BIODEGRADATION OF CHLOROBENZENES AT OXIC-ANOXIC
GROUNDWATER INTERFACES: ASSESSING THE INFLUENCES OF
BIOGEOCHEMICAL INTERACTIONS AND AMENDMENT CONDITIONS

by
Steven Jordan Chow

A dissertation submitted to Johns Hopkins University in conformity with the
requirements for the degree of Doctor of Philosophy

Baltimore, Maryland
October 2019

Abstract

Chlorobenzenes (CBs) are persistent groundwater contaminants of concern at hundreds of industrial sites around the world. This work investigated microbial biodegradation of CBs at the interface between oxic and anoxic groundwater conditions as a potential strategy to remediate sites and minimize human exposure to contaminants.

Biodegradation of micromolar concentrations (<60 µM) of 1,2,4-trichlorobenzene (1,2,4-TCB) was investigated in simulated oxic-anoxic interfaces (OAIs) using packed upflow columns. Increasing doses of model electron donor sodium lactate (NaLac) from 0.14 to 1.4 mM enhanced anaerobic reductive dechlorination activity, which stalled to monochlorobenzene without further dechlorination. However, excess NaLac (1.4 mM) suppressed aerobic CB degradation by increasing demand for limiting oxygen. Inclusion of wetland sediment within the column matrix was associated with enhanced reductive dechlorination and enrichment of anaerobic CB-dechlorinator *Dehalobacter*. Dechlorinated daughter products were not associated with enhanced aerobic degradation, suggesting no benefit of an initial reductive dechlorination step for 1,2,4-TCB mineralization.

Biodegradation of 1,2,4-TCB at simulated OAIs was also tested under nitrate- and sulfate-reducing conditions, which are common in anaerobic groundwater plumes. Under constant electron donor (0.55 mM NaLac), increased nitrate and sulfate concentrations decreased reductive dechlorination activity. Complete inhibition was observed at 2.5 mM nitrate and 10 mM sulfate. Re-oxidation of reduced sulfur negatively impacted aerobic CB degradation. In contrast, nitrate enhanced aerobic CB degradation by serving as a sink for

reduced compounds that compete with CB for limited concentrations of oxygen. Under excess nitrate (2.5 mM), a 270% increase in aerobic degradation was observed.

In separate batch experiments, effects of granular activated carbon (GAC) amendment on aerobic CB biodegradation were investigated. GAC seeded with an aerobic enrichment culture was shown to effectively facilitate mineralization of 1,2-dichlorobenzene in synthetic media and in site water. Increased GAC dose (0.13-6.7 mg/L) decreased degradation activity while increased wetland sediment loads (0.33-333 g/L) increased degradation. Results highlighted potential tradeoffs between sorption and biodegradation.

Overall, these findings emphasize the complex interactions between site and amendments at OAIs that warrant careful consideration in order to implement successful remediation strategies. Results from these studies demonstrate the potential for substantial CB bioremediation under optimal environmental conditions.

Advisor:

Dr. Edward Bouwer, Johns Hopkins University

Dissertation Readers:

Dr. William Ball, Johns Hopkins University

Dr. Michelle Lorah, US Geological Survey

Dr. Sarah Preheim, Johns Hopkins University

Acknowledgements

I would like to acknowledge some of the countless individuals and organizations that helped guide my journey to earn a PhD and made the past 6 years in Baltimore memorable.

My DoGEE colleagues, past and present, have been an integral part of my learning experience. Michael Rose and Stephanie Lau were instrumental in my development as a part-time analytical chemist and shared the highs and lows of instrument troubleshooting and method development. Keith Arora-Williams and Eric Sakowski generously shared their passion and knowledge for molecular biology and microbial community analysis. I'll never forget my day-one Master's cohort including Ali, Sonali, Kameron, Alex, and Aliza holding down the Ames lounge. Thanks to my current colleagues with whom I have interesting and enriching discussions: Andrea Fraser, Weichen Liao, Yue Zhang, and Cassie Cosans. I cherish the time spent with former colleagues with whom I've exchanged ideas, celebrated achievements, and commiserated the struggle: Dano Wilusz, Shane Putnam, David Goodwin, Jessica Lawson, Chris Kelley, Robin Hytowitz, and Elina Spyrou. I am especially grateful to Pavlo Bohutskyi, whose work inspired me to come to Johns Hopkins. His mentorship and passion for research were highly influential in my early stages of graduate school. Finally, I thank my brilliant and supportive laboratory group: Chris Brueck, Hannah Gray, and Margaret Fleming. From Bouwer family power to thesis bailouts, you were the best. The lines between colleagues, friends, and family are completely blurred; and I would not have it any other way.

I thank all of the students that have worked with me over the years, putting up with my missteps and misguidance. I specifically appreciate Shun Che, Amanda Sun, Nichole Cohen, and Annabel Mungan for their significant contributions to my work. I hope you gained as much working with me as I did from mentoring you.

I appreciate the current and past front office staff who have kept our department and my research running behind the scenes: Michael Lester, Denise Nowlin, Jessica Elroy, Zoe Peterson, Tugba Yildiz, Adena Rojas, and Keith Ritchie. A special thank-you to Huan Luong, who went above and beyond the call of laboratory manager duty to help keep my experiments and analyses running during my most critical times in the lab.

 I would like to acknowledge my sources of funding: the NSF Water, Climate, and Health IGERT program and the NIEHS Superfund Research Program. I would like to thank my project collaborators from our R01 grant: Drs. Michelle Lorah, Amar Wadhawan, and Neal Durant for their thoughtful input and guidance. I would especially like to thank Dr. Grace Brush for leading the IGERT program, which was a wonderful and enriching experience. Thank you also to Shahin Zand for making the program feel like family. And thank you to Dr. Margaret Kosek and Pablo Yori for being welcoming hosts and international research mentors during my time in Iquitos, Peru.

Thank you to my dissertation committee members for taking the time to provide guidance and thoughtful research advice over the years. Dr. Bill Ball, whose standards of rigorous and impactful research were highly appreciated to sharpen my own skills as a researcher. I am very grateful to have your mentorship and instruction, especially during the beginning of my PhD studies. Dr. Sarah Preheim, whose instruction in microbial community analysis opened my eyes new and enjoyable field of study and guided a major

This thesis is dedicated to my advisor, Dr. Edward J. Bouwer. A devoted mentor, a caring

friend, an exemplary human.

"Keep up the good work."

Table of Contents

List of Tables

List of Figures

Chapter 1.
Introduction, Objectives, and Motivation

1.1 Dissertation Objectives

The persistence of chlorobenzene (CB) contamination in subsurface environments and high costs of remediation highlight the need to better understand the factors affecting biodegradation at contaminated sites in order to develop and validate effective remediation strategies. This research fills crucial gaps in understanding CB biodegradation under anaerobic conditions, aerobic conditions, and in particular the transition zones between these conditions. In this research, we used long-term column systems to model complex contaminant transport and degradation through the subsurface. Additionally, we used batch microcosms to more carefully measure the rates and extents of biodegradation. The primary objectives of this research were:

1. Investigate the mechanisms and extent of CB biodegradation across oxic-anoxic groundwater interfaces in continuous-flow biofilm systems.

2. Determine the effects of variable biogeochemical (organic carbon, oxygen availability, and alternative electron acceptors) and bioamendment parameters (activated carbon dose, sediment presence) on CB biodegradation.

3. Characterize the microbial communities present in actively degrading systems and determine how composition relates to changes in biogeochemical conditions and observed function.

1.2   Chlorobenzene Background

1.2.1   Production and Prevalence of Contamination

CBs are a group of chlorinated aromatic compounds that consist of one to six chlorine atoms substituted onto a single aromatic ring. Historically, CBs have been used as deodorants, as carrier solvents, and as intermediates for products such as dyes, plastics, and pesticides [1]. The most industrially important CB congeners include monochlorobenzene (MCB), 1,2-dichlorobenzene (1,2-DCB), 1,4-dichlorobenzene (1,4-DCB), 1,2,4-trichlorobenzene (1,2,4-TCB), and hexachlorobenzene (HCB); HCB is banned as of 2004 under the Stockholm Convention [1, 2]. These compounds are produced synthetically through reaction of benzene with excess chlorine in the presence of a catalyst such as iron or aluminum chloride [3]. A mixture of CB congeners is produced nonspecifically in this process, requiring subsequent fractional distillation to separate products.

Thanks to increased scientific research and regulation, environmental releases of CBs have decreased steadily over the past few decades. Based on data from the EPA Toxic Release Inventory, significant reductions were made in the release of 1-3 CB congeners over a 13-year period from 2003 to 2015 [4]. According to the 2015 inventory, the majority of recent releases consisted of air emissions (267 metric tons) while a much smaller amount was attributed to land and surface water disposal (<0.2 metric tons), both of which have been significantly mitigated over the inventory history [4]. Despite this progress, there is a substantial legacy reservoir resulting from historic and unreported spills that continues to persist in the environment. Of 1854 EPA National Priorities List (NPL) sites evaluated by the Agency for Toxic Substances and Disease Registry (ATSDR), several hundred sites

have documented CB contamination (over 26% of the total database) and several dozen pathways to human exposure have been identified (Table 1.1).

Table 1.1. CB contamination at EPA NPL sites and associated regulatory limits (2017)

Substance Name	SPL Rank [b]	Occurrences at NPL Sites (% Frequency) [a]		EPA MCL (μg/L) [e]
		Sites Contaminated [c]	Exposure Pathways [d]	
Benzene	6	972 (52.4%)	143 (7.7%)	5
PeCB	76	14 (0.8%)	2 (0.1%)	NR [f]
HCB	93	111 (6.0%)	12 (0.6%)	1
MCB	128	491 (26.5%)	33 (1.8%)	100
1,2,3-TCB	137	30 (1.6%)	1 (0.1%)	NR
1,4-DCB	163	322 (17.4%)	10 (0.5%)	75
1,2-DCB	179	277 (14.9%)	5 (0.3%)	600
1,2,4-TCB	202	183 (9.9%)	4 (0.2%)	70
1,3-DCB	208	170 (9.2%)	3 (0.2%)	NR
1,2,3,4-TeCB	413	12 (0.6%)	-	NR
1,3,5-TCB	527	4 (0.2%)	-	NR
1,2,4,5-TeCB	567	16 (0.9%)	-	NR
Total NPL Sites		1854		

a. Adapted from 2017 ATSD Substance Priority List Complete Exposure Pathway Report Data [5]
b. Rank on 2017 ATSDR Substance Priority List
c. Number of NPL sites with documented substance contamination including NPL Site File records
d. Number of documented pathways to human exposure for substance at NPL sites
e. Maximum Contaminant Level from EPA National Primary Drinking Water Regulations [6]
f. NR - Not Regulated

1.2.2   Health Risks and Ecotoxicity

CBs are recognized as substances hazardous to human health and are consequently regulated contaminants [6]. CBs are nonpolar narcosis chemicals, which disrupt cell membranes and have toxicity generally proportional to concentration [7]. Studies have found that toxicity has been correlated to the number of substituted Cls attached to the aromatic ring as well as hydrophobicity [7-9]. In humans, CBs are partially metabolized in the liver by cytochrome P450 2E1 to form chlorocatechol urinary metabolites [10]. Although evidence of mortality is low, these compounds are suspected carcinogens and at high doses have been shown to cause skin irritation, damage the liver, and suppress central

nervous system functionality [11]. Benzene, a common CB co-contaminant and degradation product, is a proven multipotential carcinogen [12]. In the workplace, the Occupational Safety and Health Administration (OSHA) has placed permissible limits on air exposure for workers. MCB, for example, is limited to a 75 ppm (350 mg/m^3) time weighted average vapor concentration (concentrations above 1000 ppm pose immediate hazardous health conditions) [13]. Eleven different CB congeners plus benzene are included on the 2017 ATSDR Substance Priority List (SPL) due to their prevalence, toxicity, and potential for human exposure (Table 1.1) [5]. Additionally, five different CB compounds and benzene are nationally regulated drinking water contaminants in the US, with maximum contaminant levels of 600 µg/L and below (Table 1.1) [6].

Despite regulations to limit high dose exposure and limited recorded physiological effects in humans, recent studies have found evidence of potential negative health effects at concentrations far below regulated limits. Lehmann et al. (2008) found that cultured lung cells exposed to vapor phase MCB at concentrations above 10 µg/m^3 resulted in production of inflammatory mediator compounds, which have been linked to increased allergic sensitivity and respiratory inflammations [14]. This inflammation was found to be a result of oxidative stress from reactive oxygen species produced during CB metabolism [15]. Prolonged subtoxic doses (0.1 µg/kg daily) of a 1,2,4-TCB and HCB mixture given to mice led to anxiety-related effects and potential behavior changes, which may occur in humans as well [16]. Workers exposed to benzene at air concentrations below the OSHA-regulated limit of 1 ppm were found to have significantly lower white blood and platelet cell counts than control groups [17]. Given the limited number of studies conducted with humans and the subtle effects elucidated in studies thus far, many health effects of CBs on humans may

still be unknown. However, the evidence suggests that health concerns exist for CBs well below established regulatory limits.

In addition to potential human health effects, CBs possess ecotoxicity that may disrupt natural systems and biogeochemical cycles near areas of contamination. Boyd et al. (1998) used bioluminescence to measure toxicity in a terrestrial *Pseudomonas* bacteria species and found half maximal effective concentration (EC_{50}) values ranging from 0.54 mg/L for TCB to 118.5 mg/L for MCB [8]. Toxicity studies on methanogenic bacteria in granular sludge found half maximal inhibitory concentrations (IC_{50}) of 94-380 mg/L in 1-3 CBs and 1.5 g/L in benzene with a positive linear correlation between toxicity and hydrophobicity (log P) [9]. A study by Calamari et al. (1983) found both growth and photosynthetic inhibition in Eukaryotic algae *Raphidocelis subcapitata* at EC_{50} values from 0.9 mg/L for 1,2,3-TCB to 12.5 mg/L for MCB [18]. This same study tested lethal CB doses on rainbow trout and found 48 hour 50% lethal concentration (LC_{50}) values from 1.95 mg/L for 1,2,4-TCB to 4.1 mg/L for MCB [18]. Chronic exposure of zebrafish to 1,2,3-TCB was found to decrease the number eggs produced by females with an EC_{50} value of 40 μg/L [19]. These studies highlight significant observed and potential risks of CB contamination on flora and fauna in the environment. These same CBs may also affect higher organisms through pathways such as consumption of water, volatilization into air, and predation of contaminated organisms.

1.2.3 Subsurface Fate and Transport

CBs can be collectively classified as dense non-aqueous phase liquids (DNAPLs), which are organic liquids sparingly soluble in water with a specific gravity greater than 1. These compounds readily dissolve in nonpolar solvents and are also co-soluble. Some CBs

(1,4-DCB and 1,2,3-TCB, 1,3,5-TCB, TeCBs, PeCB, HCB) form solid crystals at room temperature, but are readily soluble in liquid CB congeners. As the number of substituted chlorines on the aromatic ring increases, aqueous solubility decreases, density increases, volatility decreases, and partitioning to sediment increases [1, 20]. Liquid CBs released into the environment tend to travel downward through sediment and aquifer pore space, displacing water until eventually being impounded by impermeable aquitards [21]. Because of low groundwater velocities and sparing aqueous CB solubility (maximum 498 mg/L for MCB), dissolution and removal of these chemicals from groundwater under natural conditions can span decades or possibly longer [22]. This slow flushing of neat CBs leads to a persistent source of dissolved aqueous concentrations that are orders of magnitude lower than the organic phase yet still well above "safe" regulatory standards [22]. All CBs (especially more chlorinated congeners) have strong sorption potential for organic sediments. Less chlorinated CBs (especially MCB) may undergo volatilization in shallow water and shallow sediment [23, 24]. Highly chlorinated CBs, more often found in lower dissolved concentrations and higher sorbed sediment concentrations, can continue to persist in surface water due to their low vapor pressures [1]. CBs in dissolved, neat liquid, and vapor phases each present unique challenges for cleanup as well as exposure for biota in the environment.

1.2.4 Biodegradation

CBs are recalcitrant to most abiotic transformations relevant to the environment, with the exception of atmospheric degradation by free radicals [25]. However, they can be transformed biologically by a variety of bacteria in both energy-yielding and fortuitous biochemical reactions, both aerobically and anaerobically [24]. Thermodynamically, the

aerobic oxidation reaction is favorable for all CB congeners with standard free energy

change $\Delta G^{o\prime}$ ranging from -3014.5 kJ/mol for MCB to -2130.95 kJ/mol for HCB; similarly,

the anaerobic reductive dechlorination of CBs coupled to oxidation of H_2 is also

thermodynamically favorable with $\Delta G^{o\prime}$ ranging from -171.4 kJ/mol for HCB to -139.6

kJ/mol for MCB [24, 26]. Under optimal environmental conditions, various bacteria have

been shown to transform all CB congeners, following at least one of the two transformation

pathways described below.

1.2.4.1 Anaerobic Reductive Dechlorination
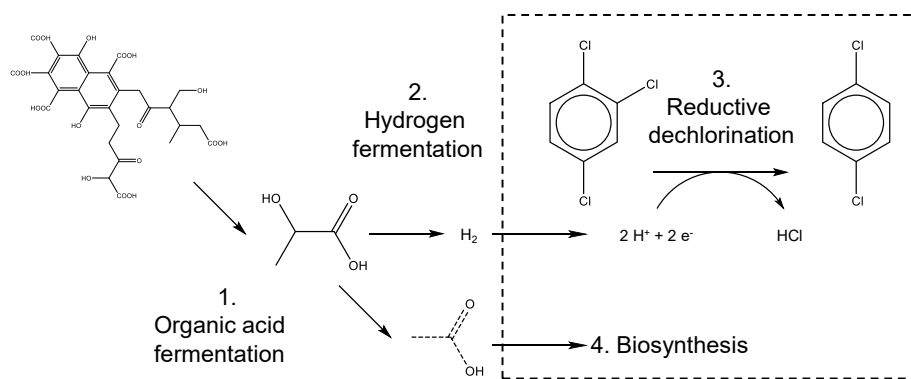
Figure 1.1. Generalized anaerobic CB reductive dechlorination pathway in a microbial consortium (steps inside dotted box occur specifically in dehalorespiring organism).

Under anaerobic conditions, CBs can be sequentially dechlorinated in a coupled

reductive dechlorination reaction known as dehalorespiration. Here, CBs serve as electron

acceptors to a coupled electron donor, H_2, in an energy-yielding process [27]. Figure 1.1

illustrates a conceptualized dechlorination pathway in a mixed anaerobic culture with a

single organic carbon source. An external carbon source such as acetate is required for

biosynthesis. This degradation reaction is catalyzed by a group of enzymes known as

reductive dehalogenases, which have diverse orthologies but similar function among their

parent organisms. Collectively, reductive dehalogenases are highly sensitive to oxygen and

require an enzymatic cofactor, cobalamin (vitamin B12) to function [27, 28]. These enzymes are contained in a small group of organohalide respiring bacteria (OHRB), capable of reducing a variety of aromatic and aliphatic halogenated compounds [27]. Several OHRB have been isolated from mixed communities. Specialist organisms in genera such as *Dehalococcoides*, *Dehalogenimonas*, and *Dehalobacter* [29] have strict metabolisms relying exclusively on dehalorespiration of H_2 for growth, but contain many different reductive dehalogenase genes that potentially reduce a variety of halogenated compounds [27, 30]. In contrast, bacteria from genera such as *Desulfitobacterium* and *Geobacter* have more diverse metabolisms, capable of using alternate anaerobic electron donors and acceptors at the expense of fewer reductive dehalogenase genes [27]. Presently, CB dehalorespiration has only been directly attributed to strict OHRB in genera *Dehalococcoides*, *Dehalobacter*, *Dehalobium*, and *Dehalogenimonas* [24, 29, 31-34]. Outside of carefully controlled laboratory conditions, strict OHRB exist as functional members of mixed microbial communities. These dechlorinators rely on other community members to synthesize necessary growth factors including H_2, assimilable organic carbon, and cobalamin.

Chemically, reductive dechlorination can be confirmed through the proportional concentration increase of dechlorinated daughter products relative to the parent CB compound. Because CBs are not used as a carbon source in this process, ^{14}C from radiolabeled CBs would not tend to accumulate in cell biomass or evolved CO_2. However, increases in OHRB population can indirectly indicate dechlorination activity [35]. Anaerobic dechlorination of MCB, 123 TCB, and 124 TCB has been shown to undergo ^{13}C

stable isotope fractionation in contrast to aerobic degradation, highlighting another potential method to identify active degradation pathways [36-38].

Reductive dechlorination has been reported for all CB congeners from MCB to HCB [28, 29, 39-43]. The pathway of CB dechlorination generally follows the most thermodynamically favorable route, with decreasing affinity for C-Cl bod cleavage from doubly flanked, to singly flanked, and finally to unflanked Cl atoms [24]. In the context of this project, 1,2,4-TCB is preferentially dechlorinated to 1,4-DCB and 1,3-DCB over 1,2-DCB; all DCB congeners can subsequently be dechlorinated to MCB [24, 41]. Transformation of more highly chlorinated CBs is thermodynamically more favorable than lower CBs, though overall degradation rates in the environment can be limited by decreased aqueous solubility and bioavailability [44]. In this case, higher CBs released into the environment will partition strongly to sediment organic matter and may exhibit slower rates of dissolution and degradation than observed in batch liquid cultures [45]. MCB exhibits much lower rates of dechlorination than DCB and TCB congeners, presenting a potential limiting step that can lead to MCB accumulation in the environment [46, 47]. Additionally, the accumulation of benzene in the environment, with greater human toxicity and more strict drinking water limits (5 µg/L) than less chlorinated CBs, is an undesirable degradation outcome [6, 40]. However, complete mineralization of CBs anaerobically has been shown to occur through isotope fractionation studies [48, 49] in the field and in laboratory microcosms [40], where produced benzene can be degraded under a variety of reducing conditions.

Aerobically, CBs can be degraded as a source of carbon and electron donor for cell growth using O_2 as an electron acceptor. Organisms capable of aerobic degradation have been identified in CB-contaminated sites around the world [24, 50, 51]. Degradation is initiated by dioxygenase enzymes, which activate the aromatic ring structure to facilitate C-C bond cleavage [24]. Typically, these adapted dioxygenases have versatile substrate specificity, with the ability to cleave aromatic homologues such as chlorophenols, chlorobenzoates and naphthalene [52-54]. Because dioxygenase enzymes are common in aerobic organisms, aerobic CB degradation is observed frequently in CB-contaminated sites. This has been attributed to modification of similar metabolic pathways over time as well as horizontal gene transfer between organisms [55, 56]. Some of the most frequently studied isolates are Gram-negative Proteobacteria in order Burkholderiales and genera *Alcalingenes, Pseudomonas*, *Xanthobacter [24, 53, 57-60]*.

1.	2.	3.	4.	5.
Chlorocatechol formation	Ring cleavage	Chloride cleavage	Organic metabolism	Oxidative phosphorylation
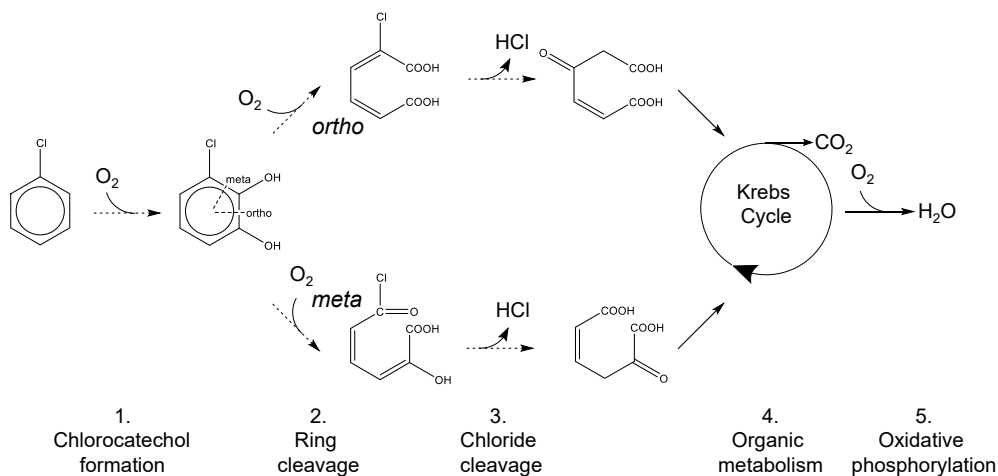
Figure 1.2. Generalized aerobic CB degradation pathway.

All CB congeners that undergo aerobic biodegradation follow a similar metabolic pathway (Figure 1.2), where a dioxygenase enzyme uses an O_2 molecule to hydroxylate the CB molecule at two adjacent carbons, eventually forming a chlorocatechol.

10

Subsequently, another O_2 molecule is used by a dioxygenase to hydroxylate the chlorocatechol again at the same carbon pair, causing cleavage of the aromatic ring. This cleavage can either occur in the *ortho* position (adjacent to both hydroxylated carbons) or *meta* position (only adjacent to one hydroxylated carbon), forming an aliphatic chloromuconic acid compound. The *ortho* cleavage pathway is much more common in chloroaromatic degraders than *meta* due to suicide inactivation of the *meta* dioxygenase enzyme by its acylchloride product [57, 61]. Subsequent hydrolysis reactions cleave the attached Cl atom from the molecule, yielding free Cl^- and H^+. The non-halogenated product can then be metabolized in the Krebs Cycle, with additional O_2 serving as a terminal electron acceptor during oxidative phosphorylation to yield H_2O and CO_2 [26, 62].

Aerobic degradation has been demonstrated in CB congeners with 4 or less attached chlorines in the environment and in controlled laboratory experiments [24, 50, 54, 63, 64]. Verification of aerobic CB degradation can be accomplished measuring disappearance of CBs in conjunction with increased dissolved Cl^- concentrations [58], $^{14}CO_2$ evolution using radiolabeled CBs [50], or increased bacterial populations when CB is the sole source of carbon [65]. In addition, increased expression of dioxygenase-coding genes has been used to infer degradation [52, 66]. There have been varying reported differences in degradability and rates of aerobic degradation between CB congeners. Some studies have reported a generally increasing trend in aerobic degradation with decreasing degree of chlorination with particular congeners more recalcitrant than others [53, 60, 67, 68]. Specifically, there is reported lower degradability of 1,3-DCB compared to other DCB congeners [69] [70] and 1,2,3-TCB compared to 1,2,4-TCB [64]. Others have reported similar degradation rates between MCBs, DCBs, and 1,2,4-TCB [64]. However, some reported differences in rate

11

appeared to be the result of prior substrate acclimation in microbial cultures rather than intrinsic metabolic rate limitations [53, 64].

1.3   Research Motivation

Remediation of groundwater contaminants is an expensive and long-term challenge, with an estimated $110-$127 billion cost to complete cleanup of the thousands of known contaminated sites in the US alone [71]. DNAPL source zones are often inaccessible and can persist for decades due to low contaminant solubility, slow groundwater flow, and sorption to sediments [72]. As a result, site remediation must often focus on removal of contaminants from dissolved groundwater plumes and sorbed sediment rather than removal of the source [73]. Because the hydrology, contaminant profiles, geochemical conditions, and risk of human exposure are heterogeneous and unique to each contaminated site, there is no "one size fits all" approach to remediation. Rather, it has been suggested by numerous prominent environmental experts, including Perry McCarty, that a combination of different technical strategies, both existing and novel, is required to achieve satisfactory results [73, 74]. This research is motivated by the need to further develop techniques and an understanding of appropriate conditions for CB bioremediation at contaminated sites. The following sections describe topics covered by this dissertation and important research needs that will be addressed.

1.3.1   *"Standard Chlorine of Delaware" Field Site*

The Standard Chlorine of Delaware (SCD) EPA Superfund site is the field site that served as motivation for this research. During the former CB manufacturer's operation from 1966 to 2002, two major spill events led to the discharge of 5000 gallons of MCB from a rail car in 1981 and 569,000 gallons of mixed DCBs and TCBs spill from

aboveground storage tanks in 1986 [75]. Substantial remedial action has since occurred at the main industrial site, under strategies that have included sediment removal, barrier wall installation, and active groundwater pump and treat [75]. Nonetheless, significant contamination has been identified in the adjacent wetland site, and remedial action at that location has not yet been taken. In a USGS site assessment from 2009-2012, DNAPL-level concentrations of mixed 1-3 CBs were detected in aquifer material, shallow sediments, and porewater throughout the wetland (Figure 1.3) [76].
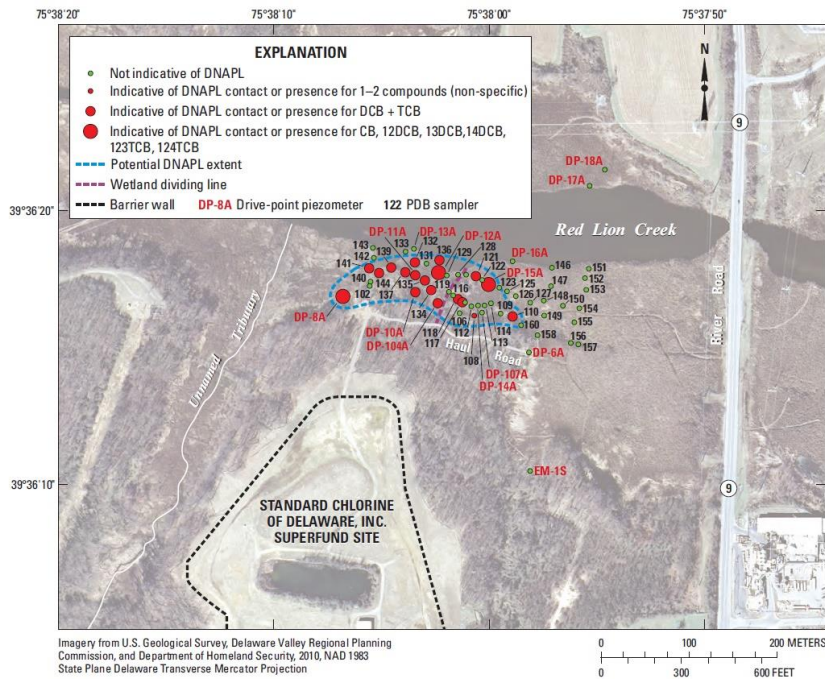
Figure 1.3. Site assessment of wetland contamination adjacent to Red Lion Creek at Standard Chlorine of Delaware Superfund site. Red circles indicate varying levels of potential CB DNAPL contamination in wetland porewater (Lorah et al., 2014 [76]).

Like many wetland systems, there is a vertical hydraulic gradient that causes upwelling of groundwater through the wetland and into the adjacent Red Lion Creek watershed (Figure 1.4) [76]. Here, site surveys have shown predominantly anaerobic porewater in shallow wetland sediments, with redox indicators methane, ferric iron, and sulfides present [76]. However, microbial community data and ^{13}C tracer uptake into cell

biomass and CO_2 have strongly suggested that both anaerobic and aerobic CB degradation processes may be occurring concurrently in this system. Similar observations have been made by Burns et al. (2013) at another contaminated site in Michigan [77] and by Braeckevelt et al. (2007) in a constructed wetland system [78]. Because of the heterogeneity in site measurements, it is incredibly difficult to assess the rates or degree to which degradation may be occurring *in situ*. Instead, model systems and microcosms simulating site conditions are necessary to determine potential treatability [67, 79].
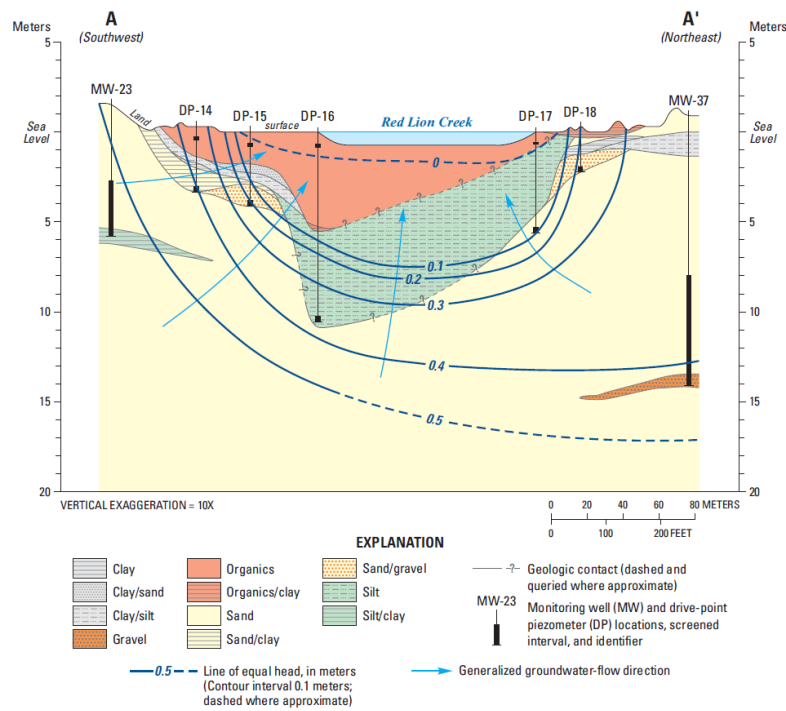
Figure 1.4. Hydraulic head distributions and groundwater flow along southwest-northeast transect at SCD wetland site. Upward arrows indicate vertical groundwater flow through organic layer in wetland adjacent to Red Lion Creek (Lorah et al., 2014 [76]).

1.3.2   Incomplete CB Reductive Dechlorination

Biological treatment strategies for anaerobic sites can be highly dependent on the contaminant present. Much of the current understanding of halogenated organic compound remediation has been developed for the treatment of more prevalent chlorinated ethenes and ethanes such as trichloroethene (TCE) and tetrachloroethane (TeCA) [73]. Initially,

anaerobic reductive dechlorination of chloroethenes was found to be problematic due to incomplete dechlorination to toxic dichloroethene and vinyl chloride daughter products [80]. However, the discovery of vinyl chloride-degrading *Dehalococcoides mccartyi*, and optimization of conditions to support its growth have helped to remedy this process-limiting step [81-83]. Thanks to this paradigm-shifting research, reductive dechlorination is a widely established remediation strategy to detoxify chloroethenes in the field [73].

With CBs, however, dechlorination as a remediation pathway remains elusive. Dechlorination of MCB to benzene has been described in several recent laboratory enrichment microcosm studies, yet rates of dechlorination are significantly lower than that for more highly chlorinated CBs [29, 38, 40, 46]. Although *Dehalobacter spp.* have been implicated in this process, no specific organisms have been isolated or characterized [29]. To our knowledge, no enrichment cultures have been developed to optimize dechlorination of MCB. Furthermore, benzene, the aromatic analog for completely dechlorinated aliphatic ethene, itself is highly toxic and is regulated at even lower levels than CBs [6]. Anaerobic dechlorination of CBs would thus need to proceed one step further to benzene mineralization in order to reach a satisfactory outcome. Innovative research by Liang et al. (2013) demonstrated coupled anaerobic benzene oxidation and MCB dechlorination processes, suggesting the potential for a self-sustaining anaerobic treatment strategy without the need for external electron donor [40]. However, until future research can better develop and demonstrate anaerobic CB mineralization in continuous and field-like conditions, this pathway remains currently non-viable for remediation treatments. Rather, aerobic degradation is the accepted standard for biological CB and benzene treatment; this has been the subject of substantial remediation research [23, 51, 52, 67, 84-87].

1.3.3 Biodegradation at Oxic-anoxic Interfaces

Naturally-occurring oxic-anoxic interfaces (OAIs) at wetlands present a naturally-occurring niche for potential aerobic CB degradation in previously anoxic groundwater. These interfaces occur often in aqueous systems, where mass transfer of atmospheric oxygen is limited by low diffusion and ppm-level aqueous solubility. At steady-state, high biomass and microbial activity are supported at overlapping gradients of limiting nutrients such as carbonaceous electron donors and oxygen [88]. Gradients can be very steep, with dramatic concentration changes occurring on the scale of several millimeters in organic rich sediments and microbial mats; or they can be much more gradual, with changes occurring on the order of several meters in sediment-free water columns [88]. In the cases of wetlands and hyporheic zones, the flux of electron donor-rich water often moves counter to the flux of oxygen from the air-water interface, forming gradient conditions. The flux of oxygen can be complex, with heterogeneities in both magnitude and direction. Processes such as turbation [89], plant root oxygenation [23], photosynthesis [90], and water table fluctuation [23, 91] have all been shown to contribute to aeration of shallow groundwater.

Several studies have quantified CB degradation under various interfacial conditions. Kurt et al. (2012) found substantial MCB degradation at the sediment-water interface of a continuously-flowing saturated water column in a completely aerobic system [79]. In a separate study, Kurt and Spain (2013) found high rates of aerobic degradation of CBs at the OAI in the unsaturated capillary fringe above anoxic groundwater [92]. Additionally, batch experiments have shown high rates of aerobic degradation after temporally sequencing anaerobic and aerobic conditions [58, 67]. Less certain is the fate of CBs in the transition from anaerobic to aerobic conditions under limiting oxygen flux

experienced in saturated groundwater. At highly contaminated sites such as SCD, a variety of reduced electron donors including CBs may all compete for the same pool of oxygen, potentially limiting aerobic CB degradation much more than these simple model systems may suggest [67]. Consequently, there is a need to assess CB degradation in systems that more accurately reflect the vertically-stratified groundwater aeration that occurs in the field.

1.3.4   Influences of Competing Redox Processes

Many studies have investigated the competition between reductive dechlorination and alternative reduction processes such as acidogenesis, methanogenesis, sulfate reduction, and nitrate reduction using chlorinated ethenes as model compounds [93-97]. Although there is substantial overlap between reaction thermodynamics and microbiology of OHRB, much less of this fundamental work has been validated in CB-dechlorinating systems [41, 98]. Even in the small body of CB literature, there is no consensus on the reducing conditions that support CB dechlorination. At low µg/L concentrations, Bosma et al. (1996) found biological CB transformations to occur under methanogenic and sulfate-reducing conditions, but not under nitrate-reducing conditions [70, 99]. Adrian et al. (1998), however, found that sulfate reduction inhibited CB reductive dechlorination at mg/L concentrations [98]. It would therefore be important to determine CB dechlorination activity under explicitly controlled reducing conditions to help clarify geochemical conditions where this process is viable.

With aerobic CB degradation, the challenge for remediation is supplying an adequate amount of oxygen to facilitate degradation. Numerous competing processes, such as ferric iron, methane, and sulfide oxidation exert O_2 demand, limiting availability for CB

17

degradation. CB degradation under very low oxygen fluxes has been verified, but can lead to incomplete mineralization to chlorinated intermediates such as chloromuconates and chlorocatechols [100]. Efforts to increase oxygen availability through air and oxygen sparging [52, 101] and hydrogen peroxide amendment [86, 102] have helped stimulate degradation, but have been shown to be costly and inefficient. While CB oxidation has only been validated as an oxygen-mediated process, there has been some suggestion that nitrate can serve as a terminal electron acceptor for CB degradation and increase CB degradation under oxygen-limited conditions [62, 66]. This would be particularly beneficial in highly contaminated sites, where the demand for oxygen is often much greater than availability. At OAIs where both anaerobic and aerobic processes are occurring, it is crucial to understand the tradeoffs and balance between anaerobically reduced substrates and potential for aerobic degradation downgradient.

1.3.5 *Innovative Amendments to Enhance Biodegradation*

There have been numerous developments in passive amendments to enhance remediation of contaminated sites. Complex carbon sources such as olive oil [103], chitin [104], peat [105], and corn cobs [106] have all been successfully demonstrated as slow-release long-term electron donors for chloroethene reductive dechlorination. These compounds are slowly hydrolyzed into soluble fermentable substrates, which limits the rate of H_2 generation [106]. Reductive dechlorination has been shown to favorably outcompete undesirable methanogenesis, sulfate reduction, and acetogenesis when H_2 partial pressures are kept below thermodynamic thresholds for these other processes [93, 96]. Oxygen amendments have been used to overcome low DO concentrations in groundwater and enhance aerobic degradation of chlorinated and aromatic contaminants. Hydrogen peroxide

has been used through active injection and decomposition to oxygen [86, 105]. Solid phase calcium and magnesium peroxide compounds, which slowly hydrolyze in water, have successfully been used to stimulate aerobic degradation [107, 108]. Oftentimes, these anaerobic and aerobic amendments have been emplaced in aquifers through permeable barriers perpendicular to groundwater flow in order to create reducing, oxidizing, or sequentially combined "biobarriers" [109-111].

Sorptive amendments such as granular activated carbon (GAC) have been proven to be highly effective in sequestering hydrophobic organic contaminants and reducing bioavailability *in situ* [112-115]. Additionally, they have been shown to be excellent delivery matrices for bioaugmentation cultures in order to stimulate combined sorption and biodegradation [116-118] . Sorption may temporarily sequester contaminants in a flowing system where high contaminant concentrations or limiting nutrient availability limit biodegradation activity, effectively providing a stabilizing sink to for variable chemical fluxes [102]. However, strong sorbents have also shown to limit rates and extents of contaminant biodegradation due to aging and desorption mass transfer limitations, which may increase overall contaminant destruction time [85, 119, 120]. Very little work has focused on applying these amendments for *in situ* CB biodegradation. In particular, tradeoffs between sorptive contaminant sequestration and potential limits to CB biodegradation must be investigated further in order to develop sustainable and effective amendment strategies.

1.3.6   *Microbial Community Interactions in Degradative Systems*

Much of the fundamental understanding of enzymatic pathways and microbial diversity of contaminant degradation has been achieved through enriched and pure cultures

of degraders [32, 98, 121-123]. While microbial community composition of various contaminant-degrading bioreactors has been described in numerous studies, it has often been achieved using highly specific targets (quantitative PCR) [97, 124] and/or low sampling depth (clone libraries) [29, 97, 122, 125]. Next-generation sequencing can reveal detailed diversity with great depth, allowing comparison of highly abundant organisms with less abundant organisms that may potentially be implicated, directly or indirectly, with contaminant degradation processes. For example, most strict OHRB require an exogenous cobalamin co-factor typically produced by sulfate-reducing and methanogenic bacteria for use in reductive dehalogenase enzymes [35]. PCB-degrading *Dehalobium* strain DF-1 was found to require an unknown factor from *Desulfovibrio* for growth [34]. Observing co-occurrence between geochemical function, specific degraders, and other taxa can potentially uncover other unknown relationships between different organisms. Further, characterizing shifts in community composition across redox conditions, space, and time may yield new insights into the stability of degradation processes, species succession, and functional redundancies [46, 121].

1.4   Dissertation Outline

This dissertation is organized into the following chapters:

Chapter 2 introduces a novel continuous-flow column system used to study interactions at a stable OAI. Two model column matrices consisting of wetland sediment from SCD site (SSC) and clean filter sand (SC) were operated continuously for 295 days to investigate dynamics of reductive dechlorination and aerobic degradation along the OAI. Biodegradation of 1,2,4-TCB at low ppm concentrations was evaluated while the dose of a model organic carbon source, sodium lactate, was cycled between concentrations of 0.14

and 1.4 mM. The stratified biofilm microbial communities in these actively-degrading columns were carefully analyzed for spatial trends across the interface.

Chapter 3 investigates the effects of alternative reducing conditions on 1,2,4-TCB biodegradation at the OAI using the experimental system developed in Chapter 2. Parallel filter sand columns were operated to evaluate the effects of changing the nitrate-reducing (0-2.5 mM nitrate) and sulfate-reducing (0.15-10 mM sulfate) conditions on CB transformations and on the electron balance of redox processes. Additionally, porewater microbial communities were assessed under these conditions to determine how structure and composition relate to changes in redox and degradation over time.

Chapter 4 evaluates factors affecting aerobic degradation of 1,2-DCB using bioaugmented GAC. Sorption can complement biodegradation in removing HOCs from groundwater, but may also create bioavailability limitations for degraders. The influence of GAC loading, site sediment, inoculation, and water characteristics on kinetics and extent of CB biodegradation were evaluated through simple batch microcosms.

Finally, Chapter 5 summarizes key experimental results, discusses important environmental implications, and presents prospects for future research resulting from this work.

1.5   References

1. Malcolm, H.; Howe, P.; Dobson, S., Chlorobenzenes other than hexachlorobenzene: environmental aspects. *Concise international chemical assessment document* **2004**.
2. Karlaganis, G.; Marioni, R.; Sieber, I.; Weber, A., The elaboration of the 'Stockholm Convention' on Persistent Organic Pollutants (POPs): A negotiation process fraught with obstacles and opportunities. *Environmental Science and Pollution Research* **2001,** *8*, (3), 216-221.
3. Auger, V. E. Process of manufacturing chlorobenzene. 1916.
4. US EPA Supporting Data Files for the 2015 TRI National Analysis. https://www.epa.gov/trinationalanalysis/supporting-data-files-2015-tri-national-analysis
5. Agency for Toxic Substances Disease Registry Substance priority list (SPL) resource page. https://www.atsdr.cdc.gov/spl/resources/index.html (07-13),

6. US EPA, National Primary Drinking Water Regulations, 40 CFR, Parts 141-143. In *Federal Registrar*, Ed. 1995.

7. Zhang, T.; Li, X.; Min, X.; Fang, T.; Zhang, Z.; Yang, L.; Liu, P., Acute toxicity of chlorobenzenes in Tetrahymena: Estimated by microcalorimetry and mechanism. *Environmental Toxicology and Pharmacology* **2012**, *33*, (3), 377-385.

8. Boyd, E. M.; Meharg, A. A.; Wright, J.; Killham, K., Toxicity of chlorobenzenes to a lux-marked terrestrial bacterium, Pseudomonas fluorescens. *Environmental Toxicology and Chemistry* **1998**, *17*, (11), 2134-2140.

9. Sierra-Alvarez, R.; Lettinga, G., The effect of aromatic structure on the inhibition of acetoclastic methanogenesis in granular sludge. *Applied microbiology and biotechnology* **1991,** *34*, (4), 544-550.

10. Nedelcheva, V.; Gut, I.; Souček, P.; Frantík, E., Cytochrome P450 catalyzed oxidation of monochlorobenzene, 1,2- and 1,4-dichlorobenzene in rat, mouse, and human liver microsomes. *Chemico-Biological Interactions* **1998**, *115*, (1), 53-70.

11. Chlorobenzene: Acute Exposure Guideline Levels. In *Acute Exposure Guideline Levels for Selected Airborne Chemicals: Volume 12*, Council, N. R., Ed. National Academies Press: Washington, DC, 2012; Vol. 12.

12. Maltoni, C.; Ciliberti, A.; Cotti, G.; Conti, B.; Belpoggi, F., Benzene, an experimental multipotential carcinogen: results of the long-term bioassays performed at the Bologna Institute of Oncology. *Environmental Health Perspectives* **1989**, *82*, 109-124.

13. Ludwig, H. R. C., Susan G.; Whalen, John J., Documentation for Immediately Dangerous To Life or Health Concentrations (IDLHs). In NIOSH, Ed. Cincinnati, OH, 1994.

14. Lehmann, I.; Röder-Stolinski, C.; Nieber, K.; Fischäder, G., In vitro models for the assessment of inflammatory and immuno-modulatory effects of the volatile organic compound chlorobenzene. *Experimental and Toxicologic Pathology* **2008,** *60*, (2–3), 185-193.

15. Feltens, R.; Mögel, I.; Röder-Stolinski, C.; Simon, J.-C.; Herberth, G.; Lehmann, I., Chlorobenzene induces oxidative stress in human lung epithelial cells in vitro. *Toxicology and Applied Pharmacology* **2010,** *242*, (1), 100-108.

16. Valkusz, Z.; Nagyéri, G.; Radács, M.; Ocskó, T.; Hausinger, P.; László, M.; László, F. A.; Juhász, A.; Julesz, J.; Pálföldi, R.; Gálfi, M., Further analysis of behavioral and endocrine consequences of chronic exposure of male Wistar rats to subtoxic doses of endocrine disruptor chlorobenzenes. *Physiology & Behavior* **2011**, *103*, (5), 421-430.

17. Lan, Q.; Zhang, L.; Li, G.; Vermeulen, R.; Weinberg, R. S.; Dosemeci, M.; Rappaport, S. M.; Shen, M.; Alter, B. P.; Wu, Y.; Kopp, W.; Waidyanatha, S.; Rabkin, C.; Guo, W.; Chanock, S.; Hayes, R. B.; Linet, M.; Kim, S.; Yin, S.; Rothman, N.; Smith, M. T., Hematotoxicity in Workers Exposed to Low Levels of Benzene. *Science* **2004**, *306*, (5702), 1774-1776.

18. Calamari, D.; Galassi, S.; Setti, F.; Vighi, M., Toxicity of selected chlorobenzenes to aquatic organisms. *Chemosphere* **1983**, *12*, (2), 253-262.

19. Roex, E. W. M.; Giovannangelo, M.; van Gestel, C. A. M., Reproductive Impairment in the Zebrafish, Danio rerio, upon Chronic Exposure to 1,2,3-Trichlorobenzene. *Ecotoxicology and Environmental Safety* **2001,** *48*, (2), 196-201.

20. Mackay, D.; Shiu, W. Y.; Ma, K. C., Illustrated handbook of physical-chemical properties and environmental fate for organic chemicals. Volume II: polynuclear aromatic hydrocarbons, polychlorinated dioxins, and dibenzofurans. *Lewis Publishers, Boca Raton, FL. 1992. 597* **1992**.

21. Hunt, J. R.; Sitar, N.; Udell, K. S., Nonaqueous phase liquid transport and cleanup: 1. Analysis of mechanisms. *Water Resources Research* **1988**, *24*, (8), 1247-1258.

22. Mercer, J. W.; Cohen, R. M., A review of immiscible fluids in the subsurface: properties, models, characterization and remediation. *Journal of Contaminant Hydrology* **1990**, *6*, (2), 107-163.

23. Braeckevelt, M.; Reiche, N.; Trapp, S.; Wiessner, A.; Paschke, H.; Kuschk, P.; Kaestner, M., Chlorobenzene removal efficiencies and removal processes in a pilot-scale constructed wetland treating contaminated groundwater. *Ecological Engineering* **2011**, *37*, 903-913.

24. Field, J. A.; Sierra-Alvarez, R., Microbial degradation of chlorinated benzenes. *Biodegradation* **2007,** *19*, 463-480.

25. Schwarzenbach, R. P.; Gschwend, P. M.; Imboden, D. M., *Environmental organic chemistry*. John Wiley & Sons: 2005.

26. Rittmann, B. E.; McCarty, P. L., *Environmental biotechnology: principles and applications*. McGraw-Hill: New York, 2001; Vol. 173, p 755.

27. Richardson, R. E., Genomic insights into organohalide respiration. *Current Opinion in Biotechnology* **2013,** *24*, (3), 498-505.

28. Adrian, L.; Szewzyk, U.; Görisch, H., Bacterial growth based on reductive dechlorination of trichlorobenzenes. *Biodegradation 11*, 73-81.

29. Nelson, J. L.; Fung, J. M.; Cadillo-Quiroz, H.; Cheng, X.; Zinder, S. H., A Role for Dehalobacter spp. in the Reductive Dehalogenation of Dichlorobenzenes and Monochlorobenzene. *Environmental Science & Technology* **2011,** *45*, (16), 6806-6813.

30. Löffler, F. E.; Yan, J.; Ritalahti, K. M.; Adrian, L.; Edwards, E. A.; Konstantinidis, K. T.; Müller, J. A.; Fullerton, H.; Zinder, S. H.; Spormann, A. M., Dehalococcoides mccartyi gen. nov., sp. nov., obligately organohalide-respiring anaerobic bacteria relevant to halogen cycling and bioremediation, belong to a novel bacterial class, Dehalococcoidia classis nov., order Dehalococcoidales ord. nov. and family Dehalococcoidaceae fam. nov., within the phylum Chloroflexi. *International Journal of Systematic and Evolutionary Microbiology* **2013,** *63*, (2), 625-635.

31. Hölscher, T.; Görisch, H.; Adrian, L., Reductive dehalogenation of chlorobenzene congeners in cell extracts of Dehalococcoides sp. strain CBDB1. *Applied and environmental microbiology* **2003,** *69*, (5), 2999-3001.

32. Adrian, L.; Szewzyk, U.; Wecke, J.; Gorisch, H., Bacterial dehalorespiration with chlorinated benzenes. *Nature* **2000,** *408*, (6812), 580-583.

33. Qiao, W.; Luo, F.; Lomheim, L.; Mack, E. E.; Ye, S.; Wu, J.; Edwards, E. A., A Dehalogenimonas Population Respires 1,2,4-Trichlorobenzene and Dichlorobenzenes. *Environmental Science & Technology* **2018,** *52*, (22), 13391-13398.

34. Wu, Q.; Milliken, C. E.; Meier, G. P.; Watts, J. E. M.; Sowers, K. R.; May, H. D., Dechlorination of Chlorobenzenes by a Culture Containing Bacterium DF-1, a PCB Dechlorinating Microorganism. *Environmental Science & Technology* **2002,** *36*, (15), 3290-3294.

35. Hug, L. A.; Maphosa, F.; Leys, D.; Löffler, F. E.; Smidt, H.; Edwards, E. A.; Adrian, L., Overview of organohalide-respiring bacteria and a proposal for a classification system for reductive dehalogenases. *Philosophical Transactions of the Royal Society of London B: Biological Sciences* **2013,** *368*, 20120322.

36. Griebler, C.; Adrian, L.; Meckenstock, R. U.; Richnow, H. H., Stable carbon isotope fractionation during aerobic and anaerobic transformation of trichlorobenzene. *FEMS Microbiology Ecology* **2004,** *48*, (3), 313-321.

37. Kaschl, A.; Vogt, C.; Uhlig, S.; Nijenhuis, I.; Weiss, H.; Kästner, M.; Richnow, H. H., Isotopic fractionation indicates anaerobic monochlorobenzene biodegradation. *Environmental Toxicology and Chemistry* **2005,** *24*, 1315-1324.

38. Liang, X.; Howlett, M. R.; Nelson, J. L.; Grant, G.; Dworatzek, S.; Lacrampe-Couloume, G.; Zinder, S. H.; Edwards, E. A.; Sherwood Lollar, B., Pathway-Dependent Isotope Fractionation during Aerobic and Anaerobic Degradation of Monochlorobenzene and 1,2,4-Trichlorobenzene. *Environmental Science & Technology* **2011,** *45*, 8321-8327.

39. Fathepure, B. Z.; Vogel, T. M., Complete degradation of polychlorinated hydrocarbons by a two-stage biofilm reactor. *Applied and Environmental Microbiology* **1991,** *57*, 3418-3422.

40. Liang, X.; Devine, C. E.; Nelson, J.; Sherwood Lollar, B.; Zinder, S.; Edwards, E. A., Anaerobic Conversion of Chlorobenzene and Benzene to CH4 and CO2 in Bioaugmented Microcosms. *Environmental Science & Technology* **2013,** *47*, 2378-2385.

41. Bosma, T. N. P.; Meer, J. R. v. d.; Schraa, G.; Tros, M. E.; Zehnder, A. J. B., Reductive dechlorination of all trichloro- and dichlorobenzene isomers. *FEMS Microbiology Ecology* **1988,** *4*, 223-229.

42. Nowak, J.; Kirsch, N. H.; Hegemann, W.; Stan, H.-J., Total reductive dechlorination of chlorobenzenes to benzene by a methanogenic mixed culture enriched from Saale river sediment. *Applied Microbiology and Biotechnology* **1996,** *45*, (5), 700-709.

43. Middeldorp, P.; De Wolf, J.; Zehnder, A.; Schraa, G., Enrichment and properties of a 1, 2, 4-trichlorobenzene-dechlorinating methanogenic microbial consortium. *Applied and environmental microbiology* **1997,** *63*, (4), 1225-1229.

44. Pavlostathis, S. G.; Prytula, M. T., Kinetics of the Sequential Microbial Reductive Dechlorination of Hexachlorobenzene. *Environmental Science & Technology* **2000,** *34*, (18), 4001-4009.

45. Prytula, M. T.; Pavlostathis, S. G., Effect of contaminant and organic matter bioavailability on the microbial dehalogenation of sediment-bound chlorobenzenes. *Water Research* **1996,** *30*, (11), 2669-2680.

46. Puentes Jácome, L. A.; Edwards, E. A., A switch of chlorinated substrate causes emergence of a previously undetected native Dehalobacter population in an established Dehalococcoides-dominated chloroethene-dechlorinating enrichment culture. *FEMS Microbiology Ecology* **2017,** *93*, (12), fix141-fix141.

47. Fung, J. M.; Weisenstein, B. P.; Mack, E. E.; Vidumsky, J. E.; Ei, T. A.; Zinder, S. H., Reductive Dehalogenation of Dichlorobenzenes and Monochlorobenzene to Benzene in Microcosms. *Environmental Science & Technology* **2009,** *43*, (7), 2302-2307.

48. Nijenhuis, I.; Stelzer, N.; Kästner, M.; Richnow, H.-H., Sensitive Detection of Anaerobic Monochlorobenzene Degradation Using Stable Isotope Tracers. *Environmental Science & Technology* **2007,** *41*, (11), 3836-3842.

49. Qiao, W.; Luo, F.; Lomheim, L.; Mack, E. E.; Ye, S.; Wu, J.; Edwards, E. A., Natural Attenuation and Anaerobic Benzene Detoxification Processes at a Chlorobenzene-Contaminated Industrial Site Inferred from Field Investigations and Microcosm Studies. *Environmental Science & Technology* **2017**.

50. Nishino, S. F.; Spain, J. C.; Belcher, L. A.; Litchfield, C. D., Chlorobenzene degradation by bacteria isolated from contaminated groundwater. *Applied and Environmental Microbiology* **1992,** *58*, 1719-1726.

51. Heidrich, S.; Weiß, H.; Kaschl, A., Attenuation reactions in a multiple contaminated aquifer in Bitterfeld (Germany). *Environmental Pollution* **2004,** *129*, (2), 277-288.

52. Dominguez, R. F.; Silva, M. L. B. d.; McGuire, T. M.; Adamson, D.; Newell, C. J.; Alvarez, P. J. J., Aerobic bioremediation of chlorobenzene source-zone soil in flow-through columns: performance assessment using quantitative PCR. *Biodegradation* **2007,** *19*, 545-553.

53. Spain, J. C.; Nishino, S. F., Degradation of 1,4-dichlorobenzene by a Pseudomonas sp. *Applied and Environmental Microbiology* **1987,** *53*, 1010-1019.

54. Adebusoye, S. A.; Picardal, F. W.; Ilori, M. O.; Amund, O. O.; Fuqua, C.; Grindle, N., Aerobic degradation of di- and trichlorobenzenes by two bacteria isolated from polluted tropical soils. *Chemosphere* **2007,** *66*, (10), 1939-1946.

55. van der Meer, J. R.; Werlen, C.; Nishino, S. F.; Spain, J. C., Evolution of a Pathway for Chlorobenzene Metabolism Leads to Natural Attenuation in Contaminated Groundwater. *Applied and Environmental Microbiology* **1998,** *64*, (11), 4185-4193.

56. Werlen, C.; Kohler, H.-P. E.; van der Meer, J. R., The Broad Substrate Chlorobenzene Dioxygenase and cis-Chlorobenzene Dihydrodiol Dehydrogenase of Pseudomonas sp. Strain P51 Are Linked Evolutionarily to the Enzymes for Benzene and Toluene Degradation. *Journal of Biological Chemistry* **1996,** *271*, (8), 4009-4016.

57. Mars, A. E.; Kasberg, T.; Kaschabek, S. R.; Agteren, M. H. v.; Janssen, D. B.; Reineke, W., Microbial degradation of chloroaromatics: use of the meta-cleavage pathway for mineralization of chlorobenzene. *Journal of Bacteriology* **1997,** *179*, 4530-4537.

58. Balcke, G. U.; Turunen, L. P.; Geyer, R.; Wenderoth, D. F.; Schlosser, D., Chlorobenzene biodegradation under consecutive aerobic–anaerobic conditions. *FEMS Microbiology Ecology* **2004,** *49*, 109-120.

59. Jiang, X.-W.; Liu, H.; Xu, Y.; Wang, S.-J.; Leak, D. J.; Zhou, N.-Y., Genetic and biochemical analyses of chlorobenzene degradation gene clusters in Pandoraea sp. strain MCB032. *Archives of Microbiology* **2009,** *191*, 485-492.

60. Schraa, G.; Boone, M. L.; Jetten, M. S.; van Neerven, A. R.; Colberg, P. J.; Zehnder, A. J., Degradation of 1,4-dichlorobenzene by Alcaligenes sp. strain A175. *Applied and Environmental Microbiology* **1986,** *52*, (6), 1374-1381.

61. Bartels, I.; Knackmuss, H.-J.; Reineke, W., Suicide inactivation of catechol 2, 3-dioxygenase from Pseudomonas putida mt-2 by 3-halocatechols. *Applied and Environmental Microbiology* **1984,** *47*, (3), 500-505.

62. Nestler, H.; Kiesel, B.; Kaschabek, S. R.; Mau, M.; Schlömann, M.; Balcke, G. U., Biodegradation of chlorobenzene under hypoxic and mixed hypoxic-denitrifying conditions. *Biodegradation* **2007,** *18*, (6), 755-767.

63. Rapp, P.; Timmis, K. N., Degradation of Chlorobenzenes at Nanomolar Concentrations byBurkholderia sp. Strain PS14 in Liquid Cultures and in Soil. *Applied and Environmental Microbiology* **1999,** *65*, 2547-2552.

64. Sander, P.; Wittich, R. M.; Fortnagel, P.; Wilkes, H.; Francke, W., Degradation of 1,2,4-trichloro- and 1,2,4,5-tetrachlorobenzene by pseudomonas strains. *Applied and Environmental Microbiology* **1991,** *57*, 1430-1440.

65. Nishino, S. F.; Spain, J. C.; Pettigrew, C. A., Biodegradation of chlorobenzene by indigenous bacteria. *Environmental Toxicology and Chemistry* **1994,** *13*, (6), 871-877.

66. Vogt, C.; Simon, D.; Alfreider, A.; Babel, W., Microbial degradation of chlorobenzene under oxygen-limited conditions leads to accumulation of 3-chlorocatechol. *Environmental Toxicology and Chemistry* **2004,** *23*, 265-270.

67. Elango, V.; Cashwell, J. M.; Bellotti, M. J.; Marotte, R.; Freedman, D. L., Bioremediation of Hexachlorocyclohexane Isomers, Chlorinated Benzenes, and Chlorinated Ethenes in Soil and Fractured Dolomite. *Bioremediation Journal* **2010,** *14*, 10-27.

68. Dermietzel, J.; Vieth, A., Chloroaromatics in groundwater: chances of bioremediation. *Environmental Geology* **2002,** *41*, (6), 683-689.

69. Bouwer, E. J.; McCarty, P. L., Removal of trace chlorinated organic compounds by activated carbon and fixed-film bacteria. *Environmental Science & Technology* **1982,** *16*, 836-843.

70. Bosma, T. N. P.; Marlies, E.; Ballemans, W.; Hoekstra, N. K.; te Welscher, R. A. G.; Smeenk, J. G. M. M.; Schraa, G.; Zehnder, A. J. B., Biotransformation of Organics in Soil Columns and an Infiltration Area. *Groundwater* **1996,** *34*, (1), 49-56.

71. National Research Council, *Alternatives for Managing the Nation's Complex Contaminated Groundwater Sites*. The National Academies Press: Washington, DC, 2013; p 422.

72. Kavanaugh, M. C.; Suresh, P.; Rao, C. *The DNAPL remediation challenge: Is there a case for source depletion?*; EPA/600/R-03/143; Environmental Protection Agency: Cincinnati, OH, December 2003, 2003.

73. McCarty, P. L., Groundwater Contamination by Chlorinated Solvents: History, Remediation Technologies and Strategies. In *In Situ Remediation of Chlorinated Solvent Plumes*, Springer, New York, NY: 2010; pp 1-28.

74. Perelo, L. W., Review: In situ and bioremediation of organic pollutants in aquatic sediments. *Journal of Hazardous Materials* **2010,** *177*, 81-89.

75. US EPA *Amendment No. 2 to the 1995 Record of Decision For The Standard Chlorine of Delaware Inc. Superfund Site Operable Unit Two*; US Environmental Protection Agency: February 24, 2016, 2016.

76. Lorah, M. M.; Walker, C. W.; Baker, A. C.; Teunis, J. A.; Majcher, E. H.; Brayton, M. J.; Raffensperger, J. P.; Cozzarelli, I. M. *Hydrogeologic characterization and assessment of bioremediation of chlorinated benzenes and benzene in wetland areas, Standard Chlorine of Delaware, Inc. Superfund Site, New Castle County, Delaware, 2009-12*; 2328-0328; US Geological Survey: 2014.

77. Burns, M.; Sublette, K. L.; Sobieraj, J.; Ogles, D.; Koenigsberg, S., Concurrent and Complete Anaerobic Reduction and Microaerophilic Degradation of Mono-, Di-, and Trichlorobenzenes. *Remediation Journal* **2013,** *23*, (3), 37-53.

78. Braeckevelt, M.; Rokadia, H.; Imfeld, G.; Stelzer, N.; Paschke, H.; Kuschk, P.; Kästner, M.; Richnow, H.-H.; Weber, S., Assessment of in situ biodegradation of monochlorobenzene in contaminated groundwater treated in a constructed wetland. *Environmental Pollution* **2007,** *148*, (2), 428-437.

79. Kurt, Z.; Shin, K.; Spain, J. C., Biodegradation of Chlorobenzene and Nitrobenzene at Interfaces between Sediment and Water. *Environmental Science & Technology* **2012,** *46*, 11829-11835.

80. Vogel, T. M.; McCarty, P. L., Biotransformation of tetrachloroethylene to trichloroethylene, dichloroethylene, vinyl chloride, and carbon dioxide under methanogenic conditions. *Applied and Environmental Microbiology* **1985,** *49*, (5), 1080-1083.

81. He, J.; Ritalahti, K. M.; Yang, K.-L.; Koenigsberg, S. S.; Löffler, F. E., Detoxification of vinyl chloride to ethene coupled to growth of an anaerobic bacterium. *Nature* **2003,** *424*, (6944), 62-65.

82. Freedman, D. L.; Gossett, J. M., Biological reductive dechlorination of tetrachloroethylene and trichloroethylene to ethylene under methanogenic conditions. *Applied and Environmental Microbiology* **1989,** *55*, 2144-2151.

83. Maymó-Gatell, X.; Nijenhuis, I.; Zinder, S. H., Reductive Dechlorination of cis-1,2-Dichloroethene and Vinyl Chloride by "Dehalococcoides ethenogenes". *Environmental Science & Technology* **2001,** *35*, (3), 516-521.

84. Guerin, T. F., Ex-situ bioremediation of chlorobenzenes in soil. *Journal of Hazardous Materials* **2008,** *154*, 9-20.

85. Lee, S.; Pardue, J. H.; Moe, W. M.; Kim, D. J., Effect of sorption and desorption-resistance on biodegradation of chlorobenzene in two wetland soils. *Journal of Hazardous Materials* **2009,** *161*, 492-498.

86. Vogt, C.; Alfreider, A.; Lorbeer, H.; Hoffmann, D.; Wuensche, L.; Babel, W., Bioremediation of chlorobenzene-contaminated ground water in an in situ reactor mediated by hydrogen peroxide. *Journal of Contaminant Hydrology* **2004,** *68*, 121-141.

87. Wenderoth, D. F.; Rosenbrock, P.; Abraham, W.-R.; Pieper, D. H.; Höfle, M. G., Bacterial community dynamics during biostimulation and bioaugmentation experiments aiming at chlorobenzene degradation in groundwater. *Microbial Ecology* **2003,** *46*, 161-176.

88. Brune, A.; Frenzel, P.; Cypionka, H., Life at the oxic-anoxic interface: microbial activities and adaptations. *FEMS Microbiol Rev* **2000,** *24*, (5), 691-710.

89. Jørgensen, B. B.; Revsbech, N. P., Diffusive boundary layers and the oxygen uptake of sediments and detritus1. *Limnology and Oceanography* **1985,** *30*, (1), 111-122.

90. Baillie, P. W., Oxygenation of intertidal estuarine sediments by benthic microalgal photosynthesis. *Estuarine, Coastal and Shelf Science* **1986,** *22*, 143-159.

91. Weishaar, J. A.; Tsao, D.; Burken, J. G., PHYTOREMEDIATION OF BTEX HYDROCARBONS: POTENTIAL IMPACTS OF DIURNAL GROUNDWATER FLUCTUATION ON MICROBIAL DEGRADATION. *International Journal of Phytoremediation* **2009,** *11*, (5), 509-523.

92. Kurt, Z.; Spain, J. C., Biodegradation of Chlorobenzene, 1,2-Dichlorobenzene, and 1,4-Dichlorobenzene in the Vadose Zone. *Environmental Science & Technology* **2013,** *47*, 6846-6854.

93. Aulenta, F.; Beccari, M.; Majone, M.; Papini, M. P.; Tandoi, V., Competition for H2 between sulfate reduction and dechlorination in butyrate-fed anaerobic cultures. *Process Biochemistry* **2008,** *43*, (2), 161-168.

94. Aulenta, F.; Di Tomassi, C.; Cupo, C.; Petrangeli Papini, M.; Majone, M., Influence of hydrogen on the reductive dechlorination of tetrachloroethene (PCE) to ethene in a methanogenic biofilm reactor: role of mass transport phenomena. *Journal of Chemical Technology & Biotechnology* **2006,** *81*, 1520-1529.

95. Mao, X.; Polasko, A.; Alvarez-Cohen, L., Effects of Sulfate Reduction on Trichloroethene Dechlorination by Dehalococcoides-Containing Microbial Communities. *Applied and Environmental Microbiology* **2017,** *83*, e03384-16.

96. Yang, Y.; McCarty, P. L., Competition for Hydrogen within a Chlorinated Solvent Dehalogenating Anaerobic Mixed Culture. *Environmental Science & Technology* **1998,** *32*, (22), 3591-3597.

97. Azizian, M. F.; Marshall, I. P. G.; Behrens, S.; Spormann, A. M.; Semprini, L., Comparison of lactate, formate, and propionate as hydrogen donors for the reductive dehalogenation of trichloroethene in a continuous-flow column. *Journal of Contaminant Hydrology* **2010,** *113*, (1–4), 77-92.

98. Adrian, L.; Manz, W.; Szewzyk, U.; Görisch, H., Physiological characterization of a bacterial consortium reductively dechlorinating 1, 2, 3-and 1, 2, 4-trichlorobenzene. *Applied and environmental microbiology* **1998,** *64*, (2), 496-503.

99. Meer, J. R. v. d.; Bosma, T. N. P.; Bruin, W. P. d.; Harms, H.; Holliger, C.; Rijnaarts, H. H. M.; Tros, M. E.; Schraa, G.; Zehnder, A. J. B., Versatility of soil column experiments to study biodegradation of halogenated compounds under environmental conditions. *Biodegradation* **1992,** *3*, 265-284.

100. Balcke, G. U.; Wegener, S.; Kiesel, B.; Benndorf, D.; Schlömann, M.; Vogt, C., Kinetics of chlorobenzene biodegradation under reduced oxygen levels. *Biodegradation* **2007,** *19*, 507-518.

101. Balcke, G. U.; Paschke, H.; Vogt, C.; Schirmer, M., Pulsed gas injection: A minimum effort approach for enhanced natural attenuation of chlorobenzene in contaminated groundwater. *Environmental Pollution* **2009,** *157*, (7), 2011-2018.

102. Tiehm, A.; Gozan, M.; Müller, A.; Schell, H.; Lorbeer, H.; Werner, P., Sequential anaerobic/aerobic biodegradation of chlorinated hydrocarbons in activated carbon barriers. *Water Science and Technology: Water Supply* **2002,** *2*, 51-58.

103. Yang, Y.; McCarty, P. L., Comparison between Donor Substrates for Biologically Enhanced Tetrachloroethene DNAPL Dissolution. *Environmental Science & Technology* **2002,** *36*, (15), 3400-3404.

104. Brennan, R. A.; Sanford, R. A.; Werth, C. J., Biodegradation of tetrachloroethene by chitin fermentation products in a continuous flow column system. *Journal of environmental engineering* **2006,** *132*, (6), 664-673.

105. Tartakovsky, B.; Manuel, M.-F.; Guiot, S. R., Trichloroethylene Degradation in a Coupled Anaerobic/Aerobic Reactor Oxygenated Using Hydrogen Peroxide. *Environmental Science & Technology* **2003,** *37*, 5823-5828.

106. Brennan, R. A.; Sanford, R. A.; Werth, C. J., Chitin and corncobs as electron donor sources for the reductive dechlorination of tetrachloroethene. *Water Research* **2006,** *40*, (11), 2125-2134.

107. Kao, C. M.; Chen, S. C.; Su, M. C., Laboratory column studies for evaluating a barrier system for providing oxygen and substrate for TCE biodegradation. *Chemosphere* **2001,** *44*, 925-934.

108. Nebe, J.; Baldwin, B. R.; Kassab, R. L.; Nies, L.; Nakatsu, C. H., Quantification of Aromatic Oxygenase Genes to Evaluate Enhanced Bioremediation by Oxygen Releasing Materials at a Gasoline-Contaminated Site. *Environmental Science & Technology* **2009,** *43*, (6), 2029-2034.

109. Lu, X.; Wilson, J. T.; Shen, H.; Henry, B. M.; Kampbell, D. H., Remediation of TCE-contaminated groundwater by a permeable reactive barrier filled with plant mulch (Biowall). *Journal of Environmental Science and Health, Part A* **2007,** *43*, 24-35.

110. Kao, C. M.; Chen, S. C.; Wang, J. Y.; Chen, Y. L.; Lee, S. Z., Remediation of PCE-contaminated aquifer by an in situ two-layer biobarrier: laboratory batch and column studies. *Water Research* **2003,** *37*, (1), 27-38.

111. Careghini, A.; Saponaro, S.; Sezenna, E., Biobarriers for groundwater treatment: a review. *Water Science and Technology* **2012,** *67*, (3), 453-468.

112. Pavoni, B.; Drusian, D.; Giacometti, A.; Zanette, M., Assessment of organic chlorinated compound removal from aqueous matrices by adsorption on activated carbon. *Water Research* **2006,** *40*, 3571-3579.

113. Song, Y.; Wang, F.; Kengara, F. O.; Bian, Y.; Yang, X.; Gu, C.; Ye, M.; Jiang, X., Does powder and granular activated carbon perform equally in immobilizing chlorobenzenes in soil? *Environmental Science: Processes & Impacts* **2015,** *17*, 74-80.

114. Oen, A. M. P.; Beckingham, B.; Ghosh, U.; Kruså, M. E.; Luthy, R. G.; Hartnik, T.; Henriksen, T.; Cornelissen, G., Sorption of Organic Compounds to Fresh and Field-Aged Activated Carbons in Soils and Sediments. *Environmental Science & Technology* **2012,** *46*, 810-817.

115. Quinlivan, P. A.; Li, L.; Knappe, D. R. U., Effects of activated carbon characteristics on the simultaneous adsorption of aqueous organic micropollutants and natural organic matter. *Water Research* **2005,** *39*, 1663-1673.

116. Payne, R. B.; Ghosh, U.; May, H. D.; Marshall, C. W.; Sowers, K. R., A Pilot-Scale Field Study: In Situ Treatment of PCB-Impacted Sediments with Bioamended Activated Carbon. *Environmental Science & Technology* **2019,** *53*, (5), 2626-2634.

117. Payne, R. B.; Fagervold, S. K.; May, H. D.; Sowers, K. R., Remediation of polychlorinated biphenyl impacted sediment by concurrent bioaugmentation with anaerobic halorespiring and aerobic degrading bacteria. *Environmental science & technology* **2013,** *47*, (8), 3807-3815.

118. Lorbeer, H.; Starke, S.; Gozan, M.; Tiehm, A.; Werner, P., Bioremediation of Chlorobenzene-Contaminated Groundwater on Granular Activated Carbon Barriers. *Water, Air and Soil Pollution: Focus* **2002,** *2*, (3), 183-193.

119. Cornelissen, G.; Gustafsson, Ö.; Bucheli, T. D.; Jonker, M. T. O.; Koelmans, A. A.; van Noort, P. C. M., Extensive Sorption of Organic Compounds to Black Carbon, Coal, and Kerogen in Sediments and Soils: Mechanisms and Consequences for Distribution, Bioaccumulation, and Biodegradation. *Environmental Science & Technology* **2005,** *39*, 6881-6895.

120. Rhodes, A. H.; McAllister, L. E.; Chen, R.; Semple, K. T., Impact of activated charcoal on the mineralisation of 14C-phenanthrene in soils. *Chemosphere* **2010,** *79*, (4), 463-469.

121. Brisson, V. L.; West, K. A.; Lee, P. K.; Tringe, S. G.; Brodie, E. L.; Alvarez-Cohen, L., Metagenomic analysis of a stable trichloroethene-degrading microbial community. *The ISME Journal* **2012,** *6*, 1702-1714.

122. Wintzingerode, F. v.; Selent, B.; Hegemann, W.; Göbel, U. B., Phylogenetic Analysis of an Anaerobic, Trichlorobenzene-Transforming Microbial Consortium. *Applied and Environmental Microbiology* **1999,** *65*, 283-286.

123. Nelson, J. L.; Jiang, J.; Zinder, S. H., Dehalogenation of Chlorobenzenes, Dichlorotoluenes, and Tetrachloroethene by Three Dehalobacter spp. *Environmental Science & Technology* **2014,** *48*, (7), 3776-3782.

124. Behrens, S.; Azizian, M. F.; McMurdie, P. J.; Sabalowsky, A.; Dolan, M. E.; Semprini, L.; Spormann, A. M., Monitoring Abundance and Expression of "Dehalococcoides" Species Chloroethene-Reductive Dehalogenases in a Tetrachloroethene-Dechlorinating Flow Column. *Applied and Environmental Microbiology* **2008,** *74*, 5695-5703.

125. Manchester, M. J.; Hug, L. A.; Zarek, M.; Zila, A.; Edwards, E. A., Discovery of a trans-Dichloroethene-Respiring Dehalogenimonas Species in the 1,1,2,2-Tetrachloroethane-Dechlorinating WBC-2 Consortium. *Applied and Environmental Microbiology* **2012,** *78*, (15), 5280-5287.

Chapter 2.

Sequential Biodegradation of 1,2,4-Trichlorobenzene at Oxic-anoxic Groundwater Interfaces in Model Laboratory Columns[*]

2.1   Abstract

Halogenated organic solvents such as chlorobenzenes (CBs) are frequent groundwater contaminants due to legacy spills. When contaminated anaerobic groundwater discharges into surface water through wetlands and other transition zones, it can experience aeration from various physical and biological processes at shallow depths. This study investigated the potential for 1,2,4-trichlorobenzene (1,2,4-TCB) biodegradation at these oxic-anoxic interfaces (OAIs). A novel upflow column system was used to create stable anaerobic and aerobic zones, simulating a natural groundwater OAI. Two columns containing (1) sand and (2) a mixture of wetland sediment and sand were operated continuously for 295 days with varied doses of 0.14-1.4 mM sodium lactate (NaLac) as a model electron donor. Both column matrices supported reductive dechlorination and aerobic degradation of 1,2,4-TCB spatially separated between anaerobic and aerobic zones. Reductive dechlorination, with maximum observed rates up to 31.1 μM/hr, produced a mixture of di- and monochlorobenzene daughter products, but did not further reduce CBs. Aerobic CB degradation, limited by available dissolved oxygen, occurred for 1,2,4-TCB

---

and all dechlorinated daughter products at aggregate rates of 4.9-11.3 µM/hr. Initial reductive dechlorination did not enhance the overall observed extent or rate of subsequent aerobic CB degradation. Increasing NaLac dose increased the extent of reductive dechlorination, but suppressed aerobic CB degradation at 1.4 mM NaLac due to increased oxygen demand. 16S-rRNA sequencing of biofilm microbial communities revealed strong stratification of functional anaerobic and aerobic organisms between redox zones including the sole putative reductive dechlorinator detected in the columns, *Dehalobacter*. The sediment mixture column supported enhanced reductive dechlorination at all tested NaLac doses and growth of *Dehalobacter* populations up to 4.1×10^8 copies/g (51% relative abundance) compared to the sand column, highlighting the potential benefit of sediments in reductive dechlorination processes. Results from these model systems suggest both substantial anaerobic and aerobic CB degradation can co-occur along the OAI at contaminated sites where bioavailable electron donors and oxygen are both present.

2.2 Introduction

Chlorobenzenes (CBs) are aromatic chlorinated organic solvents historically produced and used in industry. Exposure at low concentrations has been associated with negative human health effects including oxidative stress, respiratory inflammation, and possible carcinogenesis [1]. Due to spills and improper disposal at manufacturing and end-use sites, CBs in the subsurface often become persistent sources of legacy groundwater contamination, occurring as dense nonaqueous phase liquids (DNAPL) and resulting in high (mg/L) aqueous CB concentrations. Persistent DNAPL source zones can result in large dissolved aqueous plumes where contaminant concentrations are often in excess of 1% aqueous solubility [2]. At least 491 EPA National Priorities List sites have documented

CB contamination, most frequently mono- (MCB), di- (DCB), tri- (TCB), and hexachlorobenzene congeners [3].

Biodegradation, either through natural attenuation or engineered *in situ* or *ex situ* treatment (bioremediation), is a significant environmental fate process for many organic contaminants, including CBs [4]. Bioremediation is an appealing treatment approach for CBs due to its relatively low cost, minimal site impact, and potential to be self-sustaining [5, 6]. Under anaerobic conditions, CBs can be reductively dechlorinated as terminal electron acceptors to less chlorinated congeners by organohalide respiring bacteria (OHRB) [7]. Though complete anaerobic mineralization of CBs through benzene metabolism has been demonstrated in laboratory microcosms and in trace amounts *in situ* [8-10], dechlorination of MCB to benzene is a known rate-limiting bottleneck in the degradation process [11]. Anaerobic bioremediation of CBs, in general, has been avoided in field-scale applications due, in part, to concerns regarding possible inadvertent accumulation of MCB and benzene in groundwater. CBs with four or less chlorines and benzene, however, are particularly amenable to aerobic mineralization, where no toxic daughter products are produced [7]. Aerobic bioremediation is often employed for treatment of less-chlorinated CB congeners; however, the costs and difficulty of oxygenating groundwater can limit treatment effectiveness [6, 10].

Groundwater discharged to surface water through wetland sediments and hyporheic zones often encounters redox gradients, which support diverse microbial communities and activity [12, 13]. In these environments organic carbon turnover can create reducing conditions in subsurface porewater, while surface processes such as turbation, plant root oxygenation, and photosynthesis contribute to aerobic conditions [12, 14]. The oxic-anoxic

interfaces (OAIs) formed in such environments offer a niche to potentially support both anaerobic and aerobic CB degradation pathways. The extent of such interfaces, and hence degradation, can vary considerably depending on the heterogenous characteristics of field sites such as organic carbon loading, competing electron acceptors, and mass transfer limitations [13]. Contaminant degradation has been described across a variety of interfacial scales in groundwater, from steep millimeter-length anoxic boundaries [15, 16] to gradual microaerophilic permeation into deeper anaerobic zones [17, 18].

At the Standard Chlorine of Delaware (SCD) Superfund site (New Castle, DE), over 1 million liters of mixed MCBs, DCBs, and TCBs were released into the environment from spill events [19]. A previous site assessment conducted by the US Geological Survey found that subsurface CB DNAPL had contaminated the wetland adjacent to the industrial site, with mixed CB concentrations in excess of 50 mg/L and 1 g/kg in porewater and sediments respectively [20]. *In situ* Bio-Trap® microcosms as well as laboratory bioreactor experiments suggested that both reductive dechlorination and oxidative degradation pathways co-occur naturally in shallow SCD wetland sediments [20]. This and other studies [14, 18] have provided empirical evidence of coupled degradation at OAIs through indicators such as ^{13}C stable isotope fractionation, genetic markers, and shifts in congener distribution. However, the rates and extents to which these CB degradation pathways may occur at these interfaces remain poorly understood.

In this study, we aimed to quantify the biodegradation potential of CBs discharged through a model OAI within a laboratory column system. Here we investigated the dynamics of labile carbon amendment on the anaerobic and aerobic degradation of 1,2,4-TCB. Over a 295-day period, we cycled various influent concentrations and measured the

extents and rates of degradation in site-relevant wetland sediment and idealized sand matrices. Additionally, we surveyed the spatial stratification of degradation activity and biofilm microbial communities within the columns to better understand the distribution of microbial taxonomy and functional potential across the interface.
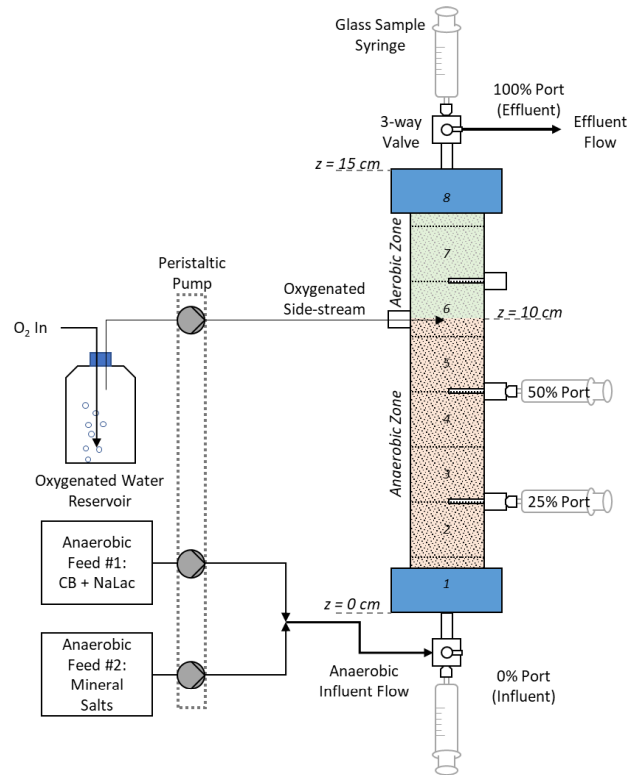
Figure 2.1. Design schematic of experimental column systems. Porewater samples were taken at positions designated 0, 25, 50, or 100% of nominal flowpath. At the end of the experiment, columns were vertically segmented into eight equal segments (1-8) to characterize the column biofilm. Segments 1-5 represent the anaerobic zone and 6-8 represent the aerobic zone after oxygenated-side-stream addition.

2.3 Materials and Methods

2.3.1 Column Design and Setup

Modified 15 cm × 2.5 cm (L × ID) glass chromatography columns (Kimble Chromaflex®) were operated as upflow packed bed reactors to simulate groundwater discharge into surface water with a discrete OAI (Figure 2.1). A side-stream of oxygen-saturated Milli-Q® water was injected into each column at 67% of the nominal length to

create aerobic conditions in the upper zone. Sample ports at 3.75 cm, 7.5 cm, and 11.25 cm from the inlet (25%, 50%, and 75% of column length, respectively) were added to vertically profile the interface. Caps, fittings, and tubing were constructed of fluoropolymers to minimize sorptive losses.

Two model matrices were tested in parallel. The first, "Sand and Sediment Column" (SSC), was packed with a 75:25 wt% (84:16 dry wt%) homogenized mixture of silica filter sand (0.55-0.65 µm) (Browns Hill Sand, Homestead, PA) and autoclaved wetland sediment sampled from the SCD site in 2016 [20]. The sediment, sieved below 1 mm, had a total organic carbon content of 33.9 mg/g and a silt loam texture consisting of 3.1% sand, 76.4% silt, and 20.5% clay. The second, "Sand Column" (SC), was packed solely with filter sand. Specific column design and packing details are provided in Appendix A (Section A.1.2).

A defined simulated anaerobic groundwater media was used to support microbial growth and minimize nutrient limitations during the experiment (Section A.1.3). Media were fed from two separate stocks containing (1) dissolved 1,2,4-TCB (from neat stock) and sodium lactate (NaLac) and (2) mineral salts, replenished every 20-30 days. Each stock was prepared by autoclaving for 30 minutes, bubbling N_2 to purge dissolved oxygen (DO), and transferring into zero-headspace feed bags to minimize re-oxygenation, volatilization, and sorption. Media entering the columns contained 0.32 mg/L Cl^-, 10.6 mg/L SO_4^{2-}, 0.25 mg/L Fe, 21.2 mg/L total N (as NH_4^+), and 39.3 mg/L total P (as phosphate buffer and counter-anions); a trace metal solution [21]; and a vitamin mixture [22]. Chloride salts were minimized to reduce background signal to allow detection of chloride released from biodegradation.

Media were delivered to the columns continuously by a multi-channel peristaltic pump (Ismatec IP 12) to achieve linear porewater velocities similar to the maximum of 2.98-4.49 cm/hr observed in the SCD wetland [20]. The anaerobic influent was diluted by a factor of 1.30 by the aerobic stream, and calculated parameters accounted for the dilution. Column hydraulics were determined mid-experiment (Day 155) by a bromide tracer test. A step-input of 25 mg/L bromide was added to the column influent with effluent samples collected in discrete 20-minute intervals and analyzed by ion chromatography. Bromide breakthrough was fitted to a 1-D advection dispersion model with a semi-infinite boundary condition (model described in detail in Section 3.3.4) using tracer interpretation application TRAC to determine column hydrodynamics for the entirety of each column [23]. Hydraulic residence times and linear velocities were then back-calculated separately for anaerobic and aerobic zones assuming a constant effective porosity throughout the entirety of each column and proportionality of linear velocities to the flow rates in each zone. Calculated hydraulic parameters for each column are described in Table 2.1.

Table 2.1. Hydraulic characteristics of experimental columns

Parameter	Sand + Sediment Column (SSC)	Sand Column (SC)
Effective porosity [a]	0.34	0.48
Effluent flow (mL/hr) [b]	7.14 ± .08	6.84 ± .09
Linear velocity (cm/hr) [a, c]	3.32 / 4.31	2.26 / 2.94
Hydraulic residence time (hr) [a, c]	3.02 / 1.16 [4.18]	4.43 / 1.70 [6.13]

[a] Calculated from hydraulic tracer test on Day 155
[b] Directly measured over course of experiment ±1 SD (n=5)
[c] Listed values: *Anaerobic zone / Aerobic zone [Total column]*

2.3.2 Column Inoculation

SSC was directly inoculated with both anaerobic and aerobic CB-degrading cultures under no-flow conditions. The anaerobic inoculum was a 1,2,4-TCB-fed subculture derived from WBC-2 (SiREM Labs, Guelph, ON); WBC-2 was previously shown to degrade CBs in field and laboratory tests at SCD [20]. The aerobic inoculum was a CB-fed culture enriched from filtered SCD wetland porewater fed with a mixture of MCB, 1,2-DCB, and 1,2,4-TCB as sole substrates. First, 40 mL of the anaerobic culture was injected by sterile syringe through the column influent port, displacing porewater media through the effluent. Ports were closed, and inoculation occurred statically for 4 days. Next, 20 mL of the aerobic culture was injected through the 50% sample port, with excess media displaced through the effluent. This inoculated the upper half of the column only, which occurred statically for 3 days. Media were then pumped continuously (Day 0) for 46 days in a startup phase to facilitate flushing of sediment-bound constituents. Detailed inoculum culture characteristics are presented in Appendix A (Section A.1.4).

At Day 43, the SSC effluent was connected to the SC influent to provide a continuous flow-through inoculum for 3 days. The entire length of the SC matrix was passively inoculated by SSC porewater, in contrast to the bifurcated SSC inoculation scheme. At Day 46, SC was connected to the same influent media as SSC and began independent operation. This marked the end of startup and beginning of Phase 1.

2.3.3 Experiment Operation

After start-up, columns were operated continuously at room temperature ($18.0\,^{\circ}$C $\pm 3.1\,^{\circ}$C SD) for 249 days. Influent 1,2,4-TCB concentrations varied between batches, with an average value of 5.8±1.6 mg/L (32±8.8 µM). Aerobic zone DO concentrations after

oxygenated side-stream injection were 7.0 ±0.9 mg/L (220 ±30 μM). NaLac, a readably fermentable source of labile carbon, was used as a model electron donor for the system. Column operation was divided into five discrete experimental phases where influent NaLac was cycled between (1) 0.28, (2) 1.4, (3) 0.14, (4) 14.4, and (5) 0.28 mM. This represented a dissolved organic carbon (DOC) range of 5-50 mg/L, similar to the range of non-volatile DOC observed at the SCD site [20]. A short phase (6) removed oxygen from the side-stream temporarily to verify oxygen dependence of aerobic zone reactions, while the final phase (7) restored oxygen and restored initial conditions before sacrificial sampling. A graphical summary of operational phases is presented in Figure 2.2a.

Porewater samples were collected at three to four-day intervals at column influent (0%) and effluent (100%) ports. Less frequently, samples were collected along the vertical profile to observe spatial trends along the column length. Samples at 25% and 50% represented the anaerobic zone of the column before oxygen addition, and samples at 75% and 100% represented the aerobic zone of the column, after oxygen dilution (Figure 2.1). Tracer measurements showed that samples at 75% were not completely-mixed, so sample data from this port were not included here. Samples were collected by filling 5 mL glass Luer Lock syringes attached to sample ports by column flow. Immediately after collection, 100 μL subsamples were taken from the syringe barrel using a gastight microsyringe and analyzed for CBs. The remaining sample volumes were passed through sterile 0.22 μm polyether sulfone syringe filters and stored in sterile polypropylene tubes for subsequent analysis.

At the end of the experiment (Day 295), columns were sacrificially sampled to analyze biofilm microbial communities. The columns were divided into eight equal-length

segments along the vertical profile, labeled 1-8 from entrance to exit (Figure 2.1). Column matrices from each segment were manually homogenized with a sterile cell scraper and stored in sterile 50 mL polypropylene tubes at -80 °C for microbial analyses.
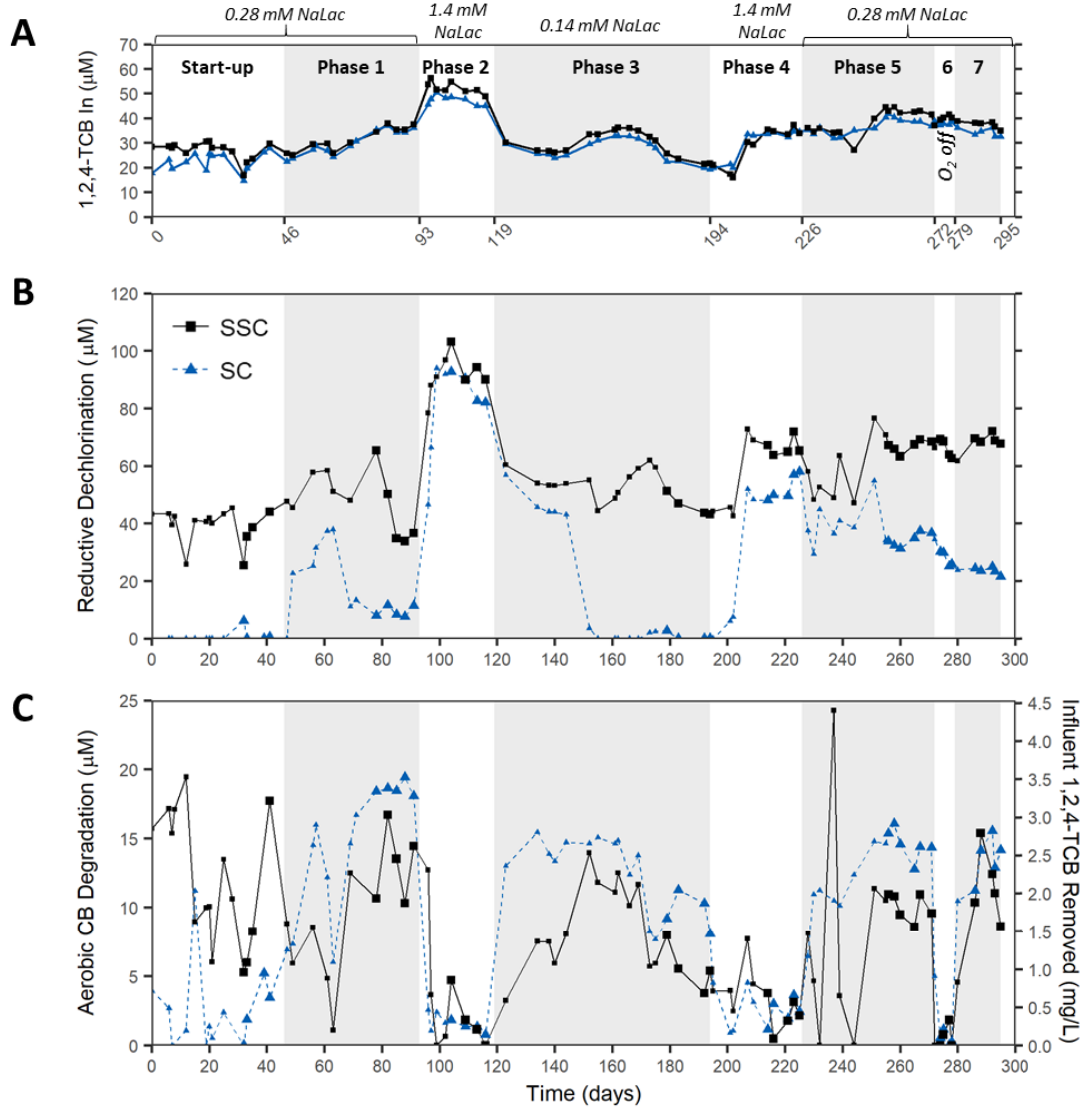
Figure 2.2. Time-series plots of experimental input phases and CB biodegradation for each column (A) Experimental input phases summary. Connected data points show influent 1,2,4-TCB measured at 0% port. Stepped lines represent theoretical NaLac amendment into columns. (B) Total anaerobic reductive dechlorination activity. (C) Aerobic degradation activity, represented as total CB removal. Bolded data points were samples used to calculate stable performance for each experimental phase.

2.3.4 Analytical Methods

Porewater CB concentrations were analyzed by gas chromatography-mass spectrometry (GC-MS; Agilent 7090B–5977). A single-step, miniaturized "in-vial" liquid-liquid extraction process was used to extract and analyze CBs directly in a single 1.5 mL autosample vial. CBs were quantitated between 0.05-10 mg/L. Benzene was analyzed separately by GC-MS using a purge and trap method described previously [20]. Ion chromatography (Thermo Fisher Dionex ICS-2100) was utilized to measure inorganic anions chloride, sulfate, and bromide, as well as organic acids from filtered aqueous samples. Anions were quantitated between 0.1-20 mg/L for inorganic anions and 1-200 μM for organic acids. Detailed descriptions of analyte extraction and chromatographic protocols are presented in Appendix A (Sections A.1.5-A.1.6).

A fiber-optic luminescence-based meter (PreSens OXY1-SMA) and an in-line sensor (PreSens FTC-PSt3) were used to measure DO concentrations at the oxygenated side-stream injection port. Column flowrates were determined gravimetrically by collection of effluent over hour-long time intervals.

2.3.5 Biodegradation Calculations

Biodegradation activity at each timepoint was enumerated on the basis of reductive dechlorination and aerobic degradation using measured concentrations of influent (0% port) and effluent (100% port) CBs in the porewater (Figure A.2). Reductive dechlorination was estimated as the total number of dechlorinations, or expected equivalent chloride released, from 1,2,4-TCB in the influent on a molar basis (μmol/L). This was calculated according to Equation 2.1, where the fractional dechlorination of the effluent was multiplied by the total influent concentration. This calculation assumed dechlorination

stalled at MCB, since benzene was not detected above the CB quantitation limit in either column.

Equation 2.1

$$\text{Reductive Dechlorination} = \frac{(2 \times \text{MCB}_{100} + \Sigma\text{DCBs}_{100})}{\Sigma\text{CBs}_{100}} \times \Sigma\text{CBs}_0$$

Aerobic CB degradation was quantified by the removal of all CB congeners from the column assuming no anaerobic mineralization occurred, as described in Equation 2.2. Since aerobic degradation occurred after the addition of the oxygen stream, all calculated extents and rates of removal were adjusted by the dilution factor (*DF*) described in Section 2.3.1 to reflect the actual removal occurring in the aerobic zone.

Equation 2.2

$$\text{Aerobic Degradation} = (\Sigma\text{CBs}_0 \div DF) - \Sigma\text{CBs}_{100}$$

Sample data from the last 15 days of each experimental phase, with the exception of shorter Phases 6 (5 days) and 7 (10 days), were used to estimate biodegradation characteristics for comparison of the experimental phases (Table 2.2). Rates of anaerobic dechlorination and anaerobic degradation were estimated based on degradation calculated in Equations 1 and 2 divided by the hydraulic retention times (HRT) of each respective redox zone (Table 2.1). A comprehensive quantitative summary of all calculated values and associated equations is presented in Appendix A (Table A.1).

2.3.6 *Microbial Community Analysis*

DNA was extracted from 0.5 g wet subsamples of each column segment using a MoBio PowerSoil® DNA extraction kit (Qiagen, Germantown, MD) following

manufacturer instructions and quantified using a Qubit® 3.0 fluorometer dsDNA high sensitivity assay kit (Thermo Fisher Scientific, Waltham, MA). Extracts were prepared for Illumina amplicon sequencing of the V4 region of 16S rRNA gene (primers U515 and E786) for bacteria and archaea [24]. Samples were sequenced by 300-base pair paired-end sequencing using an Illumina MiSeq sequencing platform (JHU Genetic Resources Core Facility, Baltimore, MD). Each column segment was extracted, quantified, and sequenced in duplicate. Sequencing data were processed using the qiime2 pipeline (v.2018.4.0) [25], and taxonomy was assigned using Greengenes 13_8 99% OTUs reference sequences [26]. Quantitative Polymerase Chain Reaction (qPCR) was used to quantify total microbial 16S rRNA gene copies using primers described by Puentes Jácome and Edwards (2017) [27]. Concentrations were normalized to the mass of column segment sampled. Details of the downstream sequence analysis and qPCR method can be found in Appendix A (Sections A.1.7-A.1.8). Raw 16S reads for each analyzed sample have been uploaded to the National Center for Biotechnology Information (NCBI) Sequence Read Archive (SRA) under BioProject Accession ID PRJNA562559.

Table 2.2. Summarized column biodegradation activity

Experimental Phase e- Donor Dose	n Samples	Column	Anaerobic Degradation [a]			Aerobic Degradation [b]			Cl- Balance [h]
			Dechlorinations (μM) [c]	Rate (μM/hr) [c,d]	e- Donor Utilization (meq %) [e]	Degradation (μM) [c] / [% Removal]	Rate (μM/hr) [c,d]	O_2 Utilization (meq %) [f] / [mg CB/ mg DO] [g]	
1 0.28 mM NaLac	5	SSC	44.2 ± 13.6	14.7 ± 4.5	2.7%	13.1 ± 2.7 [47%]	11.3 ± 2.3	47.4% [0.41]	81%
		SC	9.4 ± 1.9	2.1 ± .4	0.6%	18.6 ± .5 [68%]	10.9 ± .3	62.3% [0.58]	50%
2 1.4 mM NaLac	4	SSC	94.4 ± 6.2	31.3 ± 2.0	1.1%	1.9 ± 2.0 [5%]	1.7 ± 1.7	6.5% [0.05]	86%
		SC	86.9 ± 5.5	19.6 ± 1.2	1.0%	1.3 ± .4 [4%]	0.8 ± .3	4.5% [0.04]	95%
3 0.14 mM NaLac	4	SSC	46.3 ± 3.7*	15.4 ± 1.2*	5.8%	5.7 ± 1.7 [31%]	4.9 ± 1.5	18.8% [0.15]	113%
		SC	0.7 ± 1.3	0.2 ± .3	0.1%	9.7 ± 1.4 [60%]	5.7 ± .8	27.6% [0.26]	112%
4 1.4 mM NaLac	5	SSC	66.6 ± 3.2	22.1 ± 1.1	0.8%	2.3 ± 1.3 [8%]	1.9 ± 1.1	6.7% [0.05]	101%
		SC	52.5 ± 4.6	11.8 ± 1.0	0.6%	2.4 ± 1.0 [9%]	1.4 ± .6	7.0% [0.06]	105%
5 0.28 mM NaLac	6	SSC	66.9 ± 2.1	22.2 ± .7	4.0%	10.0 ± 1.0 [31%]	8.7 ± .9	29.0% [0.24]	93%
		SC	34.4 ± 2.4	7.8 ± .5	2.1%	14.6 ± 1.1 [48%]	8.6 ± .7	40.0% [0.35]	99%
6 0.28 mM NaLac, (O_2 Off) [i]	4	SSC	66.1 ± 3.3	21.9 ± 1.1	4.0%	0.6 ± .9 [0%]	0.6 ± .7	20.6% [0.17]	88%
		SC	27.8 ± 2.6	6.3 ± .6	1.7%	0.5 ± .5 [0%]	0.3 ± .3	14.0% [0.12]	100%
7 0.28 mM NaLac	5	SSC	69.3 ± 1.7	23.0 ± .6	4.2%	11.6 ± 2.5 [40%]	10.0 ± 2.2	35.0% [0.29]	96%
		SC	23.6 ± 1.3	5.3 ± .3	1.4%	13.6 ± 1.6 [52%]	8.0 ± 1.0	37.7% [0.34]	86%

a. Based on undiluted concentrations in column anaerobic zone
b. Based on diluted concentrations in column aerobic zone
c. Results presented as average ±1 SD
d. Calculated as Degradation ÷ HRT of respective column and zone
e. CB reductive dechlorination e- equivalent as a fraction of influent NaLac e- equivalent, assuming 2 e- per dechlorination and 12 e- per NaLac oxidized
f. CB oxidation e- equivalent as a % of available O_2 assuming 24 (TCB), 26 (DCB), and 28 (MCB) e- per CB oxidized and 4 e- per O_2 reduced
g. mg of equivalent influent 1,2,4-TCB degraded as a fraction of mg DO available in aerobic zone
h. Measured Cl⁻ change ÷ Apparent Cl loss (from CB measurements)
i. Though O_2 was purged from feed, some oxygen detected at column entrance resulting in low 0.7 mg/L DO at OAI
* Effluent completely dechlorinated to MCB, indicating CB limitation

2.4   Results and Discussion

2.4.1   Sand and Sediment Column (SSC) Activity

SSC was designed to reflect conditions similar to the SCD wetland, using sterilized sediment from SCD. Due to the high silt and clay content, sediment was mixed with filter sand to facilitate more uniform flow characteristics. This column was directly inoculated with enrichments into each redox zone to initially stratify microbial communities along the OAI.

After inoculation at Day 0, both anaerobic and aerobic biodegradation pathways were immediately apparent in SSC (Figure 2.2). At the initial 0.28 mM NaLac dose (Phase 1), degradation activity stabilized to approximately 44.2 ± 13.6 µM reductive dechlorination and 13.1 ± 2.7µM aerobic degradation (47% removal), resulting in an effluent mix of DCB and MCB congeners. Vertical sampling showed that degradation pathways were spatially separated along the OAI, with reductive dechlorination exclusive to the anaerobic zone and aerobic degradation to the aerobic zone of the column (Figure 2.3a). Sulfate transformation also reflected the two distinct redox zones. In the anaerobic zone sulfate reduction co-occurred with CB dechlorination, and in the aerobic zone re-oxidation of reduced sulfur co-occurred with CB oxidation (Figure 2.3a).

Increasing the NaLac amendment to 1.4 mM (Phase 2) caused a rapid enhancement of reductive dechlorination, more than doubling the extent of reductive dechlorination rate to 94.4 ± 6.2 µM. However, the extent of aerobic degradation decreased nearly tenfold to 1.9 ± 2.0 µM (5% removal); nearly all 1,2,4-TCB mass entering the system was conserved as reduced MCB (Figure 2.3b). This five-fold increase in NaLac increased the share of fermentation side-reactions occurring in the column. The amount of electron donor

theoretically used for reductive dechlorination decreased from 2.7% in Phase 1 to 1.1% in Phase 2, leaving the majority of the 16.6 millielectron equivalent (meq) NaLac to be used for acetate and propionate fermentation, which themselves are reduced electron donors. In the aerobic zone, only 0.81 meq O_2 was available as an electron acceptor to degrade approximately 1.1 meq MCB and the large fraction of excess fermented organic acids (approximately 9 meq). Under this high organic carbon load, residual organic acids likely outcompeted aerobic CB degradation for oxygen at the interface and led to inhibition.
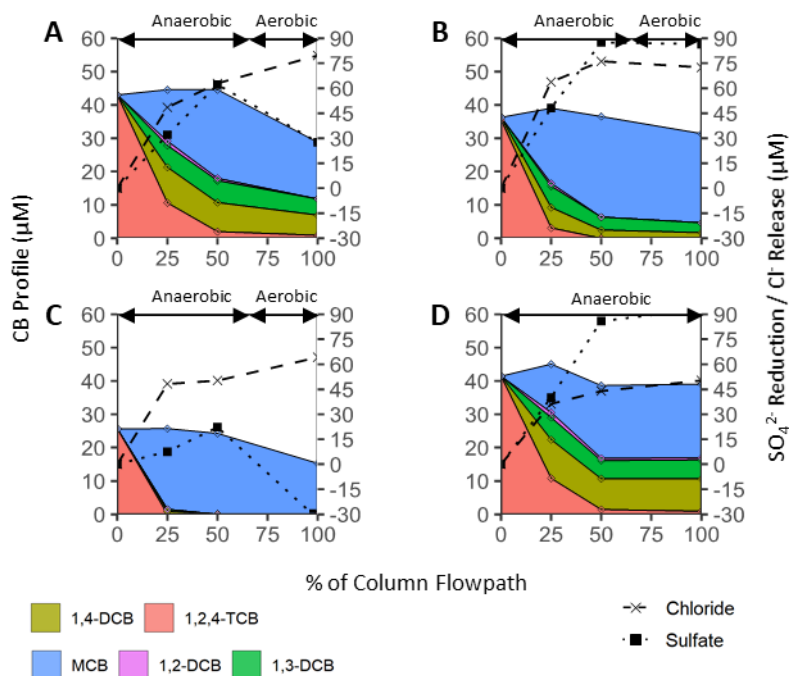
Figure 2.3. Representative SSC vertical CB biodegradation profiles during each input condition. (A) 0.28 mM NaLac; (B) 1.4 mM NaLac; (C) 0.14 mM NaLac; (D) 0.28 mM NaLac with aerobic zone anoxia. Stacked areas represent total molar CB concentrations (left axis). Points connected by lines for visual aid represent net degradative chloride release and sulfate reduction (right axis). Concentrations at the 100% port were multiplied by the side-stream dilution factor to correctly visualize mass balance of chemical processes, resulting in an exaggeration of true effluent concentrations.

After 26 days under high dosage, influent NaLac was decreased to 0.14 mM in Phase 3. Anaerobic reductive dechlorination activity decreased but remained stable at 46.3±3.7 µM, with all influent 1,2,4-TCB reduced to MCB (Figure 2.3c). Because nearly complete dechlorination occurred here, 1,2,4-TCB influent was limiting in this phase, and

the estimated dechlorination activity was likely an underestimate of the total dechlorination capacity (Table 2.2). Nevertheless, high reductive dechlorination persisted through the entire 75-day operating period of Phase 3 at a rate equal to that of Phase 1, suggesting that the dechlorinating population acclimated over time to better utilize electron donor. Aerobic degradation slowly recovered over a 30-day period before stabilizing at 5.7±1.7 µM (31% removal) (Figure 2.2c). This was less than half the extent observed in Phase 1, which was unexpected since less NaLac would be expected to lower the amount of residual O_2 demand in the aerobic zone. The decreased aerobic degradation with decreased electron donor in Phase 3 may have been related to a change in the sulfur oxidation dynamics in the column. Sulfate reduction was suppressed in the anaerobic zone and effluent sulfate concentrations were greater than influent concentrations (Figure 2.3c), suggesting transient oxidation of previously immobilized reduced sulfide species. Although sulfides weren't measured directly here, the column matrix darkened over time, a visual indicator that a sink of precipitated sulfide compounds such as iron sulfide were retained throughout the column. Conservatively, the difference in average sulfate change in Phase 3 (+28 µM) compared to Phase 1 (-12 µM) (Table A.1) would indicate an increased theoretical oxygen demand of 0.32 meq (assuming S^- oxidized to SO_4^{2-}), or 37.6% of total available oxygen (SI Calculation S2m). These results highlight that even in low sulfate systems, accumulation of reduced sulfur over time can exert substantial oxygen demand on aerobic pathways downgradient as it is re-oxidized to sulfate.

Re-amending 1.4 mM (Phase 4) and 0.28 mM NaLac (Phase 5) had similar effects seen previously in Phase 2 and 1 respectively (Table 2.2), indicating changes in organic carbon dosage did not permanently disrupt degradation functionality. In Phase 6, O_2 was

purged from the side-stream so the entire column was made anaerobic. No change in reductive dechlorination was observed. However, aerobic CB degradation and sulfide oxidation ceased (Figure 2.2c), with a vertical profile nearly identical to the high 1.4 mM NaLac inputs (Figure 2.3d). This phase provided definitive evidence that complete degradation was an oxygen-dependent process, and not an anaerobic process or artifact of dilution. The oxygen stream was restored to the column in Phase 7 after seven days of anoxia. Aerobic CB degradation was re-established within the first day of sampling and stabilized at levels observed prior to anoxia (Figure 2.2c).

2.4.2   Sand Column (SC) Activity

SC was designed to test the microbial colonization and biodegradation potential on an inert matrix without the influence of site sediment. Like SSC, degradation activity was split across the OAI (Figure 2.4a). Unlike SSC, this split was definitively a result of differences in redox zone as opposed to possibly being a result of the split inoculation. Despite these differences, overall degradation patterns in SC in response to NaLac dose were similar to SSC (Figure 2.2). In general, the extent of aerobic degradation was higher in SC than SSC. Anaerobic sulfate reduction and aerobic sulfur oxidation were both observed (Figure 2.4) across the OAI; however, the degree of sulfate reduction was consistently lower in SC compared to SSC (Table A.1). Anaerobic reductive dechlorination activity was lower in SC compared to SSC and showed a comparatively lower electron donor utilization, especially at 0.14 and 0.28 mM NaLac doses (Table 2.2). These differences may be attributed to the absence of sediment in SC compared to SSC; sediment has been shown to provide a superior surface for microbial attachment to sand [28] and may have contained additional unquantified bioavailable reductants and nutrients favoring

45

reductive processes [29]. However, the columns also had differing inoculation schemes, which could have played another important but confounding role in establishing microbial functionality (discussed in Section 3.4).

Activity during the 0.14 mM NaLac input in Phase 3 was notable. After previous inhibition at 1.4 mM, aerobic degradation was immediately re-established, more quickly than in SSC (Figure 2.2c). For the first 20 days of this phase (78 pore volumes), reductive dechlorination activity persisted to a similar extent as SSC (Figure 2.2b). Afterwards, dechlorination activity as well as sulfate reduction ceased (Figure 2.4c), indicating that the 0.14 mM NaLac dose was inadequate to support long-term degradation in the sand matrix. Dechlorination activity may have been temporarily sustained by a slow decay of excess attached biomass developed during the previous high NaLac dose, which has been demonstrated by others previously [30, 31]. Despite the lack of measured anaerobic activity, TCB degradation and sulfur oxidation were still observed in the aerobic zone (Figure 2.4c). As with SSC, effluent sulfate concentrations also increased in this phase, indicating a transient oxidation of retained sulfides that may have outcompeted aerobic CB degradation for DO (Table 2.2).

After re-amending SC with 1.4 mM NaLac in Phase 5, reductive dechlorination activity in SC resumed (Figure 2.2b). Degradation activity followed similar trends in Phases 5-8 as described above for SSC (Figure 2.2). There was, however, a gradual but significant decrease in reductive dechlorination activity between Phases 5-6 (p =.0031, Welch's 1-tailed t-test) and 6-7 (p=.020) through the end of the experiment (Figure 2.2b). This would suggest that dechlorination in SC may not have been sustainable at low NaLac doses without periodic electron donor spikes to re-stimulate activity.
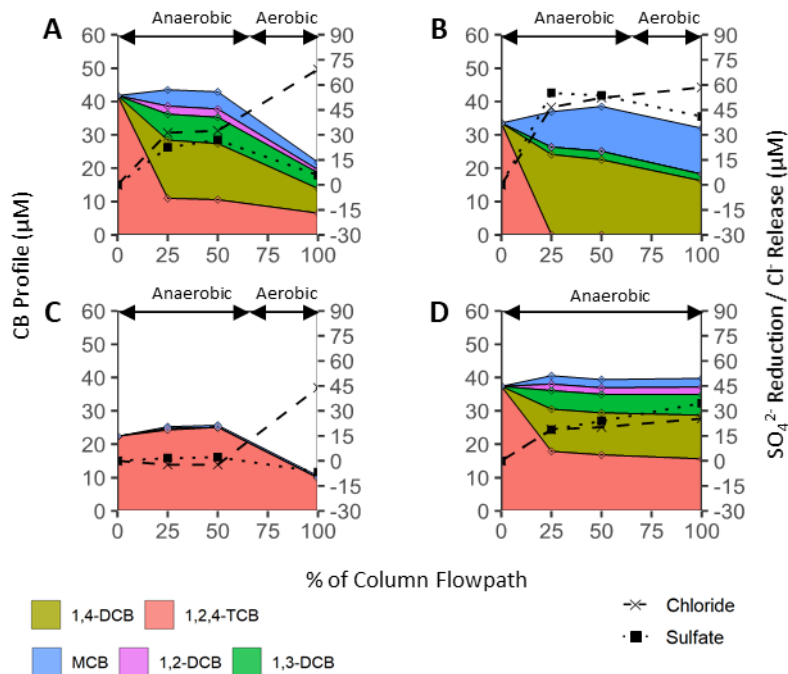
Figure 2.4. Representative SC vertical CB biodegradation profiles during each input condition. (A) 0.28 mM NaLac; (B) 1.4 mM NaLac; (C) 0.14 mM NaLac with aerobic zone anoxia; (D) 0.28 mM NaLac with aerobic zone anoxia. Data presented in a similar manner to Figure 2.3.

In both columns, influent effluent media were circumneutral, but showed slight acidification through the column. Influent pH was 7.0-7.6 in SSC and 7.0-7.5 in SC, and effluent pH was 6.7-7.3 in SSC and 6.8-7.3 in SC. This can be attributed to proton release from dechlorination reactions and sulfide oxidation. DO was depleted below detection limits (<0.1 mg/L) in SSC effluent during all phases, evidence of near-complete oxygen utilization throughout the experiment. There was good mass balance between chloride release and CB transformations in SSC (81%-113%) and SC (86%-113%) except for Phase 1 for SC (50%; Table 2.2).

2.4.3   *Dynamics of Anaerobic and Aerobic Degradation*

Anaerobic reductive dechlorination of 1,2,4-TCB resulted in nearly stoichiometric increases of 1,3-DCB, 1,4-DCB, and MCB production while 1,2-DCB was only a minor daughter product (Figure 2.3, Figure A.2). Concentrations of benzene were not measured

47

above the CB detection limit, indicating dechlorination effectively stalled at MCB. Dechlorination activity in both columns was positively correlated with NaLac dose. The highest rates of dechlorination, at 1.4 mM NaLac, were estimated to be approximately 31.3 ± 2.0 µM/hr in SSC and 19.6 ± 1.2 µM/hr in SC. These rates were over an order of magnitude higher than TCB dechlorination rates reported from prior studies by others in column [32] and batch systems [27]. When dechlorination activity was present, electron donor utilization was low and decreased with increasing NaLac dose. Donor utilization varied from 0.6% at 1.4 mM to 5.8% at 0.14 mM, consistent with other reported values from lactate-amended dechlorinating column studies: 0.2% at 20 mM NaLac [33] and 6.5% at 0.68 mM NaLac [34].

Aerobic CB degradation was consistently highest at 0.28 mM NaLac, where effects of excess electron donor and competitive sulfur oxidation were minimal. Here, maximum observed aerobic degradation rates were 11.3 ± 2.3 µM/hr in SSC and $10.9\pm.3$ µM/hr in SC. These rates were nearly an order of magnitude lower than rates measured by Kurt et al. in a different column system simulating a sediment-water interface [16]; however oxygen limitation and upgradient reduction processes, which limited apparent rates here, were excluded in that study. Oxygen utilization for CB degradation varied from 0.04 mg TCB degraded per mg O_2 consumed at 1.4 mM to 0.58 mg TCB/mg O_2 at 0.28 mM NaLac. Complete summaries of CB degradation in each phase are presented in Table 2.2.

A key question this experiment addressed was what effect the coupling of anaerobic reductive dechlorination to aerobic degradation would have on overall CB degradation. Since complete anaerobic dechlorination and mineralization were not observed here, the only path to mineralization was through the aerobic pathway. Although MCB, DCBs, and

TCBs are all aerobically degradable, some bioremediation studies have found that lower CBs degraded at significantly faster rates than 1,2,4-TCB [35, 36]. This would suggest that an initial dechlorination step could enhance the overall rates and extents of aerobic mineralization.

In Phase 3 of this experiment, we observed two very different reductive dechlorination outcomes between columns. In SSC, nearly all CBs entering the aerobic zone were dechlorinated to MCB and 1,2- and 1,4-DCB (Figure 2.3c). In SC, no dechlorination occurred, leaving only 1,2,4-TCB (Figure 2.4c). In both cases, however, significant aerobic degradation occurred (Table 2.2). Additionally, in the vertical column profiles, it can be seen qualitatively that all CB congeners show a concentration decrease within the aerobic zone (Figure 2.3a, c; Figure 2.4a, c). This would imply that all CB congeners were subject to aerobic biodegradation.

To test this observation more rigorously, we compared the measured aerobic degradation of each congener to the change in relative abundance of that congener (Equation 2.3) across the aerobic zone at each vertical sample timepoint to determine whether certain congeners degraded at a greater extent compared to others (Figure A.3).

Equation 2.3

$$\% \text{ Change in Congenr } n \text{ Abundance} = \frac{n\text{CB}_{100}}{\Sigma\text{CBs}_{100}} - \frac{n\text{CB}_{50}}{\Sigma\text{CBs}_{50}}$$

On average, the change in any individual congener abundance was 2% or less (Table A.2). Between MCB, total DCBs, and 1,2,4-TCB there was no statistically significant change ($p > .05$) in congener distribution. Thus, there was no apparent preferential degradation based on degree of congener chlorination during aerobic degradation. There was a

significant preference for 1,2- and 1,4- DCB over 1,3- DCB ($p<.05$), however the small effect size (<2.8%), small samples size (n=37), and low amount of 1,2-DCB present adds uncertainty to these results (Table A.2). This is in agreement with previous work by Sander et al. [37] showing highly similar oxygen uptake and mineralization rates between MCB, DCBs, and 1,2,4-TCB with pure cultures of *Ralstonia* sp. strain PS12 and *Burkholderia* sp. strain PS14. There is no consensus in the literature on preferential degradation rates of 1-3 CBs, and degradation capacity has shown to be highly dependent on factors such as geochemical conditions, substrate acclimation, and microbial strain [35, 37-39]. Although not explicitly tested, our experimental results demonstrated 1,2,4-TCB and all reduced daughter congeners seemingly degraded at a similar rate aerobically. Further, there was no significant correlation between the degree of CB chlorination and the extent of aerobic degradation from effluent column samples (Figure A.4). Based on these results, initial reductive dechlorination of 1,2,4-TCB did not appear to benefit subsequent aerobic degradation.

Even if aerobic CB degradation is congener-independent for lower CBs, reductive dechlorination of lower CBs may have potential benefits for site remediation, provided dechlorination stalls at MCB. Having less sorption potential to sediments and greater aqueous solubility, less chlorinated CBs are more environmental mobile and may be flushed from the subsurface more quickly than more chlorinated CBs. Yang and McCarty, for example, demonstrated a 3-fold increase in PCE DNAPL dissolution as a result of reductive dechlorination [40]. Limited ecotoxicity studies have found that MCB is significantly less toxic than DCBs and TCB to *Pseudomonas fluorescens* [41], *Daphnia*, and salmon [42]. However, this detoxification effect must be weighed against potentially

higher dissolved concentrations of the dechlorinated congeners mobilized in the aqueous phase.

2.4.4 Microbial Community Analysis

2.4.4.1 Inocula Composition

Sequenced SSC inocula revealed distinct mixed communities. The anaerobic, WBC-2-derived subculture consisted primarily of classes containing obligate anaerobes: Clostridia (50.5% relative abundance), Bacteroidia (14.2%), Methanomicrobia (8.3%), Methanobacteria (7.6%), Thermotogaea (3.5%), and Anaerolineae (3.1%) (Figure 2.5a). Among the community, three known OHRB genera [43, 44] were identified: *Dehalobacter* (1.3%), *Dehalogenimonas* (0.2%), and *Dehalococcoides* (0.05%). There was a substantial shift in abundances of OHRB from the sequenced parent WBC-2 culture, which consisted primarily of *Dehalococcoides* (8.8%) and *Dehalogenimonas* (8.7%), but only a small fraction of *Dehalobacter* (0.012%). This suggests 1,2,4-TCB dechlorination favored *Dehalobacter* enrichment over other OHRB; a similar shift was observed by others in chloroethene enrichment KB-1 when substrate was changed to 1,2,4-TCB [27]. The aerobic inoculum was dominated by Betaproteobacteria (89.3%) and Saprospirae (10.1%). Two genera associated with aerobic CB degradation [45] were highly abundant: *Pandoraea* (19.5%) and *Burkholderia* (7.2%), both in the Burkholderiaceae family. Full class- and genus-level profiles are presented in Figure A.5 and Figure A.6a.

2.4.4.2   Community Structure Across Column Interfaces
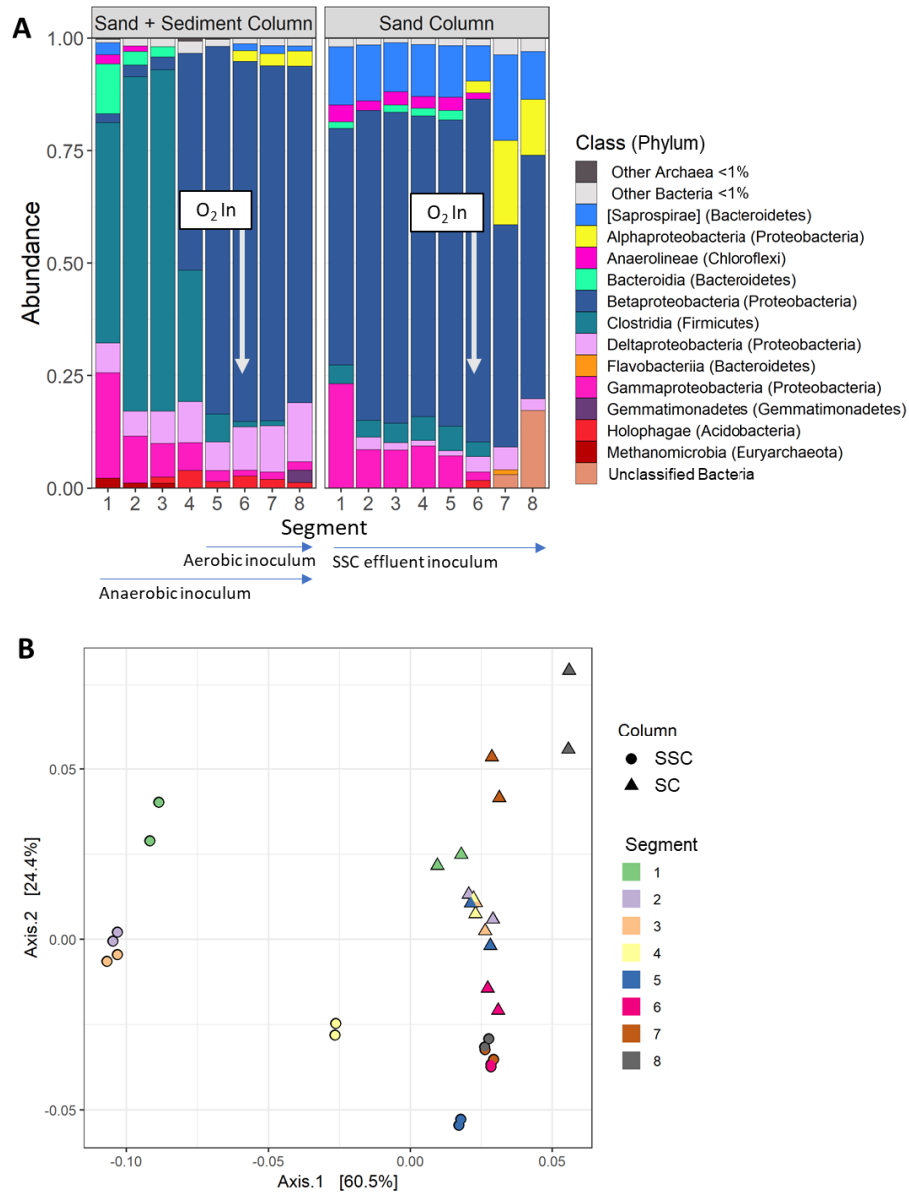
Figure 2.5. Microbial community structure of experimental columns. (A) Class-level microbial community profiles in column biofilm segments. Composition expressed as relative abundance based on 16S rRNA amplicon sequences. Bacteria and Archaea classes with <1% representation aggregated as "Other". [Bracketed groups] were not identified at class level and were identified at the next closest taxonomic level. (B) Principal coordinate analysis of beta diversity within experimental columns based on weighted Unifrac distances. The first two axes (displayed) explain 84.9% of sample distances.

Segmentation and analysis of the microbial communities found in each column matrix provided a unique cross-section of the active CB-degrading communities across the OAI. The class-level composition of each column at the end of the experiment is presented

in Figure 2.5a. Segments 1-4 of SSC, inoculated exclusively with the anaerobic WBC-2 subculture, contained high abundances of Clostridia with lower abundances of Bacteroidia, Gammaproteobacteria, Deltaproteobacteria, and others present. Clostridia, which was the largest class in the inoculum culture, persisted as the dominant class within these sections. Li et al. (2013) also found considerable abundances of both Clostridia (32%) and Deltaproteobacteria (33%) in the bottom of a lactate-fed pentachlorophenol (PCP) dechlorinating column inoculated with an anaerobic Clostridia-dominated enrichment [33]. Segments 5-8 of SSC, inoculated first with the anaerobic inoculum and then the aerobic inoculum, consisted primarily of Betaproteobacteria, which also dominated the aerobic inoculum. Interestingly, SC, which was exposed to the entire effluent of SSC, was dominated by Betaproteobacteria throughout the entire column length and more closely resembled the aerobic SSC inoculum than the anaerobic. In the transition from the anaerobic zone (segments 1-5) to aerobic zone (6-8), both columns showed decreasing Clostridia, Gammaproteobacteria, Bacteroidia, and Anaerolineae abundances and increasing Alphaproteobacteria abundances (Figure 2.5a).

A principal coordinate analysis of each segment illustrated structural changes within columns (Figure 2.5b). SSC experienced significant clustering between segments 1-4 and 5-8 (p=.0006, R^2=.28, Adonis PERMANOVA analysis, 10,000 permutations), reflective of its split inoculation. Segments 6-8 were also significantly different from segment 5 (p=.036, R^2=.53), indicating a sharp community shift across the OAI between segments 5-6. In contrast, SC did not have any statistically significant shifts between column segments. Qualitatively, SC segments 1-6 were closely clustered on the ordination plot while segment 7 and 8 samples diverged from this group (Figure 2.5b). The scatter

between segment 7 and 8 replicates suggests these communities were more spatially heterogeneous than those in segments 1-6. These observations suggest a more gradual community shift occurred along the entire length of the SC aerobic zone compared to that of SSC.

In SSC, total 16S counts were fairly evenly distributed along column length. Abundances spiked at segments 1 and 6, corresponding to influent sources of NaLac and O_2 respectively, before diminishing in subsequent samples (Figure 2.6a). In SC, total 16S counts were greatest at segment 1 before dropping drastically (Figure 2.6b). After the addition of O_2 in the aerobic zone, concentrations gradually increased through segment 8. These distributions were also reflected in total DNA and bulk protein concentrations measured (Figure A.6). The profiles suggest electron donor was more quickly depleted in the SC anaerobic zone than SSC, while oxygen was more immediately depleted in the SSC aerobic zone than SC.

2.4.4.3 Distribution of Functional Genera

Over 139 and 107 unique genera were identified in the SSC and SC column segments, respectively. *Dehalobacter, Clostridium, Pseudomonas, Thiobacillus, Rhodocyclus, Zoogloea,* and *Geobacter* were all found in at least 10% abundance in SSC segments. *Sediminibacterium, Comamonas, Rhodocyclus, Pseudomonas, Thiobacillus, Zoogloea*, an unspecified Sphingomonadaceae genus, and an unspecified Comamonadaceae genus were at least 10% abundant in SC. A full column genus profile can be found in Figure A.7. At the genus-level, the functional potential of most of the dominant organisms was not apparent. Some genera such as *Pseudomonas* and *Geobacter* are metabolic generalists known to cycle a wide range of electron donors and acceptors;

however, functionality can be highly strain- and environment- dependent, beyond the resolution of short-read 16S sequencing [46, 47]. However, we were able to identify several genera of interest that were at least 1% abundant and are broadly implicated in either CB degradation or specific redox cycling.

Dehalobacter (Clostridia) was the only OHRB identified in either column and was the presumed CB dechlorinator. Sulfate reducing bacteria (SRB) *Desulfosporosinus* (Clostridia) [48] and methanogen *Methanosarcina* (Methanomicrobia) [49] were also identified. All three of these obligate anaerobes were much more abundant in SSC compared to SC. Chemolithotrophic sulfur-oxidizer *Thiobacillus* (Betaproteobacteria) [50] was prominently abundant in both columns. Several Proteobacteria groups implicated as aerobic CB degraders by others were also abundant in both columns, including *Pandoraea* (Betaproteobacteria), *Xanthobacter* (Alphaproteobacteria), and an unspecified Sphingomonadaceae genus (Alphaproteobacteria) [7, 45]. Except for *Dehalobacter* and *Pandoraea*, the described functional genera were present in inoculum cultures at abundances less than 0.04%, indicating that enrichment and species succession occurred along the column biofilm during operation.

The absolute abundances of potentially functionally-relevant genera along the vertical column profiles were estimated by multiplying total 16S copy numbers from qPCR by relative abundances from sequencing (Figure 2.6a, b). Although 16S copy numbers vary taxonomically and PCR amplification biases exist [51], we considered the log-scale differences in copy number satisfactory to observe population trends between segments and genera.
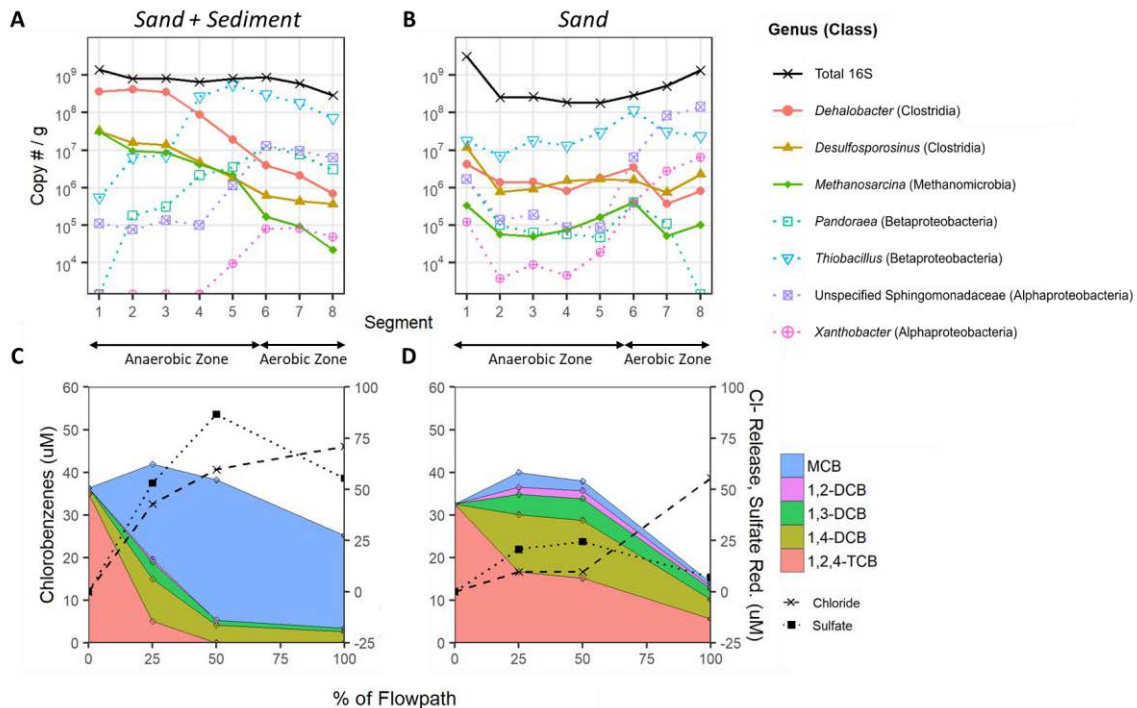
Figure 2.6. Top: Vertical biofilm profiles of functional genera and total microbial 16S copy number in (A) SSC and (B) SC. Bottom: Vertical porewater profiles of CB biodegradation, cumulative chloride release, and net sulfate reduction in (C) SSC and (D) SC. All samples taken at Day 295.

In SSC, all three identified functional anaerobes were most highly abundant in segments 1-3 of SSC before a log-scale decrease across the OAI. *Dehalobacter* was dominant genus in the anaerobic zone, nearly an order of magnitude higher than *Desulfosporosinus* and *Methanosarcina*. In segment 4, *Thiobacillus* succeeded *Dehalobacter* as the dominant genus through the end of the column. Potential aerobic degraders *Pandoraea* and *Xanthobacter* increased 2-log to become highly abundant in segment 5, but were over an order of magnitude lower than *Thiobacillus*. Measured redox processes at the time of sampling (Figure 2.6c) aligned very well with peak functional organism abundances (Figure 2.6a). The highest reductive dechlorination and sulfate reduction activity occurred in the first 25% of the column length, aligning with the highest abundances of *Dehalobacter* and *Desulfosporosinus* abundances in segments 1-3. Although methane concentrations were not measured, the presence of high

56

Methanosarcina abundances suggests methanogenesis was another prevalent anaerobic pathway in this column. Across the OAI, sulfur oxidation and CB oxidation (Figure 2.6c) co-occurred with peak abundances of the aerobic organisms in segments 5-8 (Figure 2.6a).

In SC, the previously identified functional anaerobes were over 2-log less abundant than total 16S copy numbers and thus accounted for a small fraction of the total community (Figure 2.6b). These organisms' abundance quickly dropped after segment 1, suggesting the majority of reduction processes occurred close to the column influent. Indeed, nearly all reductive dechlorination and sulfate reduction occurred within the first 25% of column length (Figure 2.6b). Interestingly, elevated abundances of *Thiobacillus* and Sphingomonadaceae were also present in segment 1. This could be a result of ongoing sulfur oxidization coupled to iron reduction [50] or potentially minor oxygen contamination since most Sphingomonadaceae species are obligate aerobes. Abundances were low and stable through the remainder of the anaerobic zone. Within the aerobic zone, *Thiobacillus* populations peaked at segment 6, while *Xanthobacter* and Sphingomonadaceae abundances continued to increase through segment 8. While peak abundances generally aligned with the observed chemical oxidations in the aerobic zone (Figure 2.6d), the resolution of chemical sampling was too coarse to determine whether greater CB degradation occurred at the end of the aerobic zone.

Dehalobacter enrichment in the bottom segments of SSC was unexpectedly high (26.2-50.9%) compared to the lower (<1.2%) abundances in SC (Figure 2.6a-b). In comparison, *Dehalobacter* abundances in CB-degrading cultures have been reported from less than 0.1% in site sediment microcosms [10] up to approximately 25% in sequentially enriched fed-batch microcosms [27]. Though limited column data is available, Li et al.

(2013) reported up to 2.4% biofilm enrichment in a PCP-dechlorinating column packed with sediment and glass [33]. We posit that the combination of shorter HRT and addition of sediment may have selectively enriched *Dehalobacter* in SSC. Decreasing the HRT in a chloroethene-dechlorinating CSTR was found to decrease H_2 concentrations, making OHRB metabolism more thermodynamically favorable than that of acetogens, methanogens, and SRB [52]. Cápiro et al. [28] found 2-fold lower interaction energy barriers and greater attachment rates for PCE dechlorinators to soil compared to fine sand. Although the causes of differences in SSC and SC cannot be determined directly from this study, the order of magnitude difference in population helps to explain the differences in activity observed throughout the time-series. SSC consistently demonstrated greater degrees of CB dechlorination (Figure 2.2b) and sulfate reduction (Table A.1) than SC, corresponding to more highly enriched *Dehalobacter* and *Desulfosporosinus*. Conversely, the extent of aerobic CB degradation was generally greater in SC (Figure 2.2c), which corresponded to the Sphingomonadaceae genus being more highly enriched in SC than any potential aerobic degraders in SSC.

Few other studies, to our knowledge, have carefully profiled the attached microbial communities in stratified systems actively degrading halogenated organic compounds [33, 53]. Liquid samples have more frequently been analyzed due to the ease of producing and collecting representative samples, however they do not always correlate well with total bacteria abundances in the subsurface [28]. In our experiment, column porewater at the time of sampling was dominated by *Pseudomonas* in SSC (81.1%) and *Comamonas* in SC (81.5%) (Figure A.7a). Based on relative abundance, dominant and functionally relevant genera from the column matrices were underrepresented in porewater by nearly a 3-log

difference, and some organisms were not even detected in the porewater (Table 2.2). Notably, putative CB degraders *Dehalobacter* and Sphingomonadaceae were underrepresented by 2.4-log in SSC and 2.8-log in SC respectively (Table 2.2). Additionally, solid-phase sampling captured much of the spatial nuances across the OAI that would have been difficult to detect solely with porewater sampling.

Profiles here provided a detailed description of changing CB-degrading community and key functional populations across an OAI. They also demonstrated a simple method to potentially interrogate other functional communities in steady-state at OAIs as a compliment to chemical data. In this experiment, the functional roles of organisms classified at genus and higher taxonomic levels often could not be determined. Most redox functionality is distributed among wide groups of taxonomically-unrelated organisms, with OHRB and methanogens notable exceptions [49, 54]. As a result, much of this taxonomically-rich dataset is uninterpretable from a functional perspective *a priori*. Even if functional potential of organisms is known with certainty, cell counts alone have been found to be poor quantitative predictors of biogeochemical fluxes in a system; intrinsic cellular regulation and environmental factors can have an even greater influence on biochemical activity [55]. As the cost of sequencing continues to decrease, employing a combination of shotgun metagenomics to qualitatively identify and annotate conserved functional genes and qPCR to quantitate them may be a more effective strategy to assess community function and quantitatively predict contaminant degradation.

2.4.5 *Practical Implications*

This proof-of-concept study demonstrated substantial and sustained degradation of dissolved CBs at OAIs in both site-relevant sediment (SSC) and a clean sand bed (SC)

matrices. Our results showed a range of potential degradation outcomes that could be reasonably expected at shallow contaminated sites contaminated with concentrations of CBs in the micromolar range. Under lower NaLac concentrations of 0.14-0.28 mM (equivalent to 5-10 mg/L DOC), substantial aerobic degradation of up to 3.5 mg/L 1,2,4-TCB was observed, implying a treatment capacity of 1.1 g/m^2-d (based on the experimental column cross-sectional area). However, under a higher NaLac concentration of 1.4 mM (50 mg/L DOC), aerobic degradation activity was inhibited, instead favoring substantial reductive dechlorination to DCBs and MCBs. This narrow window in which DOC dose expended available DO shows that aerobic degradation may not be viable at sites with modest concentrations of dissolved or sediment-bound organic carbon. Atashgahi et al. [56] found similar effects in hyporheic-zone sediments, where TOC concentrations as low as 7.3 mg/g inhibited aerobic degradation and facilitate reductive dechlorination in an aerobic environment. Additionally, the DO supplied to the columns (7.0 mg/L) approached the best-case air-saturated concentrations that could be expected in naturally aerated porewater (9.1 mg/L at 20 °C). Based on the maximum observed oxygen utilization in this experiment (0.58 mg TCB/mg O_2), it is apparent that natural aerobic degradation alone may not be a viable for remediation of sites with porewater CB concentrations greater than several mg/L.

In areas with high organic carbon and/or CB flux, alternative strategies should be considered to manage contamination. Wetland plants have been shown to significantly enhance aerobic CB degradation in constructed wetland studies, increasing oxygen flux through root zone oxygenation and enhanced diurnal water table fluctuation [57, 58]. Though they were not considered in this model, plants may already be prevalent at sites –

especially wetlands; additional planting could potentially aerate previously anoxic sediments. Sediment amendment with activated carbon has proven an effective means to immobilize hydrophobic organic contaminants and facilitate slow aerobic degradation over time, effectively stabilizing differences in oxygen supply and demand [59-61]. Additionally, amendment of solid-phase oxygen-releasing compounds has also shown effectiveness in enhancing aerobic degradation [62, 63]. Finally, future consideration should be given to the possibility of complete anaerobic mineralization at sites. Our study demonstrated that OHRB such as *Dehalobacter* could be sustained in high abundances, especially in sediment matrices. Though dechlorination stalled at MCB, recent studies have begun to identify the factors and OHRB strains implicated in complete reduction to benzene and subsequent anaerobic mineralization [9-11, 27]. In the future, development of a highly efficient MCB-dechlorinating and benzene-oxidizing bioaugmentation culture may potentially facilitate oxygen-independent site treatment of CBs.

In this experiment, we assumed steady fluxes of contaminants and available oxygen, when these are often temporally and spatially heterogeneous in the field [20]. Degradation activity may therefore be quite transient. By cycling through long periods of alternative redox conditions, our study did demonstrate that temporary inhibition of degradation did not permanently alter the microbial community's capacity to degrade CBs in the long-term, even on inert sand matrices (SC). This positively reflects on the potential for bioaugmented degraders to persist in the OAI. However, since conditions were still controlled in the lab, validation in the field, especially in the presence of native microbial communities, is warranted. In conjunction with this study, a pilot-scale bioaugmented

61

reactive barrier is currently being tested at SCD to assess anaerobic and aerobic CB degradation *in situ*.

2.5   Conclusions

- The model dual-stream column system provided an effective method to carefully measure anaerobic-aerobic processes under stable conditions. Mass balance of CB degradation was approximately 86%-113% through the majority of the experiment.

- Anaerobic reductive dechlorination and aerobic degradation of 1,2,4-TCB occurred sequentially across the simulated OAI. Reductive dechlorination of 1,2,4-TCB stalled at MCB. CB destruction only occurred through aerobic degradation, which occurred for 1,2,4-TCB and all daughter DCB and MCB daughter products. Initial reductive dechlorination did not appear to enhance subsequent aerobic degradation rates in this system.

- Degradation outcomes varied with NaLac loading. Observations included reductive dechlorination inhibition at 0.14 mM NaLac, mixed degradation pathways at 0.28 mM, and aerobic degradation inhibition at 1.4 mM. This demonstrated a narrow and sensitive window in which degradation along the OAI was affected.

- Maximum observed aerobic CB removal was low – approximately 19 µM (3.5 mg/L) degraded with oxygen utilization of 0.58 mg TCB/mg O_2. This suggests natural conditions may not facilitate adequate CB mineralization in highly contaminated water when DO is limiting.

- SSC supported high levels of reductive dechlorination across all tested NaLac doses (0.14-1.4 mM). It also supported very high enrichment of OHRB *Dehalobacter* up to

4×10^8 copies/g (50.9% relative abundance), which likely thrived on the sediment matrix.

- Prominent functional genera (CB degraders, sulfur cyclers, methanogens) showed clear stratification across the OAI, correlating with observed CB degradation and sulfur cycling. Similar shifts in microbial communities occurred in both columns, despite having different initial community structures.

- Both CB degradation pathways were resilient and remained active through the end of the 295-day experiment. Similar outcomes occurred in different columns packed with site sediments (SSC) and an inert sand (SC). Results here show that substantial anaerobic and aerobic CB degradation could occur naturally in shallow site sediments under optimal conditions.

2.6 Acknowledgements

2.7 References

1. Feltens, R.; Mögel, I.; Röder-Stolinski, C.; Simon, J.-C.; Herberth, G.; Lehmann, I., Chlorobenzene induces oxidative stress in human lung epithelial cells in vitro. *Toxicology and Applied Pharmacology* **2010,** *242*, (1), 100-108.
2. Feenstra, S.; Mackay, D. M.; Cherry, J. A., A Method for Assessing Residual NAPL Based on Organic Chemical Concentrations in Soil Samples. *Groundwater Monitoring & Remediation* **1991,** *11*, (2), 128-136.
3. Agency for Toxic Substances Disease Registry Substance priority list (SPL) resource page. https://www.atsdr.cdc.gov/spl/resources/index.html (07-13),
4. Perelo, L. W., Review: In situ and bioremediation of organic pollutants in aquatic sediments. *Journal of Hazardous Materials* **2010,** *177*, 81-89.

5. National Research Council, *Alternatives for Managing the Nation's Complex Contaminated Groundwater Sites*. The National Academies Press: Washington, DC, 2013; p 422.

6. Boopathy, R., Factors limiting bioremediation technologies. *Bioresource Technology* **2000,** *74*, (1), 63-67.

7. Field, J. A.; Sierra-Alvarez, R., Microbial degradation of chlorinated benzenes. *Biodegradation* **2007,** *19*, 463-480.

8. Nijenhuis, I.; Stelzer, N.; Kästner, M.; Richnow, H.-H., Sensitive Detection of Anaerobic Monochlorobenzene Degradation Using Stable Isotope Tracers. *Environmental Science & Technology* **2007,** *41*, (11), 3836-3842.

9. Liang, X.; Devine, C. E.; Nelson, J.; Sherwood Lollar, B.; Zinder, S.; Edwards, E. A., Anaerobic Conversion of Chlorobenzene and Benzene to CH4 and CO2 in Bioaugmented Microcosms. *Environmental Science & Technology* **2013,** *47*, 2378-2385.

10. Qiao, W.; Luo, F.; Lomheim, L.; Mack, E. E.; Ye, S.; Wu, J.; Edwards, E. A., Natural Attenuation and Anaerobic Benzene Detoxification Processes at a Chlorobenzene-Contaminated Industrial Site Inferred from Field Investigations and Microcosm Studies. *Environmental Science & Technology* **2017**.

11. Fung, J. M.; Weisenstein, B. P.; Mack, E. E.; Vidumsky, J. E.; Ei, T. A.; Zinder, S. H., Reductive Dehalogenation of Dichlorobenzenes and Monochlorobenzene to Benzene in Microcosms. *Environmental Science & Technology* **2009,** *43*, (7), 2302-2307.

12. Brune, A.; Frenzel, P.; Cypionka, H., Life at the oxic-anoxic interface: microbial activities and adaptations. *FEMS Microbiol Rev* **2000,** *24*, (5), 691-710.

13. Brunke, M.; Gonser, T. O. M., The ecological significance of exchange processes between rivers and groundwater. *Freshwater Biology* **1997,** *37*, (1), 1-33.

14. Braeckevelt, M.; Rokadia, H.; Imfeld, G.; Stelzer, N.; Paschke, H.; Kuschk, P.; Kästner, M.; Richnow, H.-H.; Weber, S., Assessment of in situ biodegradation of monochlorobenzene in contaminated groundwater treated in a constructed wetland. *Environmental Pollution* **2007,** *148*, (2), 428-437.

15. Atashgahi, S.; Maphosa, F.; Dogan, E.; Smidt, H.; Springael, D.; Dejonghe, W., Small-scale oxygen distribution determines the vinyl chloride biodegradation pathway in surficial sediments of riverbed hyporheic zones. *FEMS Microbiol Ecol* **2013,** *84*, (1), 133-42.

16. Kurt, Z.; Shin, K.; Spain, J. C., Biodegradation of Chlorobenzene and Nitrobenzene at Interfaces between Sediment and Water. *Environmental Science & Technology* **2012,** *46*, 11829-11835.

17. Gossett, J. M., Sustained Aerobic Oxidation of Vinyl Chloride at Low Oxygen Concentrations. *Environmental Science & Technology* **2010,** *44*, (4), 1405-1411.

18. Burns, M.; Sublette, K. L.; Sobieraj, J.; Ogles, D.; Koenigsberg, S., Concurrent and Complete Anaerobic Reduction and Microaerophilic Degradation of Mono-, Di-, and Trichlorobenzenes. *Remediation Journal* **2013,** *23*, (3), 37-53.

19. US EPA *Amendment No. 2 to the 1995 Record of Decision For The Standard Chlorine of Delaware Inc. Superfund Site Operable Unit Two*; US Environmental Protection Agency: February 24, 2016, 2016.

20. Lorah, M. M.; Walker, C. W.; Baker, A. C.; Teunis, J. A.; Majcher, E. H.; Brayton, M. J.; Raffensperger, J. P.; Cozzarelli, I. M. *Hydrogeologic characterization and assessment of bioremediation of chlorinated benzenes and benzene in wetland areas, Standard Chlorine of Delaware, Inc. Superfund Site, New Castle County, Delaware, 2009-12*; 2328-0328; US Geological Survey: 2014.

21. Zeyer, J.; Kearney, P. C., Microbial degradation of para-chloroaniline as sole carbon and nitrogen source. *Pesticide Biochemistry and Physiology* **1982,** *17*, 215-223.

22. Fathepure, B. Z.; Vogel, T. M., Complete degradation of polychlorinated hydrocarbons by a two-stage biofilm reactor. *Applied and Environmental Microbiology* **1991,** *57*, 3418-3422.

23. Gutierrez, A.; Klinka, T.; Thiéry, D.; Buscarlet, E.; Binet, S.; Jozja, N.; Défarge, C.; Leclerc, B.; Fécamp, C.; Ahumada, Y.; Elsass, J., TRAC, a collaborative computer tool for tracer-test interpretation. *EPJ Web of Conferences* **2013,** *50*, 03002.

24. Preheim, S. P.; Olesen, S. W.; Spencer, S. J.; Materna, A.; Varadharajan, C.; Blackburn, M.; Friedman, J.; Rodríguez, J.; Hemond, H.; Alm, E. J., Surveys, simulation and single-cell assays relate function and phylogeny in a lake ecosystem. *Nature Microbiology* **2016,** *1*, 16130.

25. Bolyen, E.; Rideout, J. R.; Dillon, M. R.; Bokulich, N. A.; Abnet, C.; Al-Ghalith, G. A.; Alexander, H.; Alm, E. J.; Arumugam, M.; Asnicar, F.; Bai, Y.; Bisanz, J. E.; Bittinger, K.; Brejnrod, A.; Brislawn, C. J.; Brown, C. T.; Callahan, B. J.; Caraballo-Rodríguez, A. M.; Chase, J.; Cope, E.; Da Silva, R.; Dorrestein, P. C.; Douglas, G. M.; Durall, D. M.; Duvallet, C.; Edwardson, C. F.; Ernst, M.; Estaki, M.; Fouquier, J.; Gauglitz, J. M.; Gibson, D. L.; Gonzalez, A.; Gorlick, K.; Guo, J.; Hillmann, B.; Holmes, S.; Holste, H.; Huttenhower, C.; Huttley, G.; Janssen, S.; Jarmusch, A. K.; Jiang, L.; Kaehler, B.; Kang, K. B.; Keefe, C.

R.; Keim, P.; Kelley, S. T.; Knights, D.; Koester, I.; Kosciolek, T.; Kreps, J.; Langille, M. G. I.; Lee, J.; Ley, R.; Liu, Y.-X.; Loftfield, E.; Lozupone, C.; Maher, M.; Marotz, C.; Martin, B. D.; McDonald, D.; McIver, L. J.; Melnik, A. V.; Metcalf, J. L.; Morgan, S. C.; Morton, J.; Naimey, A. T.; Navas-Molina, J. A.; Nothias, L. F.; Orchanian, S. B.; Pearson, T.; Peoples, S. L.; Petras, D.; Preuss, M. L.; Pruesse, E.; Rasmussen, L. B.; Rivers, A.; Robeson, I. I. M. S.; Rosenthal, P.; Segata, N.; Shaffer, M.; Shiffer, A.; Sinha, R.; Song, S. J.; Spear, J. R.; Swafford, A. D.; Thompson, L. R.; Torres, P. J.; Trinh, P.; Tripathi, A.; Turnbaugh, P. J.; Ul-Hasan, S.; van der Hooft, J. J. J.; Vargas, F.; Vázquez-Baeza, Y.; Vogtmann, E.; von Hippel, M.; Walters, W.; Wan, Y.; Wang, M.; Warren, J.; Weber, K. C.; Williamson, C. H. D.; Willis, A. D.; Xu, Z. Z.; Zaneveld, J. R.; Zhang, Y.; Zhu, Q.; Knight, R.; Caporaso, J. G., QIIME 2: Reproducible, interactive, scalable, and extensible microbiome data science. *PeerJ Preprints* **2018,** *6*, e27295v2.

26. DeSantis, T. Z.; Hugenholtz, P.; Larsen, N.; Rojas, M.; Brodie, E. L.; Keller, K.; Huber, T.; Dalevi, D.; Hu, P.; Andersen, G. L., Greengenes, a Chimera-Checked 16S rRNA Gene Database and Workbench Compatible with ARB. *Applied and Environmental Microbiology* **2006,** *72*, (7), 5069-5072.

27. Puentes Jácome, L. A.; Edwards, E. A., A switch of chlorinated substrate causes emergence of a previously undetected native Dehalobacter population in an established Dehalococcoides-dominated chloroethene-dechlorinating enrichment culture. *FEMS Microbiology Ecology* **2017,** *93*, (12), fix141-fix141.

28. Cápiro, N. L.; Wang, Y.; Hatt, J. K.; Lebrón, C. A.; Pennell, K. D.; Löffler, F. E., Distribution of Organohalide-Respiring Bacteria between Solid and Aqueous Phases. *Environmental Science & Technology* **2014,** *48*, (18), 10878-10887.

29. Maillard, J.; Holliger, C., The Genus Dehalobacter. In *Organohalide-Respiring Bacteria*, Adrian, L.; Löffler, F. E., Eds. Springer Berlin Heidelberg: Berlin, Heidelberg, 2016; pp 153-171.

30. Sleep, B. E.; Brown, A. J.; Lollar, B. S., Long-term tetrachlorethene degradation sustained by endogenous cell decay. *Journal of Environmental Engineering and Science* **2005,** *4*, (1), 11-17.

31. Yang, Y.; McCarty, P. L., Biomass, Oleate, and Other Possible Substrates for Chloroethene Reductive Dehalogenation. *Bioremediation Journal* **2000,** *4*, (2), 125-133.

32. Bosma, T. N. P.; Meer, J. R. v. d.; Schraa, G.; Tros, M. E.; Zehnder, A. J. B., Reductive dechlorination of all trichloro- and dichlorobenzene isomers. *FEMS Microbiology Ecology* **1988,** *4*, 223-229.

33. Li, Z.; Inoue, Y.; Suzuki, D.; Ye, L.; Katayama, A., Long-Term Anaerobic Mineralization of Pentachlorophenol in a Continuous-Flow System Using Only Lactate as an External Nutrient. *Environmental Science & Technology* **2013,** *47*, 1534-1541.

34. Azizian, M. F.; Marshall, I. P. G.; Behrens, S.; Spormann, A. M.; Semprini, L., Comparison of lactate, formate, and propionate as hydrogen donors for the reductive dehalogenation of trichloroethene in a continuous-flow column. *Journal of Contaminant Hydrology* **2010,** *113*, (1–4), 77-92.

35. Elango, V.; Cashwell, J. M.; Bellotti, M. J.; Marotte, R.; Freedman, D. L., Bioremediation of Hexachlorocyclohexane Isomers, Chlorinated Benzenes, and Chlorinated Ethenes in Soil and Fractured Dolomite. *Bioremediation Journal* **2010,** *14*, 10-27.

36. Dermietzel, J.; Vieth, A., Chloroaromatics in groundwater: chances of bioremediation. *Environmental Geology* **2002,** *41*, (6), 683-689.

37. Sander, P.; Wittich, R. M.; Fortnagel, P.; Wilkes, H.; Francke, W., Degradation of 1,2,4-trichloro- and 1,2,4,5-tetrachlorobenzene by pseudomonas strains. *Applied and Environmental Microbiology* **1991,** *57*, 1430-1440.

38. Schraa, G.; Boone, M. L.; Jetten, M. S.; van Neerven, A. R.; Colberg, P. J.; Zehnder, A. J., Degradation of 1,4-dichlorobenzene by Alcaligenes sp. strain A175. *Applied and Environmental Microbiology* **1986,** *52*, (6), 1374-1381.

39. Naziruddin, M.; Grady, C. P. L.; Tabak, H. H., Determination of Biodegradation Kinetics of Volatile Organic Compounds through the Use of Respirometry. *Water Environment Research* **1995,** *67*, (2), 151-158.

40. Yang, Y.; McCarty, P. L., Comparison between Donor Substrates for Biologically Enhanced Tetrachloroethene DNAPL Dissolution. *Environmental Science & Technology* **2002,** *36*, (15), 3400-3404.

41. Boyd, E. M.; Meharg, A. A.; Wright, J.; Killham, K., Toxicity of chlorobenzenes to a lux-marked terrestrial bacterium, Pseudomonas fluorescens. *Environmental Toxicology and Chemistry* **1998,** *17*, (11), 2134-2140.

42. Calamari, D.; Galassi, S.; Setti, F.; Vighi, M., Toxicity of selected chlorobenzenes to aquatic organisms. *Chemosphere* **1983,** *12*, (2), 253-262.

43. Qiao, W.; Luo, F.; Lomheim, L.; Mack, E. E.; Ye, S.; Wu, J.; Edwards, E. A., A Dehalogenimonas Population Respires 1,2,4-Trichlorobenzene and Dichlorobenzenes. *Environmental Science & Technology* **2018,** *52*, (22), 13391-13398.

44. Nelson, J. L.; Fung, J. M.; Cadillo-Quiroz, H.; Cheng, X.; Zinder, S. H., A Role for Dehalobacter spp. in the Reductive Dehalogenation of Dichlorobenzenes and Monochlorobenzene. *Environmental Science & Technology* **2011,** *45*, (16), 6806-6813.

45. Jiang, X.-W.; Liu, H.; Xu, Y.; Wang, S.-J.; Leak, D. J.; Zhou, N.-Y., Genetic and biochemical analyses of chlorobenzene degradation gene clusters in Pandoraea sp. strain MCB032. *Archives of Microbiology* **2009,** *191*, 485-492.

46. Mahadevan, R.; Palsson, B. Ø.; Lovley, D. R., In situ to in silico and back: elucidating the physiology and ecology of Geobacter spp. using genome-scale modelling. *Nature Reviews Microbiology* **2010,** *9*, 39.

47. Dos Santos, V. A. P. M.; Heim, S.; Moore, E. R. B.; Strätz, M.; Timmis, K. N., Insights into the genomic basis of niche specificity of Pseudomonas putida KT2440. *Environmental Microbiology* **2004,** *6*, (12), 1264-1286.

48. Pester, M.; Brambilla, E.; Alazard, D.; Rattei, T.; Weinmaier, T.; Han, J.; Lucas, S.; Lapidus, A.; Cheng, J.-F.; Goodwin, L.; Pitluck, S.; Peters, L.; Ovchinnikova, G.; Teshima, H.; Detter, J. C.; Han, C. S.; Tapia, R.; Land, M. L.; Hauser, L.; Kyrpides, N. C.; Ivanova, N. N.; Pagani, I.; Huntmann, M.; Wei, C.-L.; Davenport, K. W.; Daligault, H.; Chain, P. S. G.; Chen, A.; Mavromatis, K.; Markowitz, V.; Szeto, E.; Mikhailova, N.; Pati, A.; Wagner, M.; Woyke, T.; Ollivier, B.; Klenk, H.-P.; Spring, S.; Loy, A., Complete genome sequences of Desulfosporosinus orientis DSM765T, Desulfosporosinus youngiae DSM17734T, Desulfosporosinus meridiei DSM13257T, and Desulfosporosinus acidiphilus DSM22704T. *Journal of bacteriology* **2012,** *194*, (22), 6300-6301.

49. De Vrieze, J.; Hennebel, T.; Boon, N.; Verstraete, W., Methanosarcina: The rediscovered methanogen for heavy duty biomethanation. *Bioresource Technology* **2012,** *112*, 1-9.

50. Kelly, D. P.; Wood, A. P., Reclassification of some species of Thiobacillus to the newly designated genera Acidithiobacillus gen. nov., Halothiobacillus gen. nov. and Thermithiobacillus gen. nov. *International Journal of Systematic and Evolutionary Microbiology* **2000,** *50*, (2), 511-516.

51. Větrovský, T.; Baldrian, P., The Variability of the 16S rRNA Gene in Bacterial Genomes and Its Consequences for Bacterial Community Analyses. *PLOS ONE* **2013,** *8*, (2), e57923.

52. Yang, Y.; McCarty, P. L., Competition for Hydrogen within a Chlorinated Solvent Dehalogenating Anaerobic Mixed Culture. *Environmental Science & Technology* **1998,** *32*, (22), 3591-3597.

53. Lima, G. d. P.; Sleep, B. E., The spatial distribution of eubacteria and archaea in sand–clay columns degrading carbon tetrachloride and methanol. *Journal of Contaminant Hydrology* **2007,** *94*, 34-48.

54. Jugder, B.-E.; Ertan, H.; Bohl, S.; Lee, M.; Marquis, C. P.; Manefield, M., Organohalide Respiring Bacteria and Reductive Dehalogenases: Key Tools in Organohalide Bioremediation. *Frontiers in Microbiology* **2016,** *7*.

55. Röling, W. F. M., Do microbial numbers count? Quantifying the regulation of biogeochemical fluxes by population size and cellular activity. *FEMS Microbiology Ecology* **2007,** *62*, (2), 202-210.

56. Atashgahi, S.; Lu, Y.; Ramiro-Garcia, J.; Peng, P.; Maphosa, F.; Sipkema, D.; Dejonghe, W.; Smidt, H.; Springael, D., Geochemical Parameters and Reductive Dechlorination Determine Aerobic Cometabolic vs Aerobic Metabolic Vinyl Chloride Biodegradation at Oxic/Anoxic Interface of Hyporheic Zones. *Environmental Science & Technology* **2017,** *51*, (3), 1626-1634.

57. Braeckevelt, M.; Mirschel, G.; Wiessner, A.; Rueckert, M.; Reiche, N.; Vogt, C.; Schultz, A.; Paschke, H.; Kuschk, P.; Kaestner, M., Treatment of chlorobenzene-contaminated groundwater in a pilot-scale constructed wetland. *Ecological Engineering* **2008,** *33*, (1), 45-53.

58. Braeckevelt, M.; Reiche, N.; Trapp, S.; Wiessner, A.; Paschke, H.; Kuschk, P.; Kaestner, M., Chlorobenzene removal efficiencies and removal processes in a pilot-scale constructed wetland treating contaminated groundwater. *Ecological Engineering* **2011,** *37*, 903-913.

59. Payne, R. B.; Ghosh, U.; May, H. D.; Marshall, C. W.; Sowers, K. R., Mesocosm Studies on the Efficacy of Bioamended Activated Carbon for Treating PCB-Impacted Sediment. *Environmental Science & Technology* **2017,** *51*, 10691-10699.

60. Song, Y.; Wang, F.; Kengara, F. O.; Bian, Y.; Yang, X.; Gu, C.; Ye, M.; Jiang, X., Does powder and granular activated carbon perform equally in immobilizing chlorobenzenes in soil? *Environmental Science: Processes & Impacts* **2015,** *17*, 74-80.

61. Tiehm, A.; Gozan, M.; Müller, A.; Schell, H.; Lorbeer, H.; Werner, P., Sequential anaerobic/aerobic biodegradation of chlorinated hydrocarbons in activated carbon barriers. *Water Science and Technology: Water Supply* **2002,** *2*, 51-58.

62. Kao, C. M.; Chen, S. C.; Wang, J. Y.; Chen, Y. L.; Lee, S. Z., Remediation of PCE-contaminated aquifer by an in situ two-layer biobarrier: laboratory batch and column studies. *Water Research* **2003,** *37*, (1), 27-38.

63. Lin, Q.; Chen, Y. X.; Plagentz, V.; Schafer, D.; Dahmke, A., ORC-GAC-Fe-0 system for the remediation of trichloroethylene and monochlorobenzene contaminated aquifer: 1. Adsorption and degradation. *Journal of Environmental Sciences* **2004,** *16*, 108-112.

Chapter 3.

Effects of Nitrate- and Sulfate-reducing Conditions on 1,2,4-Trichlorobenzene Biodegradation at Oxic-anoxic Interfaces[*]

3.1 Abstract

Biogeochemistry within and between contaminated sites can vary drastically due to natural conditions as well as human impacts to the environment. At shallow subsurface sites such as wetlands, aerobic gradients at oxic-anoxic interfaces (OAIs) can facilitate anaerobic and aerobic biodegradation of halogenated organic chemicals such as chlorobenzenes (CBs) in natural conditions and engineered treatments. However, other side-reactions and metabolic processes may limit or confound these processes. In this study, we investigated the effects of two common electron acceptors found in groundwater, sulfate and nitrate, to determine the effects of alternative reducing conditions on CB biodegradation. Using parallel sand column systems developed in Chapter 2 to simulate a steady-state OAI, we separately increased influent nitrate (0-2.5 mM) and sulfate (0.15-10 mM) concentrations in a stepwise manner over a period of 1 year. During this experiment, we monitored the reductive dechlorination and aerobic degradation of 1,2,4-TCB, the prevailing redox activity, and the composition of porewater microbial communities over time.

Under baseline column conditions, reductive dechlorination and aerobic CB activity remained stable. An unexplained shift in microbial activity at the end of the experiment led to substantial methanogenesis and increased reductive dechlorination, but showed minimal effect on aerobic degradation. Increasing sulfate-reducing conditions were detrimental to both anaerobic and aerobic CB transformations; pathways reached near complete inhibition at a 10 mM dose. CB reductive dechlorination appeared to be negatively impacted by increased competition for electron donor by sulfate and aerobic CB oxidation by competition for oxygen by re-oxidation of reduced sulfur. Increasing nitrate-reducing conditions were also detrimental to reductive dechlorination, with nitrate outcompeting other electron acceptors for electron donor. Increasing nitrate dose led to greater aerobic CB degradation. Under nitrate excess (2.5 mM), 96% of all influent 1,2,4-TCB (4.8 mg/L) was degraded aerobically, a 270% increase from baseline degradation. Nitrate reduction served as a permeant sink for electron donor, decreasing the oxygen demand from competing reduced substrates and leaving more oxygen available for aerobic CB oxidation. Using 16S rRNA sequencing of column porewater and biofilm samples, genera associated with redox cycling were identified; their spatial and temporal changes in abundance were in agreement with observed geochemistry and degradation measurements. Results from this experiment emphasized the complex role of alternative electron acceptors in CB biodegradation at OAIs. While sulfate-reducing conditions present challenges to CB degradation, nitrate demonstrates great potential as an amendment to conserve limited oxygen and maximize aerobic degradation potential.

3.2   Introduction

Oxic-anoxic interfaces (OAIs) contain gradients in electron donor and electron acceptor (oxygen) controlled by mass transfer and reactive utilization. Oxygen, which is abundant in the atmosphere, is soluble only to low millimolar concentrations in saturated groundwater. In areas with modest dissolved organic carbon, such as wetlands, oxygen concentrations can be quickly depleted by microbial growth at depths as low as several millimeters [1]. At greater depths where anoxic conditions exist, microbial communities are adapted to use a variety of alternative metabolic processes to support growth. Hydrolysis and fermentation of organic matter as well as autotrophic reduction of CO_2 produce a variety of reduced substrates such as hydrogen, methane and volatile fatty acids. Exogenous electron acceptors such as nitrate, ferric iron, and sulfate can facilitate oxidation of these reduced substrates, and potentially become electron donors themselves (e.g. ferrous iron, sulfide) [2]. Consequently, oxidation of a single substrate upgradient can lead to a complex series of redox processes downgradient in a subsurface system.

Nitrate is a prominent nutrient and electron acceptor in groundwater [3]. Baseline concentrations in natural subsurface tend to be low (< 2 mg/L NO_3^--N); however, human impacts on the landscape from agriculture, sewage and septic leaks, landfill leachate, and industrial spills often lead to much higher concentrations [3, 4]. A USGS survey of over 120,000 groundwater wells found that 13.2% had NO_3^--N concentrations between 3.1-10 mg/L (0.2-0.7 mM) and 6.4% above 10 mg/L (0.7 mM) [5]. Biological nitrate reduction has a similar reduction potential to oxygen, which leads to high growth yields when used as an electron acceptor compared to other anaerobic substrates [6]. Dissimilatory reduction typically occurs in a multi-step process with intermediates nitrite (NO_2^-), nitric oxide (NO),

and nitrous oxide (N_2O) before reduction to N_2 gas; additionally, dissimilatory nitrate reduction to ammonia (DNRA) can also occur [7]. Due to its high aqueous solubility at ambient temperatures (>900 mg/L) compared to oxygen (8-10 mg/L), nitrate has also been utilized as a groundwater amendment to oxidize a variety of contaminants such as BTEX and ethanol [8-10].

Sulfate is a prevalent anion in many groundwater systems, resulting from atmospheric deposition, mineral dissolution, and mineral oxidation, and anthropogenic activity. Groundwater concentrations can vary significantly, with concentrations from non-detect up to 3 g/L (31 mM) reported at contaminated sites [11, 12]. Biological sulfate reduction leads to the production of sulfides, which can exist as dissolved HS^- at neutral conditions, H_2S at acidic conditions, and as precipitated metal sulfides in the presence of reactive metals such as iron [12]. Sulfate reduction is much less energetically favorable than either nitrate or oxygen reduction, with a negative redox potential closer to that of methanogenesis [13]. Sulfides also highly susceptible to biological sulfur oxidation, leading to complete oxidation back to sulfate or as intermediates such as molecular sulfur or thiosulfate [12]. Sulfate is a regulated secondary drinking water contaminant with a maximum contaminant level (MCL) of 250 mg/L (2.6 mM).

Biodegradation of hydrophobic organic compounds released into groundwater is greatly influenced by the prevailing subsurface biogeochemistry. Chlorobenzenes (CBs) with 1-4 attached chlorines can transform both anaerobically through reductive dechlorination and aerobically through oxidative pathways [14, 15]. Anaerobically, organohalide reducing bacteria (OHRB) must compete for electron donor, H_2, with other organisms that use competing electron acceptors including nitrate, ferric iron, sulfate, and

CO$_2$ [16]. Typically, only a small fraction of donor is utilized for reductive dechlorination in these complex systems [11]. Reductive dechlorination has been typically found to be inhibited under nitrate-reducing conditions through a combination of competition for H$_2$ and toxicity from nitrate reduction intermediates N$_2$O and NO [17, 18]. Reductive dechlorination has been found to co-occur frequently under sulfate-reducing conditions, but also with reported inhibition and lag [11, 17, 19, 20].

Oxidation of CBs is only known to occur through oxygen-mediated pathways, despite studies investigating the possibility of oxidation coupled to nitrate and sulfate reduction [21]. At OAIs, oxidative pathways are often limited by the availability of dissolved oxygen available to organisms [21, 22]. Common reduced groundwater species (organic acids, methane, sulfide) can negatively impact aerobic contaminant degradation by creating additional oxygen demand. Atashagahi et al. (2013), for example, found that elevated sediment-bound organic carbon inhibited vinyl chloride oxidation in microcosms under bulk aerobic conditions [23]. Reduced sulfides, resulting from sulfate oxidation, have been reported to account for up to 50% of oxygen demand in some marine sediments [1, 24]. For aerobic biodegradation treatments, some authors have noted potential beneficial use of nitrate as an alternative electron acceptor to decrease oxygen demand from these other non-contaminant substrates [21, 25].

At sites containing OAIs, such as wetlands and hyporheic zones, contaminated water can contain a variety of different redox conditions over relatively short flowpaths. From our previous work (Chapter 2) and fieldwork by others, CBs have been shown to transform anaerobically and aerobically at model and site OAIs either sequentially or concurrently [26, 27]. While limited aforementioned work has described effects of

alternative electron acceptors on either aerobic or reductive dechlorinating CB pathways, to our knowledge the effects on both pathways within a single system have been untested. This study aimed to fill the knowledge gap by testing the effects of various nitrate- and sulfate-reducing conditions on sequential CB degradation pathways occurring at a model OAI. We hypothesized that elevated sulfate would be detrimental to both CB degradation pathways, serving a re-oxidizable sink for both electron donor and acceptor. We also hypothesized that nitrate would benefit aerobic CB degradation by decreasing oxygen demand from competing substrates. Using model column systems developed in Chapter 2, we tested various doses of nitrate and sulfate in parallel to evaluate changes in biodegradation performance and explore how prevailing redox processes and their associated microbial communities shift over time.

3.3 Materials and Methods

3.3.1 Column Design and Setup

Four columns were packed with rinsed and autoclaved medium-grain filter sand (0.55-0.65 µm) using the same multi-port column system described in Chapter 2. Columns were fed by peristaltic pump in an upflow direction. Simulated groundwater consisted of the same phosphate-buffered anaerobic media described in Chapter 2 with slight modifications. The base mineral media contained 0.32 mg/L Cl^-, 14 mg/L SO_4^{2-}, 0.25 mg/L Fe, and 21.2 mg/L NH_4^+-N with supplemental trace metals and vitamins. Mineral salt stock solutions were stored in headspace-free foil-lined sampling bags for feeding. Separately, neat 1,2,4-TCB and sodium lactate (NaLac) were dissolved in anaerobic Milli-Q® water to achieve influent column concentrations of 34.3±7.4 µM (6.2±1.3 mg/L; ± 1 SD) and 0.55 mM (62 mg/L) respectively. The CB-NaLac feed solutions were stored in headspace-

free polyvinyl fluoride bag for feeding. The separate mineral media and CB-NaLac solutions were mixed at a 1:1 ratio in-line during column feed to minimize potential contamination. Mineral media were replaced every 30 days, and CB-NaLac media were replaced every 10 days. Influent tubing and fittings from the feed media to column influent were replaced and sterilized every 20 days to prevent buildup of biofilm. Sterilization consisted of a 20-minute soak in 20% bleach solution, a triple rinse in Milli-Q® water, and a 30-minute vacuum autoclave cycle. Oxygen-saturated Milli-Q® water was introduced as a side-stream at the column 67% injection ports to create the upper aerobic zone, as described in Chapter 2. A full schematic of influent media streams can be found in Appendix B (Figure B.1).

The four columns were operated under different conditions to determine the effects of varying concentrations of nitrate and sulfate (Table 3.1). An abiotic control column (AC) served as a baseline to determine potential degradation artifacts during column operation. This column was not fed NaLac, but instead 200 mg/L sodium azide as a biocide. A baseline column (BC) was operated continuously throughout the experiment with unmodified simulated groundwater. A nitrate-reducing column (NRC) was fed increasing concentrations of nitrate (0 – 2.5 mM) using filter-sterilized stocks of KNO_3. Similarly, a sulfate-reducing column (SRC) was fed increasing concentrations of sulfate (0.15 – 10 mM) as K_2SO_4. All columns had a baseline influent of 0.15 mM sulfate, which was included in the calculated SRC amendments.

3.3.2   Inoculation

Columns were flushed for over 10 days with their respective influent media streams to stabilize conditions and remove any trapped air. In the biological columns, influent

NaLac concentrations were initially dosed at 1.4 mM to stimulate biofilm formation. Inoculation occurred for 12 days prior to column data collection (day -12). Inoculation of reductive dechlorinators came from the effluent of a column packed with sand and chitin that actively dechlorinated 1,2,4-TCB. The active column effluent was connected directly into the 0% sample port of a single experimental column and continuously pumped at 0.1 mL/min for 18 hours. Subsequently, media from the continuously-stirred aerobic CB-degrading enrichment described in Chapter 2 was continuously inoculated in the same manner for 18 hours. Afterwards, the influent media feed was restored to conditions prior to inoculation. The same inoculation procedure was performed in sequence for all three biologically active experimental columns (excluding AC).

At day 0, influent NaLac concentrations were decreased to 0.28 mM, as used in the Chapter 2 experiments. However, reductive dechlorination activity could not be sustained at this concentration (Figure B.3). At day 24, influent NaLac was increased to 0.55 mM and maintained for the remainder of the experiment.

3.3.3 Experiment Operation

Columns were operated in parallel inside a laboratory fume hood. Ambient temperature, logged continuously, was $18.6 \pm 2.7\,°C$. The experiment was divided into five distinct operational phases over 351 days, summarized in Table 3.1. Concentration of nitrate in NRC and sulfate in SRC were increasing between Phases I-IV, before being lowered to equimolar 0.5 mM in Phase V. Column flow was stopped at the end of Phase V, and columns were sacrificially sampled for biofilm microbial analysis.

Column porewater was sampled every 4-5 days at the 100%, 50%, and 0% ports to profile transformations in the anaerobic zone (0-50%) and aerobic zone (50%-100%).

Samples were collected in 5 mL glass Luer-lock syringes for chemical analyses as described in Chapter 2. At each time point, samples were analyzed for dissolved CBs and inorganic anions. During steady-state operation at the end of each experimental phase, dissolved methane and organic acids were also measured at 100% and 50% ports to estimate an electron balance of redox-active chemicals.

Table 3.1. Overview of experimental phases in test columns

| Phase | Time (days) | Column Amendment | | | |
		Abiotic (AC)	Baseline (BC)	Nitrate Reducing (NRC) [mM NO_3^-] (mg/L)	Sulfate Reducing (SRC) [mM SO_4^{2-}] (mg/L) [*]
I	31-81			Unmodified	Unmodified
II	81-141	No NaLac,		0.15 (9.3)	0.5 (48)
III	141-193	200 mg/L	Unmodified	0.5 (31)	2.5 (240)
IV	193-302	NaN_3		2.5 (155)	10 (961)
V	302-351			0.5 (31)	0.5 (48)

* SO_4^{2-} concentrations include baseline concentration of 0.15 mM

3.3.4   Column Hydrodynamics

Column flow was measured gravimetrically through effluent collection. Nominal column flow was approximately 0.09 mL/min and 0.03 mL/min in the main streams and oxygenated side-streams, respectively. Dilution due to the side-stream was determined by a steady-state bromide tracer, using the ratio of bromide-spiked media concentrations at the 0% and 100% ports of each columns. Flow and dilution varied slightly between columns due to differences in pump heads and tubing. Values were measured repeatedly throughout the experiment and did not drift over time. Average and standard deviation values are presented in Table 3.5.

Three hydraulic tracer tests were performed during startup, at the end of Phase IV, and at the end of Phase V as described in Table B.1. A tracer test was not performed in Phase IV for AC. The oxygenated side-stream was turned off temporarily during these tests

to simplify analysis, leaving only the anaerobic influent feed. Tracer tests were performed using a 50 mg/L Br⁻ (as KBr) step-input spike into the CB media bag for each column. Effluent samples were collected in 20-minute intervals at the 100% port for approximately 600 minutes (11.7 hr) or until breakthrough concentrations of approximately 25 mg/L were achieved. Bromide was measured by ion chromatography. Tracer concentrations measurements are illustrated Figure B.8-10. Since clean filter sand closely approximated an idealized porous surface without sorption, data were fitted to an analytical solution for the 1-D advection-dispersion equation assuming constant injection in a semi-infinite media (Equation 3.1). Column length x was fixed at 15 cm, reaction decay constant λ was assumed to be 0, and a sorptive retardation was assumed to be 0. Fitting parameters C_0 (influent concentration), u (porewater velocity), and D_L (longitudinal dispersion) were determined by nonlinear least-square regression in R using the *nls* function.

Equation 3.1

$$C(t) = \frac{C_0}{2}\left[\mathrm{erfc}\left(\frac{(x - ut)}{\sqrt{4D_L t}}\right) + \exp\left(\frac{ux}{D_L}\right) \times \mathrm{erfc}\left(\frac{(x + ut)}{\sqrt{4D_L t}}\right)\right]\exp\left(-\lambda t\right)$$

Parameters ε (effective porosity) and HRT (hydraulic retention time) were calculated based on u, column flow, and column dimensions. A full summary of model fitting parameters is presented in Table B.6. Modeled HRT values were in agreement with values determined by moment analysis of tracer data (data not shown). Values for u and ε were used to estimate HRT values for the anaerobic and aerobic zones under the dual-stream flow, assuming effective porosity remained constant with the addition of the side-stream.

3.3.5 Analytical Methods

From the 5 mL glass syringe samples, 100 μL aliquots of column porewater were immediately transferred to GC autosample vials and extracted in-vial into cyclohexane for

CB analysis by Gas Chromatography–Mass Spectrometry as described previously in Chapter 2. Benzene was not analyzed in this experiment due to negligible production observed in inoculum cultures and previously tested column experiments (Chapter 2).

Anions in filtered porewater samples were analyzed by ion chromatography with conductivity cell detection as described in Chapter 2 with the following modifications. Inorganic ions chloride, sulfate, nitrate, nitrite, and bromide were separated isocratically in 30 mM KOH eluent at 1 mL/min using an AS18 ion exchange column. The eluent suppressor was operated at 75 mA current. Organic acids lactate, acetate, formate, propionate, and butyrate were separated in KOH eluent pumped at 1.5 mL/min using an AS11-HC column. The eluent concentration followed a gradient of 8 minutes at 1 mM, a 20 min ramp to 30 mM, and a 10 min ramp to 60 mM. The eluent suppressor was maintained at 223 mA. Samples with concentrations above upper calibration limit of 20 mg/L for inorganic ions and 200 µM for organic acids were diluted with Milli-Q® water to achieve an analyte concentration within the linear range.

Dissolved methane in porewater was collected in separate 5 mL glass syringe samples and immediately transferred to 8 mL vials sealed with butyl rubber stoppers. Equilibrated headspace was sampled, manually injected, and analyzed by GC-FID in duplicate with a gas-phase 0.05 mg/L limit of quantification. Aqueous concentrations were back-calculated using Henry's Law. A full description of this method and calculations is presented in Appendix B.1.

3.3.6 Microbial Community Analysis

3.3.6.1 Porewater Filtrate Sample Extraction

During vertical porewater sampling at each timepoint, approximately 5 mL of porewater collected in each glass syringe were passed through a disposable 0.22 μm polyether sulfone syringe filter to remove porewater biomass and particulate matter. After filtration, these filters were saved and frozen at -20° C as representative samples of porewater microbial communities.

Representative filter samples were extracted for each column at the 50% and 100% sample port during steady-state operation of every experimental phase. Under aseptic conditions, thawed filters were cut open along the radial plane using a hot knife consisting of a sterilized steel craft knife blade attached to a soldering iron, exposing the filter membrane. The membrane was carefully removed from the filter using sterilized tweezers and placed in a sterile DNA-free 5 mL polypropylene centrifuge tube. A modified Qiagen DNeasy® PowerSoil® (Germantown, MD) extraction protocol was used to elute DNA from the filter membranes. The contents of one PowerBead tube and 60 μL of Solution C1 were transferred to each 5 mL tube containing a filter. Tubes were vortexed using a MoBio vortex adapter in batches of six for 10 minutes at maximum speed. Afterwards, all liquid contents in the 5 mL tubes were transferred back into the empty PowerBead tubes. Tubes were centrifuged at $10,000 \times g$ for 30 s and transferred into clean collection tubes. The remaining protocol, beginning with the addition of solution C2, was followed according to the manufacturer's protocol.

3.3.6.2 Biofilm Sacrificial Sample Extraction

At the end of the experiment, column matrices were sacrificially sampled for microbial community analysis. Columns were divided into four equal-length segments along the vertical profile and transferred by sterile scoops into a sterile 50 mL polypropylene tubes. Tubes were vortexed at maximum speed for 30 seconds, and contents were dispensed into sterile 100 mm diameter petri dishes. The column matrices were each mixed manually for 1 minute with sterile cell spreaders. Afterwards, approximately 1 g aliquots of each mixed segment were transferred to sterile microcentrifuge tubes and stored at -80 °C. Two duplicate aliquots from each column segment were later thawed for DNA extraction. Approximately 0.5 g of each aliquot were extracted using a PowerSoil® DNA extraction kit (Qiagen, Germantown, MD) following manufacturer instructions. A visual schematic of all DNA sampling is presented in Figure B.2.

3.3.6.3 DNA Sequencing and Analysis

DNA libraries were prepared and sequenced as described in Chapter 2, following the methods of Preheim et al. to amplify the V4 region of 16S rRNA gene for Illumina sequencing [28]. 300-bp paired-end sequences were analyzed as described in Chapter 2 with the following modifications. Sequencing data were processed using the updated qiime2 pipeline (v.2019.1) [29]. Forward and reverse reads were truncated at 241 bp and 178 bp respectively, the first instances the 9th percentile quality score of each read dropped below 20; both reads were trimmed at 24 bp to remove primers sequences. Across all samples, over unique 3600 features were identified. Features were taxonomically classified using the built-in Naïve Bayes feature classifier plugin *classify-sklearn* trained with SILVA 132 99% OTU reference database [30, 31]. In addition to the R packages described in

Chapter 2, *DESeq2* was used for identification of differentially abundant OTUs between column porewater phases [32].

3.3.7 Calculations

3.3.7.1 Chlorobenzene Degradation

Anaerobic reductive dechlorination was quantified based on the appearance of daughter products at the 50% sample port (Equation 3.2). In Chapter 2, we demonstrated that nearly all anaerobic reactions in sand columns occurred within the first 25% of the column length, so it was assumed no further reaction would occur between the 50% port and the oxygenated side-stream port. Since influent 1,2,4-TCB was in excess throughout the experiment and total CB mass was conserved within the anaerobic zone, total reductive dechlorinations provide a performance metric independent of variations of influent 1,2,4-TCB concentration (Figure B.3).

Equation 3.2

$$\text{Reductive dechlorination} = 2 \times \text{MCB}_{50} + 1 \times \sum \text{DCBs}_{50}$$

Aerobic degradation was quantified based on the change in total CB mass between the 50% port (immediately before oxygen addition) and 100% port (Equation 3.3). The reported concentrations were adjusted by the side-stream dilution factor to reflect the measured concentrations observed in the column aerobic zones.

Equation 3.3

$$\text{Aerobic degradation} = \sum \text{CBs}_{50} \div DF - \sum \text{CBs}_{100}$$

For each operational phase, the final 6-7 sample points were used to calculate steady-state average values for CB degradation, nitrate transformation, and sulfate transformation. Columns were operated for a minimum 26 days (110 pore volumes) before

81

steady-state values were calculated to ensure stabilization of microbial processes. The specific time ranges used for steady-state calculations are presented in Table B.1. Differences in steady-state performance between columns and between phases were calculated for statistical significance using Welch's 2-tailed t-test. Reported p-values below 0.05 were considered to be statistically significant.

3.3.7.2 Electron Balance

Illustrative electron balances were calculated at representative steady-state timepoints in each experimental column phase (Table B.1) for both anaerobic zone and aerobic zone processes. Anaerobic zone processes quantified were CB reductive dechlorination, nitrate reduction, sulfate reduction, methanogenesis, propionate fermentation, and acetate fermentation; these were based on the concentration change of indicator analytes between the 0% and 50% sample ports. Total accounted reductions were compared to the theoretical available electron donor (0.55 mM NaLac) available at the column influent. Aerobic zone processes quantified were CB oxidation, sulfide oxidation, methane oxidation, propionate oxidation, acetate oxidation, and lactate oxidation; these were based on concentration change between the 50% and 100% ports, adjusted to the side-stream dilution concentrations in the aerobic zone. Total accounted oxidations were compared to the theoretical available electron acceptor (oxygen) in the aerobic zone (measured DO in the side stream). Calculations assumed sulfate was reduced to sulfide, nitrate was reduced to N_2, and longer-chain organic acid fermentations were negligible. Notably, these calculations did not account for transformation of other possible redox species such as iron (0.25 mg/L in the feed media) and H_2, nor transient electron sinks such

as precipitated sulfides and cell biomass. Table B.2 provides a full description of the measured quantities, electron equivalents, and calculations used in the electron balances.

3.4   Results and Discussion

CB biodegradation activity began rapidly in biologically-active columns after inoculation. Removal of CBs was immediate at time 0 in the 100% port, indicative of aerobic degradation activity (Figure B.3). Reduced CB daughter products were also immediately produced in the biological columns, but disappeared for a short period during the initial adjustment of influent NaLac concentration (Figure B.3). After the adjustment of NaLac to 0.55 mM, reductive dechlorination activity stabilized by day 57 (Figure 3.1). Degradation patterns in all three biological columns were consistent during Phase I (Figure 3.1, Figure 3.2).

Throughout the experiment, CB degradation patterns followed similar trends observed in Chapter 1. Briefly, reductive dechlorination of 1,2,4-TCB resulted in the production of 1,3-DCB, 1,4-DCB, and lower fractions of 1,2-DCB and MCB (Figure B.3). Overall dechlorination of the CBs was generally low in all columns; the steady-state degree of effluent CB chlorination was 2.6-3 Cl per CB in all column phases, with the exception of BC Phases IV and V (2-2.4; Table B.3). Concentrations of 1,2,4-TCB and all dechlorinated daughter congeners decreased within the aerobic zone only, indicative of aerobic degradation of all available MCB, DCB, and TCB congeners (Figure B.3). The extents of anaerobic reductive dechlorination (Figure 3.1) and aerobic degradation (Figure 3.2) were calculated and tracked over time in all columns throughout the experiment, based on measured CB profiles (Figure B.3). The steady-state CB degradation performance in

each phase is shown graphically in Figure 3.3. A comprehensive summary of all tabulated

metrics is presented in Table B.3.
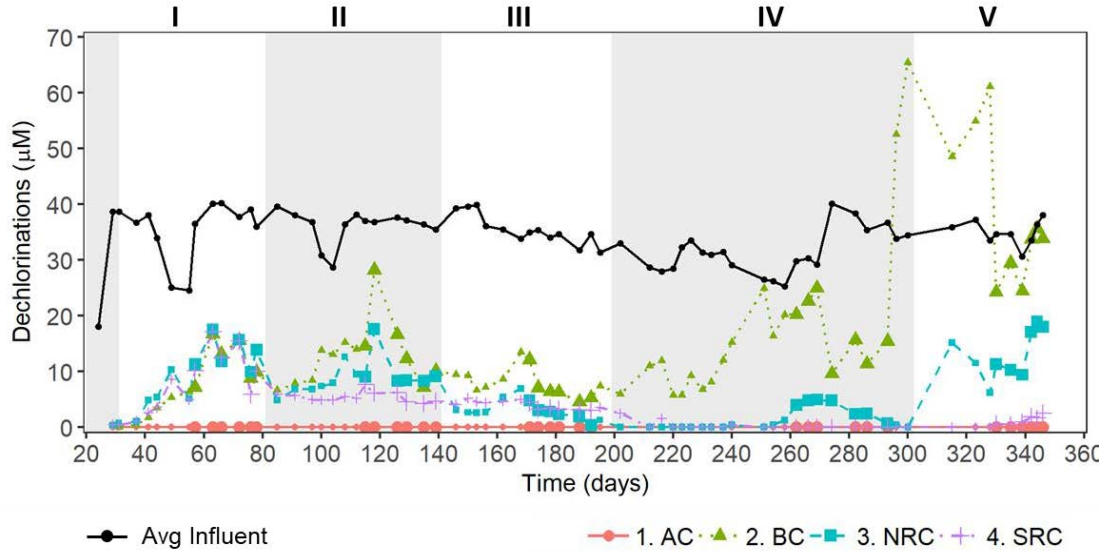
Figure 3.1 Time-series of measured reductive dechlorination observed in each column at the 50% port. Solid black data points were average 1,2,4-TCB influent into each column. Bold data points were samples used to calculate steady-state performance for each experimental phase.
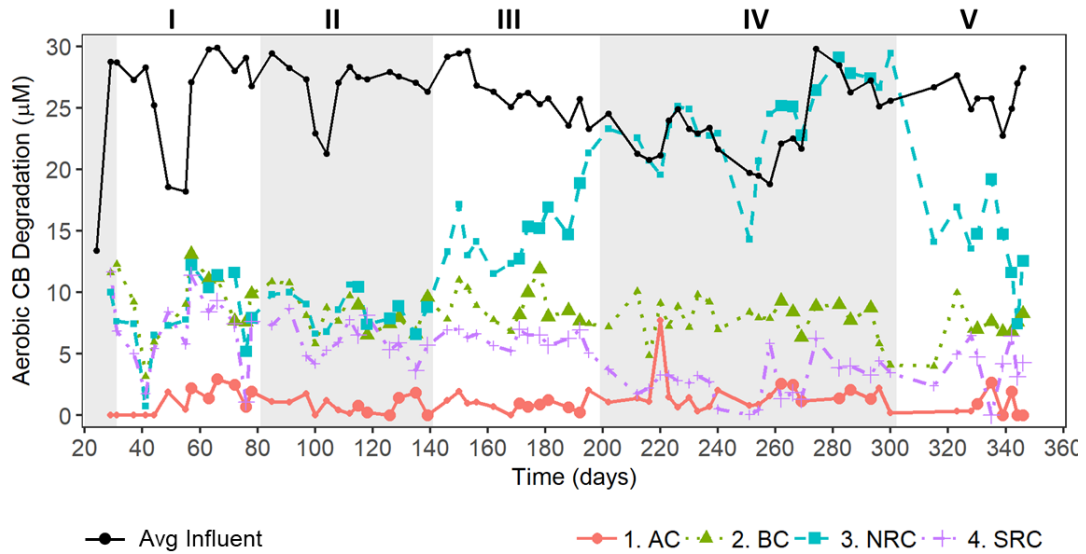
Figure 3.2. Time-series of measured aerobic degradation observed in each column. Solid black data points were average 1,2,4-TCB influent into each column, divided by the dilution factor from the aerobic zone side-stream. Bold data points were samples used to calculate steady-state performance for each experimental phase.

Within all columns, effluent pH was measured during steady-state of each phase.

pH remained circumneutral (7.12-7.61) throughout the experiment without any apparent

differences between biological columns or experimental phases (Table B.5). pH in the Abiotic Column (AC) (7.37-7.61) was slightly higher than the biological columns (7.12-7.43) likely due to the absence of lactate and addition of sodium azide.

In AC, the abiotic control, no dechlorinated daughter products were detected and calculated reductive dechlorination was 0 throughout the experiment (Figure 3.1). There was low apparent CB removal measured in this column (0.7-1.8 µM steady-state range), which may be a result of potential sampling losses or variation due to side-stream dilution. This nonzero loss provided a baseline for which to compare the biologically active columns, which are described in the following sections.
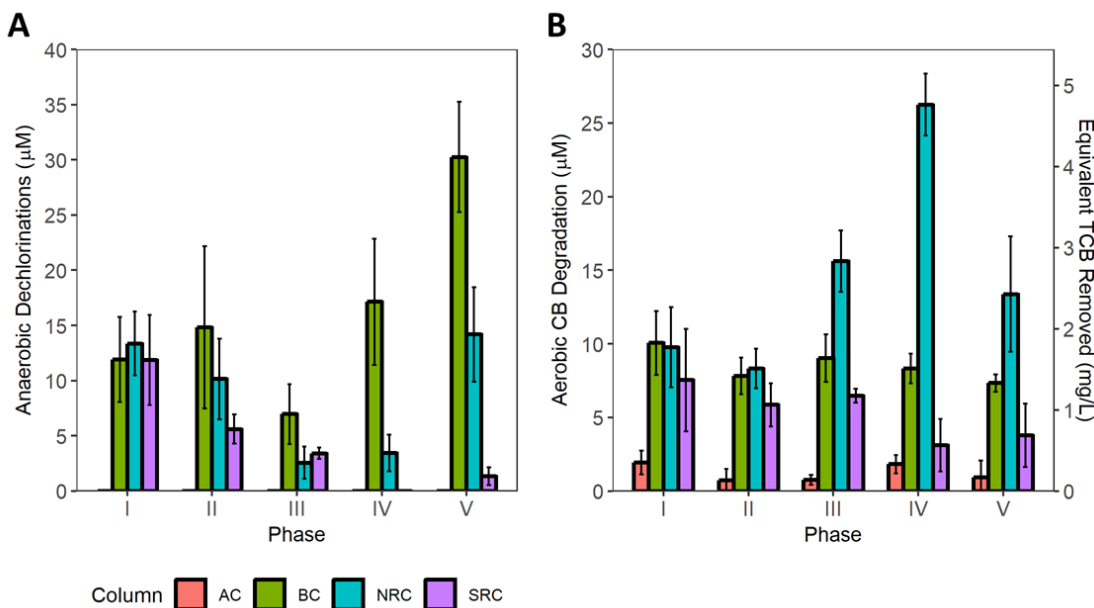
Figure 3.3. Steady-state averaged CB degradation in each column experimental phase. (A) Anaerobic reductive dechlorination; (B) Aerobic degradation Error bars represent ±1 SD

3.4.1 Baseline Column (BC) Activity

The BC was designed to demonstrate long-term CB degradation across an OAI without any intentional changes to operating conditions and serve as a baseline biological

control to the NRC and SRC. Initial degradation activity (Phase I) was 11.9 µM anaerobic dechlorinations and 10.1 µM aerobic degradations. Reductive dechlorination in BC was stable in Phases I-II before decreasing in Phase III. However, in the second half of Phase IV and beginning of Phase V reductive dechlorination activity increased from approximately 10 µM to nearly 55 µM, before stabilizing at a steady-state value of 30.3 µM at the end of the experiment, a 250% increase from Phase I (Figure 3.1). An electron balance of anaerobic processes (Figure 3.4a) illustrates an apparent shift in redox processes also co-occurring with this increase in dechlorination. In Phases I and II when degradation was stable, approximately 90% of accounted reduction resulted in formation of organic acids acetate and propionate while the remaining 10% resulted in sulfate reduction. Reductive dechlorination utilize less than 1% of the total available electron donor. Beginning Phase III and continuing to Phase V, methanogenesis began to account for an increasingly large fraction of total electron flow at the expense of acetate (Figure 3.4a). In Phase V, methanogenesis was the dominant reductive process and there was almost no acetate present, indicative of acetolactic methanogenesis (discussed in Section 3.4.5.3).

Table 3.2. Steady-state redox activity in the BC during each operational phase

	Anaerobic Zone		Aerobic Zone		
Phase	CB Reductive Dechlorination (µM)	Electron Donor Utilization (% e⁻ equiv)	CB Degradation (µM)	Aerobic Zone DO (mg/L)	Specific Degradation (µM CB/mM O_2)
I	11.9 ± 3.9	0.36%	10.1 ± 2.2	$7.1 \pm .5$	45.1
II	14.8 ± 7.4	0.45%	7.8 ± 1.2	$7.5 \pm .4$	33.4
III	7.0 ± 2.7	0.21%	9.0 ± 1.6	$7.8 \pm .7$	37.1
IV	17.1 ± 5.7	0.52%	8.3 ± 1.0	$6.2 \pm .2$	42.8
V	30.3 ± 5.0	0.91%	$7.3 \pm .6$	$6.2 \pm .2$	37.9
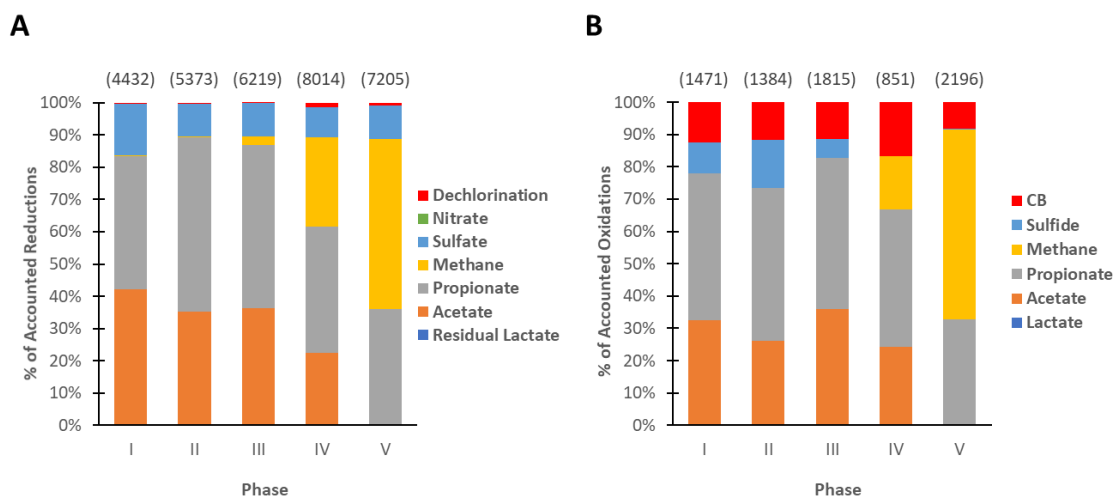
Figure 3.4. Representative BC electron balances during steady-state of each phase. Graphed percentages based only on quantified reductive processes listed in legend. Values above each bar are total accounted electron equivalents (μeq). (A) Anaerobic zone reduction processes based on constant 0.55 mM NaLac input (theoretical 6640 μeq). (B) Aerobic zone oxidation processes based on diluted DO influent from oxygenated side-stream: 7.1, 7.5, 7.8, 6.2, 6.2 mg/L (890, 940, 980, 780, 780 μeq) in Phases I-V respectively.

In contrast, aerobic degradation in BC remained stable throughout the experiment and did not show significant changes (p>.05) between consecutive phases (Figure 3.2). Maximum aerobic degradation was well below the theoretical yield for oxygen of approximately 167 μM TCB/mM O_2 (assuming aerobic degradation of TCB; Table 3.2). There was a significant 28% decrease (p=.026) in aerobic degradation from Phase I to Phase V (Table 3.2). However, adjusting aerobic degradation to the available concentration of oxygen in each phase (13% lower in Phase V compared to Phase I), this decrease was much lower (16%). Occasional measurement of column effluent and the colorless visual resazurin indicator indicated that oxygen was completely depleted in BC effluent. An electron balance of aerobic zone oxidation processes (Figure 3.4b) showed that degradation of reduced compounds generally mirrored the reduction processes in the anaerobic zone (Figure 3.4a). Propionate and acetate accounted for over 70% of accounted oxidations in Phases I-III, while CB oxidation accounted for a smaller share, approximately 10% or less. Re-oxidation of reduced sulfur species (presumed to be sulfide) to sulfate accounted for a

small (approximately 10%) fraction as well. As the BC became methanogenic in Phases IV and V, oxidations shifted to methane oxidation at the expense of organic acids and sulfide (Figure 3.4b). Despite the complete shift from acetate to methane oxidation in the column aerobic zone, aerobic CB degradation remained stable (Figure 3.4).

3.4.2   Nitrate-Reducing Column (NRC) Activity

In the NRC, Phase I degradation was nearly identical to the BC under the same influent conditions. At elevated 0.15 mM nitrate dose in Phase II, steady-state degradation was not significantly different compared to Phase I or BC Phase II. Increasing nitrate to 0.5 mM (Phase III), reductive dechlorination decreased significantly (p<.01) from 10.2 µM to 2.6 µM. (Figure 3.3a). Increasing nitrate to 2.5 mM caused reductive dechlorination to completely cease in the first 50 days of Phase IV (Figure 3.1). However, dechlorination increased slightly at the end of Phase IV, resulting in a steady-state average of 3.4 µM (Figure 3.3a). After lowering nitrate to 0.5 mM in Phase V, reductive dechlorination increased significantly (p<.001) to 14.2 µM, similar to the initial activity observed in Phase I without nitrate addition (Figure 3.3a). Elevated nitrate appeared to have an overall negative effect on reductive dechlorination; however, a shift occurred (similar to BC) at the end of Phase IV to promote reductive dechlorination.

Nitrate was completely reduced within the anaerobic zone at 0.15 mM and 0.5 mM influent (Phases II, III, V), but was in excess at 2.5 mM (approximately 1.5 mM remaining) (Table 3.3). No nitrite was detected (data not shown), and reduction of nitrate was assumed to proceed fully to N_2 for electron balance purposes. However, it is possible that incomplete reduction to NO or N_2O gas may have occurred. Figure 3.5a shows representative anaerobic electron balances in the NRC. The balance in Phase I was predictably similar to

BC (Figure 3.4), with majority organic acid fermentation and a small fraction of sulfate reduction. In Phases II and III, increased nitrate reduction occurred while all other reduction processes decreased. In Phase IV nearly all electron donor was used for nitrate reduction, outcompeting all other processes. This was unsurprising, given the substantial difference in free energy for nitrate compared to other anaerobic electron acceptors [13]. As nitrate concentration was lowered to 0.5 mM in Phase V, other reduction processes re-emerged presumably after limiting nitrate had been expended (similar to Phase III). A small fraction of methanogenesis also emerged in Phase V, similar to the shift seen in BC.

Table 3.3. Steady-state redox activity in NRC during each operational phase

Phase	NO_3^- Dose (mM)	Anaerobic Zone				Aerobic Zone		
		CB Reductive Dechlorination (μM)	Δ NO_3^- (μM)	Δ SO_4^{2-} (μM)	Residual Organic Acids (μM)	CB Degradation (μM)	Δ NO_3^- (μM)	Δ SO_4^{2-} (μM)
I	0	13.4 ± 2.9	1 ± 1	-88 ± 4	437	9.8 ± 2.7	1 ± 1	16 ± 5
II	0.15	10.2 ± 3.7	-142 ± 3	-86 ± 12	346	8.3 ± 1.3	2 ± 2	13 ± 4
III	0.5	2.6 ± 1.5	-477 ± 38	-57 ± 32	167	15.6 ± 2.1	5 ± 9	32 ± 8
IV	2.5	3.4 ± 1.6	-943 ± 54	1 ± 4	7	26.3 ± 2.1	-59 ± 44	2 ± 8
V	0.5	14.2 ± 4.3	-499 ± 0	-84 ± 18	192	13.4 ± 3.9	0 ± 0	15 ± 7
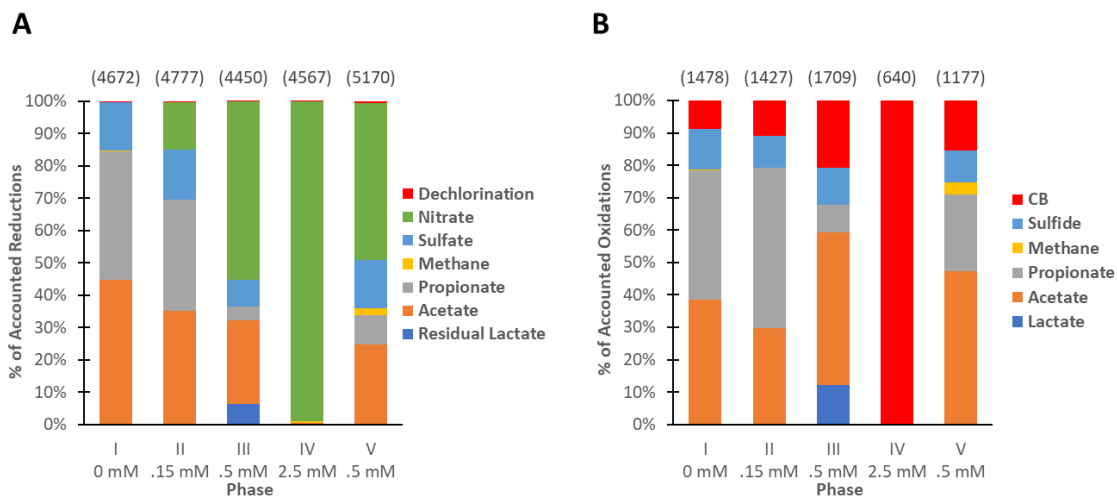
Figure 3.5. Representative NRC electron balances during steady-state of each phase. Graphed percentages based only on quantified reductive processes listed in legend. Values above each bar are total accounted electron equivalents (µeq). (A) Anaerobic zone reduction processes based on constant 0.55 mM NaLac input (theoretical 6640 µeq). (B) Aerobic zone oxidation processes based on diluted DO influent from oxygenated side-stream: 8.0, 8.4, 8.7, 7.0, 7.0 mg/L (1000, 1050, 1090, 870, 870 µeq) in Phases I-V respectively.

There was a clear positive association between nitrate dose and aerobic CB degradation (Table 3.3). Degradation in NRC increased significantly (p<.001) at 0.5 mM nitrate (Phase III) to 15.6 µM and again at 2.5 mM nitrate (Phase IV) to 26.3 µM. The latter represented a 270% increase in total CB degradation. When nitrate influent was decreased to 0.5 mM in Phase V, aerobic degradation fell to 14.2 µM, similar to Phase III. Increased nitrate dose led to decreasing concentrations of reduced substrates such sulfide and organic acids moving from anaerobic to aerobic zone, as shown quantitatively in Table 3.3 and qualitatively in the anaerobic electron balance (Figure 3.5a). Unlike competing reduction processes (e.g. methanogenesis, organic acid fermentation, and sulfate reduction), nitrate reduction to N_2 was an electron donor sink that was not readily bioavailable for re-oxidation. With lower oxygen demand from competing species, more oxygen was then available for CB metabolism in the aerobic zone (Figure 3.5b). Effluent DO measurements showed that oxygen was limiting at nitrate doses of 0.5 mM and less. However, under nitrate excess in Phase IV, nearly 2 mg/L residual oxygen was measured in the column

90

effluent. Under this dose, near-complete (95.4%) aerobic degradation of the 26.3 µM of 1,2,4-TCB in the aerobic zone occurred. When nitrate influent was lowered to 0.5 mM (Phase V), degradation activity decreased to levels previously observed in Phase III (Table 3.3).

3.4.3 Sulfate-Reducing Column (SRC) Activity

Degradation in the SRC was similar to BC in Phase I, but began to diverge from BC in Phase II (Figure 3.3). There was a clear negative association between sulfate addition and reductive dechlorination, which decreased significantly in every consecutive phase from I to IV ($p<.05$). Reductive dechlorination fell by 53% to 5.6 µM at 0.5 mM sulfate (Phase II), to 3.4 µM at 2.5 mM sulfate (Phase III), and was completely inhibited at 10 mM sulfate (Phase IV; Table 3.4). No dechlorination activity was observed for the first 25 days of Phase V, when sulfate was decreased to 2.5 mM; however, dechlorination showed a slight but significant ($p<.01$) recovery to 1.3 µM at the end of the experiment (Figure 3.1). Figure 3.6a shows the representative anaerobic electron balance in the SRC. Sulfate reduction comprised an increasing fraction of total electron donor as the dose increased and came at the expense of residual propionate, which was completely absent in Phase IV (Figure 3.6a). Similar to the BC, the SRC also become more methanogenic over the course of the experiment, with nearly 10% of electron donor utilized for methanogenesis in Phase V. Interestingly, the total accounted electron equivalents calculated in Phase IV far exceeded any other phase by at least 1700 µeq and the influent NaLac by 2300 µeq (Figure 3.6a). This over-accounting may suggest that sulfate was not completely reduced to sulfide, but instead to a less reduced compound such as sulfite or elemental sulfur. This could also be a result of increased variability of sulfate measurements in Phase IV indicated by a high

deviation in steady-state sulfate change (Table 3.4). Unlike nitrate in the NRC, sulfate was never completely utilized in any phase (Table 3.4). Competing reduction processes such as acetogenesis and methanogenesis were able to co-occur with sulfate reduction regardless of the influent dose (Figure 3.6a), reflective of the similar redox potentials between these processes [13].

Table 3.4. Steady-state redox activity in the SRC during each operational phase

Phase	SO_4^{2-} Dose (mM)	Anaerobic Zone			Aerobic Zone	
		CB Reductive Dechlorination (μM)	Δ SO_4^{2-} (μM)	Residual Organic Acids (μM)	CB Degradation (μM)	Δ SO_4^{2-} (μM)
I	0.15	11.9 ± 4.1	-95 ± 8	203	7.5 ± 3.5	12 ± 2
II	0.5	5.6 ± 1.3	-245 ± 26	392	5.9 ± 1.5	54 ± 15
III	2.5	3.4 ± .5	-329 ± 35	353	6.5 ± .5	106 ± 45
IV	10	0.0 ± .0	-252 ± 137	317	3.1 ± 1.8	70 ± 93
V	0.5	1.3 ± .8	-325 ± 31	279	3.8 ± 2.2	68 ± 8
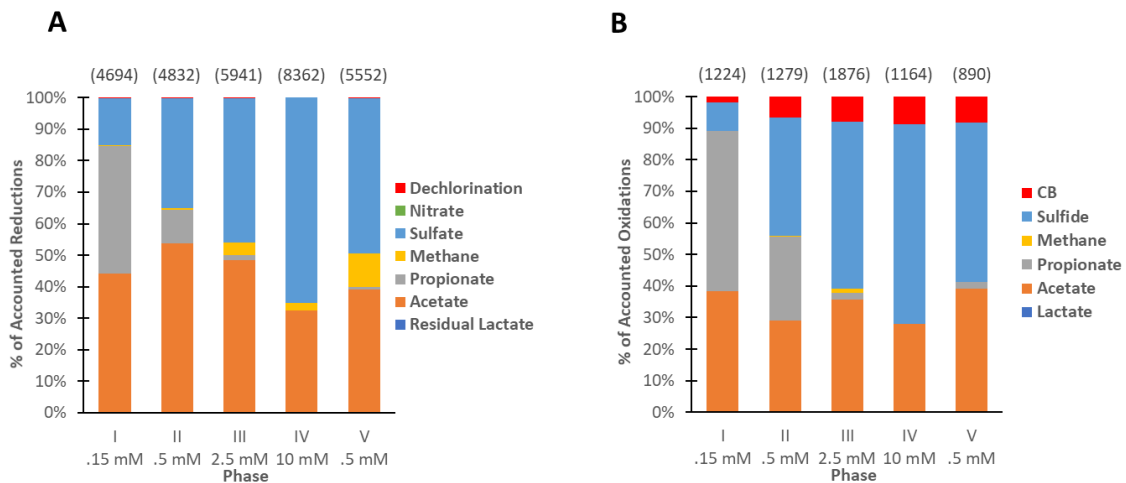
Figure 3.6. Representative SRC electron balances during steady-state of each phase. Graphed percentages based only on quantified reductive processes listed in legend. Values above each bar are total accounted electron equivalents (μeq). (A) Anaerobic zone reduction processes based on constant 0.55 mM NaLac input (theoretical 6640 μeq). (B) Aerobic zone oxidation processes based on diluted DO influent from oxygenated side-stream: 7.8, 8.2, 8.5, 6.8, 6.8 mg/L (980, 1030, 1070, 850, 850 μeq) in Phases I-V respectively.

92

Aerobic degradation also appeared to be negatively impacted by sulfate at higher doses (Figure 3.3b). From Phase II onward, aerobic CB degradation was significantly lower than in the corresponding BC phase (p<.05). However, within SRC, degradation did not decrease significantly from Phase I until the 10 mM sulfate dose in Phase IV where degradation decreased 49% to 3.1 ± 1.8 µM. This was not statistically different (p>.05) from the observed removal in AC (1.8 ± 0.6 µM), suggesting aerobic degradation may have been completely inhibited here. Lowering sulfate to 0.5 mM in Phase V, aerobic degradation did increase slightly to 3.8 µM, but this was not a statistically significant change (p>.05; Table 3.4). This suggested that aerobic degradation may have been permanently negatively impacted by the high sulfate dose. Decreased aerobic CB degradation at higher sulfate doses could likely be attributed to increased competition for oxygen from sulfide oxidation, as seen in the aerobic electron balance (Figure 3.6b). As greater fractions of sulfate were reduced, increased fractions were re-oxidized, which would increase total oxygen demand.

3.4.4   Tracer Test Results

Empty bed column tracer tests during startup showed that columns were packed similarly prior to inoculation and experimental operation (Figure B.8). Initial tracer porewater velocities and longitudinal dispersion coefficients ranged from 0.046-0.050 cm/min and 0.0026-.0037 cm^2/min respectively, with effective porosity values of 0.39-0.42 (Table B.6). Prior to Phase I, the influent peristaltic pump heads and tubing to AC were changed, decreasing influent flow by 16%. This was assumed to have a proportional impact on column velocity and retention time. Since this column was not biologically active, the lower flow compared to the biologically active columns was not considered confounding.

At the end of Phase IV, when alternative electron acceptor doses were greatest, another tracer test was performed on the biologically active columns (Figure B.9). Dispersion coefficients increased an order of magnitude (0.012-0.029 cm^2/min), indicative of additional mixing possibly due to biofilm and precipitate development (Table B.6). BC and SRC behaved similarly. Both had small (<13%) decreases in porewater velocity and proportionally higher HRTs and higher effective porosity. In contrast, NRC had an 8% increase in velocity, corresponding to a decrease in porosity and retention time (Table B.6). This difference may be due to enhanced biofilm growth in NRC occupying greater porespace compared to the other columns. Nitrate provides significantly greater energy yield for cell growth compared to sulfate and other electron acceptors, potentially enhancing biofilm development and decreasing effective porespace during this phase [6].

Table 3.5. Column hydrodynamics and estimated zonal hydraulic retention times

		AC	BC	NRC	SRC
Measured	Effluent Flow (mL/min) [a]	0.109 ± 0.004	0.121 ± 0.003	0.123 ± 0.002	0.122 ± 0.001
	Dilution Factor (*DF*) [b]	1.38	1.30	1.35	1.34
Modeled Parameters [c]	u (cm/min)	0.035	0.046	0.047	0.045
	D (cm^2/min)	0.004	0.009	0.016	0.026
	Effective Porosity, ε	0.45	0.41	0.40	0.41
	Pore Volume (mL)	33.0	30.4	29.1	30.4
Dual-stream Calculated Zonal Retention Time (hr)	Anaerobic HRT	4.6	3.6	3.5	3.7
	Aerobic HRT	1.7	1.4	1.3	1.4
	Total HRT	6.3	5.0	4.9	5.1

a. Based on 7 measurements throughout experiment
b. Based on 4 measurements throughout experiment
c. Based on Phase V tracer test at the end of the experiment

A final tracer test was performed on all columns at the end of Phase V immediately before ending the experiment (Figure B.10). Dispersion in AC remained unchanged from the initial tracer test, indicative of minimal biofilm development. Effective porosity increased slightly from 0.4 to 0.45, which may have been resultant of decreased flow. Hydrodynamics in the biological columns were similar. Dispersion remained similar to the Phase IV test (0.009-0.026 cm^2/min). Porewater velocity and effective porosity were 0.045-0.047 cm/min and 0.40-0.41 respectively, which were nearly identical to the parameters from the empty-bed tracer test. This may have been indicative of a loss of biomass within the NRC after nitrate concentrations were decreased. In general, column hydraulics within the biological columns appeared stable throughout the experiment from the beginning to the end of the experiment. The order of magnitude increases in dispersion likely resulted in some preferential flow and additional mixing within the columns. However, near-constant velocities and porosities indicated that there was no major fouling or dead space.

3.4.5   Microbial Community Analysis

3.4.5.1   Inocula Composition

CB-degrading enrichments used to inoculate the biological columns were sequenced with relative abundance profiles described in Figure B.11. The anaerobic inoculum contained approximately 11% putative reductive dechlorinator *Dehalobacter* [33] with additional fractions of *Pseudomonas* (18%), an unidentified Lahnospiraceae OTU (12%), *Sporomusa* (11%), *Fonticella* (7%), and *Dechlorosoma (6%)*. The aerobic enrichment was dominated by an unidentified Betaproteobacteriales OTU (76%) with smaller fractions of *Paraburkholderia* (9%), *Rhizobium* (6%), *Pseudomonas* (3%) also present. *Paraburkholderia* [14], *Pseudomonas* [34], and *Pandoraea* [35] (found at low

95

0.5% abundance) have all been previously identified by others as potential aerobic CB degraders. The rapid startup of CB degradation in the biological columns (Figure 3.1, Figure 3.2) was likely aided by high fractions of putative CB degraders in the inocula.

3.4.5.2 Porewater Microbial Communities

Sampling column porewater provided an opportunity to profile changes in the microbial community over shifting redox conditions. Although the distribution of bacteria between solid and aqueous phases are known to vary, shifts in porewater community originating from the column would still indicate changes in activity over time [36]. Comparing abundances between the 50% and 100% sampling port, we were able to see contrasts in profiles between the anaerobic and aerobic zones respectively. Organisms abundant at the 100% port but not at the 50% port can be assumed to be related to activity in the aerobic zone; conversely organisms abundant at both ports can be assumed to be related to anaerobic zone activity with potential additional activity in the aerobic zone. A genus-level profile of column porewater samples across each experimental phase is presented in Figure 3.7. These data provided a qualitative, but noisy, description of changing community composition and metabolic potential within the columns.
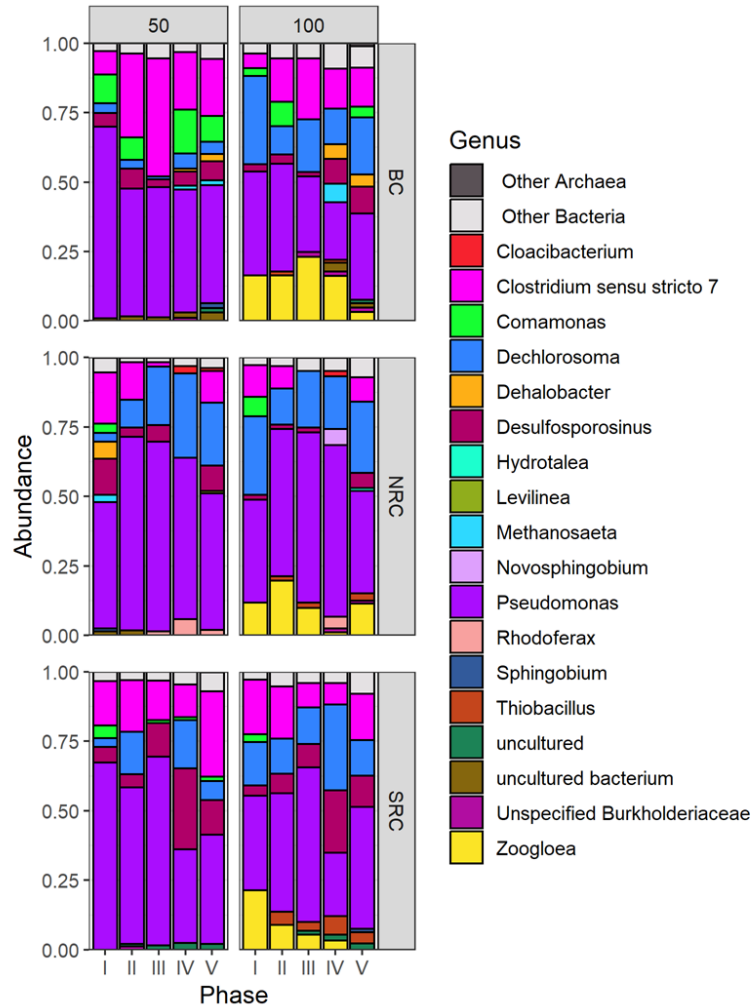
Figure 3.7. Porewater bacteria relative abundance profile in biological columns during steady-state of each phase at 50% port (left) and 100% port (right) for genera with >=1% abundance. n=2 sample dates for all samples except in BC Phases II, III, and V.

Initially, Phase I porewater in all biological columns was dominated by just five genera – *Pseudomonas*, *Dechlorosoma*, *Comamonas*, *Clostridium*, *Zoogloea* and *Desulfosporosinus* (Figure 3.7). All of these dominant genera were detected in the inocula, except for *Clostridium*, a common anaerobe associated with organic acid fermentation and hydrogen generation [37]. *Clostridium* populations may have developed as a result of a switch in primary substrate between the inocula (chitin) and the column (lactate). The presence of *Desulfosporosinus*, a genus of strictly anaerobic sulfate-reducing bacteria (SRB) [38], was expected given the baseline influent of 0.15 mM sulfate in all columns.

Dechlorosoma, Comamonas, *Zoogloea*, *and Pseudomonas* are all facultative anaerobes with additional potential for fermentation, perchlorate-reduction (*Dechlorosoma*) [39] and nitrate-reduction (*Dechlorosoma*, *Pseudomonas*) [40, 41]. *Dechlorosoma* and *Zoogloea* were found predominantly in the 100% samples, indicating an association with aerobic metabolism. With the exception of the NRC 50% sample (6%), *Dehalobacter* was present in all column porewater samples at low abundances (<1%). *Pseudomonas* was the only highly abundant potential aerobic CB degrader from the aerobic inoculum present in column porewater. However, all porewater samples were dominated by large fractions (>21%) of a single *Pseudomonas* OTU that did not show strong differential abundance patterns. Due to its ubiquity in samples and the vast number of potential strains and known metabolic functionality [42], we could not infer a specific functional role for this genus in this experiment.

Several qualitative trends were observed in these profiles (Figure 3.7). In BC, both *Dehalobacter* and methanogenic *Methanosaeta* [43] emerged in larger proportions beginning in Phase IV. In SRC, *Desulfosporosinus* and *Thiobacillus* (100% port) showed increased abundances with increased sulfate dose. In NRC, the abundance of *Dechlorosoma* increased with increasing nitrate dose at the 50% port, but trend was not apparent at 100%. Abundances of *Rhodoferax* and *Novosphingobium* also co-occurred with increasing nitrate dose. Interestingly, the *Novosphingobium* OTU identified was identical to an OTU identified in Chapter 2 as an "Unspecified Sphingomonadaceae" (using the GreenGenes database) that was highly abundant in column aerobic zones and suspected to be an aerobic CB degrader. Conversely, abundances of *Desulfosporosinus* and

Clostridium, which were prominent across BC and SRC, appeared to decrease with increased nitrate dose in NRC.

At the class level (Figure B.12), porewater was dominated by Gammaproteobacteria and Clostridia to a lesser extent. Over time, BC and SRC had increasingly larger fractions of Clostridia compared to Gammaproteobacteria independent of conditions, suggesting a shift to more strictly anaerobic organisms. The presence of Clostridia decreased with increasing nitrate dose in NRC. Alphaproteobacteria and Bacteroidia emerged in abundances greater than 1% in Phases IV and V of all columns.

3.4.5.3   Changes in Functionally Relevant Porewater Genera

Several indicator genera whose porewater abundances co-occurred with methane, sulfate, and nitrate cycling were identified. The trends are described here, but plots of relative abundances across phases and columns are presented in Appendix B (Figure B.13 - Figure B.15).

Within the BC, the loss of acetate and increase in methane production seen in the electron balance within Phases IV and V were suspected to be a result of acetoclastic methanogenesis (Figure 3.4). We identified *Methanosaeta* as the only methanogenic archaeal genera within any of the column samples. *Methanosaeta* is slow-growing obligate acetoclastic methanogen, only capable of using acetate as an electron donor for growth [43, 44]. Consequently, *Methanosaeta* in BC became substantially more abundant in the 50% porewater samples in Phases IV and V (Figure B.13), co-occurring with the observed increase in methanogenesis (Figure 3.4a). Increased methane oxidation (Figure 3.4b) was accompanied by a 2-log increase in putative methanotroph *Methylocystis* [45] in 100% porewater samples between Phases III and V (Figure B.13). Similar trends in *Methanosaeta*

were observed in SRC, but to a lesser extent, corresponding to observed methanogenesis in Phases III-V (Figure 3.6a). NRC did not show co-occurrence, despite some observed methane in Phase V (Figure 3.5a).

Two different genera in the NRC 50% porewater samples appeared to be associated with nitrate reduction. *Dechlorosoma* became highly abundant (up to 30%) with increased nitrate concentration from Phases I-IV (Figure B.14) [40]. This genus was also found in BC and SRC at moderate abundances, which was unexpected since *Dechlorosoma* is not known to have fermentative or sulfate-reducing metabolism [39]; however no patterns in abundance were apparent in those columns. *Rhodoferax,* which has also been implicated in nitrate reduction [46], showed a similar trend with nitrate dose in the NRC, but at an order of magnitude lower than *Dechlorosoma*; this genus was not present in BC or SRC (Figure B.14).

Abundances of putative SRB *Desulfosporosinus* and sulfate-oxidizer *Thiobacillus* were prominent in all columns since a baseline 0.15 mM was fed to each (Figure B.15). Under elevated sulfate-reducing conditions in the SRC, *Desulfosporosinus* and *Thiobacillus* abundances also increased, with maxima at 10 mM sulfate (Phase IV; Figure B.15). Also in Phase IV, the abundances of these sulfur-cycling organisms decreased to zero in NRC, further evidence that nitrate-reducing conditions suppressed other anaerobic processes (Figure B.15).

Porewater abundances of putative CB dechlorinator *Dehalobacter* (Figure 3.8) appeared to generally co-occur with CB dechlorination activity in all columns (Figure 3.3). We attempted to correlate steady-state reductive dechlorination to the average relative abundance *Dehalobacter* from the 50% porewater samples in each column (n=2; Figure

3.9). Excluding a single outlying point (NRC Phase I), there was a good linear fit (R^2=0.838) to the combined data from all columns. This suggests that in a simple sand matrix, abundances of planktonic *Dehalobacter* may be a useful relative measure of CB dechlorination activity.
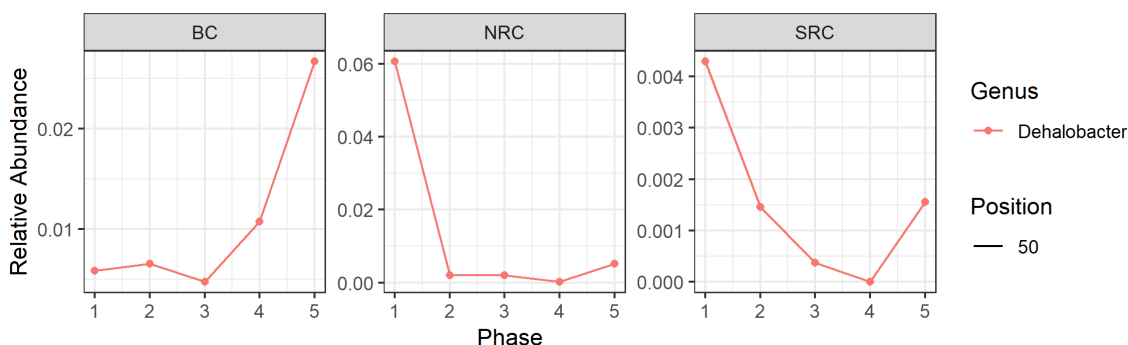
Figure 3.8. Relative abundance profiles of putative CB dechlorinator *Dehalobacter* at 50% porewater sample port during steady-state operation of each experimental phase. Each datapoint represents the average of 2 samples with the exception of BC Phases II, III, and V.
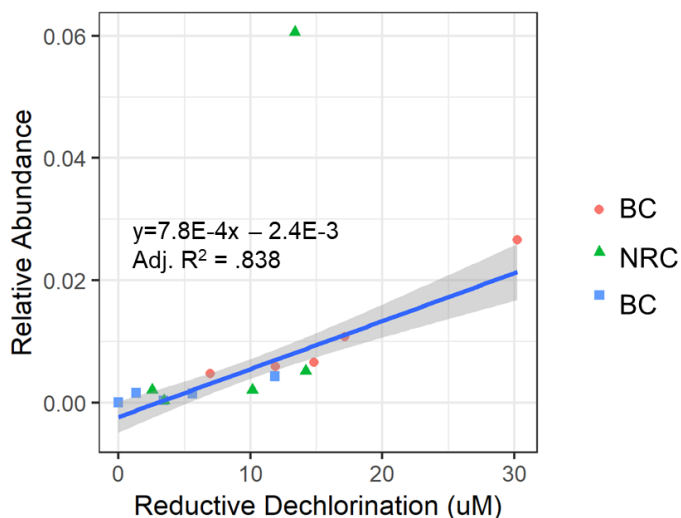
Figure 3.9. Correlation between *Dehalobacter* porewater relative abundance at the 50% sample port and the average measured reductive dechlorination in each experimental phase. Linear regression includes all data points except the outlier at the top of the plot. Shaded region represents 95% confidence interval of the regression.

Based on the increasing aerobic CB degradation observed in NRC, we identified *Novosphingobium* and an Unspecified Burkholderiaceae OTU as likely aerobic degraders. Interestingly, neither of these OTUs were detected within the aerobic inoculum culture.

101

Relative abundances of both genera qualitatively increased with increasing nitrate doses in

Phases II-IV (Figure 3.10). However, their abundances remained relatively low in BC and

SRC, not showing discernable trends over time. Unlike *Dehalobacter*, there was no

identified quantitative correlation between the abundances of these genera and the aerobic

degradation activity (Figure 3.11). While there was a monotonic increase in

Novosphingobium abundance with aerobic degradation in NRC, it was not linear (Figure

3.11a). This result is not entirely surprising since aerobic CB degraders tend to also be

heterotrophic generalists with additional function capacity for CB degradation [34, 47].

Therefore, abundances could potentially be influenced by consumption of other organic

substrates present. In contrast, *Dehalobacter* is a strict OHRB that can only reduce

halogenated substrates, limiting growth to highly specific substrates. Additionally, it is

possible that other unidentified degraders were abundant in BC and SRC; however, these

could not be determined from this experiment.
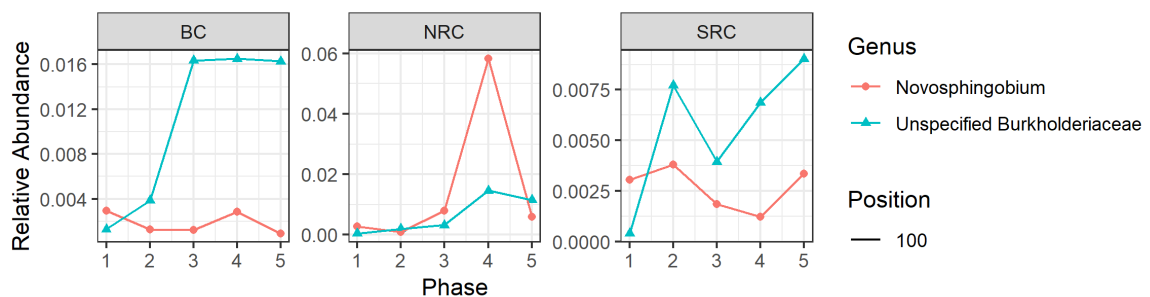
Figure 3.10. Relative abundance profiles of potential aerobic CB degraders at 100% porewater sample port during steady-state operation of each experimental phase. Each datapoint represents the average of 2 samples with the exception of BC Phases II, III, and V.
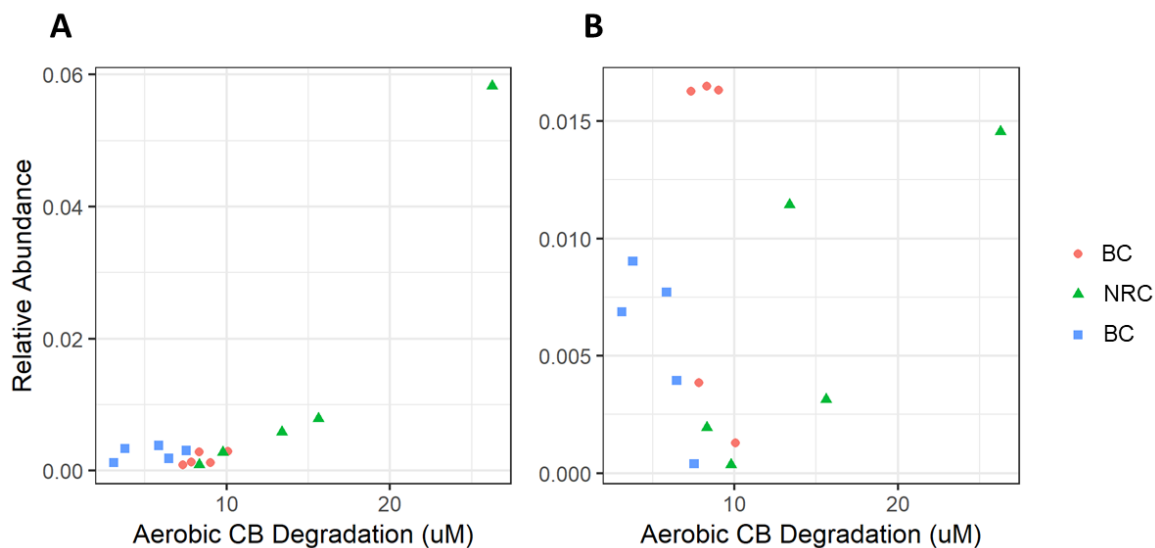
Figure 3.11. Relative abundances of potential aerobic degraders (A) *Novosphingobium* and (B) Unspecified Burkholderiaceae at 100% sample port vs. average measured aerobic degradation in each experimental phase.

In this experiment, porewater relative abundances of key organisms provided a useful confirmation of observed geochemical measurements. Similar associations were observed by others in fill-and-draw reactors with different retention times for a defined TCE dechlorinating community [48]. In our study, it was assumed that the observed communities were at a functional steady-state between cell growth and decay and cells released into the porewater were not the result of transient changes between experimental phases. However, we cannot eliminate the possibility that some of the observed community members in porewater samples the result of slow, transient shifts occurring in the biofilm. For field applications, 16S sequencing groundwater samples at multiple timepoints and locations may be prohibitively expensive and time-consuming with no guarantee of positively identifying functionally-relevant organisms compared to this closed, controlled system. Additionally, direct measurement of redox indicators such as sulfate, sulfide, nitrate, nitrite, ammonia, and iron can be analyzed faster, at less cost, and with more certainty than microbial analysis. However, these indicators may be difficult to measure

103

with high spatial resolution. Greater value may be derived from quantification of niche specialists such as OHRB compared to metabolic generalists, as shown in our quantification of *Dehalobacter* (Figure 3.9). Though 16S copy number is already frequently used as a qualitative predictor of biodegradation potential [49], it is currently not viewed as a particularly reliable quantitative predictor of absolute metabolic activity in the field [50]. With a better prior understanding of the diversity of organisms occurring in a system and their functionality, targeting conserved functional genes such as reductive dehalogenases [51] and ring oxidizing dioxygenases [52] through qPCR may be a more viable means to quantify CB degradation activity in the field. Identifying such functional genes specific to CB biodegradation remains an important research need.

3.4.5.4   Biofilm Microbial Communities

Sacrificial sampling at the end of the experiment (Phase V) revealed descriptive spatial trends between columns under baseline and moderately nitrate- and sulfate-reducing conditions (0.5 mM). Columns were divided into four sequential segments labeled 1-4 from influent to effluent; segments 1 and 2 represented the anaerobic zone, segment 3 represented the transition from anaerobic to aerobic conditions, and segment 4 represented the aerobic zone (Figure B.2). Bulk DNA extracted from each of the four vertical sand segments provided an approximation of the biomass density along the OAI (Figure 3.12). All biological columns showed greatest anaerobic zone DNA concentration in the bottom segment (1) followed by a 1-log decrease in concentrations, indicating the majority of biological activity occurred close to the column entrance. Notably, NRC had over 8-fold greater biomass in segment 1 compared to BC or SRC, reflective of the much higher energy yield available to bacteria with nitrate reduction compared to sulfate reduction or

fermentation. After addition of oxygen, biomass densities increased in segment 4, which were similar between all biological columns (Figure 3.12).

Community structure within columns, based on weighted Unifrac distances [53], showed a strong bifurcation along the anaerobic-aerobic interface (Figure 3.13). In BC and SRC, anaerobic segments (1, 2) were separated from aerobic segments (3, 4) along the first principal coordinate (61.2% of explained difference). NRC segments did not show as substantial separation between anaerobic and aerobic conditions. Rather, they clustered more closely to the BC and SRC aerobic samples, with segment 1 separated from segments 2-4 along the second principal coordinate (Figure 3.13).
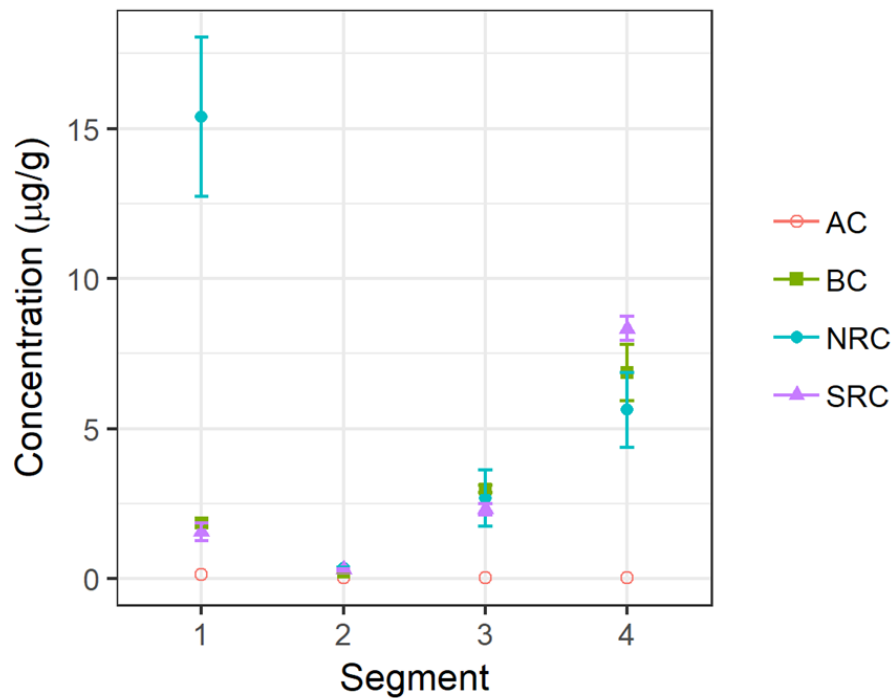
Figure 3.12. Distribution of DNA through sacrificial column segmentation. Error bars represent ±1 SD for duplicate BC, NRC, and SRC measurements. Only a single measurement was taken for AC.
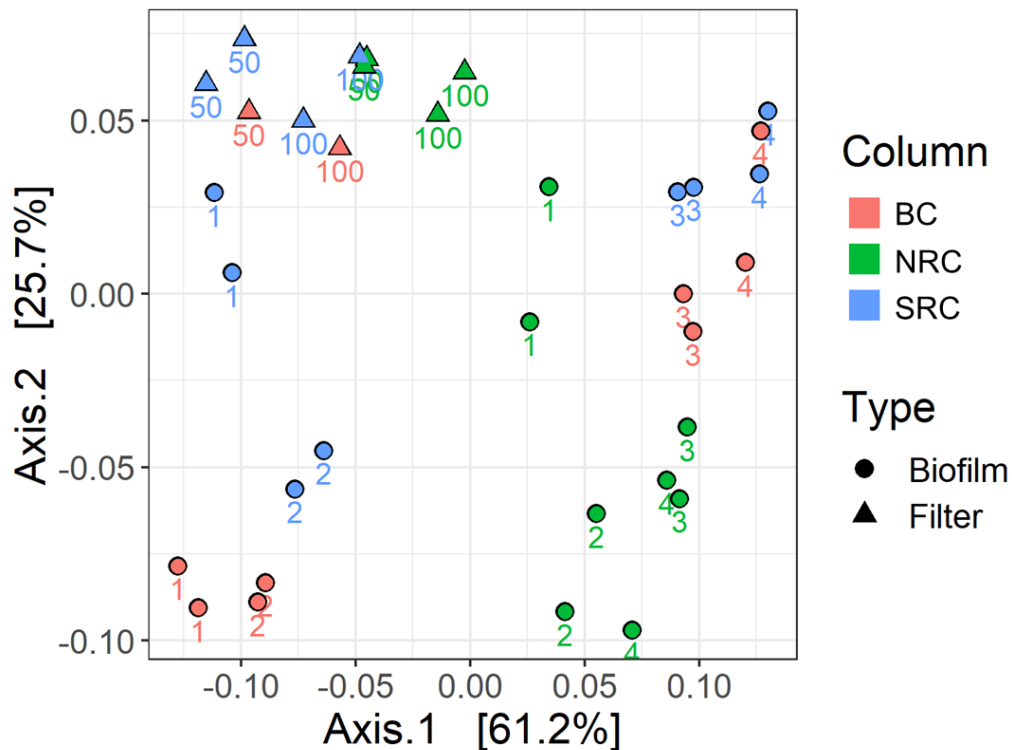
Figure 3.13. Principal coordinate analysis of Weighted Unifrac distances between biofilm and porewater (Filter) samples sampled at the end of the experiment in Phase V. Biofilm samples were segmented from 1 to 4 from bottom to top in duplicate. Porewater samples were collected at 50% and 100% of column length in duplicate (except for BC; n=1). The first two axes (displayed) explain 86.9% of sample distances.

A genus-level taxonomic plot of the four columns is presented in Figure B.16 of Appendix B showing the most abundant genera in each column. Functionally relevant organisms identified in column porewater were also identified and profiled along the lengths of each column (Figure B.17, Figure B.18). These profiles were confirmatory of all of the observed porewater trends observed in Phase V. Despite the porewater carrying similar patterns for individual functional bacteria, the overall community structures (based on weighted abundances) were distinctly different between biofilm and porewater. Comparing porewater samples and biofilm samples taken in Phase V for all columns (Figure 3.13), there was significant clustering of all porewater samples distinct from biofilm samples (p=0.0323, Adonis PERMANOVA test; 10,000 permutations). In contrast, ordination of Unweighted Unifrac distances, measuring qualitative community

composition, did not cluster based on sample type (Figure 3.14). Rather, all samples generally clustered by column and redox zone (anaerobic = 1, 2, 50% samples; aerobic = 3, 4, 100% samples; Figure 3.14). This is in agreement with the past literature comparing biofilm and planktonic groundwater microbial communities. These studies found that porewater communities represent some subset of the total biofilm population, but in lower and typically unpredictably different relative abundances [54, 55]. A multitude of physiological and environmental conditions such as attachment energy, shear stress, and cell growth can influence the distribution of cell mass between phases [36]. Because cell densities are typically orders of magnitude higher in biofilm than in porewater [56], an inter-taxonomic comparison of porewater abundances between phases may not be representative of changes within the actual biofilm. However, comparing porewater abundance changes for individual organisms between phases, as conducted with the functional degraders in Section 3.4.5.3, may be a more valid representation of changes within the biofilm. Since the partitioning of a specific organism between biofilm and porewater would be expected to be relatively constant throughout the experiment given uniform physiological characteristics and column hydrodynamics, changes in abundance over time would signal proportional changes occurring in the biofilm as well.
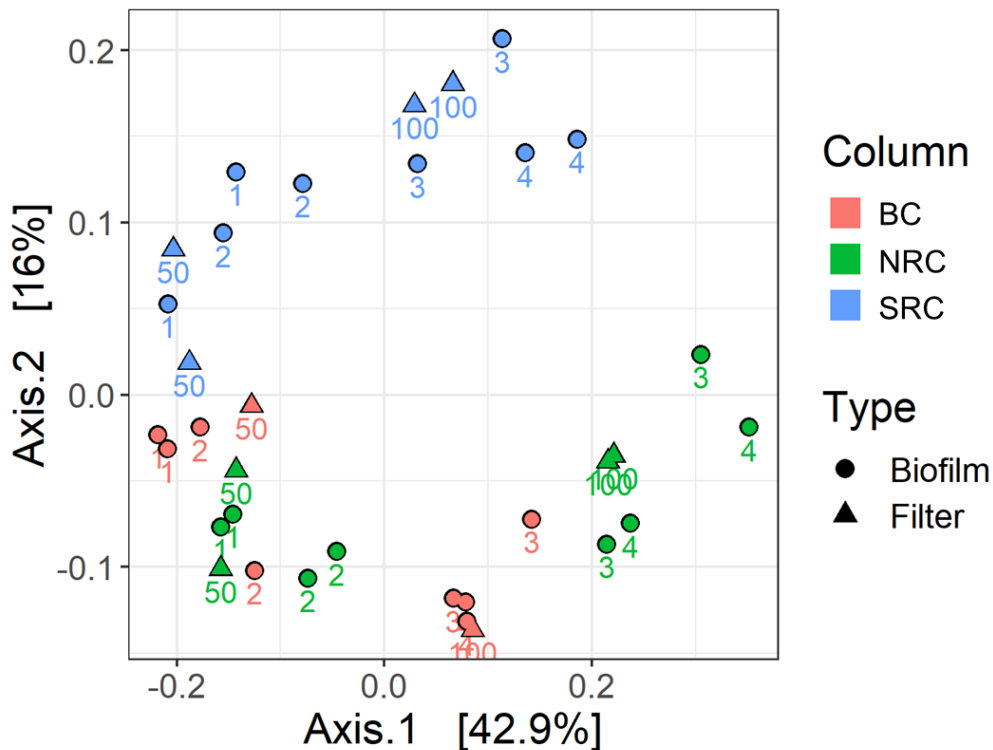
Figure 3.14. Principal coordinate analysis of Unweighted Unifrac distances between biofilm and porewater (Filter) samples sampled at the end of the experiment in Phase V. Biofilm samples were segmented from 1 to 4 from bottom to top in duplicate. Porewater samples were collected at 50% and 100% of column length in duplicate (except for BC; n=1). The first two axes (displayed) explain 58.9% of sample distances.

3.4.6 Impacts of Alternative Electron Acceptors on Reductive Dechlorination

In the SRC, reductive dechlorination was negatively impacted by sulfate doses of at least 0.5 mM and completely suppressed at 10 mM (Figure 3.3). Prior literature on CB dechlorination had reported varying outcomes from sulfate addition. Bosma et al. (1988) found that reductive dechlorination of low micromolar concentrations of TCBs and DCBs proceeded without issue in sediment columns with approximately 20 mM sulfate [57]. Adrian et al. (1998) found that low (1 mM) sulfate stimulated reductive dechlorination in batch, serving as a necessary source of elemental S [58]. However, Chang et al. (1998) and Adrian et al. found that increasing sulfate concentrations (0.02-0.5 mM and 2-7 mM respectively) delayed CB dechlorination until after sulfate was reduced and inhibited

dechlorination when sulfate was in excess [58, 59]. Work by Pantazidouof et al. (2011) combined observations from multiple field sites and laboratory tests and found generally decreasing TCE dechlorination with increasing sulfate concentration [60]. That study also found that under electron donor excess, dechlorination was delayed in the presence of sulfate; but under electron donor limitation, dechlorination activity decreased up to 50% [60].

Our results appear to be in agreement with these observations of decreased dechlorination activity under increasing sulfate excess and electron-donor limitation. Residual propionate was observed in SRC at 0.15- and 0.5-mM sulfate doses, indicating a pool of electron donor was still available to drive sulfate- and CB reduction (Figure 3.6). Propionate fermentation can produce the H_2 needed for sulfate-reduction and CB-reduction as described in Equation 3.4, but is not energetically favorable under standard conditions (ΔG_0'=+76.1 kJ/reaction) [61].

Equation 3.4

$$Propionate + 3\ H_2O \rightarrow Acetate + HCO_3^- + H^+ + 3H_2$$

However, increased sulfate dose co-occurred with increased sulfate reduction and depletion of excess propionate, suggesting higher sulfate drove consumption of H_2 to levels below the required threshold of 10^{-6}-10^{-4} atm to drive the reaction in Equation 3.4 forward [61]. This supports that notion that under increasing sulfate concentrations, SRB out-competed OHRB for limiting H_2. Despite OHRB generally having a higher affinity than SRB for low concentrations of H_2 [16, 19], slow growth of OHRB compared to other organisms can put them at a competitive disadvantage if they cannot limit H_2 concentrations below thresholds required to prevent sulfate reduction.

Sulfide toxicity is another mechanism of dechlorination inhibition that warrants consideration. Recent work by Mao et al. (2017) systematically investigated sulfur inhibition in a TCE dechlorinating triculture with *Dehalococcoides mccartyi* and found that high concentrations of sulfide (5 mM) were directly responsible for reductive dechlorination inhibition, and not sulfate itself; sulfide was believed to inactivate metal-containing enzymes such as dehalogenases [11]. Though we did not directly measure sulfide, no more than 0.5 mM of sulfate was reduced at any sulfate dose in SRB (Table 3.4). Additionally, Adrian et al. (1998) did not note inhibition of CB dechlorination in the presence of 1 mM sulfide [58]. This suggests that in our donor-limited system, sulfide toxicity may not have been a factor. However, in systems where sulfate concentrations are high and electron donor is in excess, the production of excess sulfide could be inhibitory.

In NRC, the generally decreasing reductive dechlorination activity with increasing nitrate dose was expected based on prior literature. Reductive CB dechlorination has rarely been observed under denitrifying conditions [58, 59, 62], and it has generally required prior depletion of nitrate before proceeding due to much more favorable energetics of nitrate-reducing organisms [63]. With specific regard to CBs, limited studies of nitrate-reducing conditions found no reductive dechlorination in the presence of excess (5 mM) [62] nor limiting (0.2-0.6 mM) nitrate [57, 59]. Additionally, it was found by others that intermediate gaseous nitrate reduction products NO and N_2O can also cause toxic inhibition of OHRB when nitrate is at low millimolar concentrations through interference with iron-containing proteins [18]. Regardless of the mode of inhibition, it was clear that high nitrate concentrations were not conducive to enhanced dechlorination.

At the end of Phase IV, it was therefore surprising that reductive dechlorination activity increased from 0 despite an excess of nearly 1.5 mM nitrate (Figure 3.1). A potential explanation for the dechlorination activity could be the development of a thick biofilm coating along the surface area of the sand matrix. At the end of the Phase IV tracer test, we observed an 8%-12% decrease in porosity compared to the empty bed and Phase V tracer test (Table B.6); additionally the bulk DNA profile of NRC at column harvest showed greater DNA concentrations (and likely cell mass) compared to other columns (Figure 3.12). Both points suggest enhanced biofilm mass could have developed under nitrate excess. *Dehalobacter* and other syntrophic organisms could have persisted under nitrate-free protected microniches deeper in the biofilm in a similar manner to methanogenic bacteria in anaerobic granules [64]. Even though nitrate-reducing bacteria were assumed to have utilized all of the available electron donor dosed to the column, decay of biomass within the film could potentially provide a local source of electron donor for dechlorination. Decaying biomass has been shown by others to be a viable source of electron donor for OHRB consortia [65, 66].

3.4.7   *Impacts of Alternative Electron Acceptors on Aerobic Degradation*

In the SRC, increased sulfate reduction was accompanied by increased sulfur oxidation and decreased CB oxidation in the aerobic zone (Table 3.4). Theoretically, in the absence of an unreactive electron sink, similar fluxes of electron carriers should move from the anaerobic zone to the aerobic zone at steady-state in both BC and SRC. In BC, these equivalents were delivered primarily as acetate, propionate, and methane (Figure 3.4), while in SRC they were delivered as reduced sulfur, acetate, propionate, and methane (Figure 3.6). Consequently, the reduced compounds entering the aerobic zones of the

columns should exhibit similar degrees of oxygen demand, but distributed among different reduced carriers. The fact that aerobic CB degradation was inhibited in SRC at high sulfate doses but not in BC suggests that the sulfur oxidizers could more effectively compete for limiting oxygen than CB oxidizers. This was reflected in the biofilm composition of columns in Phase V, where relative abundances of sulfur-oxidizing *Thiobacillus* were greater in SRC compared to BC but CB-oxidizing *Novosphingobium* were much lower (Figure B.18). A preference for oxidation of sulfur over other substrates had previously been described by Hatamoto et al. (2012) in a treatment system for anaerobic waste [67]. Under conditions of oxygen excess, sulfur oxidation co-occurred with methane, ammonia, and COD oxidation; however under oxygen-limiting conditions, sulfur-oxidation outcompeted methane and ammonia oxidation [67]. Similarly, Matsuura et al. (2010) found that sulfur-oxidizing bacteria had a high oxygen affinity even in microaerophilic conditions; in a downflow reactor, sulfur oxidation preceded both organic carbon and methane oxidation activity [68]. Our previous results in Chapter 2 also support that sulfur-oxidizing bacteria have a higher affinity for oxygen than CB degraders. Immediately after the introduction of oxygen in packed columns, sulfate-oxidizing *Thiobacillus* abundances increased log-fold along the column flowpath before similar increases occurred in CB-oxidizing organisms (Figure 2.6a, b). These results suggest that sulfur-oxidizing bacteria may be more effective in outcompeting CB-degraders for oxygen than other competing heterotrophic bacteria.

The presence of anaerobic nitrate-reducing conditions showed greatly enhanced CB degradation at OAIs. Under excess nitrate in Phase IV (2.5 mM), near complete-removal of the 26.3 µM (4.8 mg/L) 1,2,4-TCB entering the aerobic zone was degraded with residual

oxygen remaining in the column (Table 3.3). With approximately 5 mg/L (156 μM) DO consumed, the observed oxygen utilization of 5.9 mol O_2 per mol 1,2,4-TCB was nearly equal to the theoretical TCB utilization of 6 mol/mol (Equation 3.5).

Equation 3.5

$$C_6H_3Cl_3 + 6O_2 \rightarrow 6CO_2 + 3H^+ + 3Cl^-$$
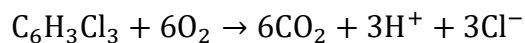
Although we did not observe any CB oxidation directly under nitrate-reducing conditions, in agreement with past literature [21, 69, 70], nitrate was able facilitate oxidation of competing electron donors and conserve limiting oxygen for CB degradation. Despite nitrate reduction having apparent detrimental effects on reductive dechlorination, CB oxidation still proceeded for 1,2,4-TCB. This reinforces findings from Chapter 2 that reductive dechlorination was not a necessary step to facilitate aerobic degradation. In fact, from an oxygen-limiting standpoint, it may be beneficial to inhibit reductive dechlorination activity to facilitate greater oxidative yield. Based on theoretical oxygen demand, only 6 mol O_2 are required to completely oxidize TCB, compared to 6.5 and 7 mol O_2 for more highly reduced DCBs and MCBs.

Despite the inability for CB to oxidize under strict nitrate-reducing conditions, a laboratory study by Nestler et al. (2007) suggested the potential for nitrate to enhance CB degradation under oxygen-limiting aerobic conditions [41]. Using sensitive oxygen sensors to maintain and measure micromolar dissolved oxygen concentrations, they found nitrate addition reduced total oxygen demand by 16% compared to an unamended control, with nitrate utilization occurring simultaneously with CB degradation; nitrate was also able to degrade aliphatic chloromuconate, a CB ring-fission product under anoxic conditions [41]. Under their proposed model, oxygen is exclusively required by ring-hydroxylating

dioxygenases to activate the aromatic structure for ring cleavage. However, the oxygen needed as a terminal electron acceptor for metabolism of aliphatic products could be replaced by nitrate. Follow-up field studies by co-authors were not able to replicate this result [71], and to our knowledge no other studies have re-addressed this finding. Under nitrate excess (Phase IV) in our experiment, no degradation was observed in the anaerobic zone of NRC. However, in the aerobic zone we did notice significant ($p<.05$), but highly variable 59 ± 44 μM disappearance of nitrate in the aerobic zone despite apparent utilization of nearly all organic acid and no sulfate reduction occurring (Table 3.3, Figure B.5). This raises the possibility that nitrate may have also been utilized in small amounts in addition to oxygen to facilitate complete CB oxidation. On the other hand, other potentially unquantified reduced compounds such as precipitated iron sulfide, may have also led to additional nitrate reduction in the aerobic zone (or in the short distance in the anaerobic zone between the 50% port and the oxygen injection port). While not conclusive, this observation provides some anecdotal support of Nestler and others' paradigm, which may warrant additional study.

3.4.8   Remediation Implications

Results from this experiment have expanded our understanding of bioremediation potential at the OAI to include redox effects (NRC, SRC) as well as long-term stability in an unmodified system (BC). In the Chapter 2 column experiments, we periodically increased the dose of influent NaLac into the column, which re-stimulated degradation activity. This caused some uncertainty whether degradation could be maintained long-term in an unperturbed system. Results from the BC, where influent conditions were held constant for nearly a year, showed high degradation stability over time at constant NaLac

input. Using sand as an inert growth matrix and a completely defined synthetic media, we conducted the experiment under a "base-case" scenario, where potential benefits of attachment [36] and additional nutrient availability [72] from sediment and site water were eliminated. In contrast to more site-specific experiments, this study should have high potential for reproducibility, with well-defined experiment parameters. One unexplained change observed in all columns was the shift to more methanogenic conditions in Phases IV and V. While it is possible that growth and species succession may have occurred slowly over the course of the experiment, we cannot eliminate the possibility that an unknown change in input or operating conditions may have perturbed all of the systems.

The tracer test results demonstrated that the column hydrodynamics stayed generally stable over the entire column operation, without major changes in porosity or porewater velocity. Pore clogging due to biofilm development, gas evolution (e.g. N_2, methane), and mineral precipitation are notable potential problems for biostimulated remediation strategies, leading to preferential flow outside of treatment areas and decreased contact time in bioactive zones [9, 73, 74]. In our experiment, this did not appear problematic based on stable hydraulic tests and CB degradation. However, effects could potentially be more problematic in less porous finer-grain media such as clay sediments found in wetlands and at higher substrate concentrations.

Results from this experiment suggest that nitrate could be a viable amendment to aid aerobic degradation at OAIs. Nitrate injection has been used previously in field trials to stimulate anaerobic degradation for reduced contaminants such as BTEX at contaminated groundwater sites [8, 9, 75, 76]. However, use of nitrate as a remediation amendment in shallow wetland sites such as SCD must also be weighed against known

ecological and health concerns such as hypoxia and algal blooms in surface water as well as contamination of drinking water sources [77-79]. Nitrate is regulated to 10 mg/L NO_3^--N (0.7 mM) in drinking water by the EPA (MCL) due to known human health effects related to methemoglobinemia, especially in infants [79, 80]. Through careful oxygen demand measurements and amendment dosing, it may be possible to make highly anaerobic groundwater much more amenable to aerobic degradation at OAIs using nitrate. Excess sulfate present at a site would appear to be challenging for CB bioremediation remediation, especially if accompanied by high concentrations of reduced sulfur compounds. Nitrate has been used previously to remove sulfide generated at waste sites [75], and conceivably be used to oxidize reduced sulfur. However, the cost of impacts of the required dose must be considered.

While observed effects on degradation pathways were largely in agreement with concepts found for other contaminants such as TCE, the current remediation challenge is unique for CBs. With chlorinated ethenes, complete anaerobic reductive dechlorination to ethene is a feasible and desirable end-goal [81]. Therefore, there is incentive to further amend sites with electron donor to overcome competing electron acceptors and stimulate dechlorination. In contrast, bioremediation of CBs is currently contingent upon successful aerobic degradation. Results here emphasize that maximizing oxygen availability for CB degradation can drastically enhance remediation outcome. Prior studies have shown that vegetation [82-84] and groundwater saturation conditions [85] can have a profound impact on oxygen availability and aerobic CB degradation. Future research should consider how these factors can affect redox cycling in aerobic sites and potentially enhance CB degradation at OAIs.

3.5 Conclusions

- Anaerobic CB reductive dechlorination and aerobic CB degradation were maintained stably in a completely defined, controlled sand column system over a period of a year. Reductive dechlorination was characterized by low (<1%) utilization of dosed electron donor (0.55 mM NaLac) and relatively low degrees of reductive dechlorination activity. Residual products from "side-reactions" (sulfate reduction, acidogenesis, methanogenesis) exerted oxygen demand in the column aerobic that limited downgradient aerobic CB degradation.

- Increased sulfate-reducing conditions in SRC were detrimental to anaerobic and aerobic CB degradation processes with limited electron donor input. Significant changes ($p<.05$) in steady-state performance were observed at doses of at least 0.5 mM sulfate, and both pathways showed near-complete inhibition at 10 mM. Increased aerobic re-oxidation of reduced sulfur to sulfate appeared to outcompete aerobic CB degradation for limiting oxygen.

- Increased nitrate-reducing conditions in NRC were detrimental to reductive dechlorination at doses of at least 0.5 mM nitrate and led to complete inhibition at 2.5 mM. Preferential use of nitrate as an anaerobic electron acceptor prevented formation of competitive reduced substrates that could be oxidized in the aerobic zone. Under nitrate excess (2.5 mM), near complete aerobic degradation of 26.3 µM (3.8 mg/L) 1,2,4-TCB occurred with residual oxygen still remaining in column effluent. Nitrate may be useful as an alternate electron acceptor for other site substrates to conserve limited oxygen available at OAIs for aerobic CB oxidation.

- Similar to findings in Chapter 2, reductive dechlorination of 1,2,4-TCB did not increase aerobic degradability in this experiment. Under optimal aerobic degrading conditions (NRC Phase IV), 95% of 1,2,4-TCB was degraded, with oxygen utilization (5.9 mol O_2/mol CB) nearly equal to theoretical value of 6. More dechlorinated CBs require additional O_2 to facilitate mineralization, suggesting a disadvantage of dechlorinated daughter products under oxygen-limited conditions.

- Relative abundances of specific functionally-associated microbial genera in column porewater related to sulfate, nitrate, methane, and CB transformations were qualitatively reflective of the observed chemical shifts during operation. Spatial and inter-column differences for specific taxa were in agreement between biofilm and porewater samples at the end of the experiment (Phase V). However, overall community compositional structures were distinct between sample type, suggesting porewater taxonomic structure would not be reflective of the majority of microbial activity within biofilms.

3.6   References

1. Brune, A.; Frenzel, P.; Cypionka, H., Life at the oxic-anoxic interface: microbial activities and adaptations. *FEMS Microbiol Rev* **2000,** *24*, (5), 691-710.
2. Babcsányi, I.; Meite, F.; Imfeld, G., Biogeochemical gradients and microbial communities in Winogradsky columns established with polluted wetland sediments. *FEMS Microbiology Ecology* **2017,** *93*, (8).
3. Wakida, F. T.; Lerner, D. N., Non-agricultural sources of groundwater nitrate: a review and case study. *Water Research* **2005,** *39*, (1), 3-16.
4. Forster, S. S. D.; Cripps, A. C.; Smith-Carington, A.; Stewart William Duncan, P.; Rosswall, T., Nitrate leaching to groundwater. *Philosophical Transactions of the Royal Society of London. B, Biological Sciences* **1982,** *296*, (1082), 477-489.
5. Power, J. F.; Schepers, J. S., Nitrate contamination of groundwater in North America. *Agriculture, Ecosystems & Environment* **1989,** *26*, (3), 165-187.
6. Rittmann, B. E.; McCarty, P. L., *Environmental biotechnology: principles and applications*. McGraw-Hill: New York, 2001; Vol. 173, p 755.
7. Tiedje, J. M., Ecology of denitrification and dissimilatory nitrate reduction to ammonium. *Biology of anaerobic microorganisms* **1988,** *717*, 179-244.
8. Cunningham, J. A.; Rahme, H.; Hopkins, G. D.; Lebron, C.; Reinhard, M., Enhanced In Situ Bioremediation of BTEX-Contaminated Groundwater by Combined Injection of Nitrate and Sulfate. *Environmental Science & Technology* **2001,** *35*, (8), 1663-1670.

9. Da Silva, M. L. B.; Ruiz-Aguilar, G. M. L.; Alvarez, P. J. J., Enhanced anaerobic biodegradation of BTEX-ethanol mixtures in aquifer columns amended with sulfate, chelated ferric iron or nitrate. *Biodegradation* **2005,** *16*, (2), 105-114.

10. Zeyer, J.; Kuhn, E. P.; Schwarzenbach, R. P., Rapid Microbial Mineralization of Toluene and 1,3-Dimethylbenzene in the Absence of Molecular Oxygen. *Applied and Environmental Microbiology* **1986,** *52*, 944-947.

11. Mao, X.; Polasko, A.; Alvarez-Cohen, L., Effects of Sulfate Reduction on Trichloroethene Dechlorination by Dehalococcoides-Containing Microbial Communities. *Applied and Environmental Microbiology* **2017,** *83*, e03384-16.

12. Miao, Z.; Brusseau, M. L.; Carroll, K. C.; Carreón-Diazconti, C.; Johnson, B., Sulfate reduction in groundwater: characterization and applications for remediation. *Environmental Geochemistry and Health* **2012,** *34*, (4), 539-550.

13. Schwarzenbach, R. P.; Gschwend, P. M.; Imboden, D. M., *Environmental organic chemistry*. 2nd ed. ed.; Wiley,: Hoboken, N.J., 2003.

14. Field, J. A.; Sierra-Alvarez, R., Microbial degradation of chlorinated benzenes. *Biodegradation* **2007,** *19*, 463-480.

15. Fung, J. M.; Weisenstein, B. P.; Mack, E. E.; Vidumsky, J. E.; Ei, T. A.; Zinder, S. H., Reductive Dehalogenation of Dichlorobenzenes and Monochlorobenzene to Benzene in Microcosms. *Environmental Science & Technology* **2009,** *43*, (7), 2302-2307.

16. Yang, Y.; McCarty, P. L., Competition for Hydrogen within a Chlorinated Solvent Dehalogenating Anaerobic Mixed Culture. *Environmental Science & Technology* **1998,** *32*, (22), 3591-3597.

17. Nelson, D. K.; Hozalski, R. M.; Clapp, L. W.; Semmens, M. J.; Novak, P. J., Effect of Nitrate and Sulfate on Dechlorination by a Mixed Hydrogen-Fed Culture. *Bioremediation Journal* **2002,** *6*, (3), 225-236.

18. Okutman Tas, D.; Pavlostathis, S. G., Effect of Nitrate Reduction on the Microbial Reductive Transformation of Pentachloronitrobenzene. *Environmental Science & Technology* **2008,** *42*, (9), 3234-3240.

19. Aulenta, F.; Beccari, M.; Majone, M.; Papini, M. P.; Tandoi, V., Competition for H2 between sulfate reduction and dechlorination in butyrate-fed anaerobic cultures. *Process Biochemistry* **2008,** *43*, (2), 161-168.

20. Berggren, D. R. V.; Marshall, I. P. G.; Azizian, M. F.; Spormann, A. M.; Semprini, L., Effects of Sulfate Reduction on the Bacterial Community and Kinetic Parameters of a Dechlorinating Culture under Chemostat Growth Conditions. *Environmental Science & Technology* **2013,** *47*, (4), 1879-1886.

21. Vogt, C.; Alfreider, A.; Lorbeer, H.; Hoffmann, D.; Wuensche, L.; Babel, W., Bioremediation of chlorobenzene-contaminated ground water in an in situ reactor mediated by hydrogen peroxide. *Journal of Contaminant Hydrology* **2004,** *68*, 121-141.

22. Kurt, Z.; Shin, K.; Spain, J. C., Biodegradation of Chlorobenzene and Nitrobenzene at Interfaces between Sediment and Water. *Environmental Science & Technology* **2012,** *46*, 11829-11835.

23. Atashgahi, S.; Maphosa, F.; Dogan, E.; Smidt, H.; Springael, D.; Dejonghe, W., Small-scale oxygen distribution determines the vinyl chloride biodegradation pathway in surficial sediments of riverbed hyporheic zones. *FEMS Microbiol Ecol* **2013,** *84*, (1), 133-42.

24. Jørgensen, B. B.; Postgate John, R.; Postgate John, R.; Kelly, D. P., Ecology of the bacteria of the sulphur cycle with special reference to anoxic—oxic interface environments. *Philosophical Transactions of the Royal Society of London. B, Biological Sciences* **1982,** *298*, (1093), 543-561.

25. da Silva, M. L. B.; Corseuil, H. X., Groundwater microbial analysis to assess enhanced BTEX biodegradation by nitrate injection at a gasohol-contaminated site. *International Biodeterioration & Biodegradation* **2012,** *67*, 21-27.

26. Lorah, M. M.; Walker, C. W.; Baker, A. C.; Teunis, J. A.; Majcher, E. H.; Brayton, M. J.; Raffensperger, J. P.; Cozzarelli, I. M. *Hydrogeologic characterization and assessment of bioremediation of chlorinated benzenes and benzene in wetland areas, Standard Chlorine of Delaware, Inc. Superfund Site, New Castle County, Delaware, 2009-12*; 2328-0328; US Geological Survey: 2014.

27. Burns, M.; Sublette, K. L.; Sobieraj, J.; Ogles, D.; Koenigsberg, S., Concurrent and Complete Anaerobic Reduction and Microaerophilic Degradation of Mono-, Di-, and Trichlorobenzenes. *Remediation Journal* **2013,** *23*, (3), 37-53.

28. Preheim, S. P.; Olesen, S. W.; Spencer, S. J.; Materna, A.; Varadharajan, C.; Blackburn, M.; Friedman, J.; Rodríguez, J.; Hemond, H.; Alm, E. J., Surveys, simulation and single-cell assays relate function and phylogeny in a lake ecosystem. *Nature Microbiology* **2016,** *1*, 16130.

29. Bolyen, E.; Rideout, J. R.; Dillon, M. R.; Bokulich, N. A.; Abnet, C.; Al-Ghalith, G. A.; Alexander, H.; Alm, E. J.; Arumugam, M.; Asnicar, F.; Bai, Y.; Bisanz, J. E.; Bittinger, K.; Brejnrod, A.; Brislawn, C. J.; Brown, C. T.; Callahan, B. J.; Caraballo-Rodríguez, A. M.; Chase, J.; Cope, E.; Da Silva, R.; Dorrestein, P. C.; Douglas, G. M.; Durall, D. M.; Duvallet, C.; Edwardson, C. F.; Ernst, M.; Estaki, M.; Fouquier, J.; Gauglitz, J. M.; Gibson, D. L.; Gonzalez, A.; Gorlick, K.; Guo, J.; Hillmann, B.; Holmes, S.; Holste, H.; Huttenhower, C.; Huttley, G.; Janssen, S.; Jarmusch, A. K.; Jiang, L.; Kaehler, B.; Kang, K. B.; Keefe, C. R.; Keim, P.; Kelley, S. T.; Knights, D.; Koester, I.; Kosciolek, T.; Kreps, J.; Langille, M. G. I.; Lee, J.; Ley, R.; Liu, Y.-X.; Loftfield, E.; Lozupone, C.; Maher, M.; Marotz, C.; Martin, B. D.; McDonald, D.; McIver, L. J.; Melnik, A. V.; Metcalf, J. L.; Morgan, S. C.; Morton, J.; Naimey, A. T.; Navas-Molina, J. A.; Nothias, L. F.; Orchanian, S. B.; Pearson, T.; Peoples, S. L.; Petras, D.; Preuss, M. L.; Pruesse, E.; Rasmussen, L. B.; Rivers, A.; Robeson, I. I. M. S.; Rosenthal, P.; Segata, N.; Shaffer, M.; Shiffer, A.; Sinha, R.; Song, S. J.; Spear, J. R.; Swafford, A. D.; Thompson, L. R.; Torres, P. J.; Trinh, P.; Tripathi, A.; Turnbaugh, P. J.; Ul-Hasan, S.; van der Hooft, J. J. J.; Vargas, F.; Vázquez-Baeza, Y.; Vogtmann, E.; von Hippel, M.; Walters, W.; Wan, Y.; Wang, M.; Warren, J.; Weber, K. C.; Williamson, C. H. D.; Willis, A. D.; Xu, Z. Z.; Zaneveld, J. R.; Zhang, Y.; Zhu, Q.; Knight, R.; Caporaso, J. G., QIIME 2: Reproducible, interactive, scalable, and extensible microbiome data science. *PeerJ Preprints* **2018,** *6*, e27295v2.

30. Pedregosa, F.; Varoquaux, G.; Gramfort, A.; Michel, V.; Thirion, B.; Grisel, O.; Blondel, M.; Prettenhofer, P.; Weiss, R.; Dubourg, V.; Vanderplas, J.; Passos, A.; Cournapeau, D.; Brucher, M.; Perrot, M.; Duchesnay, É., Scikit-learn: Machine learning in Python. *Journal of machine learning research* **2011,** *12*, (Oct), 2825-2830.

31. Quast, C.; Pruesse, E.; Yilmaz, P.; Gerken, J.; Schweer, T.; Yarza, P.; Peplies, J.; Glöckner, F. O., The SILVA ribosomal RNA gene database project: improved data processing and web-based tools. *Nucleic Acids Research* **2012,** *41*, (D1), D590-D596.

32. Love, M. I.; Huber, W.; Anders, S., Moderated estimation of fold change and dispersion for RNA-seq data with DESeq2. *Genome Biology* **2014,** *15*, (12), 550.

33. Wintzingerode, F. v.; Selent, B.; Hegemann, W.; Göbel, U. B., Phylogenetic Analysis of an Anaerobic, Trichlorobenzene-Transforming Microbial Consortium. *Applied and Environmental Microbiology* **1999,** *65*, 283-286.

34. Spain, J. C.; Nishino, S. F., Degradation of 1,4-dichlorobenzene by a Pseudomonas sp. *Applied and Environmental Microbiology* **1987,** *53*, 1010-1019.

35. Jiang, X.-W.; Liu, H.; Xu, Y.; Wang, S.-J.; Leak, D. J.; Zhou, N.-Y., Genetic and biochemical analyses of chlorobenzene degradation gene clusters in Pandoraea sp. strain MCB032. *Archives of Microbiology* **2009,** *191*, 485-492.

36. Cápiro, N. L.; Wang, Y.; Hatt, J. K.; Lebrón, C. A.; Pennell, K. D.; Löffler, F. E., Distribution of Organohalide-Respiring Bacteria between Solid and Aqueous Phases. *Environmental Science & Technology* **2014,** *48*, (18), 10878-10887.

37. Matsumoto, M.; Nishimura, Y., Hydrogen production by fermentation using acetic acid and lactic acid. *Journal of Bioscience and Bioengineering* **2007,** *103*, (3), 236-241.

38. Pester, M.; Brambilla, E.; Alazard, D.; Rattei, T.; Weinmaier, T.; Han, J.; Lucas, S.; Lapidus, A.; Cheng, J.-F.; Goodwin, L.; Pitluck, S.; Peters, L.; Ovchinnikova, G.; Teshima, H.; Detter, J. C.; Han, C. S.; Tapia, R.; Land, M. L.; Hauser, L.; Kyrpides, N. C.; Ivanova, N. N.; Pagani, I.; Huntmann, M.; Wei, C.-L.; Davenport, K. W.; Daligault, H.; Chain, P. S. G.; Chen, A.; Mavromatis, K.; Markowitz, V.; Szeto, E.; Mikhailova, N.; Pati, A.; Wagner, M.; Woyke, T.; Ollivier, B.; Klenk, H.-P.; Spring, S.; Loy, A., Complete genome sequences of Desulfosporosinus orientis DSM765T, Desulfosporosinus youngiae DSM17734T, Desulfosporosinus meridiei DSM13257T, and Desulfosporosinus acidiphilus DSM22704T. *Journal of bacteriology* **2012,** *194*, (22), 6300-6301.

39. Achenbach, L. A.; Michaelidou, U.; Bruce, R. A.; Fryman, J.; Coates, J. D., Dechloromonas agitata gen. nov., sp. nov. and Dechlorosoma suillum gen. nov., sp. nov., two novel environmentally dominant (per)chlorate-reducing bacteria and their phylogenetic position. *International Journal of Systematic and Evolutionary Microbiology* **2001,** *51*, (2), 527-533.

40. Xu, J.; Trimble, J. J.; Steinberg, L.; Logan, B. E., Chlorate and nitrate reduction pathways are separately induced in the perchlorate-respiring bacterium Dechlorosoma sp. KJ and the chlorate-respiring bacterium Pseudomonas sp. PDA. *Water Research* **2004,** *38*, (3), 673-680.

41. Nestler, H.; Kiesel, B.; Kaschabek, S. R.; Mau, M.; Schlömann, M.; Balcke, G. U., Biodegradation of chlorobenzene under hypoxic and mixed hypoxic-denitrifying conditions. *Biodegradation* **2007,** *18*, (6), 755-767.

42. Peix, A.; Ramírez-Bahena, M.-H.; Velázquez, E., Historical evolution and current status of the taxonomy of genus Pseudomonas. *Infection, Genetics and Evolution* **2009,** *9*, (6), 1132-1147.

43. Smith, K. S.; Ingram-Smith, C., Methanosaeta, the forgotten methanogen? *Trends in Microbiology* **2007,** *15*, (4), 150-155.

44. PATEL, G. B.; SPROTT, G. D., Methanosaeta concilii gen. nov., sp. nov. ("Methanothrix concilii") and Methanosaeta thermoacetophila nom. rev., comb. nov.†. *International Journal of Systematic and Evolutionary Microbiology* **1990,** *40*, (1), 79-82.

45. Auman, A. J.; Stolyar, S.; Costello, A. M.; Lidstrom, M. E., Molecular Characterization of Methanotrophic Isolates from Freshwater Lake Sediment. *Applied and Environmental Microbiology* **2000,** *66*, (12), 5259-5266.

46. Finneran, K. T.; Johnsen, C. V.; Lovley, D. R., Rhodoferax ferrireducens sp. nov., a psychrotolerant, facultatively anaerobic bacterium that oxidizes acetate with the reduction of Fe(III). *International Journal of Systematic and Evolutionary Microbiology* **2003,** *53*, (3), 669-673.

47. Rapp, P.; Timmis, K. N., Degradation of Chlorobenzenes at Nanomolar Concentrations byBurkholderia sp. Strain PS14 in Liquid Cultures and in Soil. *Applied and Environmental Microbiology* **1999,** *65*, 2547-2552.

48. Ziv-El, M.; Popat, S. C.; Parameswaran, P.; Kang, D.-W.; Polasko, A.; Halden, R. U.; Rittmann, B. E.; Krajmalnik-Brown, R., Using electron balances and molecular techniques to assess trichoroethene-induced shifts to a dechlorinating microbial community. *Biotechnology and Bioengineering* **2012,** *109*, (9), 2230-2239.

49. Environmental Biotechnology Testing Lab.

50. Röling, W. F. M., Do microbial numbers count? Quantifying the regulation of biogeochemical fluxes by population size and cellular activity. *FEMS Microbiology Ecology* **2007,** *62*, (2), 202-210.

51. Payne, R. B.; Fagervold, S. K.; May, H. D.; Sowers, K. R., Remediation of polychlorinated biphenyl impacted sediment by concurrent bioaugmentation with anaerobic halorespiring and aerobic degrading bacteria. *Environmental science & technology* **2013,** *47*, (8), 3807-3815.

52. Dominguez, R. F.; Silva, M. L. B. d.; McGuire, T. M.; Adamson, D.; Newell, C. J.; Alvarez, P. J. J., Aerobic bioremediation of chlorobenzene source-zone soil in flow-through columns: performance assessment using quantitative PCR. *Biodegradation* **2007,** *19*, 545-553.

53. Lozupone, C.; Lladser, M. E.; Knights, D.; Stombaugh, J.; Knight, R., UniFrac: an effective distance metric for microbial community comparison. *The ISME Journal* **2011,** *5*, (2), 169-172.

54. Lehman, R. M.; Colwell, F. S.; Bala, G. A., Attached and Unattached Microbial Communities in a Simulated Basalt Aquifer under Fracture- and Porous-Flow Conditions. *Applied and Environmental Microbiology* **2001,** *67*, (6), 2799.

55. Holm, P. E.; Nielsen, P. H.; Albrechtsen, H. J.; Christensen, T. H., Importance of unattached bacteria and bacteria attached to sediment in determining potentials for degradation of xenobiotic organic contaminants in an aerobic aquifer. *Applied and Environmental Microbiology* **1992,** *58*, (9), 3020.

56. Alfreider, A.; Krössbacher, M.; Psenner, R., Groundwater samples do not reflect bacterial densities and activity in subsurface systems. *Water Research* **1997,** *31*, (4), 832-840.

57. Bosma, T. N. P.; Meer, J. R. v. d.; Schraa, G.; Tros, M. E.; Zehnder, A. J. B., Reductive dechlorination of all trichloro- and dichlorobenzene isomers. *FEMS Microbiology Ecology* **1988,** *4*, 223-229.

58. Adrian, L.; Manz, W.; Szewzyk, U.; Görisch, H., Physiological characterization of a bacterial consortium reductively dechlorinating 1, 2, 3-and 1, 2, 4-trichlorobenzene. *Applied and environmental microbiology* **1998,** *64*, (2), 496-503.

59. Chang, B.-V.; Su, C.-J.; Yuan, S.-Y., Microbial hexachlorobenzene dechlorination under three reducing conditions. *Chemosphere* **1998,** *36*, (13), 2721-2730.

60. Pantazidou, M.; Panagiotakis, I.; Mamais, D.; Zikidi, V., Chloroethene Biotransformation in the Presence of Different Sulfate Concentrations. *Groundwater Monitoring & Remediation* **2012,** *32*, (1), 106-119.

61. Fukuzaki, S.; Nishio, N.; Shobayashi, M.; Nagai, S., Inhibition of the Fermentation of Propionate to Methane by Hydrogen, Acetate, and Propionate. *Applied and Environmental Microbiology* **1990,** *56*, (3), 719.

62. Bouwer, E. J.; McCarty, P. L., Transformations of halogenated organic compounds under denitrification conditions. *Applied and Environmental Microbiology* **1983,** *45*, (4), 1295-1299.

63. Adrian, L.; Görisch, H., Microbial transformation of chlorinated benzenes under anaerobic conditions. *Research in Microbiology* **2002,** *153*, 131-137.

64. Kato, M. T.; Field, J. A.; Lettinga, G., High tolerance of methanogens in granular sludge to oxygen. *Biotechnology and Bioengineering* **1993,** *42*, (11), 1360-1366.

65. Yang, Y.; McCarty, P. L., Biomass, Oleate, and Other Possible Substrates for Chloroethene Reductive Dehalogenation. *Bioremediation Journal* **2000,** *4*, (2), 125-133.

66. Sleep, B. E.; Brown, A. J.; Lollar, B. S., Long-term tetrachlorethene degradation sustained by endogenous cell decay. *Journal of Environmental Engineering and Science* **2005,** *4*, (1), 11-17.

67. Hatamoto, M.; Miyauchi, T.; Kindaichi, T.; Ozaki, N.; Ohashi, A., Dissolved methane oxidation and competition for oxygen in down-flow hanging sponge reactor for post-treatment of anaerobic wastewater treatment. *Bioresource Technology* **2011,** *102*, (22), 10299-10304.

68. Matsuura, N.; Hatamoto, M.; Sumino, H.; Syutsubo, K.; Yamaguchi, T.; Ohashi, A., Closed DHS system to prevent dissolved methane emissions as greenhouse gas in anaerobic wastewater treatment by its recovery and biological oxidation. *Water Science and Technology* **2010,** *61*, (9), 2407-2415.

69. Vogt, C.; Simon, D.; Alfreider, A.; Babel, W., Microbial degradation of chlorobenzene under oxygen-limited conditions leads to accumulation of 3-chlorocatechol. *Environmental Toxicology and Chemistry* **2004,** *23*, 265-270.

70. Tiehm, A.; Gozan, M.; Müller, A.; Schell, H.; Lorbeer, H.; Werner, P., Sequential anaerobic/aerobic biodegradation of chlorinated hydrocarbons in activated carbon barriers. *Water Science and Technology: Water Supply* **2002,** *2*, 51-58.

71. Balcke, G. U.; Paschke, H.; Vogt, C.; Schirmer, M., Pulsed gas injection: A minimum effort approach for enhanced natural attenuation of chlorobenzene in contaminated groundwater. *Environmental Pollution* **2009,** *157*, (7), 2011-2018.

72. Rogers, J. R.; Bennett, P. C., Mineral stimulation of subsurface microorganisms: release of limiting nutrients from silicates. *Chemical Geology* **2004,** *203*, (1), 91-108.

73. Seki, K.; Thullner, M.; Hanada, J.; Miyazaki, T., Moderate Bioclogging Leading to Preferential Flow Paths in Biobarriers. *Groundwater Monitoring & Remediation* **2006,** *26*, (3), 68-76.

74. Ye, S.; Sleep, B. E.; Chien, C., The impact of methanogenesis on flow and transport in coarse sand. *Journal of Contaminant Hydrology* **2009,** *103*, 48-57.

75. Londry, K. L.; Suflita, J. M., Use of nitrate to control sulfide generation by sulfate-reducing bacteria associated with oily waste. *Journal of Industrial Microbiology and Biotechnology* **1999,** *22*, (6), 582-589.

76. Reinhard, M.; Shang, S.; Kitanidis, P. K.; Orwin, E.; Hopkins, G. D.; LeBron, C. A., In Situ BTEX Biotransformation under Enhanced Nitrate- and Sulfate-Reducing Conditions. *Environmental Science & Technology* **1997,** *31*, (1), 28-36.

77. Valiela, I.; Costa, J.; Foreman, K.; Teal, J. M.; Howes, B.; Aubrey, D., Transport of groundwater-borne nutrients from watersheds and their effects on coastal waters. *Biogeochemistry* **1990,** *10*, (3), 177-197.

78. Paerl, H. W., Coastal eutrophication and harmful algal blooms: Importance of atmospheric deposition and groundwater as "new" nitrogen and other nutrient sources. *Limnology and Oceanography* **1997,** *42*, (5part2), 1154-1165.

79. Squillace, P. J.; Scott, J. C.; Moran, M. J.; Nolan, B. T.; Kolpin, D. W., VOCs, Pesticides, Nitrate, and Their Mixtures in Groundwater Used for Drinking Water in the United States. *Environmental Science & Technology* **2002,** *36*, (9), 1923-1930.

80. US EPA, National Primary Drinking Water Regulations, 40 CFR, Parts 141-143. In Federal Registrar, Ed. 1995.

81. Aulenta, F.; Majone, M.; Verbo, P.; Tandoi, V., Complete dechlorination of tetrachloroethene to ethene in presence of methanogenesis and acetogenesis by an anaerobic sediment microcosm. *Biodegradation* **2002,** *13*, (6), 411-424.

82. Braeckevelt, M.; Mirschel, G.; Wiessner, A.; Rueckert, M.; Reiche, N.; Vogt, C.; Schultz, A.; Paschke, H.; Kuschk, P.; Kaestner, M., Treatment of chlorobenzene-contaminated groundwater in a pilot-scale constructed wetland. *Ecological Engineering* **2008,** *33*, (1), 45-53.

83. Braeckevelt, M.; Reiche, N.; Trapp, S.; Wiessner, A.; Paschke, H.; Kuschk, P.; Kaestner, M., Chlorobenzene removal efficiencies and removal processes in a pilot-scale constructed wetland treating contaminated groundwater. *Ecological Engineering* **2011,** *37*, 903-913.

84. Chen, Z.; Wu, S.; Braeckevelt, M.; Paschke, H.; Kästner, M.; Köser, H.; Kuschk, P., Effect of vegetation in pilot-scale horizontal subsurface flow constructed wetlands treating sulphate rich groundwater contaminated with a low and high chlorinated hydrocarbon. *Chemosphere* **2012,** *89*, (6), 724-731.

85. Kurt, Z.; Spain, J. C., Biodegradation of Chlorobenzene, 1,2-Dichlorobenzene, and 1,4-Dichlorobenzene in the Vadose Zone. *Environmental Science & Technology* **2013,** *47*, 6846-6854.

Chapter 4.

Influence of Initial Amendment Parameters on the Aerobic Biodegradation of 1,2-Dichlorobenzene with Granular Activated Carbon

4.1 Abstract

Chlorobenzenes (CBs) and other hydrophobic organic chemicals (HOCs) are persistent groundwater contaminants that can sorb strongly to soils and sediments. Amendment of strong sorbents such as granular activated carbon (GAC) at contaminated sites has been recognized as effective means to decrease environmental concentrations of HOCs and lower their bioavailability and toxicity to biota. In this study, we investigated the aerobic biodegradation of 1,2-dichlorobenzene (1,2-DCB) under simulated GAC bioaugmentation treatments. Using batch microcosms, we tested degradation under various amendment conditions modifying GAC loading, sediment amendment, pH, supplemental carbon addition, and inoculation dose. Groundwater and sediment from a contaminated wetland at the Standard Chlorine of Delaware Superfund site were used as representative site matrices. Mineralization of 5 mg 1,2-DCB was tracked over time through the release of aqueous chloride. Under an increasing GAC load, biodegradation over a 63-day period decreased from nearly 95% at 0.13 mg/L to 1% at 6.7 mg/L. Increasing ratios of sediment to GAC increased the apparent rates and extents of degradation; in the absence of GAC, all sediment loadings (0.33-333 g/L) led to rapid and complete mineralization within 8 days. Increasing inoculum dose in microcosms decreased the apparent lag before substantial degradation occurred. In the presence of GAC, observed initial mineralization rates varied from 0.006 mg/day to 0.347 mg/day in synthetic media and 0.014 mg/day to 0.238 mg/day

in site water. Results from this study show that initial CB degradation in freshly amended GAC can be greatly impacted by a number of simple site factors. For field applications, these raise important considerations for bioremediation strategies involving GAC.

4.2 Introduction

Chlorobenzenes (CBs) are a class of chlorinated hydrophobic organic contaminants (HOCs) that form pools of dense nonaqueous phase liquid (DNAPL) in the subsurface that are difficult to delineate and remove compared to less dense contaminants such as gasoline and other hydrocarbons [1]. Spills often result in decades-long contaminant plumes due to the difficulty in treating the contaminant source zone. Sediments and soils also form a natural sink for HOCs such as CBs, which partition favorably from water into the organic carbon fraction, effectively becoming secondary sources of contamination [2]. Desorption over time from these contaminated materials can lead to bioaccumulation in biota and pose potential human health risks [3].

Natural black carbon (BC) sources such as soot and coal, with sorption capacity 1 to 2-log greater than the more abundant amorphous organic carbon (AOC), have substantial HOC-sequestration capacity within natural soils and sediments [4]. High surface area manufactured BC amendments such as granular activated carbon (GAC) have been actively investigated to manage contaminated sediments in aquatic environments [3, 5-9]. GAC and powdered AC have been shown to significantly reduce bioavailability and volatilization of CBs by 1-2 log when amended at 1% (wt) into contaminated soils [10]. Additionally, packed GAC beds have been shown to be effective systems to quickly immobilize and biodegrade CBs and other HOCs [5, 11, 12]. GAC and other black carbon amendments have been shown to be amenable to biofilm formation due to their high surface area,

making them suitable carriers for contaminant-degrading bacteria used in bioaugmentation [13-15]. Payne et al. (2013), for example, found that GAC inoculated with a combination of aerobic and anaerobic degraders was able to reduce harbor sediment polychlorinated biphenyl (PCB) concentrations of 8 mg/kg by 80% [14]. With the dual benefit of promoting sorption and degradative biofilm formation, there is great potential for *in situ* contaminated site remediation using GAC.

Past research investigating the sorption mechanisms and biodegradation effects of GAC amendments in contaminated soils and sediments have primarily focused on well-known polyaromatic hydrocarbons (PAHs), PCBs, and pesticides; these are ubiquitous global contaminants characterized by high hydrophobicity, sorption potential, and toxicity [7, 9, 14, 16-21]. Notably, irreversible sorption and slow desorption kinetics have consistently been shown to limit biodegradation in GAC and highly sorbent sediments [4, 18, 22]. Research on the interactions between sorption and biodegradation of CBs at contaminated sites has been much more limited to empirical studies investigating degradation in soil [23-25] or pilot studies using flow-through columns [5, 26]. Though CBs share structural similarity to PCBs and PAHs, less chlorinated CBs (1-3 attached Cls) tend to be more soluble and partition less strongly to organic carbon by at least 1 order of magnitude [27]. Additionally, notable differences in degradation mechanisms and degradability between compound classes exist, such as recalcitrance of highly chlorinated PCBs to aerobic degradation [9]. Therefore, there is a need to investigate how CB degradation, in particular, is affected by sorptive matrices amended to contaminated sites.

At the Standard Chlorine of Delaware Superfund site (SCD), wetland sediment and porewater was found to be highly contaminated with a mix of 1-3 CBs and benzene, with

125

measured total porewater concentrations up to 75 mg/L [28]. Dichlorobenzenes (DCBs), especially 1,2-DCB, were found to be major groundwater constituents; accounting for greater than half of the total CB mix in many different samples [28]. Application of bioaugmented GAC has been proposed as a possible remediation strategy within the shallow wetland sediments, with the potential to desorb CBs from contaminated sediment and intercept porewater CBs discharging to the surface. This could be achieved through mixing bioaugmented GAC with existing sediment or embedding it in a reactive barrier. The goal of this study was to determine the influence of simple site and amendment parameters on the biodegradation of CBs using freshly amended GAC. Using batch microcosms to simulate contaminated aerobic groundwater environments, we monitored the biodegradation of model contaminant 1,2-DCB over time. We investigated the influence of GAC loading, site sediment, inoculation scheme, pH, and supplemental organic carbon on the extent and kinetics of biodegradation. Results of this study offer insight into CB remediation outcomes associated with GAC.

4.3   Methods

4.3.1   Chemicals

1,2-DCB (99% purity) was purchased from Millipore Sigma (Burlington, MA). Inorganic anion analytical standards were purchased from Thermo Fisher Scientific (Waltham, MA). All reagent water used in experiments and analyses was distilled and treated with a Milli-Q® purification system (Millipore Sigma).

4.3.2   Microcosm Preparation

GAC used in the experiment (Calgon Filtrasorb F600) was sieved between 500 and 1000 μm and autoclaved in a vacuum cycle for 30 minutes at 121 °C with a 20-minute dry

time. CB-free wetland sediment was sampled from SCD in 2016. Sediment was stored at 4 °C until further processing. Sediment was prepared for the experiment by placing a 100 g aliquot in a glass beaker and autoclaving in a liquid cycle for 30 minutes at 121 °C. It was subsequently oven dried for 24 hours at 105 °C and homogenized with mortar and pestle into a fine powder. Powdered sediment was dry sieved below 500 µm and dried in the oven for an additional 24 hours. Sediment was removed and stored at room temperature in a desiccator until use. Dry sediment amendments were weighed and added to their respective microcosm bottles during experimental setup. Sodium lactate and sodium benzoate amendments were prepared as 100 g/L stock solutions sterilized through 0.22 µm polyether sulfone syringe filters.

Synthetic groundwater media was a previously described phosphate-buffered defined media with ammonium as a nitrogen source and additional trace metal and vitamin solutions (Chapter 1). Media concentrations were 8.5 mg/L KH_2PO_4; 22 mg/L K_2HPO_4; 33 mg/L Na_2HPO_4; 5.0 mg/L $CaH_4(PO_4)_2$; 1.25 mg/L $FeSO_4·7H_2O$; 100 mg/L $(NH_4)_2HPO_4$; 25 mg/L $MgSO_4·7H_2O$. Trace elements consisted of 1.0 mg/L $MnSO_4·4H_2O$; 0.25 mg/L $(NH_4)_6Mo_7O_{24}·4H_2O$; 0.25 mg/L $Na_2B_4O_7·10H_2O$; 0.25 mg/L $CoCl_2·6H_2O$; 0.25 mg/L $CuCl_2·2H_2O$; 0.25 mg/L $ZnCl_2$; 1.0 mg/L $NaVO_3$ [29]. Vitamin concentrations were 0.1 mg/L pyridoxine-HCl; 0.05 mg/L thiamine-HCl; 0.05 mg/L riboflavin; 0.05 mg/L nicotinic acid; 0.05 mg/L biotin; 0.02 mg/L folic acid; 0.005 mg/L cobalamin; 0.05 mg/L p-aminobenzoic acid [30]. Prepared media were sterilized using 0.2 µm cellulose membrane vacuum filter units.

Site groundwater was sampled from the SCD wetland site in 2014 and stored in the dark at 4 °C. Site water characteristics were measured immediately before experiments, as

follows: pH 4.60, 16.5 mg/L NO_3^-, 67 mg/L Cl^-, 450 mg/L SO_4^{2-}, and 1.46 mg/L TOC. No organic acids were detected.

The inoculum culture was a semi-continuous aerobic batch reactor fed with a mixture of vapor-phase monochlorobenzene (MCB), 1,2-DCB, and 1,2,4-trichlorobenzene (1,2,4-TCB) previously described in Chapter 2. Aliquots from this reactor were used to inoculate microcosms within the same tests simultaneously either by seeding GAC granules or adding pelleted liquid culture directly to the media. For GAC seeding, 2 mL inocula were added to 5 mL sterile polypropylene centrifuge tubes containing prepared GAC. Tubes were vortexed for 5 seconds to remove evolved gas bubbles, capped, and stored upright at room temperature for 24 hours. Liquid culture was removed from the tubes by pipette, and the GAC was rinsed 3 times with the media to be used for the microcosm experiment. Pelleted liquid inocula were prepared by adding 2 mL liquid culture to sterile tubes and centrifuging for 5 minutes at 3197×g (Eppendorf 5810R). Culture supernatant was removed, and the pellets were resuspended in 0.25 mL of the media to be used for the microcosm experiment. During inoculation of the first degradation experiment, 5 mL of liquid culture were sampled, pelleted, and resuspended as 0.25 mL for DNA sampling. DNA was extracted using a Qiagen DNeasy® PowerSoil® (Germantown, MD) kit following manufacturer's instructions. 16S rRNA from extracted DNA was amplicon sequenced in the same run and followed the sample upstream and downstream protocol as described in Chapter 3.

4.3.3   Degradation Experiments

Seven degradation experiments were designed to test different parameters of GAC amendment and aerobic degradation of 1,2-DCB over time. A summary of each

experiment, amendment conditions, and varied parameters is presented in Table 4.1. Batch microcosms were conducted in 250 mL amber borosilicate glass bottles sealed with screw caps containing removable polytetrafluoroethylene (PTFE) septa. Bottles and septa were cleaned, triple-rinsed with distilled water, and autoclaved before use. Each microcosm consisted of 150 mL liquid media with 100 mL nominal headspace. Unless otherwise noted, 0.2 g GAC was utilized as a baseline amendment condition for comparison. Microcosms were prepared with synthetic groundwater media or SCD site water and additional amendments (described below) for each specific experiment. All experiments were spiked with 5 mg neat 1,2-DCB, equivalent to a nominal aqueous concentration of 33.3 mg/L. Degradation was tracked through the release of chloride into solution. Experimental microcosms were prepared and run simultaneously in duplicate unless otherwise noted.

Experiments 1 and 2 tested the influence of GAC loading on biodegradation. Increasing doses of 0.02-1 mg were added to each microcosm, corresponding to 0.13 to 6.7 mg/L GAC suspension and approximately 5-250 mg CB / g GAC loading. Experiment 1 was conducted in synthetic media with seeded GAC while Experiment 2 was conducted in site water with a pelleted inoculum. Experiment 3 tested the mixture of GAC with site sediment with increasing ratios of sediment to GAC of 0 to 25 (g/g). This experiment used seeded GAC (0.2 g) and tested both synthetic media and site water. Experiment 4 tested potential benefits of supplemental organic carbon (OC) sources added to microcosms using sodium lactate and sodium benzoate as model aliphatic and aromatic compounds. Doses were chosen to provide OC content equivalent to the 0.5 and 5 g sediment microcosms from Experiment 2, with 1.7 and 17 mg total C respectively. This experiment used 0.2 g

seeded GAC in synthetic media. Experiment 5 tested the potential for biodegradation of site water with seeded GAC (0.2 g) under varied site water pH values of 3, 4.6 (unadjusted), 7, 10, and 12. pH was adjusted with either NaOH or H_2SO_4 and subsequently re-filtered through a 0.2 μm vacuum filter. Experiments 1-5 were all conducted in parallel using the same subsample of the inoculum culture.

Experiments 6 and 7 were conducted in parallel as a follow-up to the previous experiments. Experiment 6 tested the influence of increasing sediment dose in microcosms without GAC. Sediment doses of 0 to 50 g (0-333 g/L) were tested using a pelleted inoculum. Experiment 7 tested the influence of increasing inoculum concentrations on biodegradation using clean GAC. Volumes of 0.002 to 20 mL of inoculum were pelleted, resuspended, and amended directly to the microcosm bottles as described previously. Subsamples of the inoculum culture were taken 2 months after experiments 1-5, which may have caused some variation in the specific activity and composition of CB degraders in the inoculum between these two experimental datasets.

Table 4.1. Summary of microcosm degradation experiments (modified conditions in bold)

Experiment 1: GAC Loading	**GAC Amendment**	**0, 0.02, 0.05, 0.2, 1 g**
	(GAC Load)	0, 0.13, 0.33, 1.3, 6.7 mg / L
	(Sorption Density)	0, 250, 100, 25, 5 mg CB/ g GAC
	Media	Synthetic
	Inoculation	Seeded
Experiment 2: GAC Loading	**GAC Amendment**	**0.02, 0.05, 0.2 g**
	(GAC Load)	0.13, 0.33, 1.3 mg / L
	(Sorption Density)	250, 100, 25 mg CB/ g GAC
	Media	Site
	Inoculation	2 mL Pelleted
Experiment 3: Sediment to GAC Ratio	GAC Amendment	0.2 g
	Sediment Amendment	**0, 0.05, 0.5, 5, .5 (no GAC) g**
	(Sediment:GAC Ratio)	0, 0.25, 2.5, 25, ∞ g/g
	Media	Synthetic + Site
	Inoculation	Seeded
Experiment 4: Supplemental Carbon	GAC Amendment	0.2 g
	Supplemental Carbon	**1.7, 17 mg C as Lactate and Benzoate**
	Media	Synthetic
	Inoculation	Seeded
Experiment 5: Site Water pH	GAC Amendment	0.2 g
	pH Adjustment	**Unadjusted (4.6), 3, 7, 10, 12**
	Media	Site
	Inoculation	Seeded
Experiment 6: Sediment Loading	GAC Amendment	None
	Sediment Amendment	**0, 0.05, 0.5, 5, 50 g**
	(Sediment Load)	0, 0.33, 3.3, 33, 333 g/L
	Media	Synthetic
	Inoculation	2 mL Pelleted
Experiment 7: Inoculum Dose	GAC Amendment	0.05 g
	Media	Synthetic
	Inoculation	**0.002, 0.02, 0.2, 2, 20 mL Pelleted**

For each degradation experiment, designated media and amendments were added to microcosm bottles, excluding DCB. Bottles were sealed, shaken for 2 hours at 150 rpm to equilibrate amendments, and sampled using the protocol described below as a baseline measurement (zero timepoint). Each bottle was subsequently spiked with neat 1,2-DCB, immediately sealed, and returned to the shaker for 36 hours at 150 rpm to ensure complete CB dissolution. Bottles were again sampled, including a porewater CB measurement, to determine the extent of dissolution and CB sorption. GC-MS results indicated high sorption in each GAC-amended microcosm, with at least 88% of total CB mass sorbed. After preparation, bottles were stored horizontally on temperature controlled orbital shakers (New Brunswick Scientific Innova 4000). Bottles were shaken at 100 rpm at a 25 °C to ensure complete mixing and oxygenation in the liquid media and sampled at regular intervals.

At each sample point, bottles were removed from the shaker and stored upright on the lab bench for 1 hour. Sample bottles were opened and 1 mL of liquid media was removed by micropipette into sterile 1.5 mL microcentrifuge tubes. When bottles were sampled directly for GC-MS analysis, liquid was directly transferred to extraction vials for analysis. Bottles were re-capped and returned to the shaker. Microcentrifuge tubes were capped and centrifuged for 2 minutes at 13362×g (Eppendorf 5810R). Avoiding any pelleted material, an aliquot of these samples (0.1-0.5 mL depending on dilution) was transferred to ion chromatography (IC) autosample vials for immediate analysis. pH was intermittently measured using the sample liquid remaining in the tubes.

4.3.4   Analytical Methods

Chloride was analyzed by IC as described previously in Chapter 3. Immediately prior to IC analysis, samples were filtered in-line through 20 μm PolyVial filter caps. Concentration values were quantitated linearly between 0.1-30 mg/L. Higher concentration samples were diluted within this calibration range, and lower concentrations were treated as 0 during analysis.

Aqueous-phase 1,2-DCB was measured by Gas Chromatography - Mass Spectrometry using the protocol described in Chapter 2. After sampling, analytes were immediately extracted into cyclohexane and were stored at 4 °C until analysis. Concentrations above the 10 mg/L linear calibration limit were diluted and below the 0.05 mg/L limit were treated as 0.

pH was measured directly in microcentrifuge tubes using a semi-micro combination probe (Thermo Fisher Orion 9103BNWP) after removing samples for chemical analysis. The probe was calibrated immediately before each measurement using a 3-point curve (pH 4, 7, 10).

Sediment total organic carbon (TOC) was measured using a Shimadzu 5000A TOC Analyzer with a Solid Sample Combustion Unit (SSM-5000A) as described by Grossman and Ghosh [31]. The texture of the sediment, a hydric soil, was measured in triplicate using a micropipette method as described by Miller and Miller [32].

GAC surface area was measured by gas adsorption isotherm using a Micromeritics ASAP 2010 instrument (Norcross, GA). Samples were degassed at 300 °C for 3 hours, in accordance with other activated carbon studies [33, 34]. The instrument was operated using

standard settings for carbon black. Nitrogen adsorption data at 77 K from the relative pressure range of 0.01-0.1 were used to calculate surface area according to the Brunauer, Emmet, and Teller (BET) isotherm [35]. Surface area measurements were performed in technical duplicate.

4.3.5 Calculations

Degradation of 1,2-DCB at a given timepoint D_t was calculated as the difference between the total mass of chloride released at time t ($M_{Cl^-,t}$) and the initial chloride mass ($M_{Cl^-,0}$) measured at time 0 converted to mass of DCB (Equation 4.1). This calculation assumed 1 mol of 1,2-DCB degraded per 2 mol Cl$^-$ released.

Equation 4.1

$$D_t = (M_{Cl^-,t} - M_{Cl^-,0}) \times \frac{MW_{DCB}}{MW_{Cl^-}} \times \frac{2\ Cl^-}{1\ DCB}$$

$$M_{Cl^-,0} = [Cl_0^-] \times V_0$$

Equation 4.2

$$M_t = [Cl_t^-] \times V_t + \sum_{t_1}^{t} (V_t - V_{t-1}) \times [Cl_{t-1}^-]$$

$M_{Cl^-,t}$ was not simply calculated on the basis of concentration measured in solution at the time because the fraction of chloride removed during previous sampling events would not be accounted for. To correct for this small mass loss, the cumulative mass of chloride removed during each prior sampling event (based on prior concentration measurements) was added to the measured mass in solution to more accurately represent the total chloride release associated with 1,2-DCB degradation (Equation 4.2). To calculate percent extent

of degradation (%), concentrations were normalized to the initial 5 mg spike added in each microcosm. All reported ± values represent 1 standard deviation.

Degradation kinetics were modeled using a modified first-order rate of production equation, tracking the total mass of 1,2-DCB degraded over time (Equation 4.3). P is the predicted mass degraded at a given time (mg), A is the asymptotic maximum theoretical mass degraded (mg), k (days^{-1}) is the first-order rate constant, and t is the time (days). A lag term λ (days) was added to model data that did not immediately degrade.

Equation 4.3

$$P = A[1 - \exp(-k(t - \lambda))]$$

Data from individual microcosms were fit to the model using nonlinear least-squares regression using the R package *minpack.lm*, which implements the Levenberg–Marquardt algorithm [36]. For most degradation curves, which did not show lag, λ was constrained to 0. For those with an apparent lag period, timepoints with 0 degradation were excluded from regression analysis and positive λ values could be calculated. Initial mineralization rates (IMRs) were calculated based on k and A in terms of mg/day (Equation 4.4).

Equation 4.4

$$IMR = k \times A$$

4.4   Results and Discussion

4.4.1   Amendment Characterizations

Sequencing of the inoculum culture yielded 52 unique features at a filtered sample depth of 154,845 reads with a Shannon diversity index of 1.88. Figure 1 shows the genus-level relative abundance of the microbial community. The community was dominated by

Proteobacteria (80.5% relative abundance) and Bacteroidetes (18.1%), with an unspecified Betaproteobacteria OTU accounting for 52% of the total community. Genera identified with high abundance in the Burkholderiaceae (*Pandoraea*, *Paraburkholderia*) [37, 38], Sphingomonadaceae (*Sphingomonas*) [39-41], and Xanthomonadaceae (*Stenotrophomonas*) [42, 43] families have been previously been associated with aerobic CB and aromatic degradation.
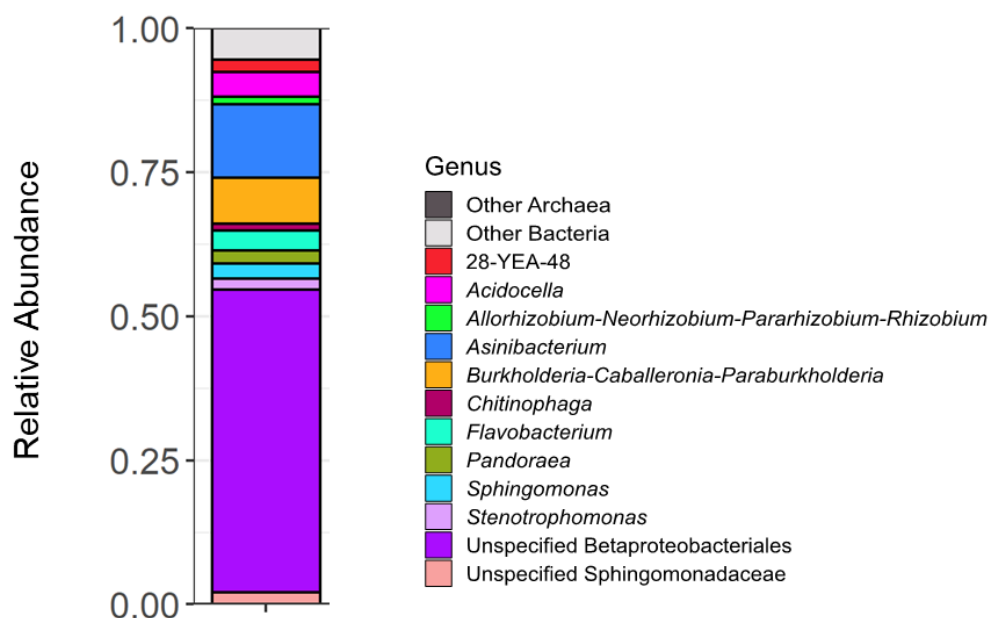
Figure 4.1. Genus-level composition of inoculum culture showing taxa with >1% relative abundance.

BET surface area of the GAC amendment was calculated to be 893 m^2/g. This was within the measured range for similar commercially available GAC (700-1200 m^2/g), but 24% greater than the only other available measurement of Calgon Filtrasorb 600 surface area (718 m^2/g) [44, 45]. Sieved sediment texture consisted of 3.4 ± 0.2% sand, 76.2 ± 2.2% silt, and 20.3 ± 2% clay. Sediment was characterized as a silt loam according to the USDA NRCS soil texture triangle. Sediment-bound TOC was measured as 33.9 mg/g. Sediment pH, in a clarified 5:1 (w/w) slurry, was 4.03 in DI water and 3.87 in 0.01 M CaCl$_2$. Indigenous CB-degrading activity in the autoclaved sediment was found to be

negligible, evidenced by no 1,2-DCB degradation in a pair of uninoculated microcosms containing 0.5 g site sediment and 0.2 g GAC in synthetic groundwater (see Figure 4.4a).

4.4.2   GAC Loading

CB degradation under varied clean GAC loads in synthetic media (Experiment 1) are shown in Figure 4.2. Overall degradation under the baseline condition of 0.2 g GAC amendment (used for comparison in other experiments) was low, with only 6% ± 1% of the initial 5 mg 1,2-DCB mineralized after 63 days. This was unexpectedly low compared to results from a preliminary experiment under similar conditions, where a higher 10 mg 1,2-DCB spike with 0.2 g GAC yielded 38% mineralization over a 56-day period (data not shown). In Experiment 1, increased GAC loading led to a decrease in the final extent of degradation and apparent rate (Figure 4.2a; discussed in Section 4.4.7). 95% ± 1% of 1,2-DCB was degraded under the lowest 0.02 g GAC, while no significant degradation (1% ± 2%) occurred at 1 g GAC dosing. No degradation occurred in the absence of GAC in the synthetic media. While this may have been an effect of toxic inhibition at high aqueous 1,2-DCB concentrations (33 mg/L), the results were surprising since the inoculum culture used the same synthetic media tested here. In other tested conditions, there was an apparent lag period before degradation began, which increased with increasing GAC dose. Closer inspection of the initial region (Figure 4.2b) showed this lag to be a convex phase of the degradation curve, which later inflected into a largely concave curve for the remainder of the time series. This lag has frequently been observed by other mineralization studies and has been attributed to a period of microbial community acclimation and cell growth before more rapid degradation occurs [7, 46, 47].
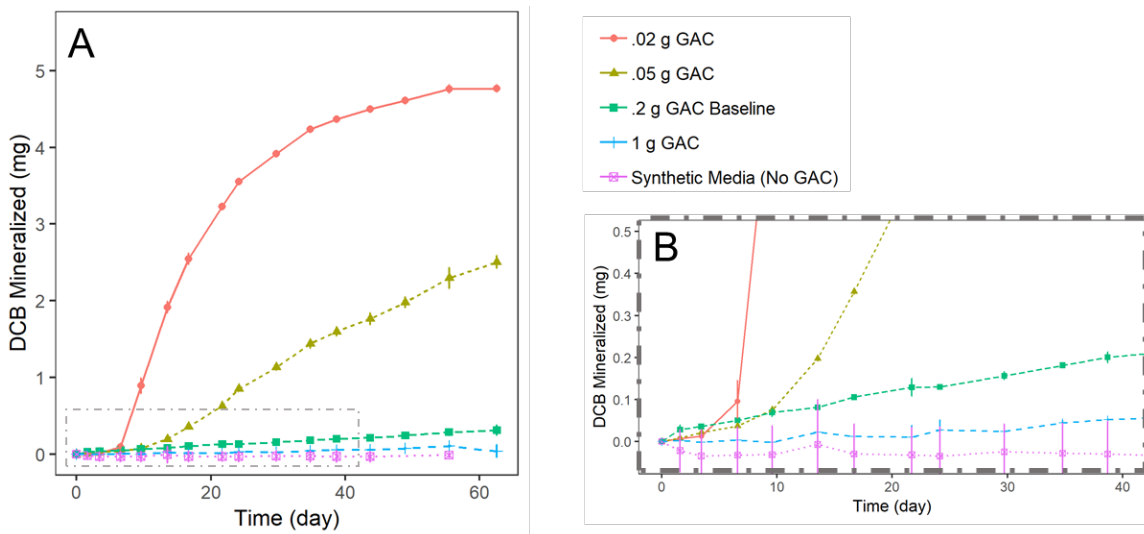
Figure 4.2. Experiment 1: Mineralization of 1,2-DCB in microcosms containing increasing loadings of inoculated GAC in synthetic groundwater media. (A) Total time-series. (B) Higher-resolution view of initial degradation patterns.

Experiment 2 tested increasing GAC dose in site water, but with equal volumes of pelleted inocula added (Figure 4.3). Degradation measurements in site water generally showed higher variability between timepoints and microcosm replicates than synthetic media, which can primarily be attributed to the higher baseline chloride (67 mg/L), necessitating a 5× sample dilution before IC analysis. Here, there was nearly identical degradation at 0.02 and 0.05 g GAC (71%), which were more than double the 0.2 g degradation (29% ± 24%) (Figure 4.3). In contrast to the synthetic media in Experiment 1, degradation in site water in the absence of GAC proceeded to near completion (92% ± 1%). This suggests better acclimation of inoculum degraders to site water or some unknown beneficial site water constituents.
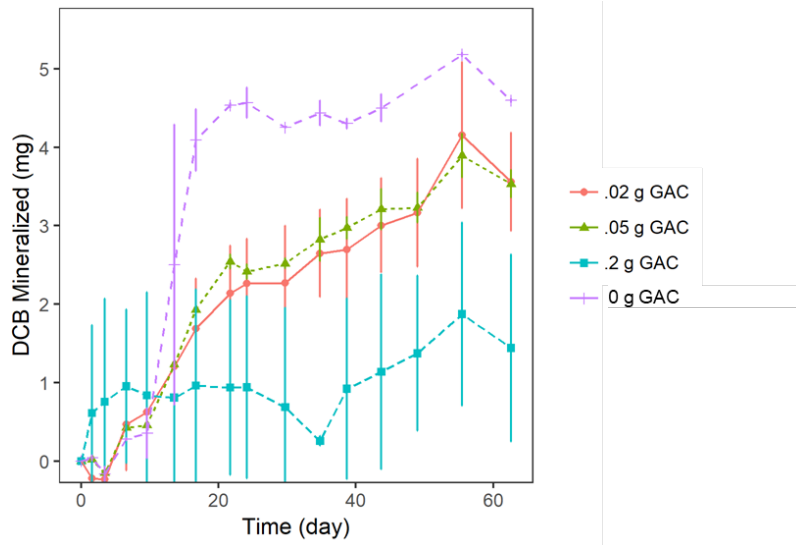
Figure 4.3. Experiment 2: Mineralization of 1,2-DCB in site water microcosms containing increasing loadings of uninoculated GAC inoculated with equal volumes of pelleted inoculum

Table 4.2. Measured aqueous-phase 1,2-DCB concentration at the beginning of degradation experiments

Experiment	Treatment	C_{aq} (mg/L) [a]
		(2-day post-spike)
Experiment 1: Synthetic Media GAC Load	0 g GAC	37.19 ± 1.81
	0.02 g GAC	$3.83 \pm .09$
	0.05 g GAC	$0.10 \pm .01$
	0.2 g GAC (Baseline)	BDL [b]
	1 g GAC	BDL [b]
		(2-day post-spike)
Experiment 2: Synthetic Media GAC Load	0 g GAC	33.28 ± 1.01
	0.02 g GAC	$0.71 \pm .85$
	0.05 g GAC	$0.09 \pm .01$
	0.2 g GAC (Baseline)	BDL [b]
Experiment 3: Sediment:GAC Load		(2-day post-spike)
	All Sediment + GAC Treatments	BDL [b]
		(1-day post-spike)
Experiment 6: Sediment Load	0 g Sediment (No GAC)	35.42 ± 2.15
	0.05 g Sediment (No GAC)	27.44 ± 12.02
	0.5 g Sediment (No GAC)	32.78 ± 1.38
	5 g Sediment (No GAC)	21.39 ± 1.14
	50 g Sediment (No GAC)	$4.38 \pm .28$ *
Experiment 7: Inoculation Dose	All Treatments	(2-day post-spike) <0.22

a. n=2 microcosms; ± 1 SD
b. Below Detection Limit (<.05 mg/L)
* Substantial degradation already occurred at this sample point

139

Biodegradation and bioavailability of HOCs has more often been associated with aqueous-phase concentrations than with sorbed-phase concentrations [4, 19, 22, 48]. Aqueous concentrations of DCB were measured 2-days after the initial spike in order to make a coarse estimate of available equilibrium concentrations (Table 4.2). Predictably, the greatest aqueous concentrations were present at the lowest GAC loadings. With the exception of the synthetic media microcosms without GAC, the extent of degradation generally appeared to increase with increasing aqueous concentration (0 g GAC > 0.02 g > 0.05 g > 0.2 g) between Experiments 1 and 2. While not quantitative in nature, this does suggest that degradation and aqueous concentrations were interrelated. If biodegradation is dependent on aqueous-phase concentrations, then the low CB degradation observed under increasing GAC amendment may be explained by sorption mechanisms. Under a constant 5 mg CB spike, the density of sorbed CB per surface area unit of GAC decreased with increasing GAC dose in our experiment (Table 4.1). At lower sorption densities, a higher fraction of contaminant may sorb to high energy sites, which in turn lead to irreversible sorption or slow desorption kinetics [4, 49, 50]. Similar phenomena were observed by others in regeneration of GAC beds [49] and in a GAC biofilm reactor [51], where greater bioregeneration and biodegradation of sorbed contaminants were observed at higher loading concentrations (greater sorbed density). This may also explain why nearly 10-fold more DCB was degraded in the preliminary experiment spiked with 10 mg 1,2-DCB instead of 5 mg, as most of the lower spike may have been desorption-resistant. These results highlight a potential tradeoff of excess sorption capacity, where low fluxes of CB may be permanently sorbed rather than degraded.

4.4.3   Sediment Amendment
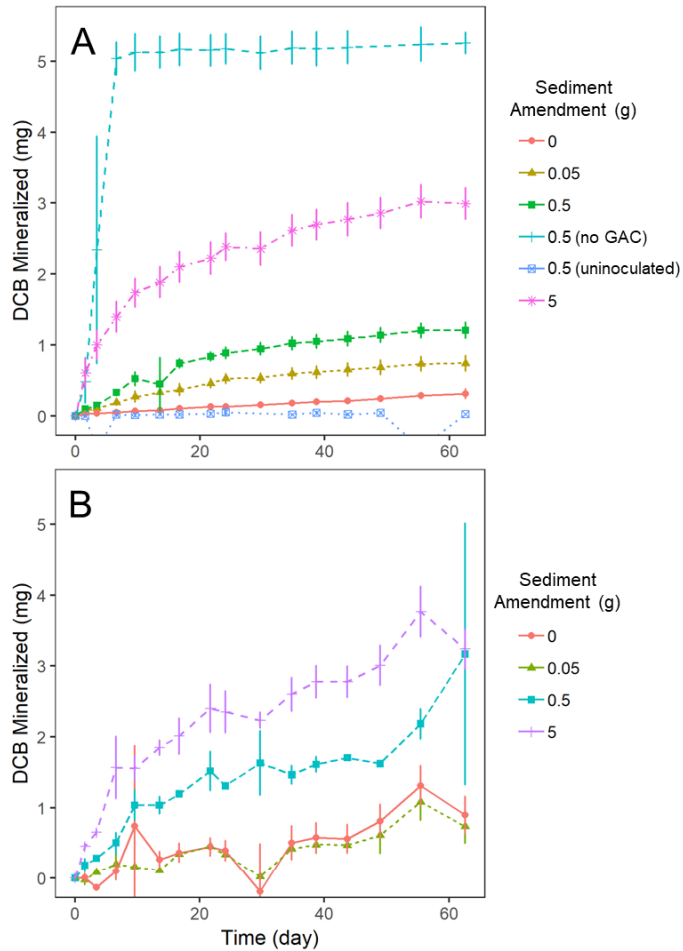
Figure 4.4. Experiment 3: Mineralization of 1,2-DCB in microcosms containing increasing ratios of sediment mass to constant 0.2 g of inoculated GAC in (A) synthetic groundwater media and (B) site water.

Experiment 3 examined the effects of DCB degradation under varying ratios of sediment to GAC, using a constant GAC amendment in both synthetic and site water (Figure 4.4). There was a clear increase in the extent and rate of degradation with increasing sediment dose in both media. In the presence of GAC, the maximum degradation of 60% $\pm$ 4% (synthetic) and 65% $\pm$ 6% (site) occurred at the highest sediment dose of 5 g (25:1 w/w ratio). The presence of GAC appeared to have an inhibitory effect on CB degradation, as complete mineralization occurred within 4 days in microcosms with 0.5 g sediment without GAC (Figure 4.4a). Enhanced degradation from native sediment bacteria was

141

eliminated as a possibility, as the uninoculated microcosm containing 0.2 g GAC and 0.5 g sediment showed no degradation activity over the course of the experiment (Figure 4.4a). In contrast to the GAC-only microcosms in Experiment 1, there was no visible initial degradation lag in the synthetic media microcosms with the addition of sediment, suggesting that sediment addition beneficially reduced the acclimation phase of bacteria.

Decreased degradation rates and extents of HOCs in GAC and soil slurry tests have been reported by others [7, 17]. Rhodes et al. (2010) reported significant reductions in phenanthrene mineralization at GAC doses greater than 0.1% (1000:1 sediment:GAC) at constant soil loads [7]. Interestingly, that study also found that soils with high organic carbon content had increased mineralization at the same GAC dose. It was suggested that soil OM may compete for sorption sites and block pores within GAC, decreasing sorption capacity and increasing the bioavailability of HOCs, similar in manner to reduction in sorption capacity of "aged" BC [7, 52, 53]. This competitive sorption with sediment OM could potentially explain the increased degradation observed at higher sediment loads. On the other hand, all amendments and DCB were introduced into our microcosms simultaneously, leaving little time for GAC to become preloaded with organic matter. Additionally, it does not explain the rapid, complete mineralization in the presence of sediment without GAC (Figure 4.4a). All aqueous CB concentrations measured in GAC-amended microcosms from Experiment 3 were below detection limits, so no variations in porewater concentrations were noted (Table 4.2). Alternatively, a simple explanation for enhanced degradation is that unidentified sediment-associated nutrients and growth factors stimulated the CB degraders. Considering that the sediment in this study was sampled from a location where previous microbial attenuation may have occurred, residual decayed

biomass may have provided a rich source of growth media beneficial to the augmented degrader population.
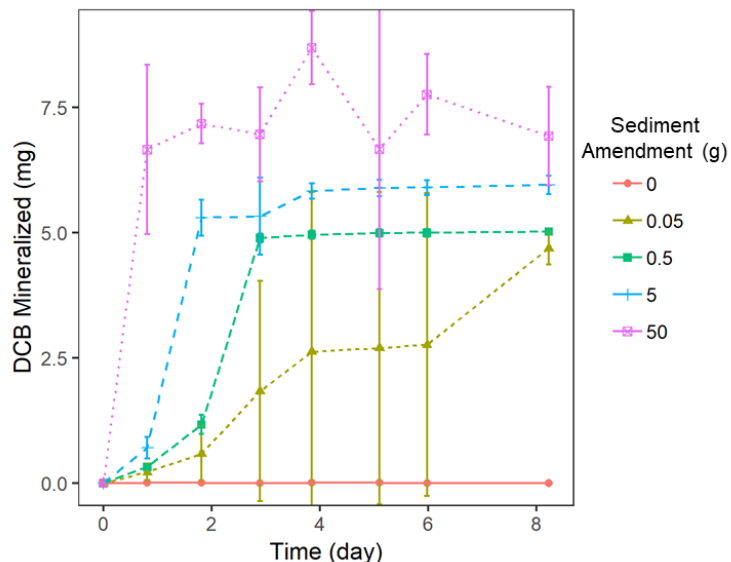
Figure 4.5. Experient 6: Mineralization of 1,2-DCB in microcosms containing increasing loadings of sediment without GAC in synthetic groundwater media.

Experiment 6 followed-up on the results of Experiment 3 to examine the effects of increasing sediment dose on degradation in the absence of GAC. Results, presented in Figure 4.5, show that order of magnitude increases in sediment addition, from 0.05 to 50 g sediment per bottle, led to apparent increasing rates of CB degradation. After only 8 days, all sediment addition conditions showed nearly complete mineralization. The final extent of mineralized mass was overestimated beyond 5 mg in the 50 g and 5 g sediment treatment due to high solids and chloride content causing variability in chloride measurements; however, these treatments quickly stabilized at these maximum values and were assumed to be 100% mineralized (Figure 4.5). Increased sediment dose also appeared to decrease the initial convex lag portion of the degradation curve.

There have been conflicting reports in the literature of the effect of soil and sediment amendment on degradation rates. Some studies have found that increasing soil loads increased the total amount of HOCs sorbed to soil, which decreased the bioavailability and degradation of HOCs [19, 25]. However, others have found enhanced degradation in the presence of soils [6, 18, 23, 24, 46]. Lee et al. (2009) found a similar stimulatory effect to our results on MCB degradation with increasing fractions of soils added to liquid microcosms; however in a second tested soil, there was no such additive benefit beyond an initial dose to a soil-free microcosm [23]. It has been suggested by others that direct interaction between biofilm-forming microorganisms and soil particles may contribute to the increased observed degradation [6, 16, 54]. Specifically, biofilm-forming strains of *Sphingomonas* (a genus identified in our inoculum) and *Pseudomonas* were found to aggregate onto soil particles in slurry microcosms contaminated with PAHs [16, 18]. It was hypothesized that these biofilm-formers could directly access sorbed HOCs, which were more concentrated in soil than in aqueous phase, and degrade the highly concentrated contaminant more quickly [54]. This may explain the discrepancy in results between various studies, as microbial physiology has not commonly been investigated in mineralization studies. In Experiments 3 and 6, greater sediment loads may have enhanced degradation by increasing the total fraction of sediment-sorbed CBs, making CBs readily accessible to biofilm-forming degraders such as *Sphingomonas*. However, this would need to be confirmed in follow-up studies investigating the distribution of microorganisms between aqueous, GAC, and sediment phases.

144

4.4.4 Supplemental Carbon

Another potential explanation for sediment-enhanced CB degradation was the presence of additional labile organic carbon to stimulate CB-degrading microorganisms, which has been suggested by others [7, 16]. Though we did not distinguish labile from recalcitrant carbon here, each gram of amended sediment contained 33.9 mg C compared to 2.4 mg C added from the 5 mg DCB spike. This may have enhanced the initial biomass density of CB degraders and facilitated higher initial CB degradation rates. CB degraders grown on benzoate were previously shown by others to rapidly biodegrade CBs [55].
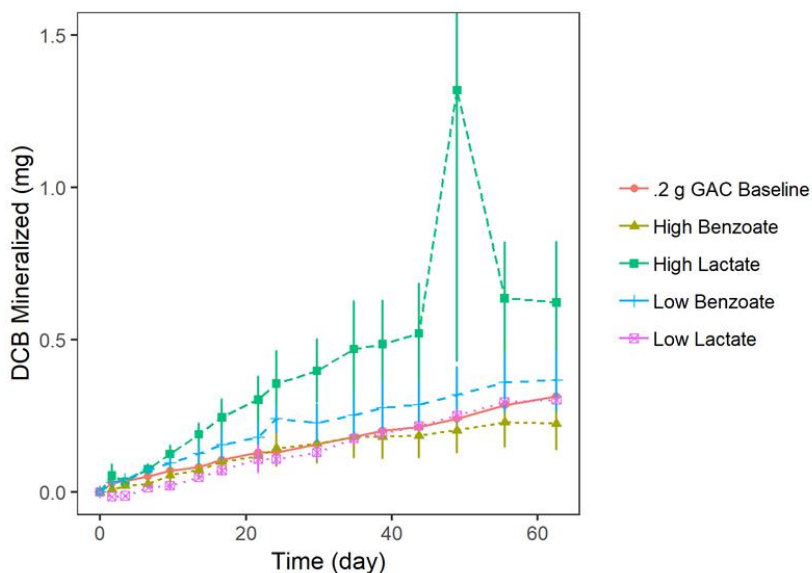
Figure 4.6. Experiment 4: Mineralization of 1,2-DCB in microcosms containing supplemental dissolved organic carbon sources compared to unsupplemented GAC microcosm in synthetic groundwater media.

To test this hypothesis, we amended simple readily-degradable model aliphatic (lactate) and aromatic (benzoate) compounds to sediment-free GAC microcosms to determine if any substrate-based enhancement was present. Two doses of each compound were amended separately – 1.7 (low dose) and 17 mg (high dose) organic C, equivalent to the TOC content in 0.05 and 0.5 g sediment respectively. Benzoate and lactate were completely degraded in all tested microcosms within the first 4 days (data not shown). CB

degradation during this test, compared to the baseline GAC condition, did not show a significant difference with either benzoate treatment or the low lactate treatment (Figure 4.6). The high lactate (17 mg) did show a significant ($p<.05$) 2-fold increase in CB degradation compared to the baseline. This treatment, however, had only ¼ of the enhancement present in the 0.5 g sediment dose. Considering the low sample size of the treatment (n=2), high relative standard deviation in the high lactate treatment (32% at the final timepoint), and lack of corroborating evidence from other supplemental C amendments, the data do not appear to support the hypothesis that supplemental labile carbon stimulated degradation. However, due to the complex structure of natural organic matter and the potential presence of natural aromatic analogs to CBs such as PAHs in soils, we cannot eliminate the possibility that degradation of sediment-bound organic matter could have provided a potential benefit as a substrate.

4.4.5   pH Effects

Overall, degradation of CBs in all microcosms did not result in substantial changes in pH over time. Synthetic media microcosms, which were well-buffered by phosphate, did not exhibit substantial changes in pH. The greatest microcosm pH change occurred in synthetic media dosed with 0.02 g GAC (Experiment 1), where pH decreased from 7.73 to 6.73 (Table 4.3). In the previous experiments, no noticeable pH effects appeared to inhibit degradation over time.

Table 4.3. Measured pH change in select microcosm conditions and Experiment 5

Media	Experiment Condition	Unamended Media	pH Measurement			
			Initial (t=0 d)	Stabilized [a] (t=2 d)	Final (t=63 d)	Δ (Final - Stabilized)
Synthetic	.2 GAC Baseline		7.47 ± .04	7.39 ± .03	7.33 ± .02	-0.07 ± .05
	.02 GAC	7.46	7.49 ± .01	7.37 ± .01	6.73 ± .01	-0.64 ± .00
	5 Sed		5.64 ± .03	6.04 ± .04	6.04 ± .04	0.00 ± .07
Site	.2 GAC Baseline	4.60	4.79 ± .01	5.06 ± .04	4.89 ± .12	-0.16 ± .10
	pH 12	11.94	11.83 ± .02	11.68 ± .01	11.87 ± .00	0.19 ± .01
	pH 10	10.08	9.56 ± .03	9.17 ± .14	8.95 ± .22	-0.23 ± .08
	pH 7	6.91	6.92 ± .04	6.89 ± .01	7.20 ± .01	0.31 ± .00
	pH 3	3.37	3.86 ± .11	4.08 ± .12	4.05 ± .10	-0.03 ± .02

a. pH measurement after DCB dissolution and additional equilibration between microcosm amendments

In Experiment 5, site water pH was adjusted to determine whether certain pH ranges may have limited biodegradation potential. A single contaminated site can have highly variable subsurface pH, potentially limiting a single bio-amendment strategy. At the SCD site, for example, measured pH varied from 3.6 to 6.8 [28]. Most laboratory examinations of aerobic CB degraders have been conducted at circumneutral pH, with some observed decrease in degradation activity with acidifying pH [56, 57]; however alkaliphilic CB degraders have also been described elsewhere [58]. The inoculum bioreactor fluctuated in pH between 4 and 8, as media self-acidified through CB degradation and was occasionally neutralized to prevent the culture from crashing. It was hypothesized that this pH fluctuation would select for a robust CB-degrading community tolerant of a wide range of pH conditions. The addition of GAC, with ionizable sites and buffering capacity, appeared to move the initial adjusted pH to more circumneutral pH, with changes of 0.02-0.91 after stabilization (t=2d) depending on the condition (Table 4.3).
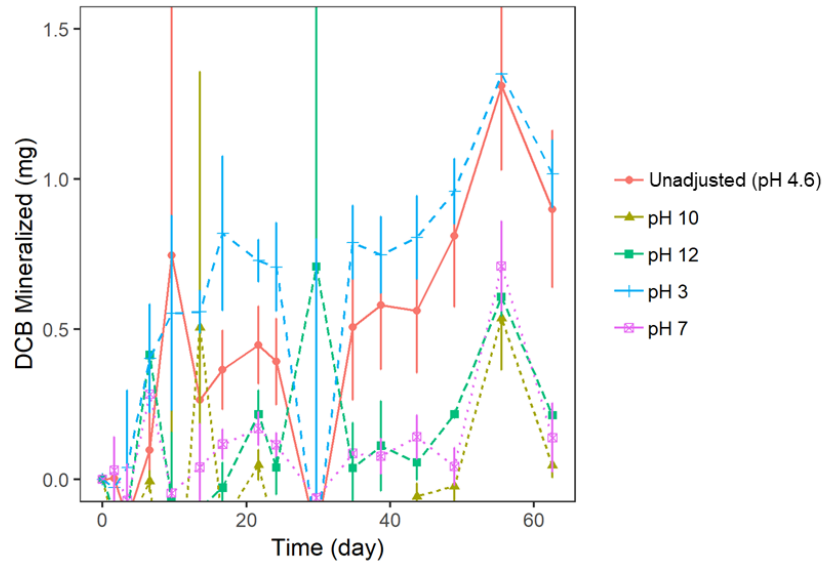
Figure 4.7. Experiment 5: Mineralization of 1,2-DCB pH-adjusted site water microcosms containing 0.2 g inoculated GAC.

Results of degradation in each adjusted site water condition are presented in Figure 4.7. There was high measured concentration variability across sample replicates and time points in most sample conditions. However, there was a significant bifurcation in end-point results between pH conditions. Degradation in adjusted media at pH 3 occurred to nearly the same extent (20% ± 2%) as the unadjusted site water (pH 4.6; 18% ± 5%). However, degradation at pH 7, 10, and 12 was significantly lower (<4%). In all treatments, pH did not drop more than 0.16 (Table 4.3). Results here confirm that substantial degradation can occur in site water with a pH as low as 4 (post-GAC stabilization). Additionally, synthetic media experiments confirm degradation can occur at a pH of 7.5 (Table 4.3). However, these results may not exclude the potential for the inoculum to degrade at higher pH values. During initial pH adjustment for the pH 10 and 12 conditions with NaOH, there was visible flocculation in solution leading to a collection of rust-colored precipitate on the vacuum filter membranes. NaOH addition may have led to the precipitation of dissolved iron as iron-hydroxide, potentially removing iron or important nutrients or constituents (such as

148

NOM) from solution. Follow-up experiments may consider the use of a chelating agent to isolate direct pH effects and prevent inadvertent loss of site water constituents.

4.4.6 Inoculum Dose

Experiment 7 attempted to determine the effects initial inoculum dose may have on initial CB degradation. Our previous experiments either used constant volume of pelleted inoculum or seeded inoculum that was proportional to the available GAC surface area. Inoculum volumes spanning 4 orders of magnitude were tested, from 0.002 to 20 mL, normalized to equal spiking volumes. With prior knowledge that baseline degradation at 0.2 g GAC amendment was low, a lower 0.05 g GAC amendment was used for these microcosms.
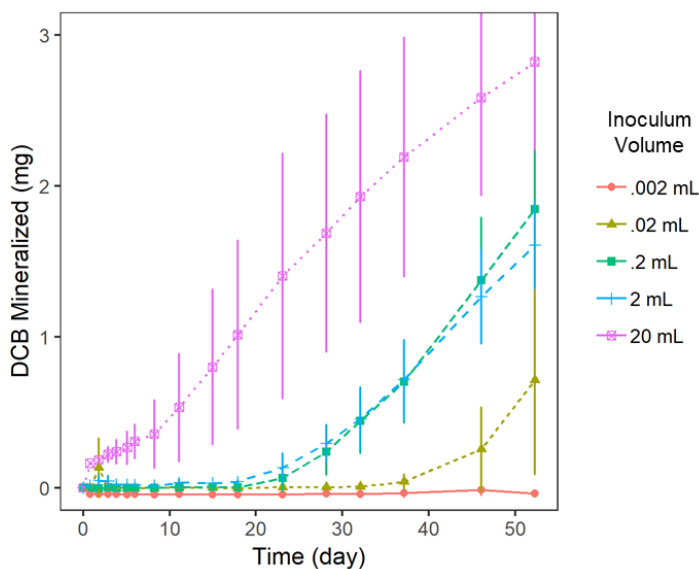
Figure 4.8. Experiment 7: Mineralization of 1,2-DCB in microcosms containing 0.05 mg GAC and separately inoculated with increasing volumes of inoculum culture (pelleted and re-suspended to equal volumes) in synthetic groundwater media.

Results over 52 days are presented in Figure 4.8. No degradation occurred at 0.002 mL inoculum. At concentrations greater than 0.002 mL, there appeared to be a lag period that decreased with increasing dose. Degradation from the 0.2 mL to 2 mL spikes were the

149

only exception, with nearly identical degradation curves. Rousseaux et al. (2003) observed similar decreased lag with log increases in inoculation dose for degradation of atrazine in four different soils [21]. At approximately day 10, the 20 mL treatment showed an inflection that likely indicated a shift from growth-limited degradation to substrate limited degradation (Figure 4.8). The degradation curve appeared convex in all doses except the 20 mL dose and did not appear to shift to a concave shape within the course of the time-series. The shapes of these degradation curves were not conducive to first-order modelling within the observed time period and no inferences could be made about how dose would affect the ultimate extent of degradation. However, the observed trends here suggest higher inoculum dose can substantially decrease degradation lag time upon initial amendment.

Past studies have noted that low native populations of HOC-degrading organisms may be unable to reach high enough biomass density to effectively remediate highly contaminated sediments when the majority of HOC was sorbed and not bioavailable to support growth of degraders [21, 48]. Consequently, bioaugmentation of degraders above some minimum threshold may be required for degradation to proceed on a reasonable timescale. In our model experiment, substantial degradation took less time to initialize with increasing inoculum dose. At the 0.002 mL dose condition, degradation was likely ongoing, but occurring at levels below detection due to small initial degrader populations. Needham et al. (2019) noted that there may be an upper limit to the effectiveness of inoculation dosages for highly sorbed contaminants, where the metabolic rate of microbial degradation exceeds the desorption mass transfer rate of the contaminants [48]. In this case, it may be possible to over-inoculate a contaminated site with degrading culture. Several studies have noted that biofilm-forming organisms may potentially overcome apparent

desorption rate limitations from sorbent to aqueous phase through direct contact with solid surfaces [6, 16, 18, 54]. One proposed mechanism was the production of biosurfactants that increased mass transfer [6]. Another more generalized mechanism was that utilization of HOCs closer to the surface of GAC may create greater concentration gradients that promote desorption [54]. As mentioned previously, specific physiological characteristics of inocula may have an impact on the rate and extent of sorbed contaminant equal to or greater than the quantity of degrader present, and warrant further consideration.

4.4.7 Kinetic Modeling

We attempted to fit time-series data to the first-order degradation model described in Equation 4.3 (Figure 4.9). For GAC microcosms with substantial mineralization (>1 mg), there was generally good fit between the model and the data (Figure 4.9a-c). However, high noise in the site-water microcosms and other samples with low mineralization made model fitting difficult (Figure 4.9d-h). Additionally, the presence of initial lag and convex portions of degradation curves did not lead to good experimental fits (Figure 4.9g-h). Adding a lag term to the model helped to increase fit where there were numerous datapoints available after the lag (Figure 4.9a). We calculated and presented the fitted model parameters for Experiments 1 and 3 (Table 4.4), where there was excellent model fitting for nearly all tested conditions (Figure 4.9a-c). The parameters A (maximum theoretical degradation) and k (first-order rate coefficient) accurately described the observed degradation in microcosms where the real extent of degradation was above 1 mg (Table 4.4). In microcosms with less mineralization, these parameters lacked physical significance and merely represented the best possible parameterized fit by the solver. Initial mineralization rates (IMRs), determined as the product of k and A more closely followed

the observed degradation trends between conditions. In clean GAC systems (Experiment 1), IMRs decreased nearly 2-log from 0.347 mg/day with 0.02 g GAC to 0.006 mg/day with 0.2 g GAC. Sediment addition to GAC (Experiment 3) increased IMRs from 0.006 mg/day (0 g) to 0.253 mg/day (5 g) in synthetic media and from 0.014 mg/day (0 g) to 0.238 mg/day (5 g). The maximum observed IMR from these experiments occurred in microcosms containing 0.5 g sediment without GAC, 1.22 mg/day (Table 4.4).

Table 4.4. First-order model degradation parameters for Experiments 1 and 3

Experiment		Treatment	Degradation Extent (mg) [a]	1st Order Model Parameters				IMR [c] (mg/day)
				A (mg)	k (1/day)	λ (day)	RMSE [b]	
1 GAC Load	Synthetic	0 g GAC	0.0 ± .0	na	na	na	na	na
		0.02 g GAC	4.8 ± .1	4.9 ± .0	0.071 ± .002	6.5 ± .2	0.002	0.347 ± .010
		0.05 g GAC	2.5 ± .1	5.9 ± .2	0.011 ± .000	9.7 ± .2	0.002	0.062 ± .003
		0.2 g GAC	0.3 ± .1	3.6 ± 4.5	0.011 ± .014	0.0 ± .0	0.0001	0.006 ± .001
		1 g GAC	0.0 ± .1	0.1 ± .1	0.110 ± .127	20.0 ± 5.1	0.0004	0.007 ± .004
3 Sediment: GAC Load	Synthetic Media	0.5 g Sed (Uninoculated)	0.0 ± .0	na	na	na	na	na
		0 g Sed	0.3 ± .1	3.6 ± 4.5	0.011 ± .014	na	0.0001	0.006 ± .001
		0.05 g Sed	0.7 ± .2	0.8 ± .2	0.039 ± .005	na	0.0006	0.032 ± .005
		0.5 g Sed	1.2 ± .9	1.3 ± .8	0.046 ± .027	na	0.0091	0.059 ± .007
		5 g Sed	3.0 ± .8	2.8 ± .9	0.089 ± .014	na	0.026	0.253 ± .051
		0.5 g Sed (No GAC)	5.3 ± .1	5.3 ± .2	0.229 ± .058	na	0.229	1.216 ± .347
	Site Media	0 g Sed	0.9 ± .2	8.0 ± .0	0.002 ± .001	na	0.065	0.014 ± .006
		0.05 g Sed	0.7 ± .2	4.2 ± 5.4	0.039 ± .052	na	0.016	0.021 ± .010
		0.5 g Sed	3.2 ± 1.8	1.8 ± .0	0.065 ± .011	na	0.023	0.118 ± .021
		5 g Sed	3.2 ± .3	2.8 ± .2	0.085 ± .010	na	0.031	0.238 ± .043

a. Measured degradation at the end of the 63-day experiment
b. Average modeled parameters from replicate microcosms ± 1 SD
c. Root mean square Error = $\sqrt{mean(Residuals^2)}$
d. Initial Mineralization Rate = A × k
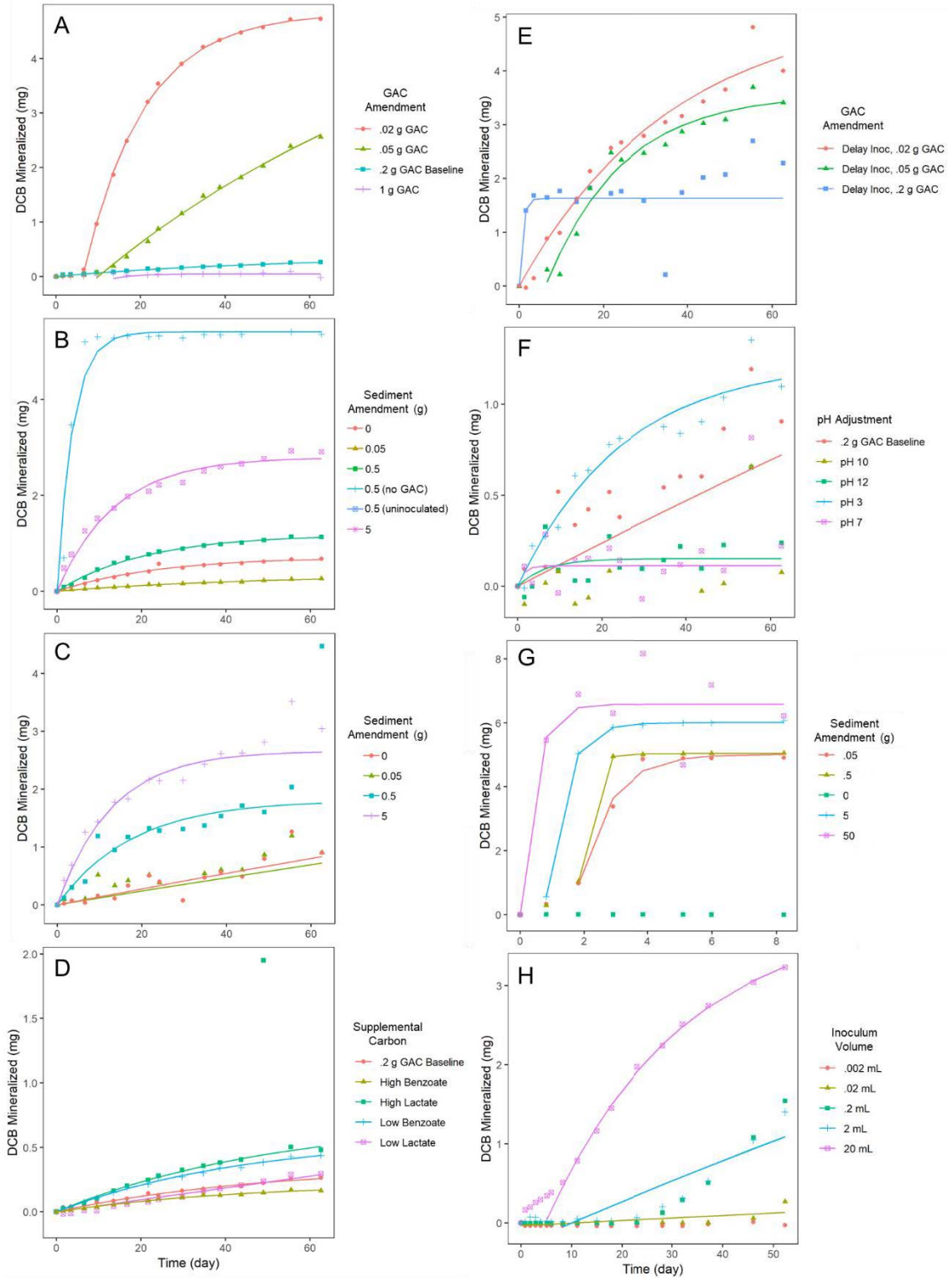
Figure 4.9. Nonlinear regression curve fitting of all experimental datasets to first-order degradation model. (A) Experiment 1 (B) Experiment 3 Synthetic Media (C) Experiment 3 Site Water (D) Experiment 4 (E) Experiment 2 (F) Experiment 5 (G) Experiment 6 (H) Experiment 7. Single representative mesocosms are shown for each treatment.

This modeling effort highlighted the difficulty in capturing kinetic parameters that accurately and universally described degradation throughout all of the tested microcosm conditions. In particular, the first-order model appeared inadequate in describing microcosms with relatively low overall degradation. The application of a lag term into the model improved curve fitting, but also relied on manual selection of initial datapoints for exclusion. Most importantly, the model did not capture the initial convex lag phase at the beginning of many of the tested microcosms. Other models may capture these details more accurately. The Gompertz equation, for example, is a sigmoidal equation with lag, rate, and final extent terms that has been shown to accurately capture growth-associated degradation of contaminants such as pesticides [21, 59]. An even more complex model, the three-half-order model, combines both second-order growth and substrate-associated kinetics with first-order substrate-only kinetics and has been shown to fit well to degradation curves with a lag [60]. These models, however, were not evaluated for this dataset.

4.4.8 Bioremediation Implications

Results from this study raise several considerations for bioremediation applications. Our tests showed that generally, the initial biodegradation in clean systems amended with GAC was low. Although observed degradation in our 0.2 g GAC base case was significantly higher in site water (18% ± 5%) compared to synthetic media (6% ± 1%), both test systems showed decreasing extents of mineralization with increased GAC amendment. This suggests that much of the initially sorbed CB may be unavailable to biodegradation. At a contaminated site, low substrate availability may cause inoculated degraders to die or slough off of GAC before reaching sustainable cell densities. This could

potentially be countered by initially seeding GAC with high cell densities of degraders, which could decrease the lag before observed degradation.

The placement and mixture of GAC relative to sediment at a contaminated site could also impact degradation. Our tests showed that in a well-mixed system, contact with SCD site sediment stimulated 1,2-DCB degradation. In more static field conditions, this suggests that mixing GAC directly with site sediment may impart similar benefits *in situ*. In contrast, applying GAC mixed in an inert sand barrier may lead to conditions more similar to our cleaner GAC system. Oxygen limitations, not considered in this study, would also be a crucial determinant of remediation outcome. The availability of oxygen has been shown to control the extent of aerobic remediation in field systems [61-64] and in our research (Chapters 2-3). Amendment of GAC into water-saturated sediments may not facilitate aerobic biodegradation as effectively as application in unsaturated sediments with greater oxygen availability. Additionally, sediments containing high DOC may reduce the available oxygen for CB degraders.

More broadly, the nature of contamination and management goals must be considered when amending GAC to a site. If the flux of contaminants is low relative to GAC sorption capacity, the GAC may simply act as a "polishing" step to sorb residual contaminant and sequester it to a less bioavailable phase [3]. This could be a viable long-term management strategy that may not require consideration for biodegradation or regeneration. On the other hand, for more highly contaminated sites with a persistent flux of contaminant, GAC could quickly become overloaded beyond its sorption capacity. In this case, facilitating adequate biodegradation of sorbed contaminant would be crucial to regenerate GAC sorption capacity and decrease downgradient concentrations to an

acceptable level. In the latter case, studies like this provide valuable insight to optimize biodegradation rates in sorptive systems.

While these tests provide useful empirical observations, future studies on CB degradation associated with GAC should consider more mechanistic partitioning of CBs and microbial communities between sediment, water, and GAC. Further investigation of biofilm interactions with CBs sorbed to activated carbon can elucidate whether close physical contact between degraders and sorbents can facilitate greater desorption and degradation. This would have wide-ranging applicability for multiple classes of HOCs.

4.5   Conclusions

- Aerobic biodegradation of 1,2-DCB was demonstrated on freshly amended GAC in synthetic media and in SCD site water using both simple GAC seeding and direct addition of inoculum culture into microcosms.

- Increased GAC loading in clean media microcosms led to decreased aqueous CB concentrations, but at decreasing sorbed densities (Experiments 1, 2). Overall extents and rates of mineralization appeared to decrease with increased loading, potentially due to low desorption of CBs from GAC at lower sorption densities.

- Increased SCD sediment loading increased the extent and rate of CB degradation in the presence (Experiment 3) and absence (Experiment 6) of a constant GAC amendment. In the absence of GAC, rapid and complete mineralization was observed within 8 days at tested loadings of 0.33-333 g sediment/L. Partitioning of CBs to sediment coupled with biofilm formation on sediment could reasonably explain observed effects, but was not tested here.

- Increased inoculum concentrations appeared to decrease the initial degradation lag time, suggesting the observed lag in experiments may be related to initial growth of degrading organisms (Experiment 7).

- When substantial degradation occurred (>20%), degradation curves could be accurately modeled with a first-order model, incorporating a lag term to account for delayed degradation in some microcosms. In other microcosms this model did not fit appropriately, and more complex models should be considered.

4.6   References

1. Mercer, J. W.; Cohen, R. M., A review of immiscible fluids in the subsurface: properties, models, characterization and remediation. *Journal of Contaminant Hydrology* **1990**, *6*, (2), 107-163.
2. Feenstra, S.; Mackay, D. M.; Cherry, J. A., A Method for Assessing Residual NAPL Based on Organic Chemical Concentrations in Soil Samples. *Groundwater Monitoring & Remediation* **1991**, *11*, (2), 128-136.
3. Ghosh, U.; Luthy, R. G.; Cornelissen, G.; Werner, D.; Menzie, C. A., In-situ Sorbent Amendments: A New Direction in Contaminated Sediment Management. *Environmental Science & Technology* **2011**, *45*, (4), 1163-1168.
4. Cornelissen, G.; Gustafsson, Ö.; Bucheli, T. D.; Jonker, M. T. O.; Koelmans, A. A.; van Noort, P. C. M., Extensive Sorption of Organic Compounds to Black Carbon, Coal, and Kerogen in Sediments and Soils: Mechanisms and Consequences for Distribution, Bioaccumulation, and Biodegradation. *Environmental Science & Technology* **2005**, *39*, 6881-6895.
5. Lorbeer, H.; Starke, S.; Gozan, M.; Tiehm, A.; Werner, P., Bioremediation of Chlorobenzene-Contaminated Groundwater on Granular Activated Carbon Barriers. *Water, Air and Soil Pollution: Focus* **2002**, *2*, (3), 183-193.
6. Leglize, P.; Alain, S.; Jacques, B.; Corinne, L., Adsorption of phenanthrene on activated carbon increases mineralization rate by specific bacteria. *Journal of Hazardous Materials* **2008**, *151*, (2), 339-347.
7. Rhodes, A. H.; McAllister, L. E.; Chen, R.; Semple, K. T., Impact of activated charcoal on the mineralisation of 14C-phenanthrene in soils. *Chemosphere* **2010**, *79*, (4), 463-469.
8. Oen, A. M. P.; Beckingham, B.; Ghosh, U.; Kruså, M. E.; Luthy, R. G.; Hartnik, T.; Henriksen, T.; Cornelissen, G., Sorption of Organic Compounds to Fresh and Field-Aged Activated Carbons in Soils and Sediments. *Environmental Science & Technology* **2012**, *46*, 810-817.
9. Payne, R. B.; May, H. D.; Sowers, K. R., Enhanced reductive dechlorination of polychlorinated biphenyl impacted sediment by bioaugmentation with a dehalorespiring bacterium. *Environmental science & technology* **2011**, *45*, (20), 8772-8779.
10. Song, Y.; Wang, F.; Kengara, F. O.; Bian, Y.; Yang, X.; Gu, C.; Ye, M.; Jiang, X., Does powder and granular activated carbon perform equally in immobilizing chlorobenzenes in soil? *Environmental Science: Processes & Impacts* **2015**, *17*, 74-80.
11. Bouwer, E. J.; McCarty, P. L., Removal of trace chlorinated organic compounds by activated carbon and fixed-film bacteria. *Environmental Science & Technology* **1982**, *16*, 836-843.
12. Tiehm, A.; Gozan, M.; Müller, A.; Schell, H.; Lorbeer, H.; Werner, P., Sequential anaerobic/aerobic biodegradation of chlorinated hydrocarbons in activated carbon barriers. *Water Science and Technology: Water Supply* **2002**, *2*, 51-58.
13. Chen, B.; Yuan, M.; Qian, L., Enhanced bioremediation of PAH-contaminated soil by immobilized bacteria with plant residue and biochar as carriers. *Journal of Soils and Sediments* **2012**, *12*, (9), 1350-1359.

14. Payne, R. B.; Fagervold, S. K.; May, H. D.; Sowers, K. R., Remediation of polychlorinated biphenyl impacted sediment by concurrent bioaugmentation with anaerobic halorespiring and aerobic degrading bacteria. *Environmental science & technology* **2013**, *47*, (8), 3807-3815.

15. Mercier, A.; Joulian, C.; Michel, C.; Auger, P.; Coulon, S.; Amalric, L.; Morlay, C.; Battaglia-Brunet, F., Evaluation of three activated carbons for combined adsorption and biodegradation of PCBs in aquatic sediment. *Water Research* **2014**, *59*, 304-315.

16. Marchal, G.; Smith, K. E. C.; Rein, A.; Winding, A.; Trapp, S.; Karlson, U. G., Comparing the desorption and biodegradation of low concentrations of phenanthrene sorbed to activated carbon, biochar and compost. *Chemosphere* **2013**, *90*, (6), 1767-1778.

17. Yang, Y.; Hunter, W.; Tao, S.; Crowley, D.; Gan, J., Effect of Activated Carbon on Microbial Bioavailability of Phenanthrene in Soils. *Environmental Toxicology and Chemistry* **2009**, *28*, (11), 2283-2288.

18. Guerin, W. F.; Boyd, S. A., Differential bioavailability of soil-sorbed naphthalene to two bacterial species. *Applied and Environmental Microbiology* **1992**, *58*, (4), 1142.

19. Zhang, W.-x.; Bouwer, E. J., Biodegradation of benzene, toluene and naphthalene in soil-water slurry microcosms. *Biodegradation* **1997**, *8*, (3), 167-175.

20. Herzberg, M.; Dosoretz, C.; Tarre, S.; Beliavski, M.; Green, M., Biological granulated activated carbon fluidized bed reactor for atrazine remediation. *Water Science and Technology* **2004**, *49*, (11-12), 215-222.

21. Rousseaux, S.; Hartmann, A.; Lagacherie, B.; Piutti, S.; Andreux, F.; Soulas, G., Inoculation of an atrazine-degrading strain, Chelatobacter heintzii Cit1, in four different soils: effects of different inoculum densities. *Chemosphere* **2003**, *51*, (7), 569-576.

22. Rhodes, A. H.; Carlin, A.; Semple, K. T., Impact of Black Carbon in the Extraction and Mineralization of Phenanthrene in Soil. *Environmental Science & Technology* **2008**, *42*, (3), 740-745.

23. Lee, S.; Pardue, J. H.; Moe, W. M.; Kim, D. J., Effect of sorption and desorption-resistance on biodegradation of chlorobenzene in two wetland soils. *Journal of Hazardous Materials* **2009**, *161*, 492-498.

24. Lee, S.; Pardue, J. H.; Moe, W. M.; Valsaraj, K. T., Mineralization of desorption-resistant 1,4-dichlorobenzene in wetland soils. *Environmental Toxicology and Chemistry* **2003**, *22*, (10), 2312-2322.

25. Lee, S.; Kommalapati, R. R.; Valsaraj, K. T.; Pardue, J. H.; Constant, W. D., Bioavailability of Reversibly Sorbed and Desorption-Resistant 1,3-Dichlorobenzene from a Louisiana Superfund Site Soil. *Water, Air, and Soil Pollution* **2004**, *158*, (1), 207-221.

26. Klečka, G. M.; McDaniel, S. G.; Wilson, P. S.; Carpenter, C. L.; Clark, J. E.; Thomas, A.; Spain, J. C., Field evaluation of a granular activated carbon fluid-bed bioreactor for treatment of chlorobenzene in groundwater. *Environmental Progress* **1996**, *15*, 93-107.

27. Schwarzenbach, R. P.; Gschwend, P. M.; Imboden, D. M., *Environmental organic chemistry*. 2nd ed. ed.; Wiley,: Hoboken, N.J., 2003.

28. Lorah, M. M.; Walker, C. W.; Baker, A. C.; Teunis, J. A.; Majcher, E. H.; Brayton, M. J.; Raffensperger, J. P.; Cozzarelli, I. M. *Hydrogeologic characterization and assessment of bioremediation of chlorinated benzenes and benzene in wetland areas, Standard Chlorine of Delaware, Inc. Superfund Site, New Castle County, Delaware, 2009-12*; 2328-0328; US Geological Survey: 2014.

29. Zeyer, J.; Kearney, P. C., Microbial degradation of para-chloroaniline as sole carbon and nitrogen source. *Pesticide Biochemistry and Physiology* **1982**, *17*, 215-223.

30. Fathepure, B. Z.; Vogel, T. M., Complete degradation of polychlorinated hydrocarbons by a two-stage biofilm reactor. *Applied and Environmental Microbiology* **1991**, *57*, 3418-3422.

31. Grossman, A.; Ghosh, U., Measurement of activated carbon and other black carbons in sediments. *Chemosphere* **2009**, *75*, (4), 469-475.

32. Miller, W. P.; Miller, D. M., A micro-pipette method for soil mechanical analysis. *Communications in Soil Science and Plant Analysis* **1987**, *18*, (1), 1-15.

33. Kumar, A.; Jena, H. M., Preparation and characterization of high surface area activated carbon from Fox nut (Euryale ferox) shell by chemical activation with H3PO4. *Results in Physics* **2016**, *6*, 651-658.

34. Peng, Z.; Guo, Z.; Chu, W.; Wei, M., Facile synthesis of high-surface-area activated carbon from coal for supercapacitors and high CO2 sorption. *RSC Advances* **2016**, *6*, (48), 42019-42028.

35. Brunauer, S.; Emmett, P. H.; Teller, E., Adsorption of Gases in Multimolecular Layers. *Journal of the American Chemical Society* **1938**, *60*, (2), 309-319.

36. Elzhov, T. V. M., Katharine M.; Spiess, Andrej-Nikolai; Bolker, Ben *minpack.lm: R Interface to the Levenberg-Marquardt Nonlinear Least-Squares*

Algorithm Found in MINPACK, Plus Support for Bound, 1.2-1; 2016.

37. Jiang, X.-W.; Liu, H.; Xu, Y.; Wang, S.-J.; Leak, D. J.; Zhou, N.-Y., Genetic and biochemical analyses of chlorobenzene degradation gene clusters in Pandoraea sp. strain MCB032. *Archives of Microbiology* **2009,** *191*, 485-492.

38. Rapp, P.; Timmis, K. N., Degradation of Chlorobenzenes at Nanomolar Concentrations byBurkholderia sp. Strain PS14 in Liquid Cultures and in Soil. *Applied and Environmental Microbiology* **1999,** *65*, 2547-2552.

39. Fang, H. H. P.; Liang, D.; Zhang, T., Aerobic degradation of diethyl phthalate by Sphingomonas sp. *Bioresource Technology* **2007,** *98*, (3), 717-720.

40. Tiirola, M. A.; Männistö, M. K.; Puhakka, J. A.; Kulomaa, M. S., Isolation and Characterization of *Novosphingobium* sp. Strain MT1, a Dominant Polychlorophenol-Degrading Strain in a Groundwater Bioremediation System. *Applied and Environmental Microbiology* **2002,** *68*, (1), 173-180.

41. Wilkes, H.; Wittich, R.; Timmis, K. N.; Fortnagel, P.; Francke, W., Degradation of Chlorinated Dibenzofurans and Dibenzo-p-Dioxins by Sphingomonas sp. Strain RW1. *Applied and Environmental Microbiology* **1996,** *62*, (2), 367-371.

42. Kurt, Z.; Shin, K.; Spain, J. C., Biodegradation of Chlorobenzene and Nitrobenzene at Interfaces between Sediment and Water. *Environmental Science & Technology* **2012,** *46*, 11829-11835.

43. Field, J. A.; Sierra-Alvarez, R., Microbial degradation of chlorinated benzenes. *Biodegradation* **2007,** *19*, 463-480.

44. Gangupomu, R. H.; Kositkanawuth, K.; Sattler, M. L.; Ramirez, D.; Dennis, B. H.; MacDonnell, F. M.; Billo, R.; Priest, J. W., Analysis and comparison of inertinite-derived adsorbent with conventional adsorbents. *Journal of the Air & Waste Management Association* **2012,** *62*, (5), 489-499.

45. Chen, W. Tailoring and regeneration of Granular Activated Carbon for perchlorate removal. The Pennsylvania State University, 2005.

46. Macleod, C. J. A.; Semple, K. T., The adaptation of two similar soils to pyrene catabolism. *Environmental Pollution* **2002,** *119*, (3), 357-364.

47. Grosser, R. J.; Warshawsky, D.; Vestal, J. R., Indigenous and enhanced mineralization of pyrene, benzo[a]pyrene, and carbazole in soils. *Applied and Environmental Microbiology* **1991,** *57*, (12), 3462.

48. Needham, T. P.; Payne, R. B.; Sowers, K. R.; Ghosh, U., Kinetics of PCB Microbial Dechlorination Explained by Freely Dissolved Concentration in Sediment Microcosms. *Environmental Science & Technology* **2019,** *53*, (13), 7432-7441.

49. Putz Andrea, R. H.; Losh Derek, E.; Speitel Gerald, E., Removal of Nonbiodegradable Chemicals from Mixtures during Granular Activated Carbon Bioregeneration. *Journal of Environmental Engineering* **2005,** *131*, (2), 196-205.

50. Aktaş, Ö.; Çeçen, F., Bioregeneration of activated carbon: A review. *International Biodeterioration & Biodegradation* **2007,** *59*, (4), 257-272.

51. Caldeira, M.; Heald, S. C.; Carvalho, M. F.; Vasconcelos, I.; Bull, A. T.; Castro, P. M. L., 4-Chlorophenol degradation by a bacterial consortium: development of a granular activated carbon biofilm reactor. *Applied Microbiology and Biotechnology* **1999,** *52*, (5), 722-729.

52. Jonker, M. T. O.; Hoenderboom, A. M.; Koelmans, A. A., Effects of sedimentary sootlike materials on bioaccumulation and sorption of polychlorinated biphenyls. *Environmental Toxicology and Chemistry* **2004,** *23*, (11), 2563-2570.

53. Kilduff, J. E.; Wigton, A., Sorption of TCE by Humic-Preloaded Activated Carbon: Incorporating Size-Exclusion and Pore Blockage Phenomena in a Competitive Adsorption Model. *Environmental Science & Technology* **1999,** *33*, (2), 250-256.

54. Poeton, T. S.; Stensel, H. D.; Strand, S. E., Biodegradation of polyaromatic hydrocarbons by marine bacteria: effect of solid phase on degradation kinetics. *Water Research* **1999,** *33*, (3), 868-880.

55. Adebusoye, S. A.; Picardal, F. W.; Ilori, M. O.; Amund, O. O.; Fuqua, C.; Grindle, N., Aerobic degradation of di- and trichlorobenzenes by two bacteria isolated from polluted tropical soils. *Chemosphere* **2007,** *66*, (10), 1939-1946.

56. Balcke, G. U.; Turunen, L. P.; Geyer, R.; Wenderoth, D. F.; Schlosser, D., Chlorobenzene biodegradation under consecutive aerobic–anaerobic conditions. *FEMS Microbiology Ecology* **2004,** *49*, 109-120.

57. Potrawfke, T.; Timmis, K. N.; Wittich, R.-M., Degradation of 1,2,3,4-Tetrachlorobenzene by *Pseudomonas chlororaphis* RW71. *Applied and Environmental Microbiology* **1998,** *64*, (10), 3798-3806.

58. Li, H.; Liu, Y. H.; Luo, N.; Zhang, X. Y.; Luan, T. G.; Hu, J. M.; Wang, Z. Y.; Wu, P. C.; Chen, M. J.; Lu, J. Q., Biodegradation of benzene and its derivatives by a psychrotolerant and moderately haloalkaliphilic Planococcus sp. strain ZD22. *Research in Microbiology* **2006,** *157*, (7), 629-636.

59. Johnsen, A. R.; Binning, P. J.; Aamand, J.; Badawi, N.; Rosenbom, A. E., The Gompertz Function Can Coherently Describe Microbial Mineralization of Growth-Sustaining Pesticides. *Environmental Science & Technology* **2013,** *47*, (15), 8508-8514.

60. Brunner, W.; Focht, D. D., Deterministic Three-Half-Order Kinetic Model for Microbial Degradation of Added Carbon Substrates in Soil. *Applied and Environmental Microbiology* **1984,** *47*, (1), 167.

61. Vogt, C.; Simon, D.; Alfreider, A.; Babel, W., Microbial degradation of chlorobenzene under oxygen-limited conditions leads to accumulation of 3-chlorocatechol. *Environmental Toxicology and Chemistry* **2004,** *23*, 265-270.

62. Vogt, C.; Alfreider, A.; Lorbeer, H.; Hoffmann, D.; Wuensche, L.; Babel, W., Bioremediation of chlorobenzene-contaminated ground water in an in situ reactor mediated by hydrogen peroxide. *Journal of Contaminant Hydrology* **2004,** *68*, 121-141.

63. Balcke, G. U.; Wegener, S.; Kiesel, B.; Benndorf, D.; Schlömann, M.; Vogt, C., Kinetics of chlorobenzene biodegradation under reduced oxygen levels. *Biodegradation* **2007,** *19*, 507-518.

64. Braeckevelt, M.; Mirschel, G.; Wiessner, A.; Rueckert, M.; Reiche, N.; Vogt, C.; Schultz, A.; Paschke, H.; Kuschk, P.; Kaestner, M., Treatment of chlorobenzene-contaminated groundwater in a pilot-scale constructed wetland. *Ecological Engineering* **2008,** *33*, (1), 45-53.

Chapter 5.
Conclusions

In this work, we sought to develop an understanding of chlorobenzene (CB) biodegradation at oxic-anoxic interfaces (OAIs) with the goal of applying the findings to the remediation of contaminated sites. Here, we summarize and discuss the key findings from this work.

5.1   Chlorobenzene Biodegradation Across Oxic-anoxic Interfaces

This research study began with the hypothesis that combined anaerobic reductive dechlorination and aerobic degradation of CBs would provide enhanced *in situ* treatment compared to a single pathway alone. Reductive dechlorination in predominantly anaerobic sediments was shown by others in general to stall at monochlorobenzene (MCB) without further dechlorination to benzene for potential anaerobic oxidation [1, 2]. Additionally, some have shown faster aerobic degradation rates for less chlorinated CBs compared to more highly chlorinated CBs [3, 4]. Combined with the known recalcitrance of highly chlorinated CBs (5-6) to aerobic degradation [1], this suggested potential synergy between coupled degradation pathways.

Our studies focused on less chlorinated mono-, di-, and tri-CBs because they are generally the most common CBs at contaminated sites such as Standard Chlorine of Delaware (SCD) and can be soluble at high micromolar concentrations in groundwater [5]. In Chapter 2 and 3, we tested the degradation of model compound 1,2,4-trichlorobenzene (1,2,4-TCB) across model OAIs at porewater velocities approximating groundwater flow (~2-4 cm/hr). Our experiments showed that both degradation pathways persisted long-term

161

(290-350 days) in simple filter sand matrices and a more complex mixture of SCD wetland sediment and sand. Vertical profiles of porewater CB concentrations showed that reductive dechlorination and aerobic degradation occurred sequentially in anaerobic and aerobic zones respectively without apparent overlap. This spatial separation allowed both pathways to be examined separately. In Chapter 2, we observed rapid rates and of reductive dechlorination; however, dechlorination stalled at MCB, emphasizing that anaerobic reductive dechlorination was not a viable path to mineralization.

After analyzing aerobic degradation patterns for the mix of dechlorinated CBs produced anaerobically, we found that all CB congeners appeared to degrade at a similar rate under oxygen-limiting conditions (Section 2.4.3). This was a crucial finding because it implied that there was no apparent aerobic degradation advantage for dechlorinated CBs compared to the parent compound. Furthermore, results from Chapter 3 suggested that more chlorinated CBs such as TCB may be more advantageous for aerobic degradation under oxygen-limiting conditions since less oxygen is theoretically required to facilitate mineralization compared to dichlorobenzenes (DCBs), and MCB. Consequently, the initial hypothesis for this research appeared incorrect in these oxygen-limited systems. Aerobic CB degradation was not aided by a prior dechlorination step, and aerobic degradation proceeded regardless of congener.

5.2   Factors Affecting Biodegradation at OAIs

In Chapter 2, we investigated the influence of electron donor dose as the primary experimental parameter controlling degradation. Labile organic carbon is frequently found in the subsurface, ranging in form from decaying biomass to simple organic acids such as the model electron donor used here, sodium lactate (NaLac). We found that reductive

dechlorination of CBs in the anaerobic zone was stimulated by increasing doses of NaLac between 0.14 and 1.4 mM, with observed transformations ranging from no dechlorination to complete dechlorination to MCB. However, with increasing electron donor dose, a decreasing fraction was utilized for reductive dechlorination; instead, more electron donor was utilized in side-reactions such as organic acid fermentation and sulfate reduction. Consequently, increased concentrations of reduced substrates decreased the extent of aerobic CB degradation. Increased competition for limited oxygen led to nearly complete inhibition of aerobic CB degradation at 1.4 mM NaLac. Under the tested conditions, this experiment showed a relatively narrow window of 5-50 mg/L DOC where aerobic CB degradation was viable given an oxygen limitation of 7 mg/L. These results emphasized that aerobic degradation at OAIs may not be viable at sites with high labile organic carbon content.

In Chapter 3, alternative electron acceptors nitrate and sulfate were investigated at model OAIs with constant electron donor dose (0.55 mM NaLac) and stable influent oxygen concentration (~7 mg/L). Sulfate, tested at doses of 0.15, 0.5, 2.5, and 10 mM was found to negatively impact reductive dechlorination and aerobic degradation of 1,2,4-TCB at concentrations of at least 0.5 mM and led to near complete inhibition at 10 mM. Anaerobically, sulfate reduction appeared to outcompete CB reductive dechlorination for limited H_2. Aerobically, the re-oxidation of reduced sulfur products appeared to outcompete CB oxidation for limited O_2. These results emphasized that high sulfate in groundwater may pose challenges for biological contaminant remediation regardless of pathway. Nitrate, a more energetically favorable electron acceptor, outcompeted nearly all other reduction processes for limited NaLac at tested concentrations of 0.15, 0.5 and 2.5

mM. Reductive dechlorination was negatively impacted at nitrate concentrations greater than 0.5 mM and completely inhibited degradation at 2.5 mM. However, preferential use of nitrate as an electron acceptor created a permanent reduced sink for electrons and prevented formation of re-oxidizable substrates such as sulfide, organic acids, and methane. This, in turn, decreased competitive oxygen demand and facilitated enhanced aerobic CB degradation at doses of at least 0.5 mM nitrate. Under excess nitrate (2.5 mM), we observed nearly complete degradation of 1,2,4-TCB (26.3 µM) with nearly 2 mg/L residual oxygen remaining, a 270% increase from baseline conditions. These results demonstrated that nitrate, whether naturally occurring or amended, would potentially be beneficial for aerobic CB degradation at contaminated sites.

Recognizing the importance of aerobic CB degradation, in Chapter 4 we investigated how aerobic degradation may be affected in a bioremediation amendment strategy involving sorptive granular activated carbon (GAC). It was found that increasing GAC loadings (0.13-6.7 mg/L) in 1,2-DCB contaminated water led to a significant decrease in aerobic 1,2-DCB mineralization over time. This emphasized a potential tradeoff between sorption capacity and bioavailability for CB-degrading organisms. Increasing mixing ratios of sediment with GAC (0.25-25 g sediment/g GAC) increased both the rate and extent of degradation, mitigating the previously observed inaccessibility of CBs for degradation. Sediment loads in the absence of GAC (0.33-333 g/L sediment) led to rapid and complete mineralization of CBs with decreasing degradation lag times at higher solids concentrations. Combined with observations in Chapter 2 of enhanced reductive dechlorination in columns containing site sediment, site sediments played a beneficial role in promoting biodegradative pathways. Potential benefits from increased

biofilm attachment, bioavailability, and trace nutrient availability were suspected, but would need to investigated directly.

5.3   Microbial Community Characterizations

Characterization of microbial communities in Chapter 2 and 3 column studies provided useful insight into ongoing microbial processes driving transformations of CBs and other redox-sensitive chemicals. In Chapter 2, the vertical stratification of microbial communities was profiled along model OAIs in active CB-degrading columns. In Chapter 3, the microbial communities in porewater were profiled between anaerobic and aerobic zone along time and shifting nitrate- and sulfate- redox conditions.

Results in both experiments showed that anaerobic reductive dechlorination was completely dependent on obligate organohalide respiring bacteria (OHRB) *Dehalobacter*, which emerged in inoculum cultures over other more prominent OHRB. *Dehalobacter* was shown to dominate the anaerobic microbial community in the tested sand and sediment column from Chapter 2, reaching abundances of up to 4×10^8 copies/g (50.9% relative abundance). Consequently, this column had fast reductive dechlorination rates (up to 31.1 µM/hr) and efficient utilization of NaLac for reductive dechlorination (up to 5.8%). In Chapter 3, the relative abundances of *Dehalobacter* in porewater samples had a nearly linear correlation with observed dechlorination activity, suggesting potential microbial signaling of dechlorination activity. Future research involving reductive dechlorination of CBs may consider studying the physiology of *Dehalobacter* more carefully due to its prominence in these tested systems.

Aerobic degradation functionality was not easily attributed to particular keystone organisms. CB degradation can occur across a number of unrelated taxa, which are also capable of degrading a wide variety of other organic substrates. Dominant organisms in aerobic inocula were often not prominent in column samples and vice-versa, indicating species succession between liquid culture and biofilm systems. In all of our tested columns, we did observe the emergence of a known aromatic-degrader *Novosphingomonas* (identified as an Unspecified Sphingogmonadaceae in Chapter 2), which co-occurred with aerobic degradation. The presence of a diverse pool of potential aerobic degraders likely contributed to the observed nonspecific degradability of CBs observed in our experiments. Attempting to track aerobic CB degradation potential may be more effective through functional genes related to CB degradation rather than through taxonomic genes.

Prominent genera associated with methane cycling, sulfate cycling, and nitrate reduction were all identified in column porewater in Chapter 3. Changes in relative abundances of these organisms were generally in agreement with changes in measured redox processes. This showed, at least in closed systems, that abundances of planktonic cell mass could qualitatively signal changes in redox processes. As expected, biofilm communities showed strong stratification across redox conditions. However, these structures were not reflected well by porewater communities. In general, the community data collected was able to reinforce and clarify observed chemical data and assumed processes. While the opportunity for robust sampling was limited in these experiments, the column sampling schemes demonstrated here show great potential for studying other relationships between community and function in model OAIs.

5.4   Practical Significance

Results from this research have several important practical implications. From a fundamental standpoint, we demonstrated a model system that can effectively interrogate changes in chemical and microbial activity across an OAI. Though our work was motivated by a contaminated wetland site, OAIs are abundant in the environment and can occur in any system where the supplies of oxygen and oxygen demand form gradients, whether in subsurface plumes, shallow bodies of water, or hyporheic zones [6].

Although demonstrating sequential reductive dechlorination and aerobic degradation of CBs within a single column was novel from a research standpoint, our results show that, for CBs, promoting both processes would not be beneficial since all tested CB congeners were degradable aerobically. Rather, efforts to enhance oxygen availability and CB degradation pathways over other aerobic oxidations appear crucial. Results from Chapter 3 suggest that nitrate amendment may be an effective tool to maximize oxygen utilization. However, costs of amendment and health concerns associated with nitrate would need to be considered. Although sequential degradation may not be effective for CBs, sequential degradation at OAIs may be more relevant to chlorinated ethenes and polychlorinated biphenyls. Highly chlorinated congeners from these classes (e.g. PCE, TCE, Archlor) are prominent groundwater contaminants and show high recalcitrance to aerobic mineralization, thus necessitating an initial dechlorination step [7, 8].

GAC amendment at sites may help to abiotically sequester CB contaminant when degradation activity is low. Our batch degradation tests in Chapter 4 suggest contact with sediments could enhance biodegradation and regeneration of CBs sorbed to carbon. From an amendment perspective, mixing amendments into sediment may be more beneficial than

stratifying amendments in separate layers. However, oxygen limitations in sediments would also need to be considered.

5.5   Future Research Directions

This work covered a breadth of subjects and methodology within contaminant remediation, microbiology, and hydrology. Our model systems made a number of simplifications and assumptions that don't necessarily capture the full complexity in the environment. Consequently, many important ideas tested here would benefit from additional elaboration and follow-up. Below, we highlight several research directions that could enhance the state of the science and merit further investigation.

The simulated OAIs in our experiments assumed a constant and steady supply of oxygen into the subsurface, approaching air-saturation. In practice, this would be unlikely. Factors including water table fluctuation, photosynthesis, and root zone transport are all transient pathways to deliver oxygen into the subsurface, with concentrations likely to fluctuate substantially [9-11]. Investigating oxygen delivery and penetration into the subsurface would be especially important in wetland systems, where photosynthetic algae and plant coverage could be extensive [12]. Some previous research by others has reported enhanced CB degradation outcomes with pilot-scale constructed wetlands [10, 13, 14]. Additionally, development of predictive models incorporating these factors to estimate oxygen flux and availability *in situ* would be a valuable tool to estimate aerobic degradation potential for a variety of contaminants.

In our model columns, we focused exclusively on biodegradation as opposed to considering abiotic processes such as volatilization and sorption. For the sake of the experiment, contaminant was generally in excess to measure maximum possible extents of

degradation. From a remediation perspective, low contaminant removal rates would be unacceptable. In practice, sites such as SCD may be amended with sorptive media such as GAC as a reactive barrier to provide abiotic sequestration capacity. After establishing baseline degradation outcomes in these experiments, important follow-up work should attempt to incorporate effects of volatilization and sorption into the system. Kurt et al. (2013) found high rates of CB degradation within the vadose zone, suggesting additional fractions of CB could be degraded in unsaturated porespace [15]. GAC amendments, as demonstrated in Chapter 4, would provide sorption capacity to remove CBs from porewater and increase the effective retention time in which biodegradation could occur. A logical extension of this column degradation and batch degradation work would be to test combined degradation and sorption dynamics of CBs in more field-relevant systems that incorporate temporal and spatial variability of contaminant and oxygen flux.

Our sequencing efforts using 16S rRNA left substantial ambiguity in identifying functionally-relevant organisms within the column experiments. Positive identification of potential aerobic CB degraders was especially difficult since CB oxidation spans wide taxonomic groups. While functional genes are often used to assess potential metabolic activity in the field, there does not appear to be an extensive database of genes available to assess aerobic CB degradation [16]. To our knowledge, very few dioxygenases specific to chlorobenzene have been catalogued or studied [17, 18]. Instead, a few nonspecific oxygenase enzymes such as toluene dioxygenase or phenol hydroxylase are currently used by practitioners as proxies for assessing aerobic CB degradation potential [18-20]. Research efforts to better catalog and identify conserved genes specific to CB degradation

would provide a more specific and accurate tool for assessing aerobic CB degradation potential at contaminated sites.

Finally, this research was premised upon the idea that aerobic oxidation of CBs was the most viable pathway to contaminant destruction. While nearly all CB bioremediation treatments in the field utilize aerobic degradation for treatment [10, 21-23], anaerobic mineralization is also a proven degradation pathway [24, 25]. However, this pathway has only been intentionally stimulated under laboratory conditions, where rates of MCB dechlorination are slow and benzene accumulation is common [24, 26, 27]. A recent study by Qiao et al. (2017) found convincing evidence of extensive anaerobic mineralization of MCB and benzene at a contaminated site in China [28]. Research investigating optimal growth conditions for MCB dechlorinators and enhanced anaerobic benzene oxidation in the field could potentially be paradigm-changing for CB bioremediation. Rather than relying on limiting oxygen concentrations, CBs could be mineralized under completely anaerobic conditions. Development of additional CB treatment strategies will help to deplete the large reservoir of legacy CB contamination that still remains at numerous complex sites and mitigate ecological and health impacts.

5.6 References

1. Field, J. A.; Sierra-Alvarez, R., Microbial degradation of chlorinated benzenes. *Biodegradation* **2007,** *19*, 463-480.
2. Fung, J. M.; Weisenstein, B. P.; Mack, E. E.; Vidumsky, J. E.; Ei, T. A.; Zinder, S. H., Reductive Dehalogenation of Dichlorobenzenes and Monochlorobenzene to Benzene in Microcosms. *Environmental Science & Technology* **2009,** *43*, (7), 2302-2307.
3. Dermietzel, J.; Vieth, A., Chloroaromatics in groundwater: chances of bioremediation. *Environmental Geology* **2002,** *41*, (6), 683-689.
4. Elango, V.; Cashwell, J. M.; Bellotti, M. J.; Marotte, R.; Freedman, D. L., Bioremediation of Hexachlorocyclohexane Isomers, Chlorinated Benzenes, and Chlorinated Ethenes in Soil and Fractured Dolomite. *Bioremediation Journal* **2010,** *14*, 10-27.
5. Lorah, M. M.; Walker, C. W.; Baker, A. C.; Teunis, J. A.; Majcher, E. H.; Brayton, M. J.; Raffensperger, J. P.; Cozzarelli, I. M. *Hydrogeologic characterization and assessment of bioremediation of chlorinated benzenes and benzene in wetland areas, Standard Chlorine of Delaware, Inc. Superfund Site, New Castle County, Delaware, 2009-12*; 2328-0328; US Geological Survey: 2014.

6. Brune, A.; Frenzel, P.; Cypionka, H., Life at the oxic-anoxic interface: microbial activities and adaptations. *FEMS Microbiol Rev* **2000,** *24,* (5), 691-710.

7. Payne, R. B.; Fagervold, S. K.; May, H. D.; Sowers, K. R., Remediation of polychlorinated biphenyl impacted sediment by concurrent bioaugmentation with anaerobic halorespiring and aerobic degrading bacteria. *Environmental science & technology* **2013,** *47,* (8), 3807-3815.

8. Tiehm, A.; Schmidt, K. R., Sequential anaerobic/aerobic biodegradation of chloroethenes—aspects of field application. *Current Opinion in Biotechnology* **2011,** *22,* (3), 415-421.

9. Baillie, P. W., Oxygenation of intertidal estuarine sediments by benthic microalgal photosynthesis. *Estuarine, Coastal and Shelf Science* **1986,** *22,* 143-159.

10. Braeckevelt, M.; Reiche, N.; Trapp, S.; Wiessner, A.; Paschke, H.; Kuschk, P.; Kaestner, M., Chlorobenzene removal efficiencies and removal processes in a pilot-scale constructed wetland treating contaminated groundwater. *Ecological Engineering* **2011,** *37,* 903-913.

11. Weishaar, J. A.; Tsao, D.; Burken, J. G., PHYTOREMEDIATION OF BTEX HYDROCARBONS: POTENTIAL IMPACTS OF DIURNAL GROUNDWATER FLUCTUATION ON MICROBIAL DEGRADATION. *International Journal of Phytoremediation* **2009,** *11,* (5), 509-523.

12. Chen, Z.; Wu, S.; Braeckevelt, M.; Paschke, H.; Kästner, M.; Köser, H.; Kuschk, P., Effect of vegetation in pilot-scale horizontal subsurface flow constructed wetlands treating sulphate rich groundwater contaminated with a low and high chlorinated hydrocarbon. *Chemosphere* **2012,** *89,* (6), 724-731.

13. Braeckevelt, M.; Rokadia, H.; Imfeld, G.; Stelzer, N.; Paschke, H.; Kuschk, P.; Kästner, M.; Richnow, H.-H.; Weber, S., Assessment of in situ biodegradation of monochlorobenzene in contaminated groundwater treated in a constructed wetland. *Environmental Pollution* **2007,** *148,* (2), 428-437.

14. Braeckevelt, M.; Mirschel, G.; Wiessner, A.; Rueckert, M.; Reiche, N.; Vogt, C.; Schultz, A.; Paschke, H.; Kuschk, P.; Kaestner, M., Treatment of chlorobenzene-contaminated groundwater in a pilot-scale constructed wetland. *Ecological Engineering* **2008,** *33,* (1), 45-53.

15. Kurt, Z.; Spain, J. C., Biodegradation of Chlorobenzene, 1,2-Dichlorobenzene, and 1,4-Dichlorobenzene in the Vadose Zone. *Environmental Science & Technology* **2013,** *47,* 6846-6854.

16. Iwai, S.; Johnson, T. A.; Chai, B.; Hashsham, S. A.; Tiedje, J. M., Comparison of the Specificities and Efficacies of Primers for Aromatic Dioxygenase Gene Analysis of Environmental Samples. *Applied and Environmental Microbiology* **2011,** *77,* (11), 3551.

17. van der Meer, J. R.; van Neerven, A. R.; de Vries, E. J.; de Vos, W. M.; Zehnder, A. J., Cloning and characterization of plasmid-encoded genes for the degradation of 1,2-dichloro-, 1,4-dichloro-, and 1,2,4-trichlorobenzene of Pseudomonas sp. strain P51. *Journal of Bacteriology* **1991,** *173,* (1), 6-15.

18. Werlen, C.; Kohler, H.-P. E.; van der Meer, J. R., The Broad Substrate Chlorobenzene Dioxygenase and cis-Chlorobenzene Dihydrodiol Dehydrogenase of Pseudomonas sp. Strain P51 Are Linked Evolutionarily to the Enzymes for Benzene and Toluene Degradation. *Journal of Biological Chemistry* **1996,** *271,* (8), 4009-4016.

19. Dominguez, R. F.; Silva, M. L. B. d.; McGuire, T. M.; Adamson, D.; Newell, C. J.; Alvarez, P. J. J., Aerobic bioremediation of chlorobenzene source-zone soil in flow-through columns: performance assessment using quantitative PCR. *Biodegradation* **2007,** *19,* 545-553.

20. Environmental Biotechnology Testing Lab.

21. Lorbeer, H.; Starke, S.; Gozan, M.; Tiehm, A.; Werner, P., Bioremediation of Chlorobenzene-Contaminated Groundwater on Granular Activated Carbon Barriers. *Water, Air and Soil Pollution: Focus* **2002,** *2,* (3), 183-193.

22. Vogt, C.; Alfreider, A.; Lorbeer, H.; Hoffmann, D.; Wuensche, L.; Babel, W., Bioremediation of chlorobenzene-contaminated ground water in an in situ reactor mediated by hydrogen peroxide. *Journal of Contaminant Hydrology* **2004,** *68,* 121-141.

23. Balcke, G. U.; Paschke, H.; Vogt, C.; Schirmer, M., Pulsed gas injection: A minimum effort approach for enhanced natural attenuation of chlorobenzene in contaminated groundwater. *Environmental Pollution* **2009,** *157,* (7), 2011-2018.

24. Liang, X.; Devine, C. E.; Nelson, J.; Sherwood Lollar, B.; Zinder, S.; Edwards, E. A., Anaerobic Conversion of Chlorobenzene and Benzene to CH4 and CO2 in Bioaugmented Microcosms. *Environmental Science & Technology* **2013,** *47,* 2378-2385.

25. Nelson, J. L.; Jiang, J.; Zinder, S. H., Dehalogenation of Chlorobenzenes, Dichlorotoluenes, and Tetrachloroethene by Three Dehalobacter spp. *Environmental Science & Technology* **2014,** *48,* (7), 3776-3782.

26. Nelson, J. L.; Fung, J. M.; Cadillo-Quiroz, H.; Cheng, X.; Zinder, S. H., A Role for Dehalobacter spp. in the Reductive Dehalogenation of Dichlorobenzenes and Monochlorobenzene. *Environmental Science & Technology* **2011**, *45*, (16), 6806-6813.

27. Puentes Jácome, L. A.; Edwards, E. A., A switch of chlorinated substrate causes emergence of a previously undetected native Dehalobacter population in an established Dehalococcoides-dominated chloroethene-dechlorinating enrichment culture. *FEMS Microbiology Ecology* **2017,** *93*, (12), fix141-fix141.

28. Qiao, W.; Luo, F.; Lomheim, L.; Mack, E. E.; Ye, S.; Wu, J.; Edwards, E. A., Natural Attenuation and Anaerobic Benzene Detoxification Processes at a Chlorobenzene-Contaminated Industrial Site Inferred from Field Investigations and Microcosm Studies. *Environmental Science & Technology* **2017**.

Appendix A.

Supplementary Information for Chapter 2

A.1 Supplemental Methods

A.1.1 Chemicals and Reagents

CB reagents and analytical standards (≥98% purity), cyclohexane (HPLC grade, ≥99.9%), organic acid analytical standards, and 60% w/w sodium DL-lactate syrup were purchased from Sigma-Aldrich (St. Louis, MO). Inorganic anion analytical standards were purchased from Thermo Fisher Scientific (Waltham, MA). Reagent water used in experiments and analyses was distilled and treated with a Milli-Q® purification system (Millipore, Burlington, MA).

A.1.2 Column Design

Columns were constructed by fusing 4 mL borosilicate glass vials at 3.75 cm intervals along the vertical column length to produce sampling ports at 25, 50, and 75% of the nominal flowpath (Glass Shop, University of Maryland Baltimore County). Customized caps were fitted with Luer Lock ports attached to short segments of 1/16" (1.59 mm) ID polytetrafluoroethylene (PTFE) tubing to facilitate sampling at the center of the column cross-section. Opposite the 3 sample ports, a fourth port was fused in the same manner 10 cm from the bottom of the column (67% of nominal flowpath) in the same manner for use as injection port for an oxygenated side-stream. The column entrance and exit were fitted with PTFE end caps attached to 3-way valves attached to the normal flowpath as well as Luer Lock sample ports. All caps and fittings were constructed of PTFE

or polyvinylidene fluoride (PVDF). All tubing was constructed of PTFE, except for peristaltic pump tubing, which was Viton rubber.

Sand was prepared by dry sieving between 0.55 and 0.65 μm, rinsing 3 times with distilled water, drying overnight at 110 °C, and autoclaving for 30 minutes. Sediment was prepared by sieving wet sediment below 1 mm to remove heterogeneous debris and autoclaving for 30 minutes. The SSC mixture was prepared by mixing autoclaved sand and sediment and autoclaving again for 30 minutes. Columns were aseptically packed within a sterile biosafety cabinet by sequentially pouring 1-cm layers into the columns and tamping.

A.1.3   Simulated Groundwater Media

Mineral media constituents were prepared as two separate 2× concentrated stock solutions to minimize contamination and reactions before being utilized in the column system. Both stocks were prepared by autoclaving 3.5 L Milli-Q® water in glass bottles for 45 minutes followed by a 60-minute N_2 purge and cool-down to sterilize influent media and remove dissolved oxygen without chemical scavenging. Cooled bottles were transferred to an anaerobic glovebag, where chemical constituents were added. Stock #1 consisted of a mixture of electron donor sodium lactate (NaLac) and dissolved model contaminant 1,2,4-trichlorobenzene (1,2,4-TCB). 70 mg of neat 1,2,4-TCB was spiked into the bottle and stirred for 2 days using a large Teflon stir bar to ensure complete dissolution of the organic phase. Concentrated NaLac stock was added to achieve desired concentrations set throughout the experiment. Stock #2 consisted of a defined mineral salt solution (described below), where 1000× concentrated filter-sterilized salt stocks were added to attain desired final concentrations. Stock #1 was anaerobically transferred to a 5 L Tedlar® fluoropolymer sampling bag and Stock #2 to a 5 L foil-lined sampling bag

(Sigma-Aldrich). These bags were used to provide zero-headspace media reservoirs outside of the glovebag to minimize re-oxygenation and CB losses during column operation. These were periodically replenished during experimental operation as the media were depleted and conditions varied.

Final diluted mineral media entering the column (from Stock #2) consisted of 8.5 mg/L KH_2PO_4; 22 mg/L K_2HPO_4; 33 mg/L Na_2HPO_4; 5.0 mg/L $CaH_4(PO_4)_2$; 1.25 mg/L $FeSO_4 \cdot 7H_2O$; 100 mg/L $(NH_4)_2HPO_4$; 25 mg/L $MgSO_4 \cdot 7H_2O$. Trace elements, modified from Zeyer and Kearney, were added to the media at final concentrations of 1.0 mg/L $MnSO_4 \cdot 4H_2O$; 0.25 mg/L $(NH_4)_6Mo_7O_{24} \cdot 4H_2O$; 0.25 mg/L $Na_2B_4O_7 \cdot 10H_2O$; 0.25 mg/L $CoCl_2 \cdot 6H_2O$; 0.25 mg/L $CuCl_2 \cdot 2H_2O$; 0.25 mg/L $ZnCl_2$; 1.0 mg/L $NaVO_3$ [1]. Vitamins from a single stock solution were added at final concentrations of 0.1 mg/L pyridoxine-HCl; 0.05 mg/L thiamine-HCl; 0.05 mg/L riboflavin; 0.05 mg/L nicotinic acid; 0.05 mg/L biotin; 0.02 mg/L folic acid; 0.005 mg/L cobalamin; 0.05 mg/L p-aminobenzoic acid [2]. 1 mg/L resazurin was also added to influent media as a qualitive redox indicator.

To minimize changes to upstream redox conditions, the media used for the oxygenated side stream consisted of autoclaved Milli-Q® water without additional nutrient addition. Water was stored in a capped 2 L glass reservoir containing a constant 100 mL/min stream of 0.22 µm-filtered O_2 from a compressed tank using a diffusive bubbler to achieve saturated concentrations.

A.1.4 Inocula Preparation

The aerobic enrichment culture used to inoculate SC was seeded by passing 1 L of site water from the SCD wetland site (USGS well 15-B) through a 0.22 µm filter. The filter, containing retained biomass, was placed in a continuously stirred, semi-continuous flow 3-

L glass spinner flask reactor containing the simulated groundwater media described here seeded and fed with a mixture of MCB, 1,2-DCB, and 1,2,4-TCB vapor as an exclusive carbon source. The culture was maintained for over a year at a hydraulic retention time of 56 days with weekly CB feeding, media replenishment, and pH neutralization. CB degradation was indicated by increase in OD_{600} and drop in culture pH.

The anaerobic enrichment was derived from chloroethene/ethane dechlorinating enrichment culture WBC-2 (SiREM Labs). As received, the original culture showed no initial capacity to degrade CBs. A subculture diluted 10× into simulated groundwater media in an anaerobic glovebag was able to stoichiometrically dechlorinate 1,2,4-TCB to monochlorobenzene using sodium lactate as an electron donor (Figure A.1). After completing two dechlorinating cycles of 10 mg/L 1,2,4-TCB to MCB, the subculture was used for column inoculation.

A.1.5   GC-MS Analysis of Chlorobenzenes

100 µL of aqueous sample was transferred via gastight microsyringe (Hamilton 1710RN) into a 1.5 mL borosilicate autosample vial filled with 1 mL of extraction solvent consisting of cyclohexane spiked with 1 mg/L bromobenzene internal standard. The vial was capped with a PTFE-lined silicone septum and vortexed in parallel with other samples in a multi-tube vortexer (VWR) for 5 min at 1800 rpm. Extraction facilitated an effective 10:1 dilution of analytes for analysis. Extracted sample phases were allowed to separate in-vial at 4 °C and were stored refrigerated in the same vial until analysis. Samples were introduced by liquid autosample injection (Agilent 7693) to a GC (Agilent 7890B) equipped with an HP-5MS column (30 m × 250 µm, 0.25 µm) coupled to a single quadrupole MS detector (Agilent 5977). The instrument was run with the following

parameters – 1 mL/min ultrapure helium (Airgas) carrier gas flow, 1 µL split injection (10:1 split ratio), 250 °C inlet temperature. The autosampler syringe was programmed to sample at a depth of 5 mm from the bottom of vials in order to prevent accidental injection of the underlying aqueous phase in the bottom. The oven was ramped from 50 °C to 160 °C at a rate of 15 °C/min followed by a ramp to 250 °C at 50 °C/min (9 min total run). The MS was run in selected ion monitoring (SIM) mode at 5.8 Hz and a Gain Factor of 3 with source and quadrupole temperatures at 230 °C and 150 °C respectively. m/z values of 112, 156, 146, and 180 were used to quantify MCB, bromobenzene, DCBs, and TCBs respectively with two qualifier ions monitored for QC. Aqueous standards were prepared from a mix of CB stocks, extracted as described above, and utilized for 5-point calibration, with a linear range between 0.05 mg/L to 10 mg/L, easily measured without dilution. In method development, calculated extraction efficiencies of aqueous standards were found to be between 95% (MCB) and 109% (1,4-DCB) (data not shown), which are already factored into calibration. Concentrations were quantified using the relative responses of the analyte peak areas normalized to the bromobenzene internal standard peak area.

A.1.6 Ion Chromatography Analysis of Anions

A Thermo Fisher Dionex ICS-2100 system equipped with a conductivity cell detector, KOH eluent generator, ASRS suppressor, 25 µL injection loop, and 0.5 mL Polyvial® autosampler (Dionex AS-40) was utilized to analyze anions. The conductivity cell and column were both maintained at 30 °C. Inorganic anions were analyzed using an AS18 ion exchange column (250 mm × 4 mm, 7.5 µm) with column guard at a flow of 0.9 mL/min run isocratically for 20 minutes with 30 mM KOH eluent and 67 mA suppressor current. Inorganic anion concentrations were determined using a 6-point linear calibration

curve from 0.1 mg/L to 20 mg/L using a combined seven-anion standard (Thermo Fisher). Organic acids were analyzed using an AS11-HC ion exchange column (250 mm × 4 mm, 9 μm) with column guard at a flow of 1 mL/min with a KOH eluent gradient and constant 75 mA suppressor current. The eluent gradient program consisted of a 20 min hold at 1 mM, 8 min ramp to 12 mM, 1 min ramp to 60 mM, 4 min hold at 60 mM, and 4 min post-run equilibration at 1 mM (37 min total run). Samples were diluted and organic acid concentrations were determined using a 6-point linear calibration from 1 μM to 200 μM.

A.1.7 *Microbial Community Analysis*

Sample sequence data was processed and classified using plugins within the qiime2 pipeline (v. 2018.4.0). Forward and reverse reads were both trimmed at 24 bp to remove primers and truncated at 218 bp to remove low quality score bases. Paired-end sequences were denoised, joined, and dereplicated with DADA2 using a 10-fold minimum parent over abundance [3]. Samples had an average of 149,000 reads. Across all samples, over unique 3600 features were identified. Features were taxonomically classified using the built-in Naïve Bayes feature classifier plugin *classify-sklearn* trained with Greengenes 13_8 99% OTUs reference sequences [4-6]. qiime2 feature table, tree, and taxonomy artifacts were imported into R (v.3.5.1) using the *qiime2R* (v.0.99.1) package [7]. Community analyses were conducted using *phyloseq* (v.1.26.0) [8] microbial community analysis package and *vegan* (v.2.5.3) community ecology package[9]. Visualizations were generated using *ggplot2* (v.3.1.0).

Column samples were sequenced in duplicate. Sample replicates did not account for significant variation in beta diversity (Weighted Unifrac, PERMANOVA analysis,

10,000 permutations, p=.32, R^2=.036). Therefore, taxa abundances from each column segment replicate were averaged based on relative abundances.

Total protein quantification was adapted from a method described by Onesios and Bouwer (2012) [10]. Approximately 1 g (wet weight) of column matrix sample was added to 4 mL of phosphate buffered saline solution. The mixture was vortexed for 10 seconds, sonicated in a bath for 5 minutes at 40 kHz (Branson 1510), and centrifuged for 5 minutes at 4000×g. The supernatant was analyzed using a BCA assay (Thermo Fisher) following the manufacturer's instructions, utilizing bovine serum albumin as a calibration standard with a quadratic calibration curve. Biomass concentrations were normalized to the mass of oven-dried subsample. Biomass subsampling and quantification were performed in duplicate. Quantified results are presented in Figure A.7.

A.1.8   qPCR Enumeration of Total Bacteria

A portion of eluted DNA was diluted 5× for quantitative analysis of total eubacteria. Conserved 16S primers 1055f (5'-ATGGYTGTCGTCAGCT-3') and 1392r (5'-ACGGGCGGTGTGTAC-3') were developed in other studies for the WBC-2 culture and chlorobenzene reductive dechlorination [11, 12].

External calibration standards were created using DNA template amplified with the total bacteria primers inserted into a plasmid vector using a pCR™Blunt II-TOPO® kit (Thermo Fisher) following the manufacturer's instructions. The vector was transformed into chemically competent *E. coli* cells using the One Shot™ TOP10 kit (Thermo Fisher) and plated following the manufacturer's instructions. Colonies containing the transformed vector were selected on the basis of kanamycin resistance, re-plated, and grown in 50 mL LB broth for 12 hours at 35 °C. Suspended cells were pelleted, and plasmid DNA was

isolated using a GeneJET Plasmid Miniprep Kit (Thermo Fisher) following the manufacturer's instructions. Plasmid DNA was visualized and purified using gel electrophoresis to ensure the exclusion of chromosomal DNA fragments. The cloned sequence identity was confirmed by Sanger sequencing. Purified plasmid concentrations were determined using Qubit® and converted to gene fragment copy number (copy # / mL) using the formula:

$$\text{Copy \#} = \frac{\text{Mass concentraton}}{(\text{Insert Length} + \text{Vector Length}) \times 660 \frac{g}{\text{mol bp}}} \times N_A$$

where each vector contains a single insert, the Vector Length is 3519 bp, the average molecular mass of 1 bp is assumed to be 660 g/mol, and N_A is Avogadro's constant $(6.02 \times 10^{23} \text{ mol}^{-1})$. These purified plasmid stocks were then serially diluted 10-fold to yield qPCR standards ranging in concentrations from 1×10^4 to 1×10^{11} copies/mL.

All samples and standards were analyzed simultaneously as 20 µL reactions in 96-well plates in a real-time PCR system (Biorad CFX96 Touch). Reactions consisted of 10 µL of 2× concentrated SsoAdvanced™ Universal SYBR® Green Supermix (BioRad), 2µL template DNA, 2 µL F primer (3 µM), 2 µL R primer (3 µM), and 4 µL ultrapure water. Sample template DNA was first diluted 5× before analysis. The amplification program utilized was 3 minutes denature step at 95 °C followed by 40 cycles of 30 seconds denaturation at 95 °C, 30 seconds annealing at 59 °C, and 30 seconds elongation at 72 °C. A calibration curve of C_q versus copy number was based on results of triplicate qPCR reactions. Calibration parameters were a slope = -3.39, intercept=46.0, R^2=.992, and efficiency=97.1%. Duplicate column DNA sample extracts were run with duplicate technical replicates. Limits of analyte quantitation in PCR tubes were 10^5 copies/mL. Bacteria copy number concentrations for each column sample were calculated relative to

the mass of matrix from which the DNA was extracted, where the copy number determined in the PCR well C_{PCR} was multiplied by the template dilution factor DF (5×), the total elution volume from the DNA extraction kit (0.1 mL), and the inverse of the total mass of solid matrix extracted M_{col}:

$$C_{col} = C_{PCR} \times DF \ \times 0.1 \text{ mL elution V} \div M_{col}$$

Limits of column sample concentration were approximately 10^5 copies/g sample, depending on exact mass of matrix sampled.

A.1.9 Sample Calculations

    a. Degree of Effluent Chlorination:

Average number of attached chlorines for the CBs in column effluent (100% port) measurement. Assessment of how dechlorinated the congener mix is. Subject to fluctuation based on influent CB concentration.

$$\text{Average Chlorination}_{100} = \frac{3 \times \sum TCB_{100} + 2 \times \sum DCBs_{100} + 1 \times MCB_{100}}{\sum CBs_{100}}$$

    b. Anaerobic Dechlorinations:

Estimated number of reductive dechlorination reactions to have occurred, based on appearance of daughter DCB (1 dechlorination) and MCB (2 dechlorinations) congeners. Presumed independent of influent CB concentration if it is in excess.

$$\text{Dechlorinations} = \frac{(2 \times MCB_{100} + \sum DCBs_{100})}{\sum CBs_{100}} \times \sum CBs_0$$

    c. Anaerobic Dechlorination Rate:

Estimated zero-order rate of degradation based on dechlorinations observed over the retention time of the anaerobic zone (Table 2.1).

$$\text{Rate} = \text{Dechlorinations}/\text{HRT}_{\text{Anaerobic Zone}}$$

d. Electron Donor Utilization:

Theoretical electron equivalent comparison of reductive dechlorination electron utilization versus availability of electrons from NaLac dose. Assume 12 mol e⁻ / mol NaLac and 2 e⁻ / dechlorination reaction.

$$\text{Donor Utilizaton} = \frac{\text{Dechlorinations}}{[\text{NaLac}]_0} \times \frac{2e^-}{\text{CB dechlorination}} \div \frac{12e^-}{\text{Lactate}} \times 100\%$$

e. Percent Removal:

Fraction of influent CBs removed due to aerobic degradation. Degradation is based on concentrations of CB entering the aerobic zone, therefore influent concentrations (0% port) must be divided by the dilution factor DF. Quantity subject to fluctuation based on influent CB concentration.

$$\% \text{ Removal} = 1 - [\Sigma\text{CBs}_{100} \div (\Sigma\text{CBs}_0 \div DF)]$$

f. Aerobic Degradation:

Removal of total CBs across column on a molar basis. Degradation is based on concentrations of CB entering the aerobic zone, therefore influent concentrations (0% port) must be divided by the dilution factor DF. Presumed independent of influent CB concentration if it is in excess.

$$\text{Aerobic Degradation} = (\Sigma\text{CBs}_0 \div DF) - \Sigma\text{CBs}_{100}$$
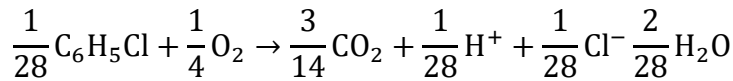
g. Aerobic Degradation Rate:

Estimated zero-order rate of degradation based on total CB removal observed over the retention time of the aerobic zone (Table 2.1).

$$\text{Rate} = \text{Aerobic Degradation}/\text{HRT}_{\text{Aerobic Zone}}$$

    h. Oxygen Utilization:

Theoretical % of available DO used for aerobic CB degradation based on electron equivalent balance. Assume 4 mol e^- / mol O_2 and 24, 26, and 28 mol e^- / mol TCB, DCB, and MCB oxidized, respectively.

Example balanced CB oxidation:

$$\frac{1}{28}C_6H_5Cl + \frac{1}{4}O_2 \rightarrow \frac{3}{14}CO_2 + \frac{1}{28}H^+ + \frac{1}{28}Cl^- \frac{2}{28}H_2O$$

Since the e^- demand varies slight depending on CB congener, we determined the average e^- demand u of CBs based on the average degree of chlorination of the effluent (S2a).

$$u = 24 + 2 \times (3 - \text{Average chlorination}_{100})$$

$$\text{Oxygen Utilization} = \frac{\text{Aerobic Degradation}}{[O_2]_{\text{aerobic zone}}} \times \frac{u\ e^-}{\text{CB oxidation}} \div \frac{4e^-}{O_2} \times 100\%$$

    i. Cl Balance

The agreement between apparent Cl loss due to CB removal and dechlorination versus the change of free chloride measured between the influent and effluent. Apparent Cl loss is based on the total number of attached Cls on CB molecules at the effluent vs influent. Chloride balance was calculated at each time point and then averaged. Therefore, phase

summary chloride balance is not reflective simply of the summary chloride change and apparent Cl loss.

$$\text{Attached Cl}_0 = 3 \times \sum\text{TCB}_0$$

$$\text{Attached Cl}_{100} = 3 \times \sum\text{TCB}_{100} + 2 \times \sum\text{DCBs}_{100} + 1 \times \text{MCB}_{100}$$

$$= \text{Average chlorination}_{100} \times \sum\text{CBs}_{100}$$

$$\text{Apparent Cl Loss} = \text{Attached Cl}_0 \div DF - \text{Attached Cl}_{100}$$

$$\text{Measured Cl}^- \text{ Change} = [\text{Cl}^-]_{100} \times \text{Dilution Factor} - [\text{Cl}^-]_0 \div DF$$

$$\text{Chloride Balance} = \frac{\text{Measured Cl}^- \text{ Change}}{\text{Apparent Cl Loss}}$$

    j.   Net Sulfate Change

The net change in sulfate concentration between influent and effluent, adjust to the effluent concentration.

$$\text{Sulfate Change} = [\text{SO}_4^{2-}]_{100} - [\text{SO}_4^{2-}]_0 \div DF$$

    k. Sulfur Oxygen Demand

Theoretical % of available DO used for sulfide oxidation CB degradation based on electron equivalent balance. Assume sulfide oxidation to sulfate and 8 mol e$^-$/ mol sulfate produced.

$$\text{Sulfate Oxygen Demand} = \frac{\text{Sulfate Increase}}{[\text{O}_2]_{\text{aerobic zone}}} \times \frac{8\text{ e}^-}{\text{Sulfide oxidation}} \div \frac{4\text{e}^-}{\text{O}_2} \times 100\%$$

    l.   Sample Calculations:

Using SSC Phase 1 summary values as an example (Table 2.2; Table A.1).

Average Chlorination $= 1.8$ Dechlorinations $= 44.2\ \mu M$

$$\text{Dechlorination Rate} = \frac{44.2\ \mu M}{3.02\ hr} = 14.7\ \mu M/hr$$

$$\text{Donor Utilizaton} = \frac{0.0442\ mM}{0.28\ mM} \times \frac{2e^-}{\text{CB dechlorination}} \div \frac{12e^-}{\text{Lactate}} \times 100\% = 2.7\%$$

$$\% \text{ Removal} = 1 - [14.7\ \mu M \div (36.1\ \mu M \div 1.30)] \times 100\% = 47.1\%$$

$$\text{Aerobic Degradation} = (36.1\ \mu M \div 1.30) - 14.7\ \mu M = 13.1\ \mu M$$

$$\text{Aerobic Rate} = \frac{13.1\ \mu M}{1.16\ hr} = 11.3\ \mu M/hr$$

$$u = 24 + 2 \times (3 - 1.8) = 26.5\ \frac{e^-}{\text{CB Effluent}}$$

$$\text{Oxygen Utilization} = \frac{0.0131\ mM\ \text{CB degraded}}{5.9\frac{mg}{L} \times \frac{1\ mmol}{32\ mg}O_2} \times \frac{26.5\ e^-}{\text{CB oxidation}} \div \frac{4e^-}{O_2} \times 100\%$$

$$= 47.4\%$$

m. Calculate increase in oxygen demand from sulfur oxidation between Phase 3 and

1:

Net sulfate change$_{\text{Phase 1}} = -12\ \mu M$ Net sulfate change$_{\text{Phase 3}} = +28\ \mu M$

Increase in sulfide oxidaton $= 28\ \mu M + 12\ \mu M = 40\ \mu M$

Sulfur Oxygen Demand Increase

$$= \frac{.04\ mM\ \text{sulfate}}{6.8\frac{mg}{L} \times \frac{1\ mmol}{32\ mg}O_2} \times \frac{8\ e^-}{\text{Sulfide oxidation}} \div \frac{4e^-}{O_2} \times 100\% = 37.6\%$$

A.2   Tables and Figures
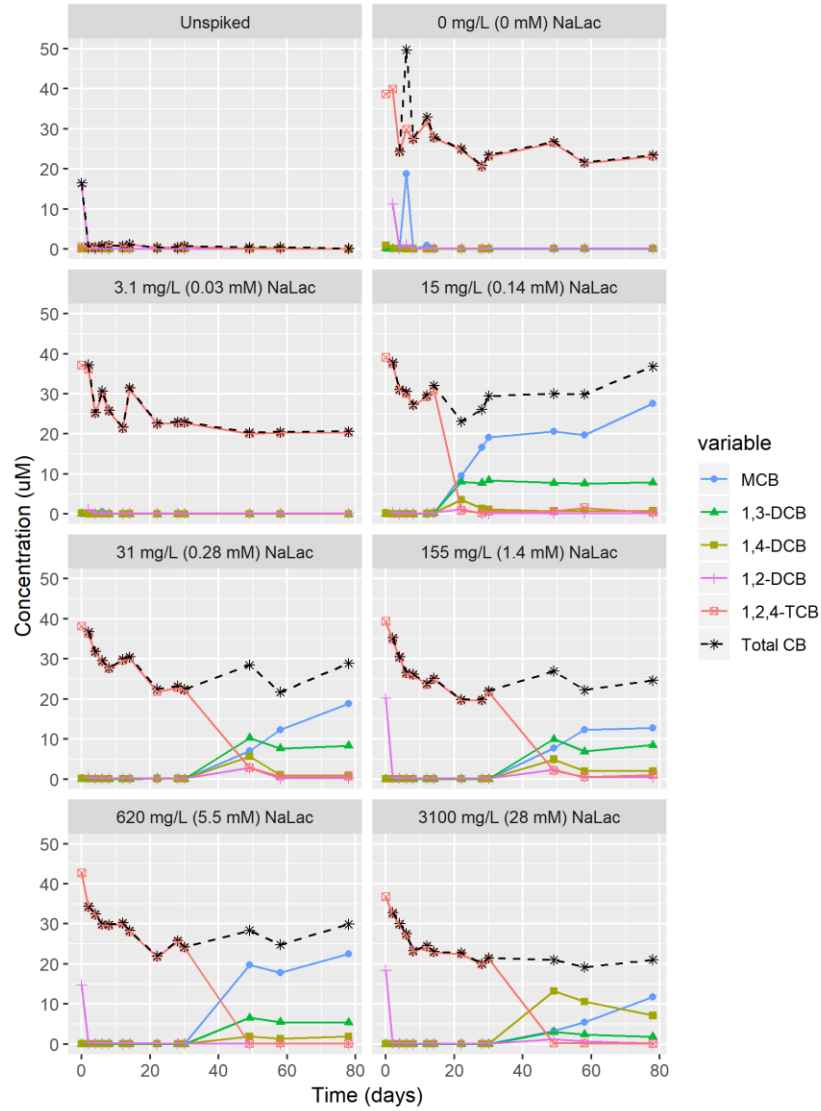
Figure A.1. Batch microcosms of anaerobic SSC inoculum culture demonstrating reductive dechlorination of 1,2,4-TCB and appearance of daughter products under varying NaLac doses. Primary daughter products were MCB; 1,3-DCB; and 1,4-DCB.
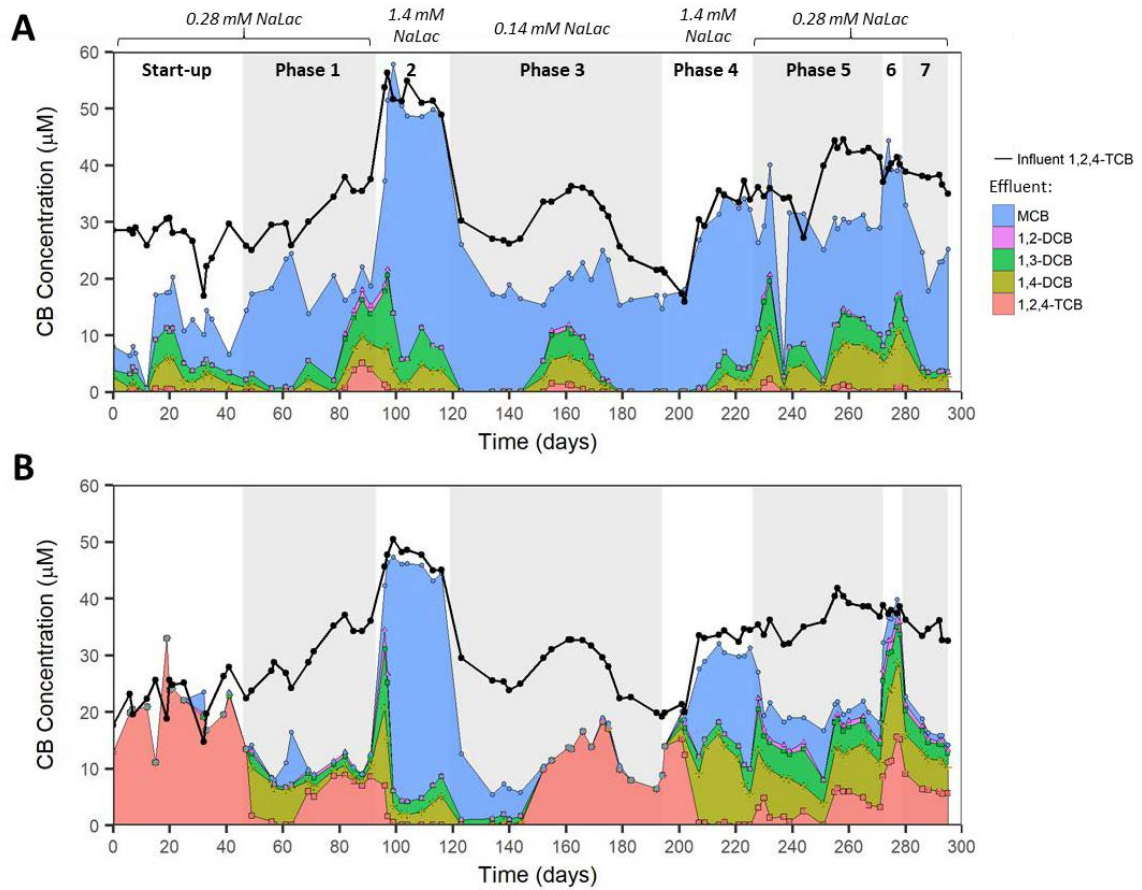
Figure A.2. Measured influent (0% port) and effluent (100% port) profiles of CB concentrations along experimental time-series for (A) Sand and Sediment Column (SSC) and (B) Sand Column (SC) Connected black data points represent influent concentration of 1,2,4-TCB, and colored stacked areas represent the combined effluent concentrations of all CB congeners. To visualize the mass balance between column influent and effluent, effluent concentrations were multiplied by the side-stream dilution factor of 1.30. This results in a visual exaggeration of the actual observed effluent concentration and aerobic degradation

Table A.1. Additional phase-summarized column measurements and calculations

Experimental Phase	Duration (days)	n	Column	Aerobic Zone DO (mg/L)	Influent 1,2,4-TCB (µM) [mg/L]	Measured Effluent Total CB (µM)	Effluent Degree of Chlorination	Expected Cl⁻ Loss from Degradation (µM)	Measured Cl⁻ Change (µM)	Net Sulfate Change (µM)
1 0.28 mM NaLac	47	5	SSC	5.9 ± 1.2	36.1 ± 1.5 (6.6 ± .3)	14.7 ± 1.8	1.8 ± .4	74.7 ± 9.7	58.1 ± 7.5	-12 ± 13
			SC		35.3 ± 1.2 (6.4 ± .2)	8.6 ± 1.2	2.7 ± .0	75.5 ± 1.6	37.5 ± 33.0	-24 ± 67
2 1.4 mM NaLac	26	4	SSC	6.5 ± 0.3	51.5 ± 2.5 (9.3 ± .4)	37.7 ± .4	1.2 ± .0	97.2 ± 8.9	83.6 ± 10.5	-143 ± 40
			SC		46.5 ± 1.9 (8.4 ± .3)	34.5 ± 1.1	1.1 ± .0	88.8 ± 6.0	84.0 ± 6.2	-56 ± 29
3 0.14 mM NaLac	75	4	SSC	6.8 ± 0.6	23.1 ± 1.9 (4.2 ± .4)	12.1 ± .8	1.0 ± .0	53.6 ± 5.9	60.4 ± 7.3	28 ± 17
			SC		21.0 ± 1.7 (3.8 ± .3)	6.5 ± 1.3	3.0 ± .1	38.1 ± 5.3	42.8 ± 7.4	9 ± 9
4 1.4 mM NaLac	32	5	SSC	7.5 ± 0.6	34.9 ± 1.5 (6.3 ± .3)	25.4 ± 1.1	1.1 ± .0	68.9 ± 4.7	70.4 ± 7.4	-69 ± 5
			SC		33.8 ± .9 (6.1 ± .2)	23.6 ± .7	1.5 ± .1	57.0 ± 5.6	59.6 ± 2.1	-39 ± 5
5 0.28 mM NaLac	46	6	SSC	7.5 ± 0.5	42.7 ± 1.1 (7.8 ± .2)	22.8 ± .8	1.4 ± .1	85.6 ± 2.8	79.8 ± 3.3	-23 ± 13
			SC		39.2 ± 1.7 (7.1 ± .3)	15.6 ± 1.1	2.1 ± .1	74.7 ± 3.2	74.0 ± 5.1	0 ± 20
6 0.28 mM NaLac, O₂ Off	7	4	SSC	0.7 ± 0.1 *	40.3 ± .9 (7.3 ± .2)	31.5 ± 1.9	1.4 ± .1	65.3 ± 4.0	57.0 ± 5.6	-67 ± 9
			SC		37.8 ± .6 (6.9 ± .1)	29.0 ± 1.2	2.3 ± .1	27.7 ± 6.1	27.0 ± 2.6	-30 ± 8
7 0.28 mM NaLac	16	5	SSC	7.3 ± 0.3	37.1 ± 1.4 (6.7 ± .2)	17.5 ± 2.2	1.2 ± .0	86.2 ± 5.1	82.5 ± 6.8	-49 ± 7
			SC		33.8 ± 1.5 (6.1 ± .3)	12.4 ± 1.3	2.3 ± .0	64.3 ± 5.2	54.8 ± 11.2	0 ± 8

Results presented as average ±1 SD
* Though O₂ was purged from feed, some oxygen detected at side-stream entrance resulting in nonzero DO
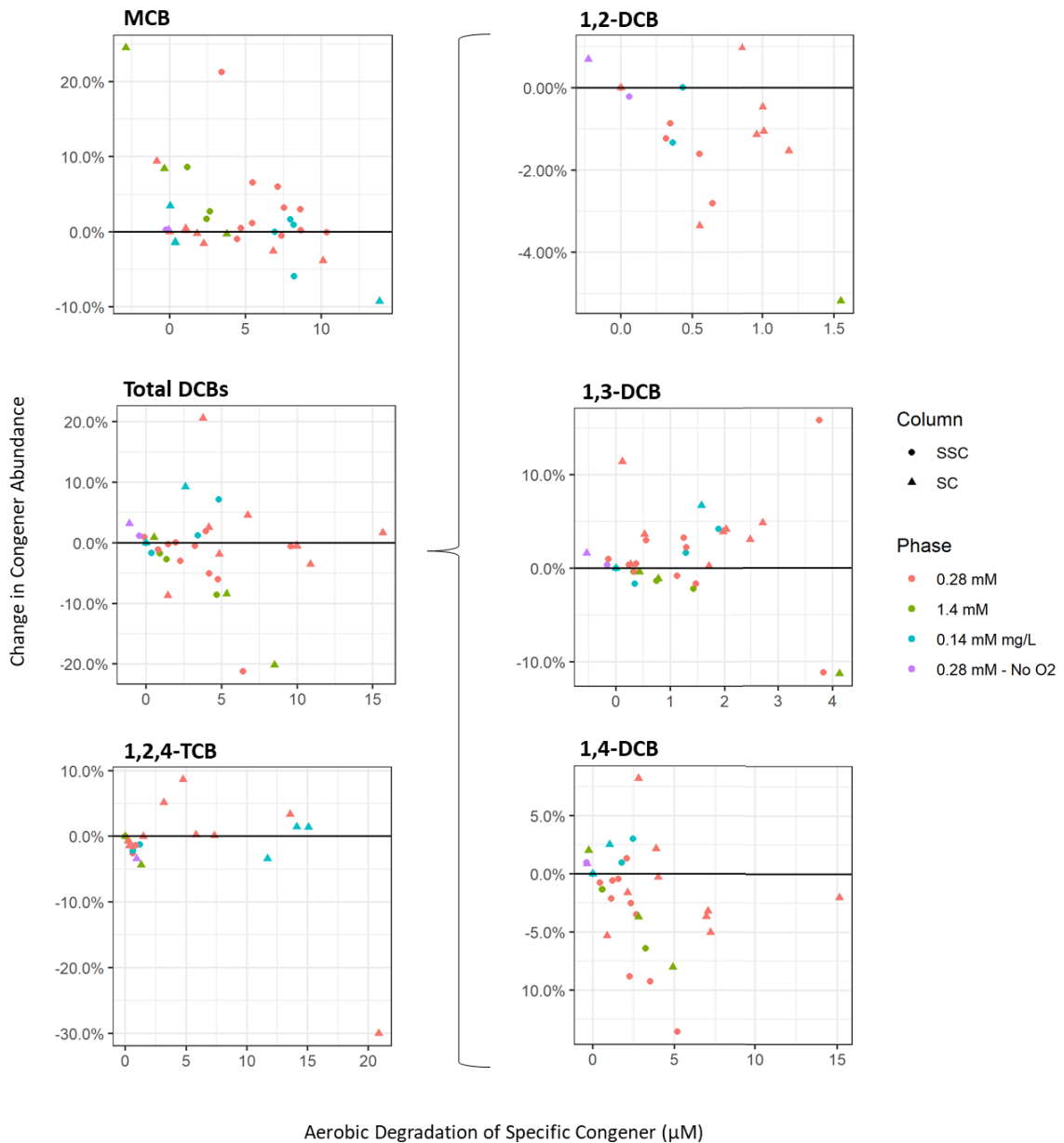
Figure A.3. Change in relative abundances of CB congeners as fraction of total CBs (y-axis) compared to aerobic degradation of each congener (x-axis) across column aerobic zone. Negative change in relative abundance (below the black line) indicates a preferential utilization of that congener in aerobic degradation. Substantial aerobic degradation typically only occurred at phases with 0.28 mM (red) and 0.14 mM (blue) influent NaLac concentrations. Substantial reductive dechlorination did not typically occur for column SC at 0.14 mM. Top row shows comparison based on degree of chlorination of congeners, with all DCBs aggregated together. Bottom rows shows DCB broken down into individual congeners. n=37 vertical sample points.

189

Table A.2. Average measured change in congener relative abundance from aerobic degradation

Congener	Average Change [a]	p-value [b]	Significance [c]
MCB	2.0%	0.058	NS
DCB (Total)	-1.1%	0.344	NS
1,2-DCB	-0.5%	0.0108	*
1,3-DCB	1.1%	0.164	NS
1,4-DCB	-1.7%	0.0154	*
TCB	-0.9%	0.3073	NS

a. Combined results from both columns; n= 37 vertical sample points
b. p-value derived from 2-tailed unpaired Student's t-test
c. NS – not significant (p>=.05); * - significant (p<.05)
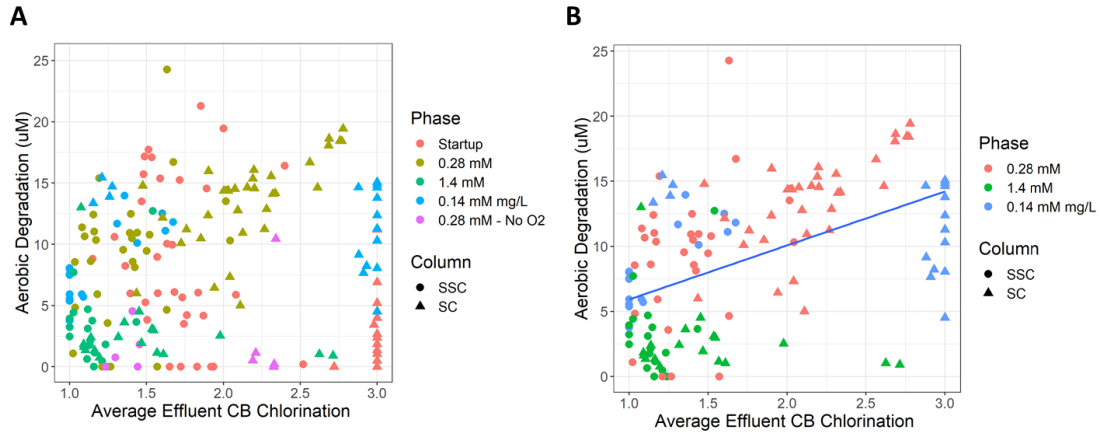
Figure A.4. Summary of all effluent (100% port) column sample time points comparing average effluent CB chlorination resulting from reductive dechlorination (x-axis) to the total observed aerobic degradation (y-axis). Higher reductive dechlorination activity indicated by lower effluent CB chlorination. (A) Total samples from entire experiment. (B) Filtered sample set removing startup and anoxic phases from comparison due to inhibited aerobic degradation. Linear regression analysis of filtered sample set yielded a poorly-fitting (R^2=.234) curve (y=4.14x+1.78) suggesting more chlorinated CB congeners were associated with higher aerobic degradation activity in the columns.
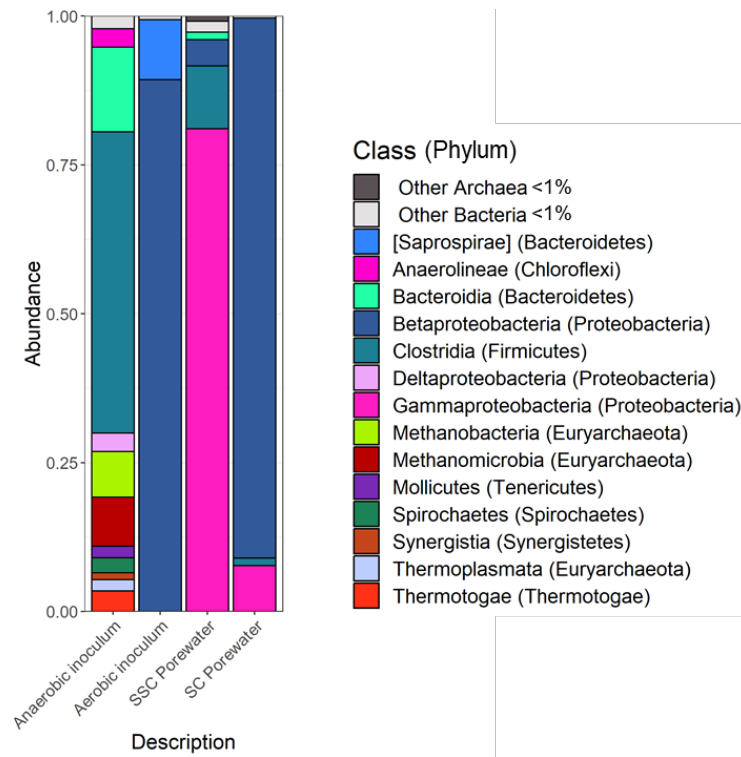
Figure A.5. Class-level microbial community profiles in inocula cultures and column porewater. Bacteria and Archaea classes with <1% representation aggregated as "Other". [Bracketed groups] were not identified at class level and were identified at the next closest taxonomic level.
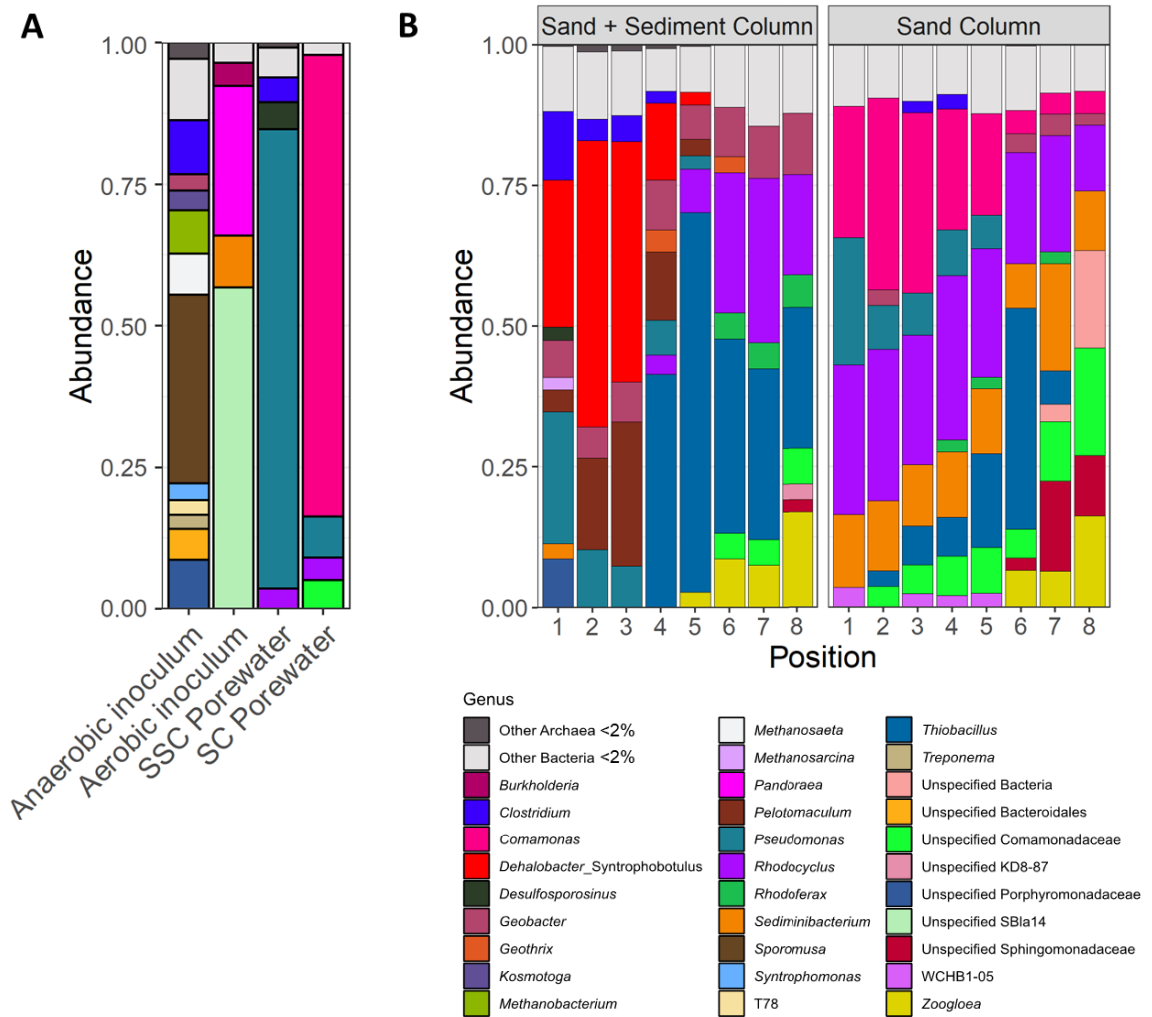
Figure A.6. Genus-level microbial community profiles in (A) inocula cultures and column porewater and (B) segmented column biofilm profiles. Bacteria and Archaea genera with <2% representation aggregated as "Other". Groups unidentified at the genus level labeled as "Unspecified" and identified at the next available taxonomic level.
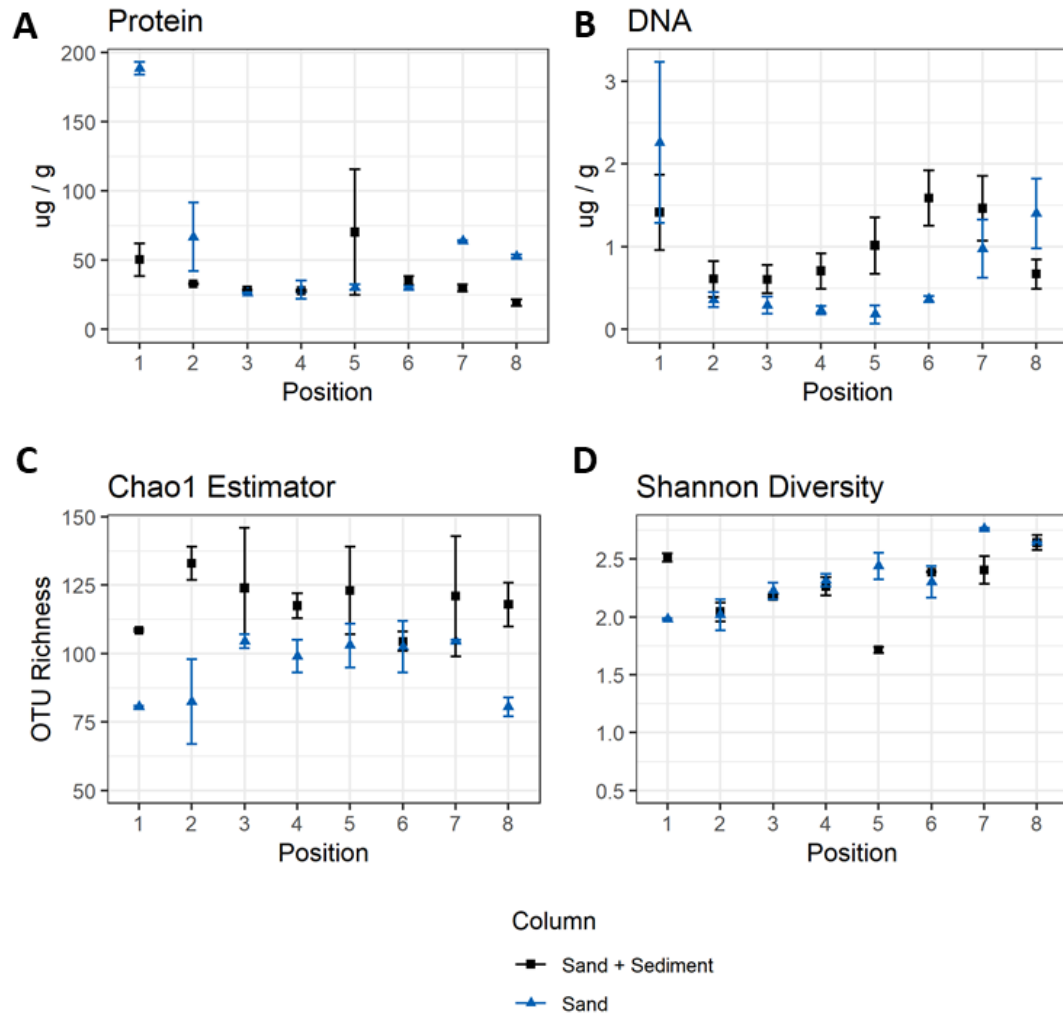
Figure A.7. Aggregate analyses of vertically-segmented column biofilm communities in Sand and Sediment Column (SSC) and Sand Column (SC). (A) Biomass estimation by crude protein extraction and quantitation with BCA assay (B) Total DNA concentrations of samples extracted by PowerSoil kit and used in sequencing. (C) Chao1 richness estimation, counting unique OTUs present in a sampled population ($S_1 = S_{obs} + \frac{F_1^2}{2F_2}$, S_{obs} = # observed OTUs, F_1 = # singletons, F_2 = # doubletons). (D) Shannon alpha diversity index, estimating relative entropy of sample OTUs, including richness and evenness ($H = -\sum_{i=1}^{R} p_i \ ln(p_i)$, R=# unique OTUs, p_i= relative abundance of each unique OTU). Data points in each plot are average values and error bars are range of values for duplicate measurements

Table A.3. Comparison of prominent genera in porewater and biofilm matrix microbial communities

Class	Genus	SSC			SC		
		Total Matrix Abundance [a]	Porewater Abundance	log (Porewater/Matrix)	Total Matrix Abundance [a]	Porewater Abundance	log (Porewater/Matrix)
Betaproteobacteria	*Thiobacillus*	22.2%	0.29%	-1.9	4.1%	0.017%	-2.4
Clostridia	*Dehalobacter*	19.9%	0.08%	-2.4	0.2%	0.034%	-0.8
Betaproteobacteria	*Rhodocyclus*	9.0%	3.6%	-0.4	22.4%	4.0%	-0.7
Gammaproteobacteria	*Pseudomonas*	8.9%	81.1%	1.0	12.8%	7.3%	-0.2
Clostridia	*Pelotomaculum*	8.1%	0.12%	-1.8	0.016%	ND [b]	-
Clostridia	*Desulfosporosinus*	1.1%	4.8%	0.6	0.35%	0.53%	0.2
Clostridia	*Clostridium*	4.2%	4.4%	0.0	1.0%	0.44%	-0.3
Bacteroidia	Unspecified Porphyromonadaceae	2.3%	1.2%	-0.3	0.70%	0.0071%	-2.0
Betaproteobacteria	*Comamonas*	0.47%	0.19%	-0.4	17.3%	81.5%	0.7
[Saprospirae]	*Sediminibacterium*	1.4%	0.49%	-0.5	12.5%	0.15%	-1.9
Betaproteobacteria	Unspecified Comamonadaceae	1.6%	0.08%	-1.3	6.9%	5.1%	-0.1
Methanomicrobia	*Methanosarcina*	0.89%	0.010%	-2.0	0.020%	0.002%	-1.1
Alphaproteobacteria	*Xanthobacter*	0.0035%	ND [b]	-	0.16%	ND [b]	-
Alphaproteobacteria	Unspecified Sphingomonadaceae	0.48%	0.004%	-2.0	3.79%	0.006%	-2.8
Betaproteobacteria	*Pandoraea*	0.48%	0.039%	-1.1	0.040%	ND [b]	-

a. Total matrix relative abundance estimated by summation of total abundances in each column segment:

$$\frac{\sum_{i=1}^{8} \% \, Abundance_i \times Total \, 16S \, Copies_i}{\sum_{i=1}^{8} Total \, 16S \, Copies_i}$$

b. ND – non-detection in porewater sequencing

A.3 References

1. Zeyer, J.; Kearney, P. C., Microbial degradation of para-chloroaniline as sole carbon and nitrogen source. *Pesticide Biochemistry and Physiology* **1982,** *17*, 215-223.

2. Fathepure, B. Z.; Vogel, T. M., Complete degradation of polychlorinated hydrocarbons by a two-stage biofilm reactor. *Applied and Environmental Microbiology* **1991,** *57*, 3418-3422.

3. Callahan, B. J.; McMurdie, P. J.; Rosen, M. J.; Han, A. W.; Johnson, A. J. A.; Holmes, S. P., DADA2: high-resolution sample inference from Illumina amplicon data. *Nature methods* **2016,** *13*, (7), 581.

4. Pedregosa, F.; Varoquaux, G.; Gramfort, A.; Michel, V.; Thirion, B.; Grisel, O.; Blondel, M.; Prettenhofer, P.; Weiss, R.; Dubourg, V.; Vanderplas, J.; Passos, A.; Cournapeau, D.; Brucher, M.; Perrot, M.; Duchesnay, É., Scikit-learn: Machine learning in Python. *Journal of machine learning research* **2011,** *12*, (Oct), 2825-2830.

5. DeSantis, T. Z.; Hugenholtz, P.; Larsen, N.; Rojas, M.; Brodie, E. L.; Keller, K.; Huber, T.; Dalevi, D.; Hu, P.; Andersen, G. L., Greengenes, a Chimera-Checked 16S rRNA Gene Database and Workbench Compatible with ARB. *Applied and Environmental Microbiology* **2006,** *72*, (7), 5069-5072.

6. McDonald, D.; Price, M. N.; Goodrich, J.; Nawrocki, E. P.; DeSantis, T. Z.; Probst, A.; Andersen, G. L.; Knight, R.; Hugenholtz, P., An improved Greengenes taxonomy with explicit ranks for ecological and evolutionary analyses of bacteria and archaea. *The Isme Journal* **2011,** *6*, 610.

7. Bisanz, J. E. *qiime2R: Importing QIIME2 artifacts and associated data into R sessions*, 0.99; 2018.

8. McMurdie, P. J.; Holmes, S., phyloseq: An R Package for Reproducible Interactive Analysis and Graphics of Microbiome Census Data. *PLOS ONE* **2013,** *8*, (4), e61217.

9. Oksanen, J.; Blanchet, F. G.; Friendly, M.; Kindt, R.; Legendre, P.; McGlinn, D.; Minchin, P. R.; O'Hara, R. B.; Simpson, G. L.; Solymos, P.; Stevens, M. H. H.; Szoecs, E.; Wagner, H. *vegan: Community Ecology Package*, 2.5-3; 2018.

10. Onesios, K. M.; Bouwer, E. J., Biological removal of pharmaceuticals and personal care products during laboratory soil aquifer treatment simulation with different primary substrate concentrations. *Water Research* **2012,** *46*, (7), 2365-2375.

11. Puentes Jácome, L. A.; Edwards, E. A., A switch of chlorinated substrate causes emergence of a previously undetected native Dehalobacter population in an established Dehalococcoides-dominated chloroethene-dechlorinating enrichment culture. *FEMS Microbiology Ecology* **2017,** *93*, (12), fix141-fix141.

12. Ferris, M. J.; Muyzer, G.; Ward, D. M., Denaturing gradient gel electrophoresis profiles of 16S rRNA-defined populations inhabiting a hot spring microbial mat community. *Applied and Environmental Microbiology* **1996,** *62*, (2), 340-346.

Appendix B.

Supplementary Information for Chapter 3

B.1   Dissolved Methane Analysis

For dissolved methane analysis, approximately 5 mL of porewater were sampled in glass syringes. After collection, samples were immediately transferred to pre-weighed 8 mL glass serum bottles and sealed with butyl rubber stoppers and crimp tops. Total sample volume was determined gravimetrically. Bottles were shaken vigorously by hand for 10 seconds and stored upright at room temperature (approximately 20 °C) for 1 hour to achieve equilibrium between the liquid samples and headspace.

100 µL of headspace were sampled using a gastight glass syringe with a sample lock and manually injected into a GC-FID (Agilent 7890) utilizing splitless injection at 200 °C inlet temperature. Methane peaks were resolved at a retention time of 1.35 minutes using helium carrier gas at 2 mL/min flow in an Agilent DB-5ms column (30 m × 250 µm, .25 µm) at a constant 40 °C oven temperature. The FID was operated at 230 °C with detector gas flows of 400 mL/min air, 40 mL/min H_2, and 40 mL/min N_2 makeup. Methane concentrations were calibrated linearly to standards prepared by spiking known volumes (2-250 µL) of pure methane calibration standard (99%; Restek, Bellefonte, PA) into sealed 160 mL serum bottles, corresponding to gas-phase concentrations of 0.05– 6.75 mg/L.

Aqueous concentrations were back-calculated from headspace concentrations using Henry's Law [1, 2]. Henry's solubility constant was calculated as a function of room temperature during each measurement according to Equation B.1, where H^0 is the Henry's

constant at T^0 (298 K), $\frac{d \ln(H)}{d\left(\frac{1}{T}\right)}$ is an empirical temperature dependence constant, and T is

the room temperature during analysis [2].

Equation B.1

$$H^{cp}(T) = H^0 \times exp\left(\frac{d\ ln(H)}{d\left(\frac{1}{T}\right)} \times \left(\frac{1}{T} - \frac{1}{T^0}\right)\right)$$

Literature values for H^0 (1.4×10^{-5} mol m^{-3} Pa^{-1}) and $\frac{d \ln(H)}{d\left(\frac{1}{T}\right)}$ (1600 K) were selected

according to Burkholder et al. (2015) [1]. Henry's constant was converted to a

dimensionless solubility constant (aqueous / gas concentration) according to Equation B.2,

where R is the ideal gas constant and T is the room temperature.

Equation B.2

$$H^{cc} = H^{cp} \times RT$$

A mass balance (Equation B.3) was used to calculate the methane concentration (C_{aq}) in

the porewater sample (V_l) based on the equilibrated concentration (C_h) measured in the gas

phase (V_h).

Equation B.3

$$C_{aq} = \frac{C_h(V_h + H^{cc}V_l)}{V_l}$$

B.2 Tables and Figures
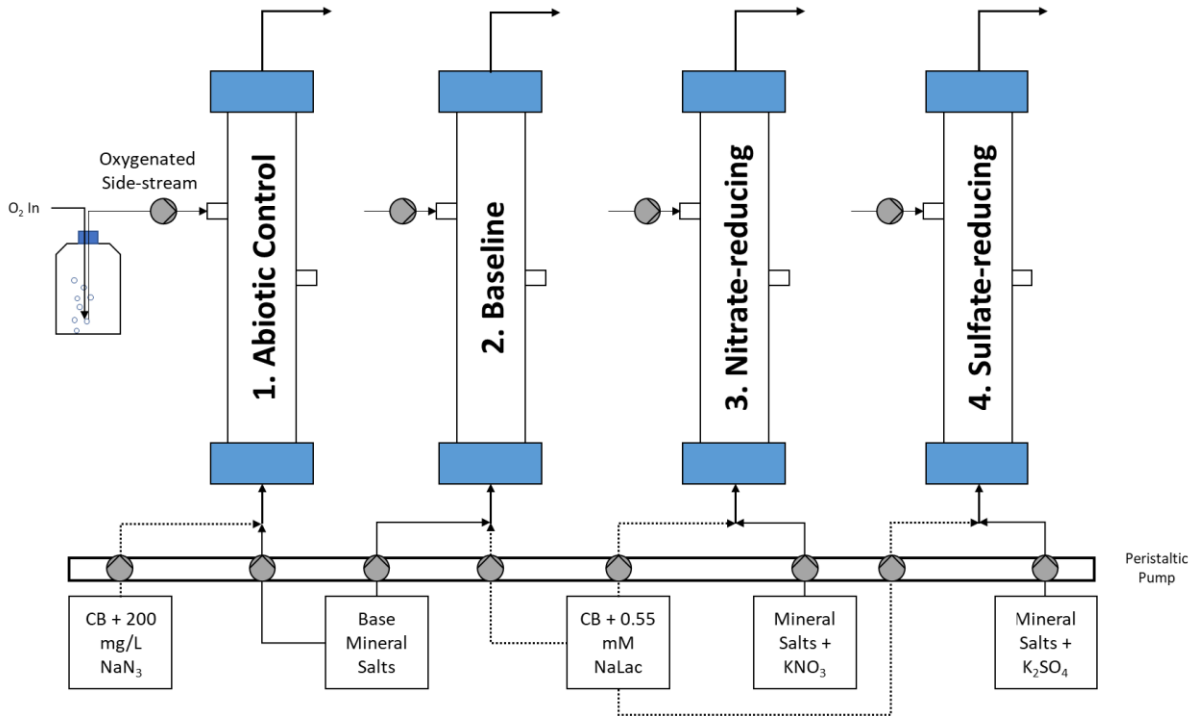
Figure B.1 Schematic diagram of parallel column experiment. Columns used shared media feed when conditions were identical and separate feeds when different. Anaerobic influent media to each column fed by single multi-channel peristaltic pump delivering equal flow to split influent. Aerobic side-stream fed by a separate multi-channel peristaltic pump.

*Table B.1* Timeline of column operation and sampling reported in Chapter 3

Phase / Activity	Operation Times	Steady-state Calculations	e⁻ Balance Sample Times	Porewater Microbial Sample Times
		Time of Activity (days)		
Startup	(-15) - 31	NA	NA	NA
Empty bed tracer test	(-15)			
Inoculation	(-12)			
Begin 100% port measurements	0			
Begin 50% port measurements	31			
I	31-81	57-80	76/79*	76 ,78
II	81-141	115-140	135/128*	129, 135
III	141-193	169-192	188/190*	188, 192
IV	193-302	260-296	296	293, 296
Tracer Test	301			
V	302-351	330-346	344	344, 346
Tracer Test	349			
Sacrificial Sample	351			

*Dissolved methane samples were collected on a different day from other analytes, listed second
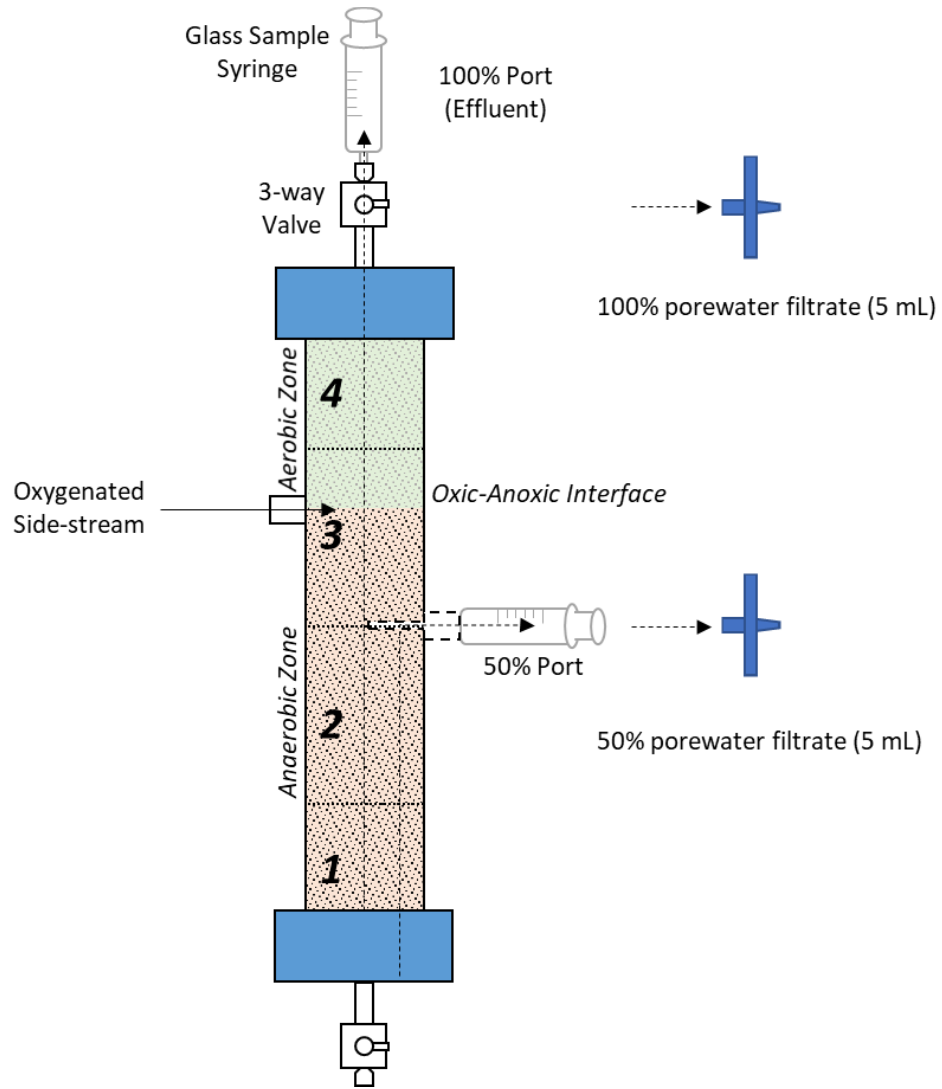
Figure B.2 DNA sampling scheme. Porewater DNA extracted from 50% sample port filtrate (anaerobic zone) and 100% port filtrate (entire column). Columns were divided into four equal length vertical segments for sacrificial sampling. Segments 1-2 represented anaerobic zone, segment 3 represented oxic-anoxic transition zone, and segment 4 represented the aerobic zone.

Table B.2. Description of reductive and oxidative processes, measured analytes, and electron equivalents used to calculate column electron balance

Redox Process	Species Measured	Assumed Half-Reactants	Calculated Analyte Change ($\Delta\mu M$)	e⁻ Equivalent ($\Delta\mu eq/\Delta\mu mol$)
Anaerobic Zone				
Available e⁻ Donor	Lactate (NaLac)	$Lactate \rightarrow CO_2$	$Lactate_0$ (theoretical) [a]	12
Reductive Dechlorination	DCBs, MCB	$nCB \rightarrow (n-1)CB$	$Dechlorination_{50} - Dechlorination_0$	2
Nitrate Reduction	Nitrate (NO_3^-)	$NO_3 \rightarrow N_2$	$Nitrate_0$ (theoretical) $- Nitrate_{50}$ [b]	5
Sulfate Reduction	Sulfate (SO_4^{2-})	$SO_4^{2-} \rightarrow S_2^-$	$Sulfate_0 - Sulfate_{50}$	8
Methanogenesis	Methane (CH_4)	$CO_2 \rightarrow CH_4$	$Methane_{50} - Methane_0$ (theoretical) [c]	8
Propionate Fermentation	Propionate	$CO_2 \rightarrow Propionate$	$Propionate_{50} - Propionate_0$ (theoretical) [c]	14
Acetate Fermentation	Acetate	$CO_2 \rightarrow Acetate$	$Acetate_{50} - Acetate_0$ (theoretical) [c]	8
Unreacted Lactate	Lactate	NA	$Lactate_{50} - Lactate_0$ (theoretical) [c]	12

$$\sum Measured\ Reductions = \sum_{Redox\ Processes} Analyte\ Change \times e^- Equivalent$$
$$\%\ e^- Donor\ Utilization = \sum Measured\ Reductions \div Available\ e^- Donor$$

Redox Process	Species Measured	Assumed Half-Reactants	Calculated Analyte Change ($\Delta\mu M$)	e⁻ Equivalent ($\Delta\mu eq/\Delta\mu mol$)
Aerobic Zone				
Available Oxygen	DO	$O_2 \rightarrow H_2O$	$DO_{side\ stream}$ [d]	4
CB Oxidation	TCB, DCBs, MCB	$nCB \rightarrow CO_2$	$nCB_{50} \div DF - nCB_{100}$	24, 26, 28
Sulfide Oxidation	Sulfate (SO_4^{2-})	$S_2^- \rightarrow SO_4^{2-}$	$Sulfate_{50} \div DF - Sulfate_{100}$	8
Methane Oxidation	Methane (CH_4)	$CH4 \rightarrow CO_2$	$Methane_{50} \div DF - Methane_{100}$	8
Propionate Oxidation	Propionate	$Propionate \rightarrow CO_2$	$Propionate_{50} \div DF - Propionate_{100}$	14
Acetate Oxidation	Acetate	$Acetate \rightarrow CO_2$	$Acetate_{50} \div DF - Acetate_{100}$	8
Lactate Oxidation	Lactate	$Lactate \rightarrow CO_2$	$Lactate_{50} \div DF - Lactate_{100}$	12

$$\sum Measured\ Oxidations = \sum_{Redox\ Processes} Analyte\ Change \times e^- Equivalent$$
$$\%\ Oxygen\ Utilization = \sum Measured\ Oxidations \div Available\ Oxygen$$

a. Influent NaLac ($Lactate_0$) was assumed to be a constant 55µM (6643 µeq) throughout the experiment
b. Influent Nitrate ($Nitrate_0$) was assumed to be equal to the theoretical nitrate dose for the given phase
c. All influent e⁻ donors besides NaLac were assumed to be zero, assuming NaLac was unreacted at influent
d. $DO_{side\ stream}$ was calculated as the measured side-stream concentration at the given phase diluted into the column aerobic zone

Table B.3. Summary of steady-state calculated and measured parameters for each column phased used in manuscript body

| Column | Phase | Influent | | Anaerobic Zone | | | | | | DO In (mg/L) | Side-stream Dilution Factor | Aerobic Zone | | | | | | Effluent | | |
| | | Amendment | Total Influent CB (μM) | CB Reductive Dechlorination | | | | | | | | Aerobic CB Degradation | | | | | | Total Effluent CB (μM) | % CB Removal | Effluent Degree of Chlorination |
				Extent (μM)	Rate (μM/hr)	% NaLac Utilization	Δ Nitrate (μM)	Δ Sulfate (μM)	Residual Organic Acids (μM)			Extent (μM)	Rate (μM/hr)	% O2 Utilization	Δ Nitrate (μM)	Δ Sulfate (μM)	Residual Organic Acids (μM)			
Abiotic Column (AC)	I	NA	34.1 ± 1.4	0.0 ± .0	0.0	NA	NA	2 ± 5	NA	8.5 ± .6		1.9 ± .8	1.2	4.4%	NA	0 ± 1	NA	22.9 ± 1.6	8 ± 3%	3.0 ± .0
	II		27.7 ± 3.5	0.0 ± .0	0.0	NA	NA	-1 ± 2	NA	8.9 ± .5		0.7 ± .8	0.4	1.5%	NA	-2 ± 2	NA	20.3 ± 1.9	-1 ± 5%	3.0 ± .0
	III		23.9 ± .9	0.0 ± .0	0.0	NA	NA	1 ± 6	NA	9.3 ± .8	1.38	0.8 ± .3	0.5	1.6%	NA	-2 ± 5	NA	16.9 ± .5	3 ± 3%	3.0 ± .0
	IV		23.8 ± 3.2	0.0 ± .0	0.0	NA	NA	0 ± 7	NA	7.4 ± .2		1.8 ± .6	1.1	4.7%	NA	-2 ± 4	NA	15.2 ± 2.7	12 ± 7%	3.0 ± .0
	V		19.5 ± 1.5	0.0 ± .0	0.0	NA	NA	2 ± 4	NA	7.4 ± .3		0.9 ± 1.2	0.5	2.4%	NA	-3 ± 2	NA	14.0 ± 1.0	0 ± 12%	3.0 ± .0
Baseline Column (BC)	I	NA	40.5 ± 1.9	11.9 ± 3.9	3.3	0.36%	NA	-94 ± 8	426	7.1 ± .5		10.1 ± 2.2	7.3	27.8%	NA	17 ± 3	92	20.2 ± 3.0	35 ± 9%	2.7 ± .1
	II		41.2 ± 1.9	14.8 ± 7.4	4.1	0.45%	NA	-88 ± 13	447	7.5 ± .4		7.8 ± 1.2	5.6	20.6%	NA	15 ± 7	242	26.0 ± 2.9	18 ± 6%	2.6 ± .2
	III		38.5 ± 1.8	7.0 ± 2.7	1.9	0.21%	NA	-83 ± 7	491	7.8 ± .7	1.30	9.0 ± 1.6	6.5	22.6%	NA	15 ± 8	235	20.7 ± 2.5	30 ± 7%	2.8 ± .1
	IV		38.1 ± 4.4	17.1 ± 5.7	4.8	0.52%	NA	-90 ± 10	304	6.2 ± .2		8.3 ± 1.0	6.0	27.0%	NA	3 ± 4	124	22.5 ± 2.7	23 ± 6%	2.4 ± .1
	V		39.4 ± 4.3	30.3 ± 5.0	8.4	0.91%	NA	-97 ± 4	200	6.2 ± .2		7.3 ± .6	5.3	24.6%	NA	6 ± 5	104	24.9 ± 1.6	17 ± 9%	2.0 ± .1

NA - not measured or calculated
Values displayed are average ± 1 SD

Table B.3. Summary of steady-state calculated and measured parameters for each column phased used in manuscript body (continued)

| Column	Phase	Influent		Anaerobic Zone — CB Reductive Dechlorination						DO In (mg/L)	Side-stream Dilution Factor	Aerobic Zone — Aerobic CB Degradation						Effluent		
		Amendment	Total Influent CB (µM)	Extent (µM)	Rate (µM/hr)	% NaLac Utilization	Δ Nitrate (µM)	Δ Sulfate (µM)	Residual Organic Acids (µM)			Extent (µM)	Rate (µM/hr)	% O2 Utilization	Δ Nitrate (µM)	Δ Sulfate (µM)	Residual Organic Acids (µM)	Total Effluent CB (µM)	% CB Removal	Effluent Degree of Chlorination
Nitrate-reducing Column (NRC)		Nitrate																		
	I	0 mM	39.0 ± 1.3	13.4 ± 2.9	3.8	0.40%	1 ± 1	-88 ± 4	437	8.0 ± .5		9.8 ± 2.7	7.4	24.2%	1 ± 1	16 ± 5	201	19.1 ± 3.3	34 ± 10%	2.6 ± .1
	II	.15 mM	39.1 ± 2.3	10.2 ± 3.7	2.9	0.31%	-142 ± 3	-86 ± 12	346	8.4 ± .4		8.3 ± 1.3	6.3	19.4%	2 ± 2	13 ± 4	139	22.2 ± 1.9	23 ± 5%	2.7 ± .1
	III	.5 mM	37.2 ± 1.6	2.6 ± 1.5	0.7	0.08%	-477 ± 38	-57 ± 32	167	8.7 ± .8	1.35	15.6 ± 2.1	11.9	34.5%	5 ± 9	32 ± 8	11	11.7 ± 2.5	58 ± 8%	2.9 ± .1
	IV	2.5 mM	36.6 ± 4.3	3.4 ± 1.6	1.0	0.10%	-943 ± 54	1 ± 4	7	7.0 ± .2		26.3 ± 2.1	20.0	72.2%	-59 ± 44	2 ± 8	5	1.3 ± .7	95 ± 2%	3.0 ± .0
	V	.5 mM	40.0 ± 2.6	14.2 ± 4.3	4.0	0.43%	-499 ± 0	-84 ± 18	192	7.0 ± .3		13.4 ± 3.9	10.2	38.2%	0 ± 0	15 ± 7	50	18.1 ± 3.6	39 ± 10%	2.6 ± .1
Sulfate-reducing Column (SRC)		Sulfate																		
	I	.15 mM	39.7 ± 3.2	11.9 ± 4.1	3.2	0.36%	NA	-95 ± 8	203	7.8 ± .5		7.5 ± 3.5	5.4	19.0%	NA	12 ± 2	183	21.3 ± 3.1	28 ± 8%	2.6 ± .1
	II	.5 mM	39.1 ± 2.0	5.6 ± 1.3	1.5	0.17%	NA	-245 ± 26	392	8.2 ± .4	1.34	5.9 ± 1.5	4.2	13.8%	NA	54 ± 15	195	24.8 ± 1.6	15 ± 6%	2.8 ± .0
	III	2.5 mM	37.5 ± 1.8	3.4 ± .5	0.9	0.10%	NA	-329 ± 35	353	8.5 ± .8		6.5 ± .5	4.6	14.7%	NA	106 ± 45	177	21.6 ± 1.1	23 ± 4%	2.9 ± .0
	IV	10 mM	36.3 ± 4.1	0.0 ± .0	0.0	0.00%	NA	-252 ± 137	317	6.8 ± .2		3.1 ± 1.8	2.2	8.8%	NA	70 ± 93	188	23.6 ± 2.1	12 ± 7%	2.9 ± .0
	V	.5 mM	39.8 ± 2.7	1.3 ± .8	0.4	0.04%	NA	-325 ± 31	279	6.8 ± .3		3.8 ± 2.2	2.7	10.7%	NA	68 ± 8	156	26.7 ± 1.6	10 ± 4%	3.0 ± .0

NA - not measured or calculated
Values displayed are average ± 1 SD

Table B.4. Summarized steady-state CB degradation significance testing

Column	Phase	Anaerobic Dechlorinations				Aerobic Degradation			
		From Previous Phase [1]		From BC Phase [2]		From Previous Phase [1]		From BC Phase [2]	
		p-value [3]	Sig. [4]	p-value [3]	Sig. [4]	p-value [3]	Sig. [4]	p-value [3]	Sig. [4]
Abiotic (AC)	I	NA		NA		NA	NA	NA	
	II	NA		NA		0.022842	*	NA	
	III	NA		NA		0.872048	ns	NA	
	IV	NA		NA		0.006553	**	NA	
	V	NA		NA		0.12665	ns	NA	
Baseline (BC)	I	NA		NA		NA		NA	
	II	0.4156	ns	NA		0.059585	ns	NA	
	III	0.0474	*	NA		0.18193	ns	NA	
	IV	0.0024	**	NA		0.380327	ns	NA	
	V	0.0010	**	NA		0.054913	ns	NA	
Nitrate Reducing (NRC)	I	NA		0.4744	ns	NA		0.84263	ns
	II	0.1246	ns	0.2057	ns	0.275188	ns	0.52938	ns
	III	0.0025	**	0.0083	**	6.65E-05	***	0.00015	***
	IV	0.3248	ns	0.0005	***	2.19E-06	***	0.00000001	***
	V	0.0010	***	0.0001	***	0.000133	***	0.01249	*
Sulfate Reducing (SRC)	I	NA		0.9912	ns	NA		0.16729	ns
	II	0.0117	*	0.0273	*	0.313048	ns	0.03126	*
	III	0.0078	**	0.0224	*	0.368484	ns	0.01024	*
	IV	0.00002	***	0.0002	***	0.002057	**	0.00007	***
	V	0.0093	**	0.00002	***	0.555386	ns	0.00873	**

1. Between current phase and previous phase within the same column
2. Between same phase in current column and Baseline Column (BC)
3. Results of Welch's 2-tailed t-test
4. Significance code: ns ($p \geq .05$), * ($p < .05$), ** ($p < .01$), *** ($p < .001$)
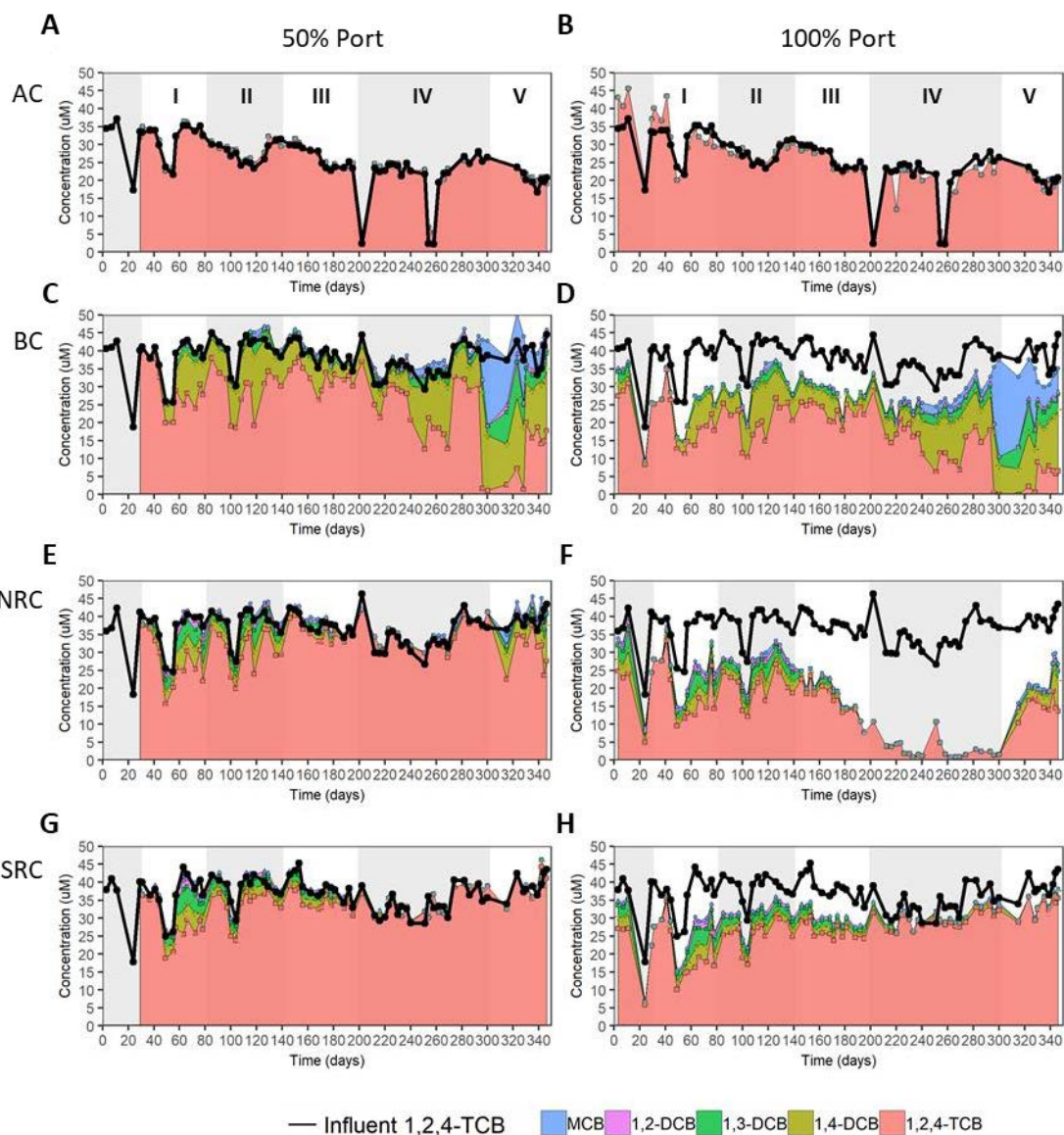
Figure B.3 Measured time-series profiles of CB concentrations at 50% port (left) and 100% port (right) for each column: (A-B) AC-Abiotic Column; (C-D) BC-Baseline Column; (E-F) NRC-Nitrate-reducing Column; (G-H) SRC Sulfate-reducing Column. Connected black data points represent influent concentration of 1,2,4-TCB at 0% port, and colored stacked areas represent the combined effluent concentrations of all CB congeners. To visualize the mass balance between column influent and effluent, concentrations for 100% port samples were multiplied by the side-stream dilution factor of each column. This results in a visual exaggeration of the actual observed effluent concentration and aerobic degradation. 50% port measurements were not adjusted.

Table B.5. Effluent pH measurements in columns during steady-state of each experimental phase

Phase	Sample Time (day)	Column			
		AC	BC	NRC	SRC
I	76	7.50	7.17	7.12	7.16
II	127	7.36	7.35	7.41	7.43
III	198	7.57	7.17	7.34	7.32
IV	261	7.61	7.20	7.36	7.36
V	344	7.37	7.19	7.32	7.32
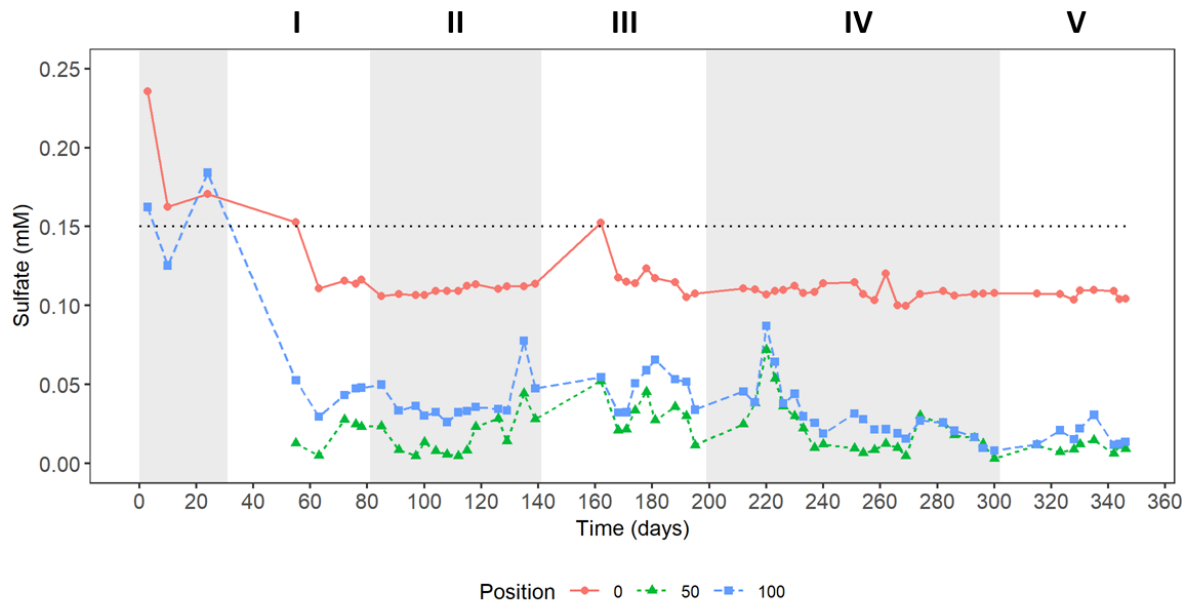
Figure B.4 Baseline Column (BC) time-series sulfate profile at 0%, 50%, and 100% sample ports. Dotted black line represents theoretical sulfate input. To visualize the mass balance between column influent and effluent, 100% port sample concentrations were multiplied by the side-stream dilution factor, resulting in displayed concentrations higher than actual sample measurements.
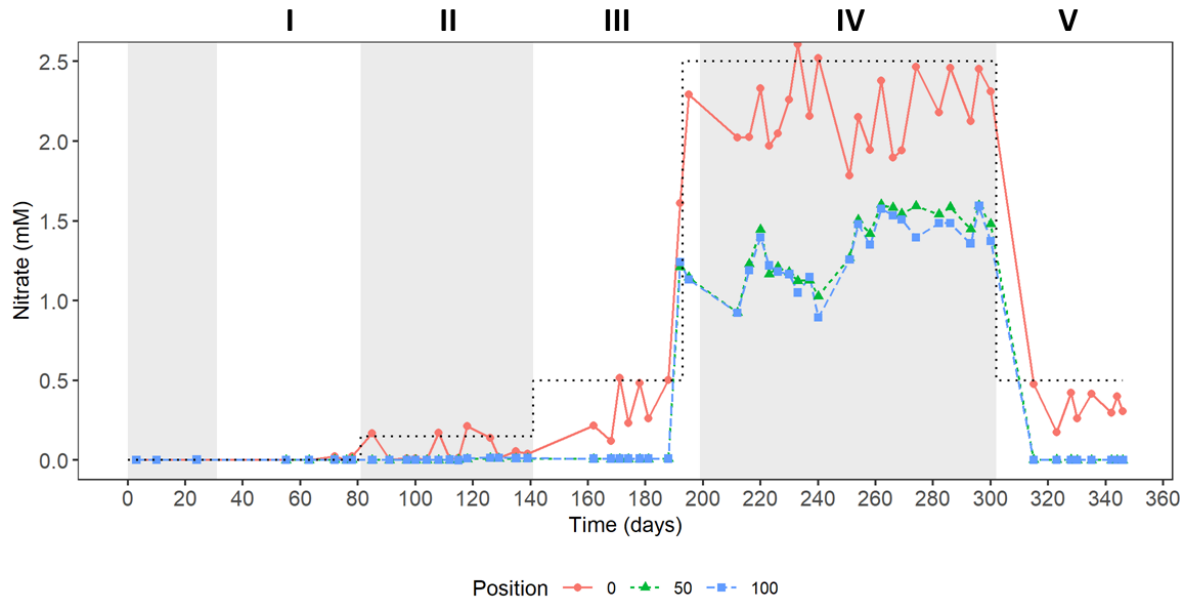
Figure B.5 Nitrate-reducing Column (NRC) time-series nitrate profile at 0%, 50%, and 100% sample ports. Dotted black line represents theoretical nitrate input. Sawtooth influent concentrations resulted from persistent nitrate utilization before 0% port and periodic sterilization of inlet lines. To visualize the mass balance between column influent and effluent, 100% port sample concentrations were multiplied by the side-stream dilution factor, resulting in displayed concentrations higher than actual sample measurements.
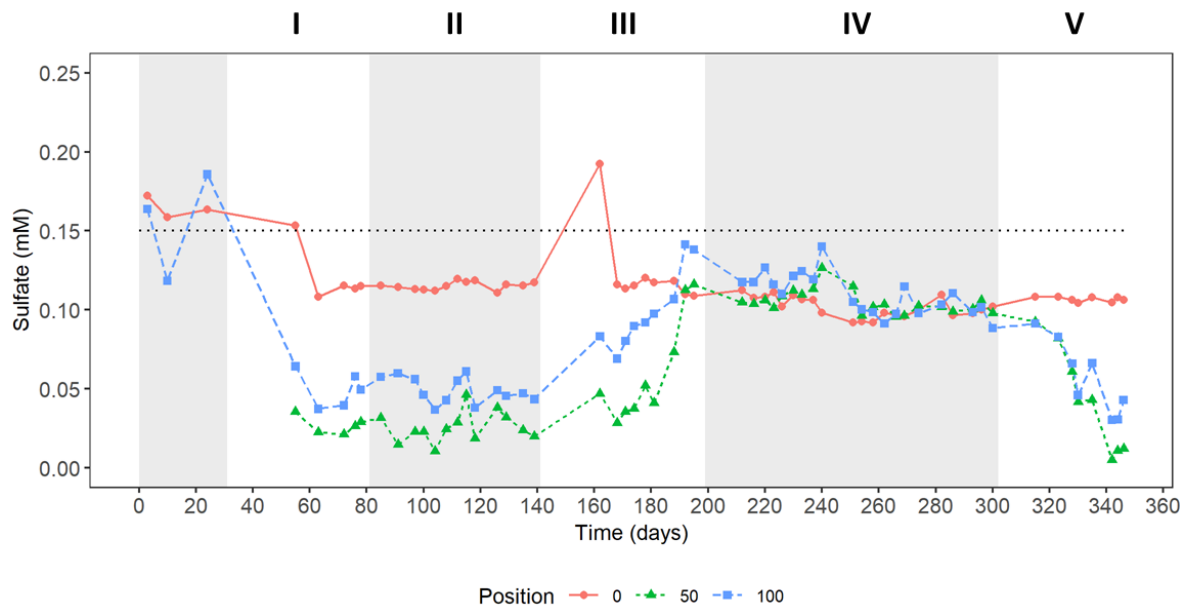

Figure B.6 Nitrate-reducing Column (NRC) time-series sulfate profile at 0%, 50%, and 100% sample ports. Dotted black line represents theoretical sulfate input. To visualize the mass balance between column influent and effluent, 100% port sample concentrations were multiplied by the side-stream dilution factor, resulting in displayed concentrations higher than actual sample measurements.

207
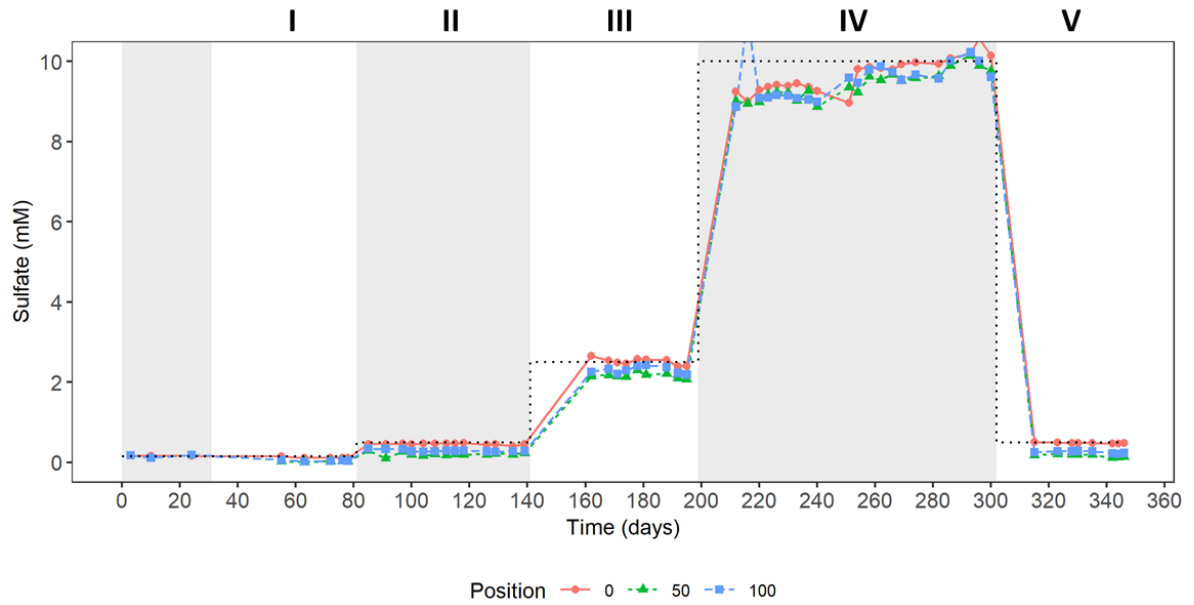
Figure B.7 Sulfate-reducing Column (BC) time-series sulfate profile at 0%, 50%, and 100% sample ports. Dotted black line represents theoretical sulfate input. To visualize the mass balance between column influent and effluent, 100% port sample concentrations were multiplied by the side-stream dilution factor, resulting in displayed concentrations higher than actual sample measurements.
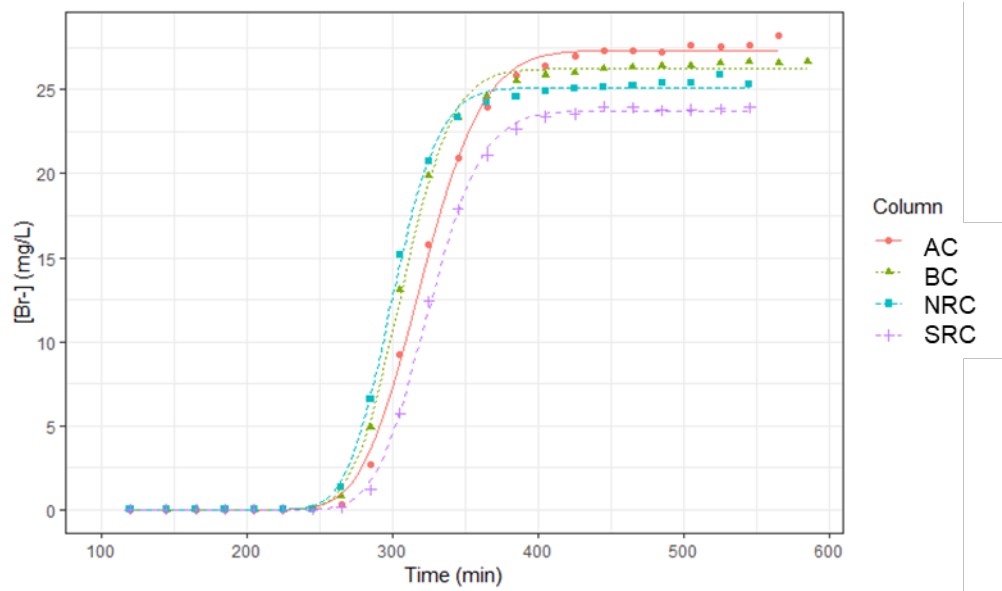
Figure B.8 Empty bed column step-input tracer test during column startup (day -15). Plotted points were measured concentrations and curves were the model fitted by nonlinear least square regression.
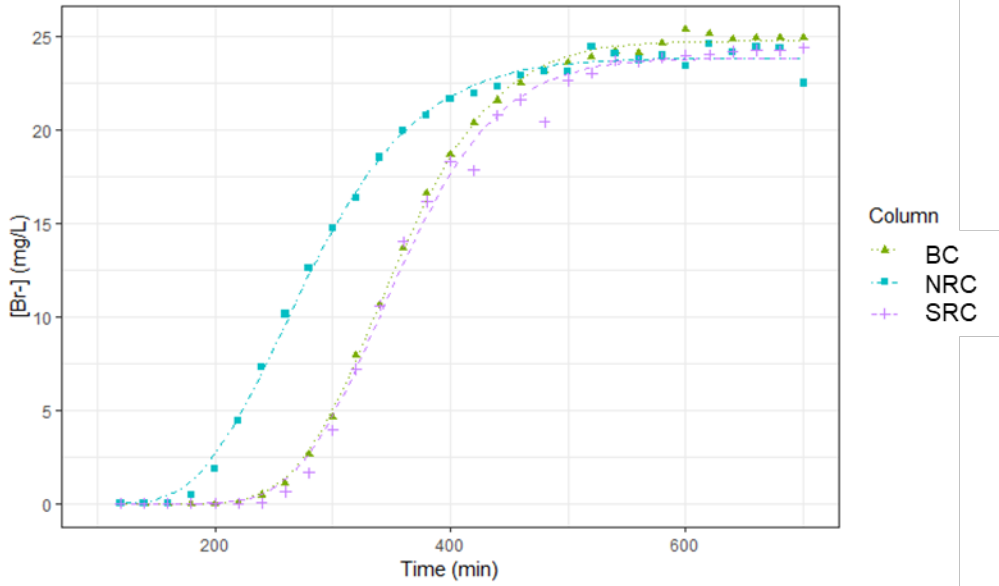
Figure B.9 Phase IV column step-input tracer test (day 301). Plotted points were measured concentrations and curves were the model fitted by nonlinear least square regression. Tracer test not run for abiotic column (AC).
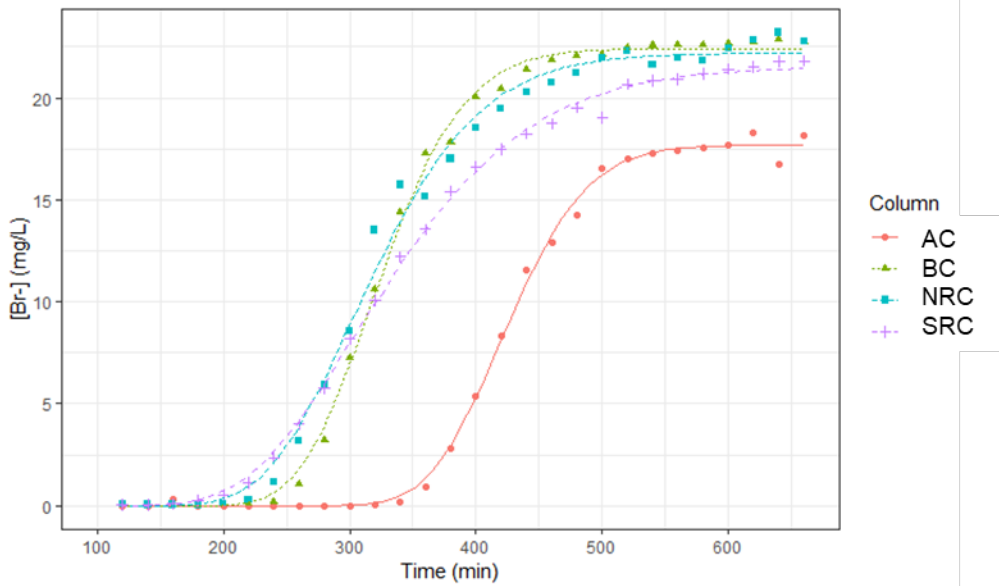

Figure B.10 Phase V column step-input tracer test (day 351) immediately before ending operation. Plotted points were measured concentrations and curves were the model fitted by nonlinear least square regression.

*Table B.6* Column hydrodynamic parameters determined by tracer test

| Column	Phase	Flow (mL/min)	C_0 (mg/L)	u (cm/min)	D (cm^2/min)	Residual Standard error	HRT, τ (min)	HRT, τ (hr)	Effective Porosity, ϵ	Pore Volume (mL)
						Fitted Model Parameters		Calculated Parameters		
	Startup	0.093	27.36	0.0468	0.0037	0.427	320	5.34	0.40	29.8
AC	V	0.078	17.67	0.0353	0.0036	0.367	425	7.09	0.45	33.0
	Startup	0.096	26.24	0.0489	0.0029	0.407	307	5.11	0.40	29.4
	IV	0.094	24.73	0.0426	0.0117	0.279	353	5.88	0.45	33.0
BC	V	0.094	22.42	0.0461	0.0088	0.443	325	5.42	0.41	30.4
	Startup	0.096	25.11	0.0500	0.0026	0.356	300	5.00	0.39	28.8
	IV	0.092	23.83	0.0538	0.0292	0.509	279	4.65	0.35	25.5
NRC	V	0.092	22.19	0.0472	0.0162	0.768	318	5.30	0.40	29.1
	Startup	0.095	23.74	0.0462	0.0028	0.233	325	5.41	0.42	30.9
	IV	0.090	23.81	0.0424	0.0118	0.702	354	5.90	0.43	31.8
SCR	V	0.092	21.54	0.0454	0.0256	0.335	330	5.50	0.41	30.4
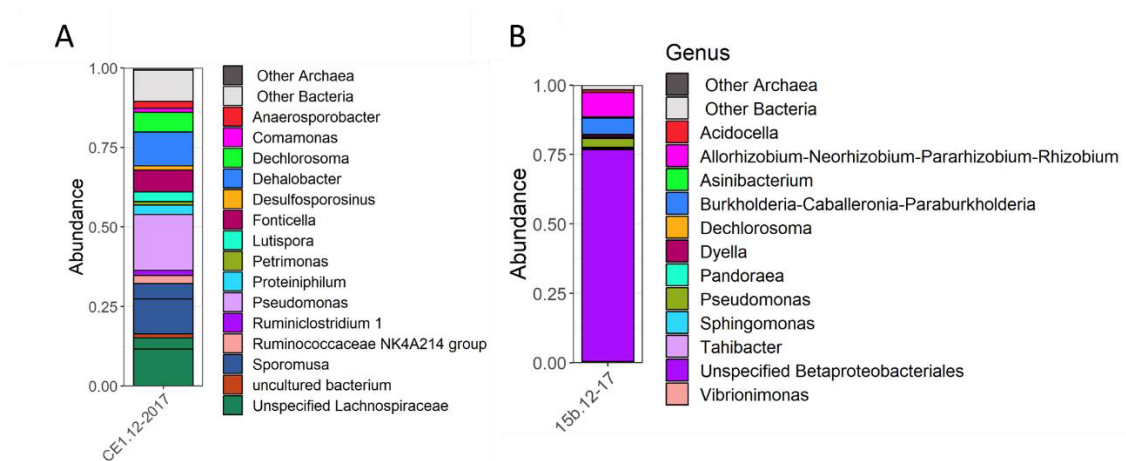
Figure B.11. 16S genus-level composition of column inocula. (A) Anaerobic CB-dechlorinating inoculum (1% relative abundance cutoff for listed genera). (B) Aerobic CB-oxidizing inoculum (0.2% cutoff).
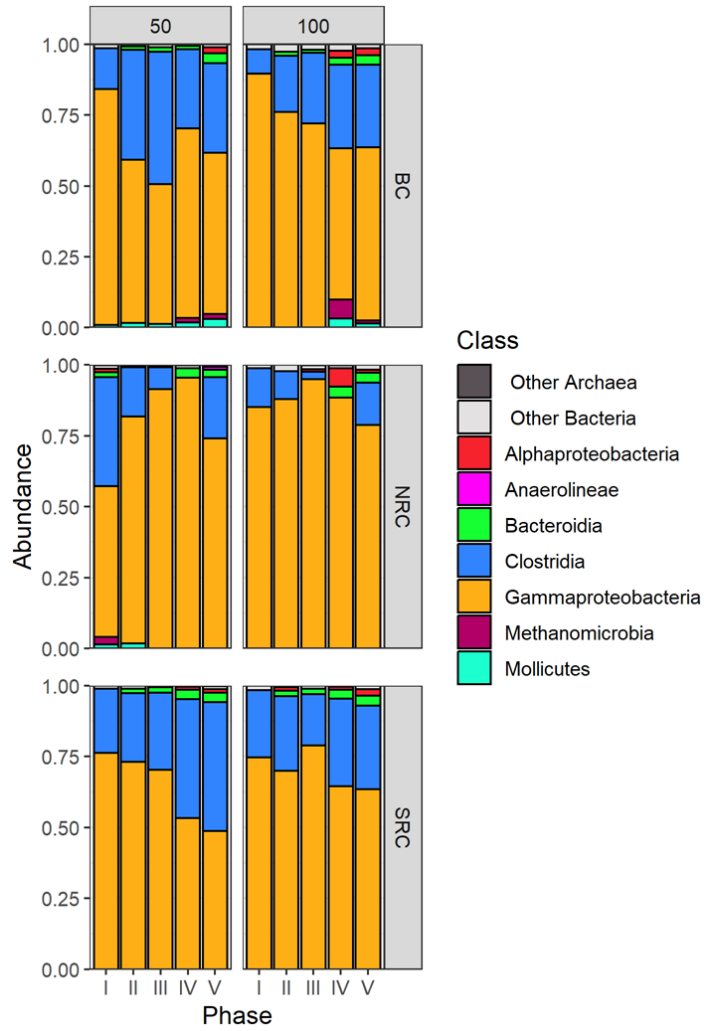
Figure B.12. Class-level porewater microbial community relative abundance profile in biological columns during steady-state of each phase at 50% port (left) and 100% port (right) for classes with >=1% abundance. n=2 sample dates for all samples except in BC Phases II, III, and V.
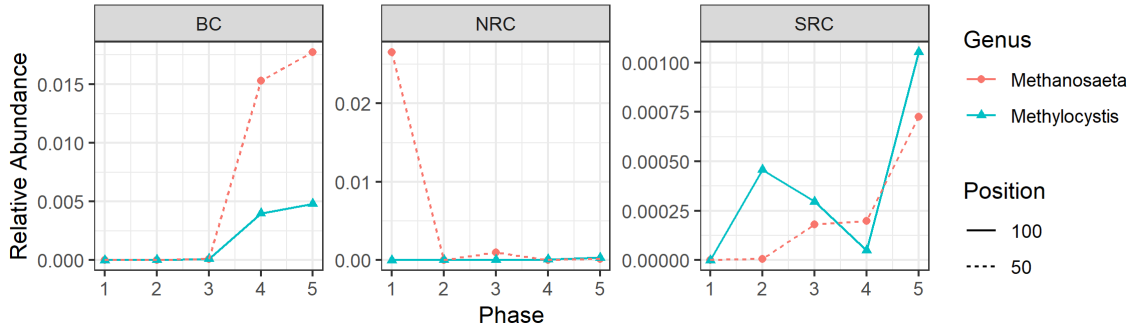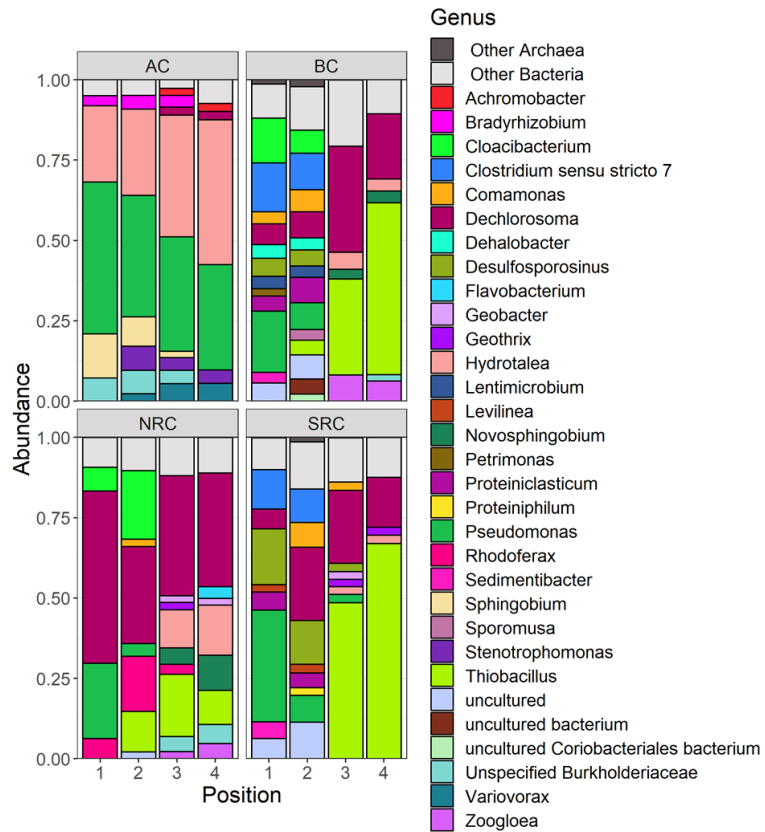
Figure B.13. Relative abundance profiles of methanogenic *Methanosaeta* at 50% porewater port and methanotroph *Methylocystis* at 100% porewater port during steady-state operation of each experimental phase. Each datapoint represents the average of 2 samples with the exception of BC Phases II, III, and V.
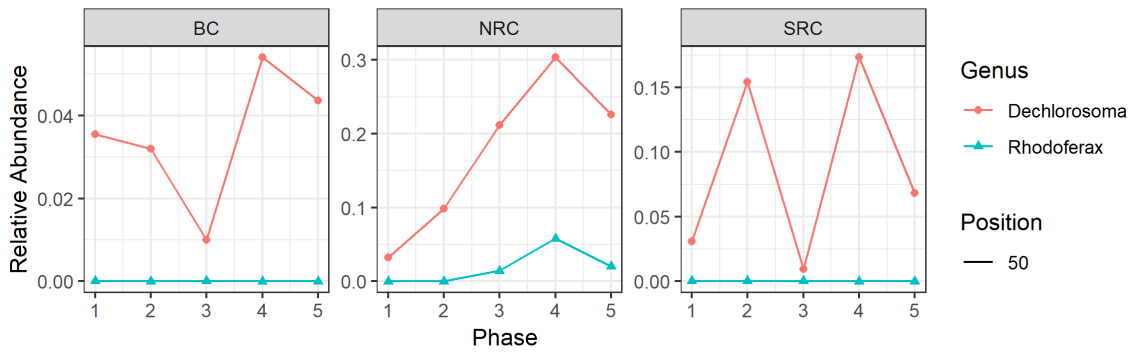
Figure B.14. Relative abundance profiles of likely nitrate-reducing bacteria *Dechlorosoma* and *Rhodoferax* at 50% porewater port during steady-state operation of each experimental phase. Each datapoint represents the average of 2 samples with the exception of BC Phases II, III, and V.
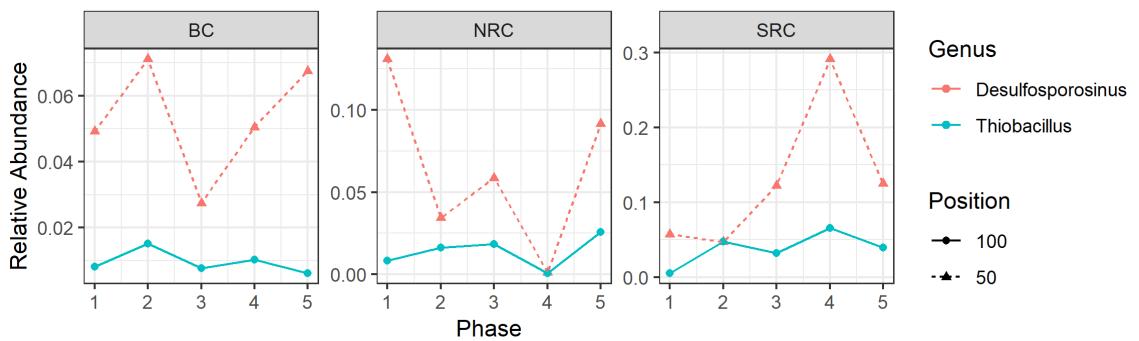
Figure B.15. Relative abundance profiles of sulfate reducer *Desulfosporosinus* at 50% porewater port and sulfur oxidizer *Thiobacillus* at 100% porewater port during steady-state operation of each experimental phase. Each datapoint represents the average of 2 samples with the exception of BC Phases II, III, and V.
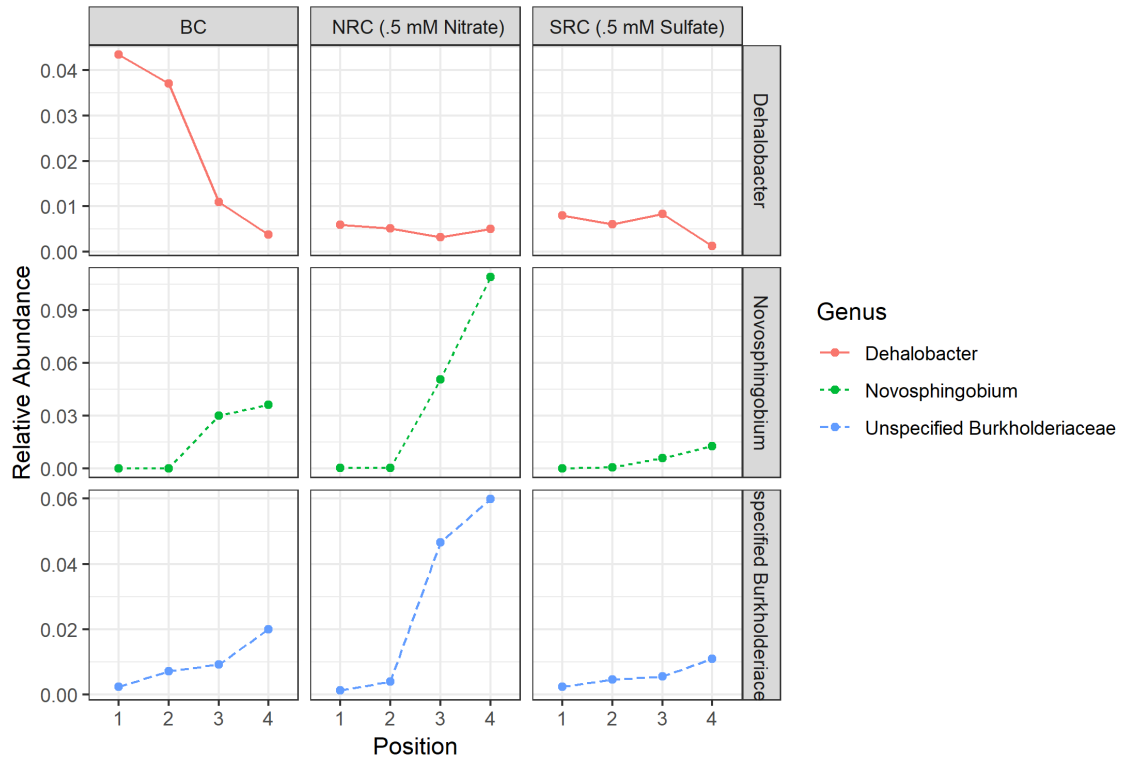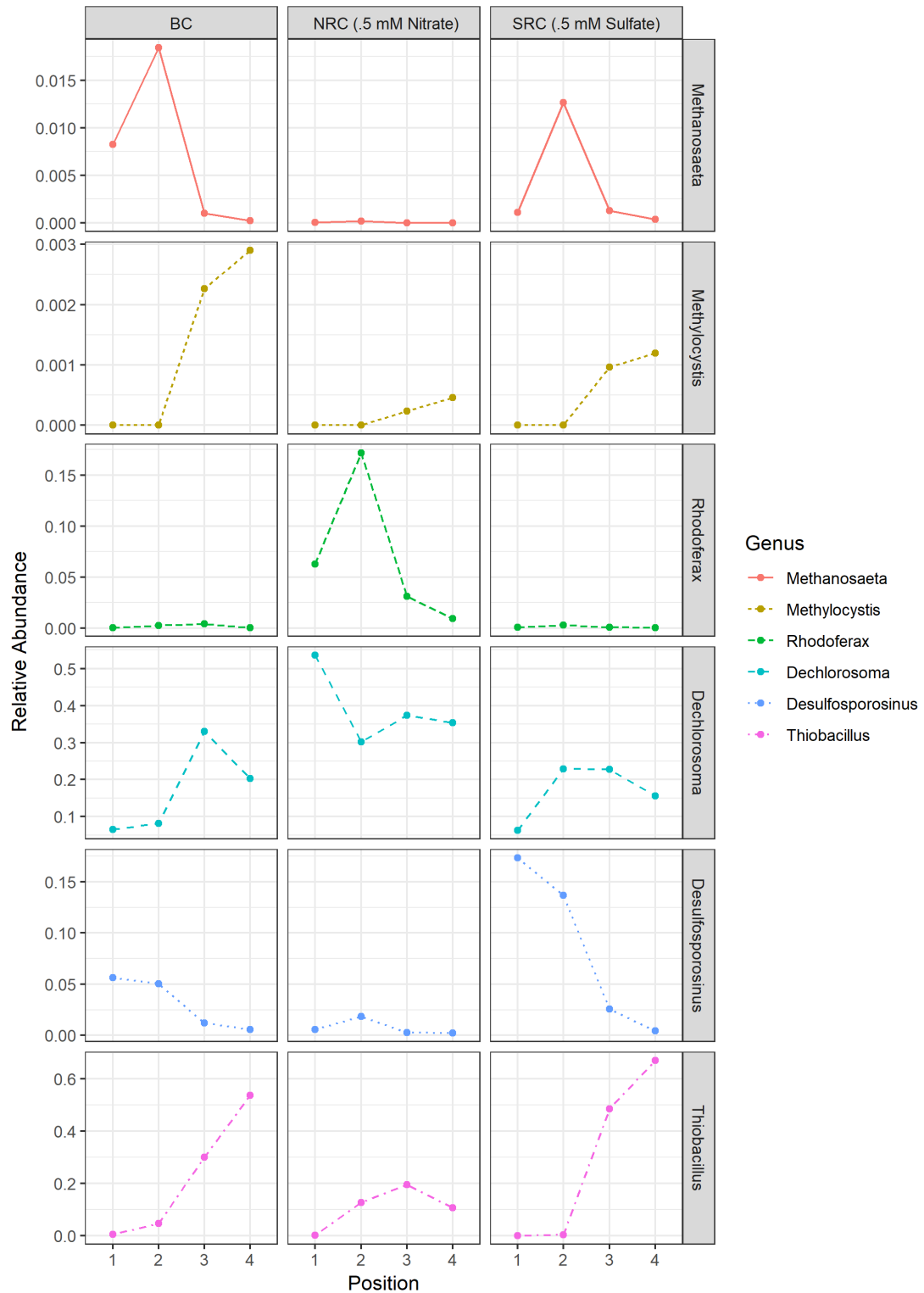
Figure B.16. Genus-level relative abundance profile of microbial biofilm community in all columns at the end of the experiment (Phase V). Genera shown are >=2% abundance. n=2 replicate samples for all segments in BC, NRC, and SRC. N=1 sample for AC.

Figure B.17. Vertical relative abundance profiles of suspected CB degrader in column biofilms at the end of Phase V. Segments 1 and 2 sampled from anaerobic zone, segment 3 in transition from anaerobic to aerobic zone, and segment 4 in the aerobic zone.

Figure B.18. Vertical relative abundance profiles of suspected functionally-relevant redox-cycling microorganisms in column biofilms at the end of Phase V. Segments 1 and 2 sampled from anaerobic zone, segment 3 in transition from anaerobic to aerobic zone, and segment 4 in the aerobic zone.

B.3   References

1. Burkholder, J.; Sander, S.; Abbatt, J.; Barker, J.; Huie, R.; Kolb, C.; Kurylo, M.; Orkin, V.; Wilmouth, D.; Wine, P., Chemical Kinetics and Photochemical Data for Use in Atmospheric Studies, Evaluation

No. 18. In *JPL Pulbication 15-10*, Laboratory, J. P., Ed. Pasadena, 2015.
2. Sander, R., Compilation of Henry's law constants (version 4.0) for water as solvent. *Atmos. Chem. Phys.* **2015,** *15*, (8), 4399-4981.

Curriculum Vitae

Steven J. Chow

3400 N. Charles Street Ames Hall 313 Baltimore, MD 21218

Spawned at the confluence of College and Spa Creeks in Annapolis, Maryland during the second fortnight of June, anno Domini 1990

Education
- Ph.D., Environmental Health and Engineering, Johns Hopkins University (JHU)
  (August 2013-Present)
- M.S.E., Geography and Environmental Engineering, JHU
  (August 2013-May 2015)
- B.S., Biosystems Engineering, Clemson University
  (August 2008-May 2012)

Major Research Experiences
Doctoral Research, PI: Dr. Edward Bouwer, JHU (Fall 2014-Present)
- Designed, operated, and analyzed long-term column experiments testing microbial chlorobenzene remediation at anaerobic-aerobic interfaces
- Developed and adapted project-specific analytical chemistry methods (GC-MS, IC) and molecular biology tools (qPCR, Illumina sequencing) to characterize experimental systems
- Utilized statistical programming (R) to quantitate and evaluate changes in dynamic time-series data for chemical and microbial community analyses

Master's Research, PI: Dr. Edward Bouwer, JHU (Fall 2013-Spring 2016)
- Evaluated algal growth rates and energy density using recycled nutrients from wastewater treatment processes
- Optimized anaerobic digestion systems to produce biogas from waste algal feedstocks
- Investigated N, P, COD, and trace metal sequestration from waste streams during microbial growth processes

Other Research Experiences
Field Research, Iquitos, Peru, Dept. of International Health, JHU, PI: Dr. Margaret Kosek (Summer 2014, 2016)
- Investigated coliform reduction efficacy of compost toilet sanitation intervention developed by local NGO
- Initial work led to conference presentations and additional funding supporting a Master's student's thesis research

Research Experience for Undergrads, Dept. of Biology, Colorado State University, PI: Dr. Marinus Pilon (Summer 2011)
- Investigated microRNA regulation of copper homeostasis in plant antioxidant proteins
- Applied plant molecular biology techniques including sterile cultivation, gel electrophoresis, and western blotting

Work Experience

Process Engineer, AMEC Power and Process. Greenville, SC (July 2012-June 2013)
- Designed chemical and mechanical processes using CAD and process modeling software
- Prepared equipment design specifications and evaluated vendor proposals for technical and budgetary acceptability

Publications

In preparation
- **Chow, S.,** Lorah, M., Wadhawan, A., Durant, N., & Bouwer, E. (2019). Sequential biodegradation of 1,2,4-trichlorobenzene at oxic-anoxic groundwater interfaces in model laboratory columns

Published
- Bohutskyi, P., Phan, D., Kopachevsky, A. M., **Chow, S.,** Bouwer, E. J., & Betenbaugh, M. J. (2018). Synergistic co-digestion of wastewater grown algae-bacteria polyculture biomass and cellulose to optimize carbon-to-nitrogen ratio and application of kinetic models to predict anaerobic digestion energy balance. *Bioresource technology*, *269*, 210-220.
- Bohutskyi, P., Kligerman, D. C., Byers, N., Nasr, L. K., Cua, C., **Chow, S.,** ... & Bouwer, E. J. (2016). Effects of inoculum size, light intensity, and dose of anaerobic digestion centrate on growth and productivity of Chlorella and Scenedesmus microalgae and their poly-culture in primary and secondary wastewater. *Algal Research*, *19*, 278-290.
- Bohutskyi, P., **Chow, S.,** Ketter, B., Shek, C. F., Yacar, D., Tang, Y., ... & Bouwer, E. J. (2016). Phytoremediation of agriculture runoff by filamentous algae poly-culture for biomethane production, and nutrient recovery for secondary cultivation of lipid generating microalgae. *Bioresource technology*, *222*, 294-308.
- Bohutskyi, P., Ketter, B., **Chow, S.,** Adams, K. J., Betenbaugh, M. J., Allnutt, F. T., & Bouwer, E. J. (2015). Anaerobic digestion of lipid-extracted Auxenochlorella protothecoides biomass for methane generation and nutrient recovery. *Bioresource technology*, *183*, 229-239.
- Bohutskyi, P., **Chow, S.,** Ketter, B., Betenbaugh, M. J., & Bouwer, E. J. (2015). Prospects for methane production and nutrient recycling from lipid extracted residues and whole Nannochloropsis salina using anaerobic digestion. *Applied energy*, *154*, 718-731.

Selected Presentations

Talks
- Battelle Bioremediation Symposium, Baltimore, MD (April 15-18, 2019)
- University of Maryland, Department of Geology Seminar (Invited), College Park, MD (December 5, 2018)
- Maryland Groundwater Symposium, Baltimore, MD (September 27, 2018)
- Central and Eastern European Conference on Health and the Environment, Krakow, Poland (June 13, 2018)
- NIEHS Superfund Research Program Annual Meeting, Philadelphia, PA (December 6-8, 2017)

- 254th American Chemical Society National Meeting, Washington, DC (August 20-24, 2017)
- International Institute for Environmental Studies Science and Policy Workshop, Shanghai, China (July 23-26, 2017)
- Water Environment Federation Annual Technical Exhibition and Conference (WEFTEC), Chicago, IL (September 28-30, 2015)

Posters
- NIEHS Superfund Research Program Annual Meeting, Sacramento, CA (November 28-30, 2018)
- JHU Colloquium on Water, Climate, and Health, Baltimore, MD (June 22, 2018)
- NIEHS Environmental Health Science FEST, Durham, NC (December 5-8, 2016)

Awards and Fellowships

- Integrative Graduate Education and Research Traineeship (IGERT) Internal Research Grant recipient, JHU (2018)
- NSF IGERT Fellow, Water, Climate, and Health program, JHU (2014-2016)
- Clark Lindsay McCaslan Biosystems Engineering Outstanding Senior Award, Clemson University (2012)
- Northrup Grumman Engineering Scholar (2008)

Teaching, Mentorship, and Outreach

- Teaching Assistant, Engineering Microbiology, JHU (Fall 2015-2018)
- Grader, Biological Processes course, JHU (Spring 2016-2017)
- Mentor, High School student research internships programs, JHU (Fall 2016-Spring 2018)
- Educational Outreach Volunteer, SABES Program, JHU (Fall 2015-Spring 2016)
- Mentor, Thread mentorship program (Fall 2015 – 2019)
- Tutor, Residents in Science and Engineering program, Clemson University (Fall 2011-Spring 2012)
- Undergraduate Teaching Assistant, General Engineering, Clemson University (Fall 2010-Spring 2011)

Professional Affiliations and Certifications

- NCEES Engineer in Training (EIT) certification (2012)
- American Academy of Environmental Engineers and Scientists – student member
- American Chemical Society – student member
- Water Environmental Federation, CWEA Chapter – student member